European Scientific Journal, ESJ
February 2026 Edition Vol. 22, No. 6

ISSN: 1857-7881 (Print)
e-ISSN 1857-7431 (Online)

European Scientific Journal, *ESJ*

February 2026

European Scientific Institute, ESI

The content is peer-reviewed

ESJ Natural/Life/Medical Sciences

February 2026 edition, vol. 22, No. 6

ISSN: 1857-7431 (Online)
ISSN: 1857-7881 (Print)

European Scientific Journal, ESJ
February 2026 Edition Vol. 22, No. 6

ISSN: 1857-7881 (Print)
e-ISSN 1857-7431 (Online)

Generativity is a Core Value of the ESJ: A Decade of Growth

Erik Erikson (1902-1994) was one of the great psychologists of the 20th century[1]. He explored the nature of personal human identity. Originally named Erik Homberger after his adoptive father, Dr. Theodore Homberger, he re-imagined his identity and re-named himself Erik Erikson (literally Erik son of Erik). Ironically, he rejected his adoptive father's wish to become a physician, never obtained a college degree, pursued independent studies under Anna Freud, and then taught at Harvard Medical School after emigrating from Germany to the United States. Erickson visualized human psychosocial development as eight successive life-cycle challenges. Each challenge was framed as a struggle between two outcomes, one desirable and one undesirable. The first two early development challenges were 'trust' versus 'mistrust' followed by 'autonomy' versus 'shame.' Importantly, he held that we face the challenge of **generativity** versus **stagnation in middle life**. This challenge concerns the desire to give back to society and leave a mark on the world. It is about the transition from acquiring and accumulating to providing and mentoring.

Founded in 2010, the European Scientific Journal is just reaching young adulthood. Nonetheless, **generativity** is one of our core values. As a Journal, we reject stagnation and continue to evolve to meet the needs of our contributors, our reviewers, and the academic community. We seek to innovate to meet the challenges of open-access academic publishing. For us,

[1] Hopkins, J. R. (1995). Erik Homburger Erikson (1902–1994). *American Psychologist*, 50(9), 796-797. doi:http://dx.doi.org/10.1037/0003-066X.50.9.796

ISSN: 1857-7881 (Print)
e-ISSN 1857-7431 (Online)

generativity has a special meaning. We acknowledge an obligation to give back to the academic community, which has supported us over the past decade and made our initial growth possible. As part of our commitment to generativity, we are re-doubling our efforts in several key areas. First, we are committed to keeping our article processing fees as low as possible to make the ESJ affordable to scholars from all countries. Second, we remain committed to fair and agile peer review and are making further changes to shorten the time between submission and publication of worthy contributions. Third, we are looking actively at ways to eliminate the article processing charges for scholars coming from low GDP countries through a system of subsidies. Fourth, we are examining ways to create and strengthen partnerships with various academic institutions that will mutually benefit those institutions and the ESJ. Finally, through our commitment to publishing excellence, we reaffirm our membership in an open-access academic publishing community that actively contributes to the vitality of scholarship worldwide.

Sincerely,

Daniel B. Hier, MD

European Scientific Journal (ESJ) Natural/Life/Medical Sciences

Editor in Chief

European Scientific Journal, ESJ
February 2026 Edition Vol. 22, No. 6

ISSN: 1857-7881 (Print)
e-ISSN 1857-7431 (Online)

International Editorial Board

ISSN: 1857-7881 (Print)
e-ISSN 1857-7431 (Online)

ISSN: 1857-7881 (Print)
e-ISSN 1857-7431 (Online)

ISSN: 1857-7881 (Print)
e-ISSN 1857-7431 (Online)

ISSN: 1857-7881 (Print)
e-ISSN 1857-7431 (Online)

ISSN: 1857-7881 (Print)
e-ISSN 1857-7431 (Online)

ISSN: 1857-7881 (Print)
e-ISSN 1857-7431 (Online)

ISSN: 1857-7881 (Print)
e-ISSN 1857-7431 (Online)

ISSN: 1857-7881 (Print)
e-ISSN 1857-7431 (Online)

ISSN: 1857-7881 (Print)
e-ISSN 1857-7431 (Online)

ISSN: 1857-7881 (Print)
e-ISSN 1857-7431 (Online)

ISSN: 1857-7881 (Print)
e-ISSN 1857-7431 (Online)

ISSN: 1857-7881 (Print)
e-ISSN 1857-7431 (Online)

ISSN: 1857-7881 (Print)
e-ISSN 1857-7431 (Online)

ISSN: 1857-7881 (Print)
e-ISSN 1857-7431 (Online)

ISSN: 1857-7881 (Print)
e-ISSN 1857-7431 (Online)

ISSN: 1857-7881 (Print)
e-ISSN 1857-7431 (Online)

ISSN: 1857-7881 (Print)
e-ISSN 1857-7431 (Online)

ISSN: 1857-7881 (Print)
e-ISSN 1857-7431 (Online)

ISSN: 1857-7881 (Print)
e-ISSN 1857-7431 (Online)

ISSN: 1857-7881 (Print)
e-ISSN 1857-7431 (Online)

ISSN: 1857-7881 (Print)
e-ISSN 1857-7431 (Online)

ISSN: 1857-7881 (Print)
e-ISSN 1857-7431 (Online)

ISSN: 1857-7881 (Print)
e-ISSN 1857-7431 (Online)

ISSN: 1857-7881 (Print)
e-ISSN 1857-7431 (Online)

ISSN: 1857-7881 (Print)
e-ISSN 1857-7431 (Online)

ISSN: 1857-7881 (Print)
e-ISSN 1857-7431 (Online)

ISSN: 1857-7881 (Print)
e-ISSN 1857-7431 (Online)

ISSN: 1857-7881 (Print)
e-ISSN 1857-7431 (Online)

ISSN: 1857-7881 (Print)
e-ISSN 1857-7431 (Online)

ISSN: 1857-7881 (Print)
e-ISSN 1857-7431 (Online)

ISSN: 1857-7881 (Print)
e-ISSN 1857-7431 (Online)

ISSN: 1857-7881 (Print)
e-ISSN 1857-7431 (Online)

ISSN: 1857-7881 (Print)
e-ISSN 1857-7431 (Online)

ISSN: 1857-7881 (Print)
e-ISSN 1857-7431 (Online)

European Scientific Journal, ESJ
February 2026 Edition Vol. 22, No. 6

ISSN: 1857-7881 (Print)
e-ISSN 1857-7431 (Online)

Table of Contents:

ISSN: 1857-7881 (Print)
e-ISSN 1857-7431 (Online)

ISSN: 1857-7881 (Print)
e-ISSN 1857-7431 (Online)

ISSN: 1857-7881 (Print)
e-ISSN 1857-7431 (Online)

ESJ Natural/Life/Medical Sciences Peer-reviewed

Machine Learning Techniques in Residential Electrical Load Forecasting: A PRISMA Review with LLM-Assisted Screening and Evidence Extraction

Nermin Siphocly, PhD
Misr International University, Egypt

Doi:10.19044/esj.2026.v22n6p1

Submitted: 08 January 2026
Accepted: 18 February 2026
Published: 28 February 2026

Cite As:
Siphocly, N. (2026). *Machine Learning Techniques in Residential Electrical Load Forecasting: A PRISMA Review with LLM-Assisted Screening and Evidence Extraction*. European Scientific Journal, ESJ, 22 (6), 1. https://doi.org/10.19044/esj.2026.v22n6p1

Abstract

This systematic review assesses machine learning (ML) techniques for residential electrical load forecasting, highlighting their effectiveness, methodologies, and challenges. Conducted under PRISMA 2020 guidelines, the review includes peer-reviewed Q1 and Q2 journal studies published between January 2020 and June 2025. These studies, sourced from the Web of Science, were selected based on their use of ML methods in residential contexts and focus on forecasting performance metrics and implementation. Extracted data covered forecasting horizons, ML algorithms, performance metrics, and limitations. Database searching yielded 712 records. After refinement and eligibility screening, 214 records were retained for title and abstract review, of which 105 were excluded. Only 93 full-text articles could be retrieved and assessed, seven of which were ultimately excluded due to methodological or contextual ineligibility, leaving the final 86 eligible studies. We present a novel multi-stage screening pipeline that incorporates semantic similarity models—specifically a zero-shot retrieval hybrid classifier—and large language models (ChatGPT-4o and Grok 3). Additionally, we examine their behavior, performance, and misclassification patterns throughout the screening process. We highlight key gaps in current literature-reproducibility issues, geographical imbalance, LLM bias, and limited use of explainable or privacy-preserving models—and suggest future research directions for residential load forecasting.

ISSN: 1857-7881 (Print)
e-ISSN 1857-7431 (Online)

Keywords: Machine Learning, Electrical Load Forecasting, Residential Areas, PRISMA, Systematic Review

Introduction

Electric energy forecasting plays a significant role in reducing energy waste by enabling more efficient management of electricity supply and demand. Accurate forecasts help utility companies anticipate energy needs, allowing them to optimize power generation and distribution Sakib et al., 2025). This reduces the need for excess energy production, which often leads to waste. Electric energy forecasting is a key tool in creating a more sustainable and efficient energy system.

In residential areas—where consumption patterns are shaped by diverse factors such as lifestyle, weather, and socioeconomic conditions—precise forecasting is particularly challenging yet vital. The International Energy Agency (IEA) projects that global electricity demand will grow significantly, with 85% of additional demand through 2026 expected from outside advanced economies International Energy Agency (IEA) (2022). This underscores the need for advanced forecasting techniques to address the complexities of residential energy use.

This paper presents a literature review on the state-of-the-art machine learning techniques used in electrical load forecasting in residential areas. Specifically, our survey addresses the following research questions:

- ***RQ1:*** *What methods and models have been used for short-term and long-term electrical load forecasting in residential areas?*
- ***RQ2:*** *What performance metrics are commonly used in the literature for evaluating the prediction of household electrical load?*
- ***RQ3:*** *What are the geographical and demographic regions most represented in residential electrical load forecasting research, and what gaps exist in terms of regional and population-based coverage?*
- ***RQ4:*** *How effective are semantic models and Large Language Models (LLMs) in supporting automated or semi-automated screening and classification in PRISMA-based systematic reviews?*
- ***RQ5:*** *What emerging trends, research gaps, and future directions can be identified in residential electrical load forecasting using machine learning?*

The main contributions of this study are summarized as follows:

- **Domain-specific focus:** This study provides a systematic review exclusively focused on residential electrical load forecasting using machine learning and deep learning approaches.

ISSN: 1857-7881 (Print)
e-ISSN 1857-7431 (Online)

- **Novel hybrid screening methodology:** We introduce an innovative multi-stage screening pipeline that integrates semantic similarity —a zero-shot retrieval hybrid classifier, large language models (ChatGPT-4o and Grok 3). We further analyze their behavior, performance, and misclassification patterns during the screening process.
- **Comprehensive categorization of forecasting techniques:** We systematically classify statistical, machine learning, hybrid, attention-based, transformer, and federated learning models, and map them to forecast horizons, data types, and application contexts, highlighting emerging trends such as privacy-preserving learning and spatio-temporal forecasting.
- **Evaluation metrics analysis:** We examine over 30 evaluation metrics, including traditional error-based metrics (RMSE, MAE, MAPE) and advanced metrics such as PTE, CRPS, DTW, ACE, and Pinball Loss, revealing a shift towards uncertainty-aware, time-sensitive, and robustness-oriented assessment practices.
- **Identification of open challenges and research gaps:** We highlight critical limitations in current literature, including geographical imbalance, LLM bias, and limited use of explainable or privacy-preserving forecasting architectures. We outline future research directions to advance residential load forecasting.

The rest of this paper is organized as follows. The Methods Section outlines the methodologies employed in this study, including the systematic literature review strategy, the inclusion and exclusion criteria for selecting manuscripts, and the PRISMA-based text analysis method. The Results Section presents, analyzes, and discusses the findings, providing further details on the PRISMA text analysis procedure. Finally, the Discussion Section discusses the implications of the results, highlights key research gaps, addresses this study's limitations, offers conclusions, and proposes directions for future research.

Methods

Eligibility Criteria

This study focuses exclusively on electrical load forecasting in residential areas, using machine learning techniques. Our review is limited to English-language journal articles published between January 2020 and June 2025, specifically those appearing in journals ranked in the first or second quartiles (Q1 and Q2) and top-tier conferences.

Information Sources

For our review, we use the WOS - Web of Science - Core collection database Clarivate (2025), which is a carefully curated database of high-

ISSN: 1857-7881 (Print)
e-ISSN 1857-7431 (Online)

quality, peer-reviewed scholarly publications—including journals, books, and conference proceedings—spanning multiple disciplines. As a central component of the Web of Science platform, it is renowned for its stringent selection criteria and is widely regarded as a reliable resource by researchers and academics.

Search Strategy

We conducted our search using the WOS search engine and exported the results as a text file, which we then converted to a CSV file using the Zotero tool. We began our process using the general search terms: ”Electrical Load Forecasting in Residential Areas”, which yielded 712 search results. We subsequently refined our search using Boolean operators: (”load forecasting” OR ”energy prediction”) AND (”residential” OR ”household”) AND (”machine learning” OR ”deep learning” OR ”statistical model”). Additionally, we included the duplicate-removal feature. This refined search produced 374 results. We then filtered the results to include only papers published between 2020 and 2025 and written in English, which reduced the count to 368. To align with our inclusion standards, we retained only articles published in journals ranked Q1 or Q2 and top-tier conferences, as previously mentioned, resulting in the exclusion of 154 papers. Therefore, the number of papers we proceeded with for the next screening phases was 214. The different screening stages are discussed as follows.

Title and Keywords Screening: Our search and filtering process was conducted in several phases; the initial phase involved title screening, during which we excluded all papers not related to ”residential” areas or ”household”. We removed titles associated with ”factory”, ”industrial”, or ”commercial” contexts, as well as those focused on load forecasting in ”agricultural”, ”irrigation”, or ”Electric Vehicles (EV)”. Since our study does not focus on anomaly detection or load monitoring (e.g., non-intrusive load monitoring), titles addressing these topics were also excluded. Additionally, we excluded any papers that were reviews or surveys. The same criteria were applied to the keywords of each paper. Following this phase, the total number of papers was reduced to 193.

Abstract Screening: In the second phase, we conducted abstract screening, applying the same exclusion criteria used during the title screening phase. Moreover, we excluded papers that focused on ”thermal load forecasting” instead of electrical load forecasting. Similarly, we removed those concerning renewable energy such as wind or solar energy resources, as these are not widely accessible to most individuals Tigo (2023).

Instead of relying exclusively on keyword matching at this stage - a method that often proves unreliable due to its disregard for contextual meaning - we developed a semantic abstract screening tool, which is described in detail

ISSN: 1857-7881 (Print)
e-ISSN 1857-7431 (Online)

in the subsequent subsection. Furthermore, we employed Large Language Models (LLMs), such as ChatGPT-4o and Grok 3, to interpret the content of each abstract and assess its relevance and conformity with our predefined inclusion criteria. The proposed methods are outlined in the following sub-sections.

Semantic Abstract Screening

To develop our semantic abstract screening tool, we experimented with three different NLP-based approaches, each designed to assess contextual relevance beyond keyword matching. The first approach used a sentence transformer model, where we created a descriptive reference paragraph reflecting inclusion and exclusion criteria, embedded both the reference and abstracts, and computed cosine similarity scores. However, this method produced very similar scores across most abstracts, making it ineffective for distinguishing relevant and irrelevant studies.

The second approach used a CrossEncoder fine-tuned for natural language inference (NLI), where each abstract was compared against predefined candidate labels (e.g., “residential load forecasting”, “anomaly detection”, “renewable energy forecasting”). The model generated entailment scores and assigned decisions such as “include,” “exclude,” or “maybe.” While this method captured contextual meaning better than the sentence transformer, it often struggled with abstracts that combined multiple forecasting topics, leading to inconsistent predictions.

The third approach implemented a zero-shot classification pipeline using a DistilBERT model trained on the Multi-Genre Natural Language Inference (MNLI) dataset, enabling semantic inference without task-specific training. It defines a set of domain-specific candidate labels, applying the classifier to infer the most probable label based solely on natural language understanding. For each abstract, it extracts the top-ranked label and its associated confidence score, storing these outputs along with the original metadata. This model demonstrated better contextual understanding, particularly in abstracts with overlapping terminology, and provided confidence scores that were useful for identifying borderline cases.

All three approaches were evaluated using a manually labeled subset of 35 abstracts sampled from the 193 abstracts entering the abstract screening phase. Each abstract was classified according to its primary application domain—such as residential electrical load forecasting, commercial or industrial energy use, renewable energy systems, thermal load forecasting, heating/cooling systems, or unclear/mixed focus—allowing structured assessment of contextual relevance.

Manual labeling yielded 25 exclusions, 6 inclusions, and 4 cases requiring further investigation. The predominance of exclusion categories

ISSN: 1857-7881 (Print)
e-ISSN 1857-7431 (Online)

reflects the diversity of non-target themes encountered during screening and provides a realistic, imbalanced benchmark for evaluating abstract-screening performance.

When evaluated on this labeled subset, the zero-shot DistilBERT classifier demonstrated the highest reliability in distinguishing residential electrical load forecasting studies from non-target domains, particularly in cases involving overlapping terminology.

Although the 35 abstracts were not sufficient to fine-tune a domain-specific model (due to overfitting concerns), we used the same labeled set to enhance the zero-shot approach for future abstract screening by incorporating retrieval-based semantic support examples. We developed a hybrid screening strategy that combines zero-shot entailment scores with similarity-weighted label borrowing from the manually labeled samples. In this approach, abstracts are embedded using SPECTER2, compared to labeled support samples using cosine similarity, and the resulting retrieval-based logits are blended with zero-shot logits using Equation 1. This enabled the model to leverage both contextual inference and sample-based guidance, improving decision robustness for future abstract screening.

$$\mathbf{F} = \alpha\mathbf{z} + (1 - \alpha)\mathbf{r} \tag{1}$$

where $\mathbf{z}$ = zero-shot logits vector, $\mathbf{r}$ = retrieval-based logits vector, and $\alpha \in [0,1]$ = blending weight.

Of the 193 abstracts entering the abstract screening phase, 35 were manually labeled for evaluation, leaving 158 abstracts to proceed through the automated hybrid screening. In subsequent steps, we focused on screening these 158 abstracts, temporarily setting aside the manually reviewed subset. The outcomes of the manual and automated screening streams were later consolidated prior to initiating the full-text screening phase.

LLMs for Abstract Screening

Recent research has begun to explore the application of ChatGPT in conducting literature reviews Teperikidis et al. (2024). In this study, we extend this line of inquiry by evaluating the performance of Grok alongside ChatGPT for the specific task of abstract screening. The models utilized in this work are ChatGPT-4o and Grok 3.

Given that neither LLM was capable of processing all 158 abstracts in a single prompt—frequently omitting entries beyond the first 40—we segmented the dataset into batches of 40 abstracts each. The following prompt was employed for each batch:

This file has a list of research papers, I want you to read and understand the abstract of each paper (column C) and decide if it complies with the following criteria:

ISSN: 1857-7881 (Print)
e-ISSN 1857-7431 (Online)

- *focuses on electrical load forecasting in residential areas only.*
- *doesn't include non-residential contexts in the study, such as commercial or manufacturing buildings.*
- *not related to agricultural energy systems*
- *doesn't study anomaly detection.*
- *doesn't study load monitoring as primary focus.*
- *not related to thermal load forecasting*
- *doesn't include electric vehicles.*
- *not a literature review or a survey paper*
- *renewable energy is not included in the study.*

You can write your decision in column E; whether this paper complies to ALL the previous criteria so it will be included or the paper fails to satisfy any of the criteria (please mention it) so the paper is considered excluded, or it is not clear from the abstract if all the criteria are satisfied.

Table 1: Breakdown of decisions of the three models regarding the papers under review

Included by all models	28
Excluded by all models	19
Included by GPT and Grok only	19
Excluded by GPT and Grok only	23
Included by our Semantic model and Grok only	3
Excluded by our Semantic model and Grok only	15
Included by our Semantic model and GPT only	19
Excluded by our Semantic model and GPT only	5
Total of unclear decision	27
Total	158

Fig. 1 visually summarizes the hybrid abstract screening workflow and the structured multi-model consensus and adjudication logic applied in this study. As illustrated in Fig. 1, abstracts were evaluated in parallel using the semantic hybrid model and two large language models (ChatGPT-4o and Grok 3). Decisions were compared to identify full consensus, partial disagreement, or unclear classifications. The numerical breakdown of these categories is presented in Table 1.

Decision-level consensus and rationale agreement*:* Following parallel evaluation (Fig. 1; Table 1), 28 abstracts were included through full consensus and advanced without further review. Nineteen abstracts were excluded by all three models; however, we examined whether this agreement extended to both the exclusion decision and its rationale.

Eight abstracts showed full agreement at both levels—that is, all models excluded them based on the same criterion (e.g., non-residential context, agricultural focus, or thermal load forecasting). These were removed without further review.

ISSN: 1857-7881 (Print)
e-ISSN 1857-7431 (Online)

The remaining 11 abstracts exhibited agreement in decision but divergence in stated reasons. These were manually reassessed to evaluate justification validity. In ten cases, ChatGPT and Grok provided identical and correct exclusion reasons. In the remaining case, Grok's reasoning was correct. In contrast, our model failed to make the correct decision for all 11 papers, suggesting that it requires additional fine-tuning to improve its classification accuracy.

Partial disagreement and adjudication outcomes: Cases with partial disagreement—where two models agreed and one differed—were manually adjudicated. Notably, in the group excluded by ChatGPT and Grok only (23 papers), the models agreed on exclusion reasons for 21 papers and disagreed on two; one disagreement favored Grok's reasoning, while in the other both models were incorrect and the paper was reinstated.

For papers excluded by the semantic model and Grok (15 papers), manual review showed that eight were wrongly excluded, two were unclear and deferred for further review, two were correctly excluded with consistent reasoning, and three were manually excluded due to lacking electrical load forecasting as their primary focus.

In the group excluded by the semantic model and ChatGPT (5 papers), two papers were wrongly excluded, one exclusion was correctly justified by ChatGPT, and two were flagged for further review due to abstract-level ambiguity.

At this stage, 111 papers remained from the initial 158 abstracts.

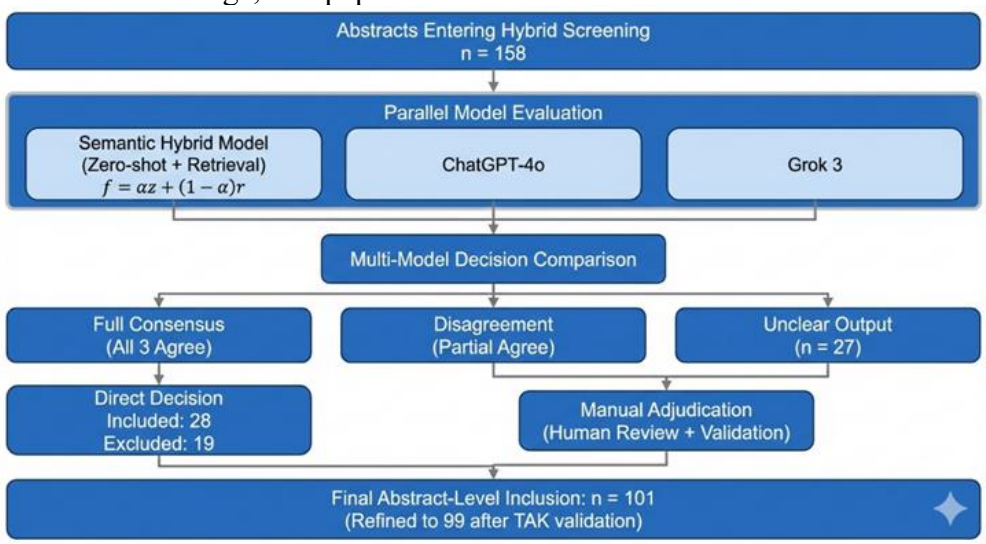

Figure 1: Hybrid Abstract Screening Workflow

ISSN: 1857-7881 (Print)
e-ISSN 1857-7431 (Online)

Unclear classifications and final resolution: The 27 abstracts classified as "unclear" by at least one model were reviewed manually, leading to three additional exclusions and reducing the count to 108 papers.

Given the strong overall performance of ChatGPT and Grok, we revisited cases where only one LLM issued an exclusion. Many of these single-model exclusions were accompanied by low-confidence language (e.g., "maybe" or "likely"), warranting further validation. Among these, 17 papers had been excluded only by Grok and 3 only by ChatGPT. Reassessment resulted in seven additional exclusions: five correctly by Grok, one excluded by Grok for an incorrect reason, and one correctly excluded by ChatGPT. This yielded a final abstract-level inclusion of 101 studies.

Interestingly, when we queried ChatGPT again about some abstracts it had previously marked for inclusion—despite being excluded by Grok—it revised its decision to exclusion. For instance, in one case, ChatGPT recognized the mention of "lodging" in the abstract (originally flagged by Grok), and identified that the dataset used was the Great Energy Predictor III, which includes various building types (e.g., educational, commercial, residential, lodging, etc.), thus not focusing exclusively on residential contexts. This process also identified a number of borderline cases where the primary focus was unclear from the abstract alone, warranting further examin

ation in the next stage. Table 2 consolidates adjudication outcomes across disagreement categories, highlighting relative model reliability and error patterns.

Table 2: Adjudication outcomes across partial-disagreement groups

Exclusion Group	Total Papers	Both Correct	One Model Correct	Both Incorrect	Unclear
ChatGPT + Grok	23	21	1 (Grok)	1	0
Semantic + Grok	15	2	0	8	2
Semantic + ChatGPT	5	0	1 (ChatGPT)	2	2

LLMs for TAK screening

TAK, an abbreviation for Title, Abstract, and Keywords, refers to the combined use of these three elements for screening purposes. In this step, instead of asking the LLMs to determine whether a paper should be included or excluded based on predefined criteria, we instructed them to summarize the scope of each paper in a single phrase using its TAK. To define the task, we provided the following prompt:

This file has the TAK (title/abstract/keywords) of some research papers. The first column is a key identifying each research paper and the second column is its TAK. I want you to process each TAK and understand it and write its scope in one phrase, neglecting the details of implementation or algorithms used. My target is to know if the paper focuses on electrical load

ISSN: 1857-7881 (Print)
e-ISSN 1857-7431 (Online)

forecasting in residential areas solely. Write the scopes on a downloadable table!

The analysis produced by Grok was notably informative, as it effectively captured the key aspects of each paper in a concise and meaningful phrase. This level of descriptive clarity enabled the identification and exclusion of two additional papers that focused on renewable energy—an aspect explicitly noted in Grok's output, such as in the following example: *"Focuses on net load forecasting for residential areas with high photovoltaic penetration."* Upon reviewing the abstracts of these two papers, we confirmed their emphasis on renewable energy, warranting their exclusion. In contrast, ChatGPT tended to generate generic summaries for nearly all entries, typically using the phrase: *"Residential electrical load forecasting"*, without providing further distinguishing details.

Of the 158 abstracts processed through hybrid screening, 99 were retained after adjudication and TAK validation. Incorporating the earlier manually screened subset of 35 abstracts (from the 193 entering abstract screening) added 6 inclusions and 4 papers flagged for further review, resulting in 109 papers advancing to full-text retrieval. Full texts were successfully obtained for 93 of these papers.

Full Paper Screening: We began the full-text screening phase by examining papers whose abstracts did not clearly indicate whether they were related to electrical load forecasting. During this stage, we made effective use of SCISPACE, a comprehensive platform designed to support the academic research process. Specifically, we utilized the "Ask the PDF" feature, an AI-powered tool that enables users to interact with research papers and other PDF documents through natural language queries.

We posed questions such as *"Is this paper concerned with electrical or thermal load forecasting?"* This tool proved especially helpful, as it not only provided answers but also highlighted the specific phrases and sections from which those answers were derived, allowing us to quickly focus on the most relevant content. Ten papers were previously identified as having abstracts with unclear focus. Upon further evaluation, four of these were excluded. In addition, we conducted full-text screening for all papers that had received an "unclear" decision from any of the models; however, no additional exclusions resulted from this group. Consequently, the final number of papers included after the full-text screening phase was 89.

The complete screening pathway and study reduction at each stage are visually summarized in Fig. 2. In total, 158 abstracts underwent hybrid screening, resulting in 101 abstract-level inclusions and 99 after TAK validation. Incorporation of the manually labeled subset added 10 abstracts (6 inclusions and 4 flagged for further review), bringing the total advancing to full-text retrieval to 109. Of these, 93 full texts were successfully obtained,

ISSN: 1857-7881 (Print)
e-ISSN 1857-7431 (Online)

leading to 86 final studies. These transitions correspond directly to the sequential screening stages described above.

Data Collection Process

Initial data extraction was semi-automated using ChatGPT (OpenAI GPT-4o) and revised by the author. Primarily, the model was prompted to extract predefined data elements from each full-text article. The extracted fields included: ***Study design, Population or setting, Intervention or primary focus, Forecasting Models Used, Outcomes measured, Time Horizon, Measured Outcomes (Evaluation Metrics), and Relevance to the review question.***

A structured prompt template was applied uniformly across all included studies to ensure consistency in the extraction process. The full-text of each article was processed by the model, focusing on the abstract, methods, and results sections.

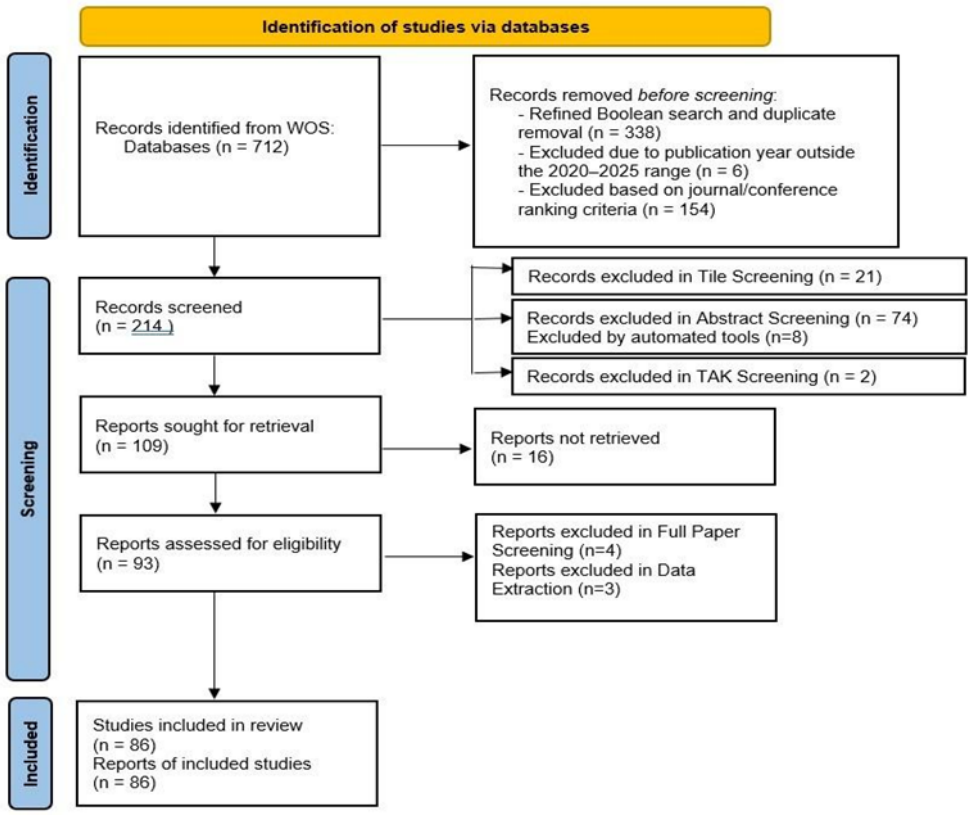

Figure 2: PRISMA 2020 flow diagram for study selection

A pilot test was conducted on a sample of five papers to assess ChatGPT's extraction accuracy and refine the prompt structure. We asked the model to act as a PRISMA reviewer and extract the required listed data. The

ISSN: 1857-7881 (Print)
e-ISSN 1857-7431 (Online)

model parsed the first research paper correctly and extracted accurate data. However, in the second paper, it parsed a wrong title and a wrong dataset, so we asked the model what is the best prompt that would minimize these types of errors, and that is what it suggested:

"Act as a systematic review assistant following PRISMA guidelines. Read the full paper carefully, and extract the following information strictly based on the actual content, not assumptions or prior knowledge:

1) *Study design (e.g., experimental, simulation, case study)*
2) *Population or setting (with precise dataset names and geographic regions)*
3) *Intervention or primary focus (e.g., forecasting, modeling, disaggregation)*
4) *Time horizon of the analysis (short-term, long-term, or annual)*
5) *Outcomes measured (specific performance metrics)*
6) *Key findings*
7) *Relevance to the review question: "What methods and models have been used for short-term and long-term electrical load forecasting in residential areas?" — clearly state if the study is directly, partially, or not relevant based on the study's forecasting goal and data granularity.*

Do not infer or fill in missing data. Be cautious with datasets and time horizons — explicitly confirm them from the text. If something is not clearly stated, write "Not specified" or "Not applicable.""

The suggested prompt improved the quality of extracted data remarkably. We added the Forecasting Models Used as a separate point to put more focus on them. Following each automated extraction, the author reviewed and verified all extracted data for accuracy and completeness. Discrepancies or ambiguities were resolved through consensus discussion. In cases of uncertainty, the original full-text was re-reviewed manually. This approach allowed for a significant reduction in manual workload while maintaining rigorous data validation, consistent with PRISMA guidelines.

During the data extraction phase, three additional studies were excluded after full-text review showed they did not meet the inclusion criteria—due to using the wrong population, having an unrelated focus, and including renewable energy, respectively. As a result, 86 studies remained for analysis.

Synthesis Methods

We conducted a narrative synthesis of the included studies, structured around key characteristics such as study design, forecasting models used, time horizon (short-term, long-term, annual), data sources, and performance

ISSN: 1857-7881 (Print)
e-ISSN 1857-7431 (Online)

metrics. Summary tables were used to organize and compare models, datasets, and outcomes across studies.

We grouped the included studies based on key characteristics to facilitate thematic and comparative analysis. These characteristics included the publication year, geographical location of the study population (countries or regions), study design (e.g., experimental, simulation-based), types of machine learning models employed, and the evaluation metrics reported. This categorization enabled us to identify trends over time, regional focus areas, methodological patterns, and variations in model performance assessment. This review adheres to the PRISMA 2020 guidelines for systematic reviews Page et al. (2021).

Results

The Results section progresses from screening outcomes (Fig. 2; Table 1) to study characteristics (Fig. 3; Table 3) and finally to methodological and evaluative trends (Figs. 4–7).

Study Selection

A total of 712 records were identified through WOS database searching. After Boolean search refinement and removing duplicates, 388 records were removed. An additional 6 records were removed due to being outside the publication range [2020-2025]. Records excluded based on Journal/Conference ranking criteria were 154. As a result, 214 records were screened by title and abstract. Of these, 105 were excluded based on eligibility criteria.

Ninety-three full-text articles were assessed for eligibility. Four were excluded for reasons such as non-residential setting, absence of forecasting models, or methodological irrelevance. Additionally, three studies were excluded during the data extraction phase after full-text re-evaluation revealed previously unrecognized ineligibility. In total, 86 studies were included in the final qualitative synthesis.

Study Characteristics

A total of 86 studies were included in qualitative synthesis. Forecasting horizons varied from short-term to long-term/annual projections. Short-term forecasting dominates the literature (85 studies), while medium-term (4), long-term (2), and annual (1) horizons appear only marginally and exclusively in combination with short-term analyses.

The included papers fall into two study design categories: Experimental and Simulation-based. Experimental studies constitute the majority, making up 74.4% of the total. The Simulation-based studies account for the remaining 25.6%, as shown in Fig. 3(a).

ISSN: 1857-7881 (Print)
e-ISSN 1857-7431 (Online)

Fig. 3(b) presents the distribution of studies by publication year. It is shown that the majority of studies were published in 2025, accounting for 20.9% of the total, followed closely by 2022 with 19.8% and 2024 with 18.6%. The years 2023, 2021, and 2020 each contributed 10.5% of the studies. Earlier years saw considerably fewer publications, with 2018 representing 5.8%, 2019 contributing 2.3%, and 2016 the least at 1.2%.

Detailed study-level mappings are provided in the following link: https://github.com/nermin-siphocly/ml-residential-load-forecasting-prisma, in a file named: "Included Studies – Tables.pdf".

RQ1: What methods and models have been used for short-term and long-term electrical load forecasting in residential areas?

A comprehensive grouping of models by category is presented in Table 3, allowing readers to quickly identify methodological patterns across studies. The studies present a vast and diverse range of machine learning and deep learning models applied to time-series forecasting and load prediction, with Long Short-Term Memory (LSTM) and its variants (BiLSTM, Seq2Seq, LSTM-AE, Co-LSTM, etc.) being the most frequently employed. Numerous hybrid architectures are introduced, such as CNN-LSTM, CNN-GRU, CNN-BiGRU, and CNN-SE, often enhanced with attention mechanisms, skip connections, or domain adaptation techniques like transfer learning, DATN, and MK-MMD. Other recurrent models include GRU, BiGRU, RNN, and DRNN, while federated learning frameworks (FedAvg, FedSGD, Ditto, FedAAVG) integrate privacy-preserving collaborative training across LSTM-based models. Traditional machine learning regressors (Random Forest, XGBoost, LightGBM, CatBoost, SVR, KNN, Decision Trees) are widely used individually or in ensemble strategies (e.g., weighted, stacked, or convex combinations). Additional techniques include autoencoders (standard, sparse, denoising, pre-trained), graph-based models (STFAG-GCN, Graph WaveNet), transformers (JITtrans, Deep-Autoformer), and statistical baselines (ARIMA, Exponential Smoothing, Prophet). Optimization and preprocessing methods such as GA, BGA-PCA, mutual information, VMD, wavelets, and k-means clustering are often integrated for feature selection or input segmentation, resulting in highly customized, task-specific predictive architectures.

RQ2: What performance metrics are commonly used in the literature for evaluating the prediction of household electrical load?

Figs. 4–6 collectively visualize the distribution of evaluation metrics across the included studies, categorized into error-based, peak-specific, probabilistic, computational, statistical, and privacy-related measures. The studies employed a wide range of evaluation metrics to assess forecasting

ISSN: 1857-7881 (Print)
e-ISSN 1857-7431 (Online)

performance, with the most frequently used being Root Mean Squared Error (RMSE), Mean Absolute Error (MAE), and Mean Absolute Percentage Error (MAPE). Additional commonly reported measures included Mean Squared Error (MSE), R-squared (R2), Normalized RMSE (NRMSE), and Coefficient of Variation (CV).

Several studies also incorporated advanced or task-specific metrics such as Dynamic Time Warping (DTW) error, Peak Timing Error (PTE), Spectrum Similarity (SS), Continuous Ranked Probability Score (CRPS), Quantile Score (QS), and probabilistic accuracy indicators like Pinball Loss, Interval Score (IS), and Average Coverage Error (ACE). Other considerations included computational efficiency (e.g., training time, runtime), model complexity (e.g., communication cost, model size), and statistical significance tests (e.g., Diebold-Mariano, Wilcoxon). This diversity reflects a comprehensive effort to evaluate both point and probabilistic forecast accuracy, robustness, and efficiency.

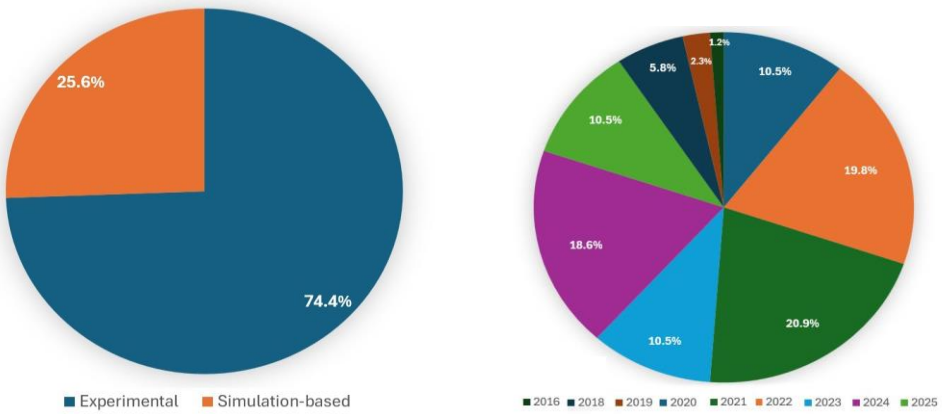

(a) Study Design Distribution. (b) Publication Years Distribution.

Figure 3: Study Design and Publication Year Distributions Among Studies

Table 3: Studies grouped by machine learning models used

Model	**Papers**
ADMIF	Fang and He (2023)
ANN	Fayaz and Kim (2018), Sulaiman et al. (2022), Truong et al. (2021), Harikrishnan et al. (2025), Dong et al. (2016)
ANFIS	Fayaz and Kim (2018)
Affinity Propagation	Dogra et al. (2023)
ATT-LSTM	Ozcan et al. (2021), Nguyen et al. (2020)
BiGRU	Aurangzeb et al. (2024), Irankhah et al. (2024)
BiLSTM	Aurangzeb et al. (2024), Kaur et al. (2024), Aurangzeb et al. (2024), Zhang et al. (2024)
CNN	Alhussein et al. (2020), Aurangzeb et al. (2024), Sakuma and Nishi (2022), Aouad et al. (2022), Jiang et al. (2021), Sajjad et al. (2020), Lotfipoor et al. (2024), Sinha et al. (2021), Shi and Wang

ISSN: 1857-7881 (Print)
e-ISSN 1857-7431 (Online)

	(2022), Cheng et al. (2021), Acharya et al. (2024), Shi and Xu (2022), Ozdemir et al. (2025), Irankhah et al. (2024), Cao et al. (2025)
CatBoost	Muqtadir et al. (2025)
DA-LSTM	Ozcan et al. (2021)
DANN	Truong et al. (2021), Truong et al. (2021)
DATN	Zhu et al. (2024)
DBN	Fan et al. (2022), Fan et al. (2022)
Deep-Autoformer	Jiang et al. (2022)
DELM	Fayaz and Kim (2018)
DFNN	Al-Jamimi et al. (2023)
DI-RNN	Yuan et al. (2020), Kiprijanovska et al. (2020)
DMLP	Nguyen et al. (2020)
DRNN	Kiprijanovska et al. (2020), Shi et al. (2018)
DT	Moldovan and Slowik (2021), Ullah et al. (2021)
ELM	Sulaiman et al. (2022), Fayaz and Kim (2018)
Exponential Smoothing	Hribar et al. (2025), Yousaf et al. (2021)
FFNN	Kong et al. (2018), Kumaraswamy et al. (2024), Imani and Ghassemian (2019)
FedAvg	Park and Son (2023), Fekri et al. (2022), Dogra et al. (2023), Widmer et al. (2023), Qu et al. (2023)
FedSGD	Fekri et al. (2022)
GAN	Qu et al. (2023)
GBR	Ullah et al. (2021), Xia et al. (2024)
GMM	Dong et al. (2016)
GPR	Dong et al. (2016), Xia et al. (2024), Dab et al. (2023)
GRU	Aurangzeb et al. (2024), Sakuma and Nishi (2022), Sajjad et al. (2020), Khan et al. (2021)
Graph WaveNet	Lin et al. (2025)
JITtrans	Benali et al. (2024)
K-means	Han et al. (2021), Dogra et al. (2023), Kell et al. (2018), Khan et al. (2021), Acharya et al. (2024)
k-medoids	Dab et al. (2023)
KNN	Ullah et al. (2021), Moldovan and Slowik (2021), Forootani et al. (2022)
LS-SVM	Dong et al. (2016)
LSTM	Han et al. (2021), Alhussein et al. (2020), Lu et al. (2022), Fekri et al. (2022), Masood et al. (2022), Dogra et al. (2023), Hou et al. (2021), Yang et al. (2022), Ji et al. (2023), Aurangzeb et al. (2024), Xu et al. (2022), Nguyen et al. (2020), Li et al. (2025), Razghandi et al. (2021), Sakuma and Nishi (2022), Kong et al. (2018), Kumaraswamy et al. (2024), Fan et al. (2020), Kim and Cho (2019), Chen et al. (2024), Flor et al. (2021), Ullah et al. (2021), Park and Son (2023), Zhao et al. (2024), Jiang et al. (2021), Taik and Cherkaoui (2020), Imani and Ghassemian (2019), Ozcan et al. (2021), Sinha et al. (2021), Manandhar et al. (2024), Kell et al. (2018), Zhu et al. (2024), Dong et al. (2024), Shi and Wang (2022), Ismail et al. (2024), Shi and Xu (2022), Zang et al. (2021), Shahsavari-Pour et al. (2025), Gong et al.

ISSN: 1857-7881 (Print)
e-ISSN 1857-7431 (Online)

	(2022), Ozdemir et al. (2025), Bai (2024), Khan et al. (2021), Qu et al. (2023), Cao et al. (2025), Fan et al. (2022)
LightGBM	Muqtadir et al. (2025), Hribar et al. (2025)
LR	Li et al. (2025), Massidda and Marrocu (2018)
MLP	Nguyen et al. (2020), Sakuma and Nishi (2022), Kell et al. (2018), Jiang et al. (2022), Lin et al. (2025)
NBEATS	Li et al. (2025)
NHiTS	Li et al. (2025)
PDNN	Jeyaraj and Nadar (2021)
PDRNN	Shi et al. (2018)
PVS	Mansoor et al. (2021)
RNN	Fekri et al. (2021), Jagait et al. (2021), Flor et al. (2021), Yuan et al. (2020), Ozcan et al. (2021), Shi et al. (2018)
Random Forest	Chaianong et al. (2022), Moldovan and Slowik (2021), Nguyen et al. (2020), Li et al. (2025), Ullah et al. (2021), Xia et al. (2024), Lotfipoor et al. (2024), Manandhar et al. (2024), Kell et al. (2018), Massidda and Marrocu (2018)
Residual LSTM	Chen et al. (2024)
SVM	Pla and Jimenez Martinez (2023)
SVR	Nguyen et al. (2020), Sulaiman et al. (2022), Ullah et al. (2021), Kell et al. (2018), Ismail et al. (2024), Dong et al. (2016)
Seq2Seq	Masood et al. (2022), Razghandi et al. (2021), Sakuma and Nishi (2022), Aouad et al. (2022), Zhu et al. (2024), Dong et al. (2024)
Sparse Autoencoder	Cheng et al. (2021)
TCN	Li et al. (2025), Widmer et al. (2023)
TFT	Li et al. (2025)
TSMixer	Li et al. (2025)
TiDE	Li et al. (2025)
XGBoost	Yang et al. (2022), Li et al. (2025), Muqtadir et al. (2025), Hribar et al. (2025), Harikrishnan et al. (2025)

RQ3: What are the geographical and demographic regions most represented in residential electrical load forecasting research, and what gaps exist in terms of regional and population-based coverage?

Fig. 7 demonstrates the geographical distribution of studies based on the country or region of the dataset (population). The USA dominates the chart, contributing the largest share at 22.1% of the studies. This is followed by Canada at 11.6%, with Australia, China, and another unidentified region each contributing 10.5%. Several countries, including South Korea, Spain, and one other, each represent 5.8% of the total. Smaller contributions (ranging from 1.2% to 4.7%) come from a wide range of countries and regions, including the UK, Belgium, Switzerland, Morocco, UAE, Pakistan, Ecuador, Ireland, India, and others.

ISSN: 1857-7881 (Print)
e-ISSN 1857-7431 (Online)

RQ4: How effective are semantic models and Large Language Models (LLMs) in supporting automated or semi-automated screening and classification in PRISMA-based systematic reviews?

This research question is answered within Section 2.3.2, where we compare the decisions of our semantic screening tool and the two LLMs (ChatGPT-4o and Grok 3). In the following section, RQ5 will be addressed.

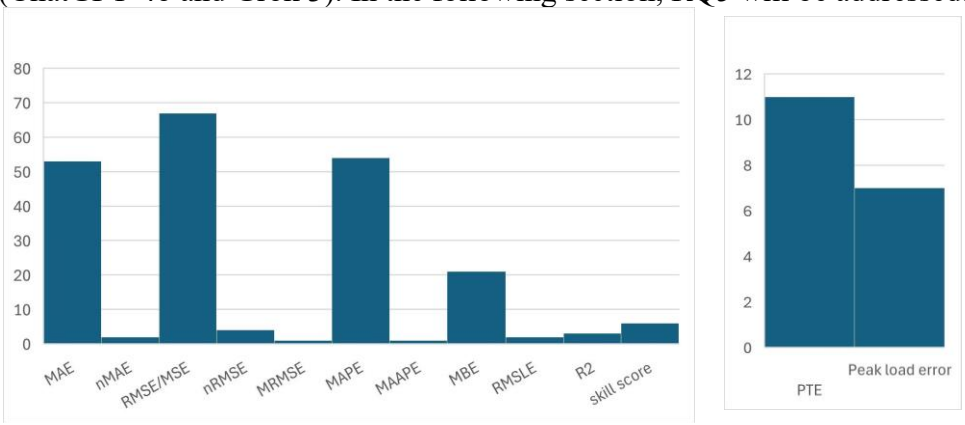

(a) Error-Based Accuracy Metrics (b)Peak and Load-Specific Error Metrics

Figure 4: Distribution of Error-Based and Peak Metrics Among Studies

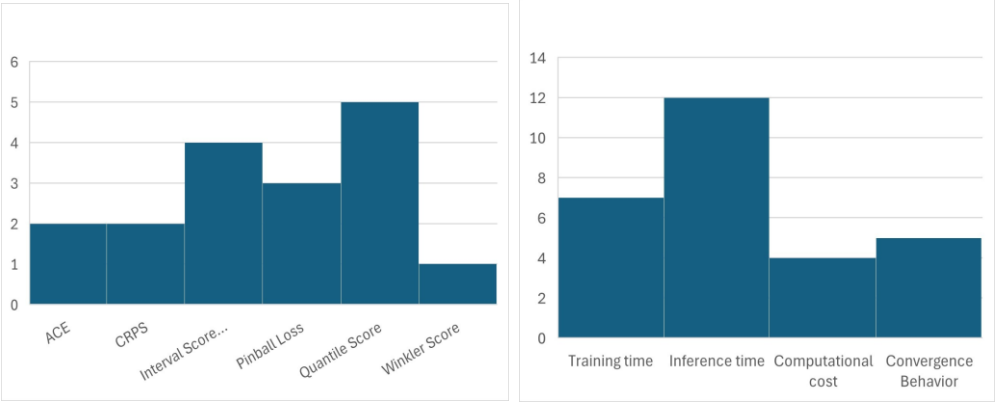

(a)Uncertainty & Probabilistic Forecasting (b)Computational Performance

Figure 5: Distribution of Probabilistic and Computation Metrics Among Studies

Discussion

Interpretation of Key Findings

The distribution of studies by publication year highlights a growing research interest in the field, with over 70% of the studies emerging between 2022 and 2025.

The geographical distribution of studies indicates a global interest in the topic of residential electrical load forecasting, with a notable

ISSN: 1857-7881 (Print)
e-ISSN 1857-7431 (Online)

concentration of research in North America and a diverse representation from Europe, Asia, and Oceania.

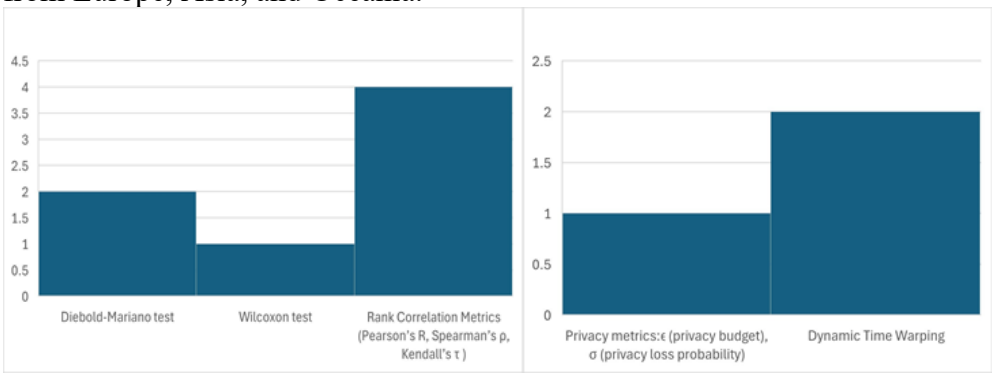

(a) Statistical Comparison Metrics (b)Privacy-Specific Metrics (for Federated /DP Models)

Figure 6: Distribution of Statistical and Privacy Metrics Among Studies

The current landscape of residential electrical load forecasting reveals a strong emphasis on deep learning models, particularly Long Short-Term Memory (LSTM) networks and their variants (e.g., CNN-LSTM, Seq2Seq, BiLSTM), reflecting the importance of modeling temporal dependencies in household energy consumption. The increasing use of hybrid and ensemble models—combining LSTM with attention mechanisms, convolutional layers, or traditional machine learning methods like Random Forest and XGBoost—suggests that no single model can capture the full complexity of load patterns. Additionally, clustering techniques and feature selection methods are often used as preprocessing steps to tailor models to specific household behaviors.

Challenges, Limitations, and Future Directions of Existing Literature

RQ5: What emerging trends, research gaps, and future directions can be identified in residential electrical load forecasting using machine learning?

Despite the breadth of existing research, several methodological weaknesses limit the maturity of residential load forecasting as a field. While the majority of studies are concentrated in countries like the USA, Canada, and Australia, regions such as Africa, South America, and parts of Asia remain significantly underrepresented, each contributing less than 2.5% of the total. This imbalance highlights a critical limitation in the global applicability of findings and underscores the need to expand research efforts in these underrepresented regions to ensure more inclusive and context-specific insights.

Emerging trends point to a growing interest in privacy-preserving approaches like federated learning, interpretable architectures using attention mechanisms, and early exploration of spatio-temporal and graph-based

ISSN: 1857-7881 (Print)
e-ISSN 1857-7431 (Online)

models. However, gaps remain in standardization, benchmarking, and reproducibility. Future research should focus on developing explainable, modular, and geographically-aware forecasting systems, while also promoting transparency through open datasets and shared evaluation frameworks. These directions will support more robust, scalable, and trustworthy forecasting solutions for smart residential energy systems.

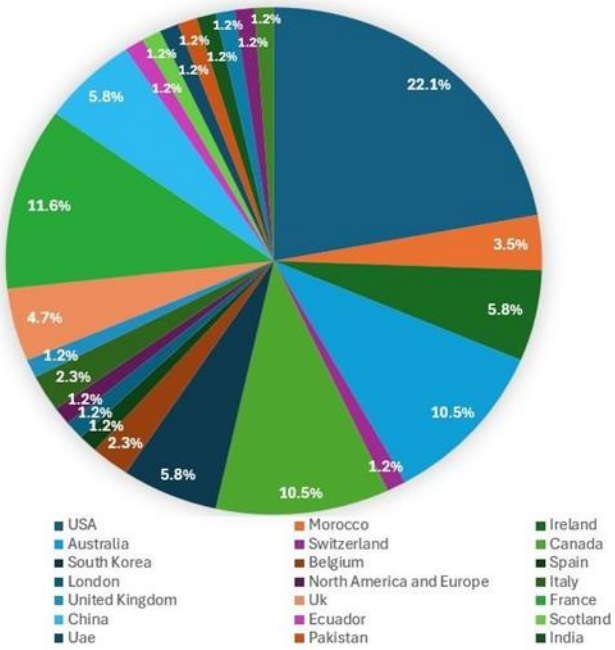

Figure 7: Studies distribution among countries

Although metrics provide a baseline understanding of model performance, they often fail to capture critical aspects like peak timing errors, uncertainty, and computational efficiency. A gradual shift is evident, however, with the emergence of specialized metrics—such as Peak Timing Error, Dynamic Time Warping (DTW), and probabilistic measures like Pinball Loss and Continuous Ranked Probability Score (CRPS)—reflecting growing interest in robustness, interpretability, and application-driven evaluation.

This trend indicates a field in transition, where future research would benefit from broader adoption of uncertainty-aware and efficiency-focused metrics, especially in real-time and resource-constrained settings. To enable meaningful model comparisons and support practical deployment, researchers are encouraged to standardize reporting practices, include peak and time-sensitive metrics, and account for computational cost and environmental impact. Ultimately, a multidimensional evaluation framework that integrates accuracy, robustness, uncertainty, and deployability is essential for advancing residential load forecasting research.

ISSN: 1857-7881 (Print)
e-ISSN 1857-7431 (Online)

The scarcity of long-term, high-resolution, and publicly accessible residential datasets makes it difficult to evaluate forecasting models in a consistent and scalable manner, especially across diverse climatic or socio-economic contexts. A large proportion of studies rely on small or short-duration datasets, often drawn from a single household or region, which increases the risk of overfitting and restricts the external validity of model performance claims. Another persistent challenge is the limited emphasis on robustness: most studies evaluate models under idealized conditions and few examine performance degradation under noise, sensor faults, data drift, or household behavioral variability. Cross-household generalization also remains problematic—models tailored to a specific home or region frequently fail to transfer to new settings without retraining. Finally, the computational complexity of many proposed architectures poses deployment challenges for real-time or edge-based environments, where limited processing power, memory constraints, and energy consumption often restrict the use of large deep learning models. These unresolved challenges highlight the need for more rigorous, standardized, and deployment-aware research practices moving forward.

Study Limitations

This review relied on a hybrid screening approach that combined semantic models, large language models (ChatGPT-4o and Grok 3), and manual adjudication. While this method improved efficiency and reduced initial screening effort, it introduced potential sources of inconsistency, particularly due to model stochasticity, potential hallucination, and prompt sensitivity. Although disagreement cases were manually reviewed, LLM-driven decisions may reflect context-driven bias.

Future research should adopt standardized benchmarks, domain-specific LLM fine-tuning, and explainable AI-based screening methods to enhance reproducibility, transparency, and comparability.

Data Availability

In Section 2.3, the search strategy, databases, keywords, and all inclusion and exclusion criteria are explicitly reported, and the PRISMA flow diagram documents each selection stage. The manually labeled set of 35 abstracts, used both for testing the semantic approaches and supporting the hybrid classifier, provides a transparent reference for screening decisions.

In the given link: https://github .com/nermin-siphocly/ml-residential-load-forecasting-prisma we provide the dataset of WOS research papers that we worked on in our systematic review, along with the codes for the Semantic Scores, Cross-Encoder, and DistilBERT Screening tools. We also provide the

ISSN: 1857-7881 (Print)
e-ISSN 1857-7431 (Online)

manually labeled support list of abstracts in addition to the Zero-Shot Hybrid screening tool code.

Reproducibility is a key concern in systematic reviews, and it becomes more complex when using LLMs and semantic models for screening. While these tools improve efficiency and recall, their decision-making is not fully deterministic. Screening outcomes can vary due to prompt sensitivity, model updates, and stochastic behavior in LLM-generated outputs. Even when using identical abstracts and prompts, we observed small inconsistencies in decisions—particularly in borderline cases.

However, to enhance reproducibility, all screening steps were conducted using fixed model versions, documented all the prompts used, and clearly defined decision rules. The semantic screening tool and LLM classifiers (ChatGPT-4o and Grok 3) were applied using identical instructions to minimize variance.

Despite the stochastic nature of LLM outputs, maintaining a consistent prompting framework and recording all screening outcomes ensures methodological transparency and facilitates reproducibility. Therefore, reproducibility in LLM-assisted screening should be interpreted as process reproducibility (i.e., using the same workflow, prompts, and reasoning framework) rather than strict duplication of classification outputs. Future reviews can improve systematic review automation through logging rationales, and treating LLMs as decision-support tools rather than fully automated classifiers.

Threats to Validity

The use of LLMs in the screening process introduces potential threats to validity, particularly related to bias and potential hallucination. LLMs may incorrectly infer eligibility based on implicit assumptions rather than explicit content, leading to overinclusion of papers with loosely related terms (semantic bias) or unjustified exclusion due to misinterpreting domain-specific contexts. Additionally, hallucinations—where the model generates false or unsupported reasoning—can distort screening decisions, especially in abstracts with ambiguous or mixed-context content. To mitigate these risks, all the conflicting LLM-based decisions were cross-checked with human validation, and disagreement cases were resolved manually. However, the lack of fully transparent decision logic and potential for model drift remain inherent limitations.

Conclusions

Global electricity demand is increasing, underscoring the importance of accurate residential forecasting in enhancing energy efficiency and sustainability. This systematic review comprehensively examined 86 studies

ISSN: 1857-7881 (Print)
e-ISSN 1857-7431 (Online)

on machine learning (ML) techniques for residential electrical load forecasting, adhering to the PRISMA 2020 framework. The review addressed two primary questions: the models and methods used in forecasting, and the evaluation metrics employed to assess their performance.

In the methodology section, a rigorous multi-stage screening process was outlined, beginning with Boolean search refinement, title and keyword filtering, and advanced abstract screening using semantic models and Large Language Models (LLMs) such as ChatGPT and Grok. A hybrid classification model combining zero-shot learning with retrieval-based similarity was developed and employed. Full-text screening and structured data extraction followed, guided by PRISMA-aligned prompts and validation from the author.

The results section detailed the final inclusion of 86 studies, most of which were experimental in design and focused on short-term forecasting. These studies spanned a diverse set of countries, though research was heavily concentrated in North America, with minimal representation from Africa and South America. A wide variety of ML models were applied, notably LSTM variants, hybrid CNN-based architectures, and ensemble methods. A diverse array of evaluation metrics was employed, including RMSE, MAE, MAPE, and more specialized metrics like PTE and CRPS, reflecting a growing attention to both accuracy and practical considerations such as efficiency and uncertainty.

The discussion emphasized the growing interest in deep learning and hybrid models, with increasing exploration into privacy-preserving, interpretable, and graph-based methods. However, it also underscored regional research gaps, limited reproducibility, and the need for broader adoption of uncertainty-aware and application-driven metrics. The field appears to be shifting toward more comprehensive, transparent, and context-sensitive forecasting frameworks.

Overall, this review consolidates current knowledge on ML-based residential load forecasting, identifies key methodological and geographical gaps, and highlights the need for standardized evaluation frameworks and more inclusive research efforts. These insights provide a foundation for advancing robust, scalable, and equitable forecasting solutions in the context of smart residential energy systems.

Conflict of Interest: The author reported no conflict of interest.

Data Availability: All data are included in the content of the paper.

Funding Statement: The author did not obtain any funding for this research.

ISSN: 1857-7881 (Print)
e-ISSN 1857-7431 (Online)

References:

1. Acharya, S. K., Yu, H., Wi, Y.-M., and Lee, J. (2024). Multihousehold load forecasting based on a convolutional neural network using moment information and data augmentation. ENERGIES, 17.0(4). Publisher: MDPI.
2. Al-Jamimi, H. A., Binmakhashen, G. M., Worku, M. Y., and Hassan, M. A. (2023). Advancements in household load forecasting: Deep learning model with hyperparameter optimization. ELECTRONICS, 12.0(24). Publisher: MDPI.
3. Alhussein, M., Aurangzeb, K., and Haider, S. I. (2020). Hybrid cnn-lstm model for short-term individual household load forecasting. IEEE ACCESS, 8.0:180544– 180557 Publisher: IEEE-INST ELECTRICAL ELECTRONICS ENGINEERS INC
4. Aouad, M., Hajj, H., Shaban, K., Jabr, R. A., and El-Hajj, W. (2022). A cnn-sequence-to-sequence network with attention for residential short-term load forecasting. ELECTRIC POWER SYSTEMS RESEARCH, 211.0. Publisher: ELSEVIER SCIENCE AS.
5. Aurangzeb, K., Haider, S. I., and Alhussein, M. (2024). Individual household load forecasting using bi-directional lstm network with time-based embedding. ENERGY REPORTS, 11.0:3963–3975. Publisher: ELSEVIER.
6. Bai, Z. (2024). Residential electricity prediction based on ga-lstm modeling. ENERGY REPORTS, 11.0:6223–6232. Publisher: ELSEVIER.
7. Benali, A. A. E., Cafaro, M., Epicoco, I., Pulimeno, M., and Schioppa, E. J. (2024). Just in time transformers. IEEE ACCESS, 12.0:178751–178767. Publisher: IEEE-INST ELECTRICAL ELECTRONICS ENGINEERS INC .
8. Cao, W., Liu, H., Zhang, X., Zeng, Y., and Ling, X. (2025). Short-term residential load forecasting based on the fusion of customer load uncertainty feature extraction and meteorological factors. SUSTAINABILITY, 17.0(3). Publisher: MDPI.
9. Chaianong, A., Winzer, C., and Gellrich, M. (2022). Impacts of traffic data on short-term residential load forecasting before and during the covid-19 pandemic. ENERGY STRATEGY REVIEWS, 43.0. Publisher: ELSEVIER.
10. Chen, Y., Obrecht, C., and Kuznik, F. (2024). Enhancing peak prediction in residential load forecasting with soft dynamic time wrapping loss functions. INTEGRATED COMPUTER-AIDED ENGINEERING, 31.0(3):327–340. USA Publisher: SAGE PUBLICATIONS INC.

ISSN: 1857-7881 (Print)
e-ISSN 1857-7431 (Online)

11. Cheng, L., Zang, H., Xu, Y., Wei, Z., and Sun, G. (2021). Probabilistic residential load forecasting based on micrometeorological data and customer consumption pattern. IEEE TRANSACTIONS ON POWER SYSTEMS, 36.0(4):3762–3775. Publisher: IEEEINST ELECTRICAL ELECTRONICS ENGINEERS INC.
12. Clarivate (2025). Web of science core collection. Accessed: 2025-06-28.
13. Dab, K., Henao, N., Nagarsheth, S., Dube, Y., Sansregret, S., and Agbossou, K. (2023). Consensus-based time-series clustering approach to short-term load forecasting for residential electricity demand. ENERGY AND BUILDINGS, 299.0. Publisher: ELSEVIER SCIENCE SA.
14. Dogra, A., Anand, A., and Bedi, J. (2023). Consumers profiling based federated learning approach for energy load forecasting. SUSTAINABLE CITIES AND SOCIETY, 98.0. Publisher: ELSEVIER.
15. Dong, B., Li, Z., Rahman, S. M. M., and Vega, R. (2016). A hybrid model approach for forecasting future residential electricity consumption. ENERGY AND BUILDINGS, 117.0:341–351. Publisher: ELSEVIER SCIENCE SA.
16. Dong, H., Zhu, J., Li, S., Miao, Y., Chung, C. Y., and Chen, Z. (2024). Probabilistic residential load forecasting with sequence-to-sequence adversarial domain adaptation networks. JOURNAL OF MODERN POWER SYSTEMS AND CLEAN ENERGY, 12.0(5):1559–1571. Publisher: STATE GRID ELECTRIC POWER RESEARCH INST.
17. Fan, C., Li, Y., Yi, L., Xiao, L., Qu, X., and Ai, Z. (2022). Multi-objective lstm ensemble model for household short-term load forecasting. MEMETIC COMPUTING, 14.0(1):115–132. Publisher: SPRINGER HEIDELBERG.
18. Fan, L., Li, H., and Zhang, X.-P. (2020). Load prediction methods using machine learning for home energy management systems based on human behavior patterns recognition. CSEE JOURNAL OF POWER AND ENERGY SYSTEMS, 6.0(3):563–571. Publisher: CHINA ELECTRIC POWER RESEARCH INST.
19. Fang, L. and He, B. (2023). A deep learning framework using multi-feature fusion recurrent neural networks for energy consumption forecasting. APPLIED ENERGY, 348.0. Publisher: ELSEVIER SCI LTD.
20. Fayaz, M. and Kim, D. (2018). A prediction methodology of energy consumption based on deep extreme learning machine and comparative analysis in residential buildings. ELECTRONICS, 7.0(10). Publisher: MDPI.

ISSN: 1857-7881 (Print)
e-ISSN 1857-7431 (Online)

21. Fekri, M. N., Grolinger, K., and Mir, S. (2022). Distributed load forecasting using smart meter data: Federated learning with recurrent neural networks. INTERNATIONAL JOURNAL OF ELECTRICAL POWER & ENERGY SYSTEMS, 137.0. Publisher: ELSEVIER SCI LTD.
22. Fekri, M. N., Patel, H., Grolinger, K., and Sharma, V. (2021). Deep learning for load forecasting with smart meter data: Online adaptive recurrent neural network. APPLIED ENERGY, 282.0(A). Publisher: ELSEVIER SCI LTD.
23. Flor, M., Herraiz, S., and Contreras, I. (2021). Definition of residential power load profiles clusters using machine learning and spatial analysis. ENERGIES, 14.0(20). Publisher: MDPI.
24. Forootani, A., Rastegar, M., and Sami, A. (2022). Short-term individual residential load forecasting using an enhanced machine learning-based approach based on a feature engineering framework: A comparative study with deep learning methods. ELECTRIC POWER SYSTEMS RESEARCH, 210.0. Publisher: ELSEVIER SCIENCE SA.
25. Gong, H., Alden, R. E., Patrick, A., and Ionel, D. M. (2022). Forecast of community total electric load and hvac component disaggregation through a new lstm-based method. ENERGIES, 15.0(9). Publisher: MDPI.
26. Han, F., Pu, T., Li, M., and Taylor, G. (2021). Short-term forecasting of individual residential load based on deep learning and k-means clustering. CSEE JOURNAL OF POWER AND ENERGY SYSTEMS, 7.0(2):261–269. Publisher: CHINA ELECTRIC POWER RESEARCH INST.
27. Harikrishnan, G. R., Sreedharan, S., and Binoy, C. N. (2025). Advanced short-term load forecasting for residential demand response: An xgboost-ann ensemble approach. ELECTRIC POWER SYSTEMS RESEARCH, 242.0. Publisher: ELSEVIER SCIENCE SA
28. Hou, T., Fang, R., Tang, J., Ge, G., Yang, D., Liu, J., and Zhang, W. (2021). A novel short-term residential electric load forecasting method based on adaptive load aggregation and deep learning algorithms. ENERGIES, 14.0(22). Publisher: MDPI.
29. Hribar, J., Fortuna, C., and Mohorcic, M. (2025). The role of age of information in enhancing short-term energy forecasting. ENERGY, 318.0. Publisher: PERGAMON-ELSEVIER SCIENCE LTD.
30. Imani, M. and Ghassemian, H. (2019). Residential load forecasting using wavelet and collaborative representation transforms. APPLIED ENERGY, 253.0. Publisher: ELSEVIER SCI LTD

ISSN: 1857-7881 (Print)
e-ISSN 1857-7431 (Online)

31. International Energy Agency (IEA) (2022). Egypt - countries & regions. https:// www.iea.org. Accessed: January 9, 2025.
32. Irankhah, A., Yaghmaee, M. H., and Ershadi-Nasab, S. (2024). Optimized short-term load forecasting in residential buildings based on deep learning methods for different time horizons. JOURNAL OF BUILDING ENGINEERING, 84.0. Publisher: ELSEVIER.
33. Ismail, L., Materwala, H., and Dankar, F. K. (2024). Machine learning data-driven residential load multi-level forecasting with univariate and multivariate time series models toward sustainable smart homes. IEEE ACCESS, 12.0:55632– 55668. Publisher: IEEE-INST ELECTRICAL ELECTRONICS ENGINEERS INC.
34. Jagait, R. K., Fekri, M. N., Grolinger, K., and Mir, S. (2021). Load forecasting under concept drift: Online ensemble learning with recurrent neural network and arima. IEEE ACCESS, 9.0:98992–99008. Publisher: IEEE-INST ELECTRICAL ELECTRONICS ENGINEERS INC.
35. Jeyaraj, P. R. and Nadar, E. R. S. (2021). Computer-assisted demand-side energy management in residential smart grid employing novel pooling deep learning algorithm. INTERNATIONAL JOURNAL OF ENERGY RESEARCH, 45.0(5):7961–7973. Publisher: WILEY.
36. Ji, X., Huang, H., Chen, D., Yin, K., Zuo, Y., Chen, Z., and Bai, R. (2023). A hybrid residential short-term load forecasting method using attention mechanism and deep learning. BUILDINGS, 13.0(1). Publisher: MDPI.
37. Jiang, L., Wang, X., Li, W., Wang, L., Yin, X., and Jia, L. (2021). Hybrid multitask multi-information fusion deep learning for household short-term load forecasting. IEEE TRANSACTIONS ON SMART GRID, 12.0(6):5362–5372. Publisher: IEEE-INST ELECTRICAL ELECTRONICS ENGINEERS INC.
38. Jiang, Y., Gao, T., Dai, Y., Si, R., Hao, J., Zhang, J., and Gao, D. W. (2022). Very short-term residential load forecasting based on deep-autoformer. APPLIED ENERGY, 328.0. Publisher: ELSEVIER SCI LTD.
39. Kaur, S., Bala, A., and Parashar, A. (2024). Ga-bilstm: an intelligent energy prediction and optimization approach for individual home appliances. EVOLVING SYSTEMS, 15.0(2):413–427. Publisher: SPRINGER HEIDELBERG
40. Kell, A., McGough, A. S., and Forshaw, M. (2018). Segmenting residential smart meter data for short-term load forecasting. E-ENERGY'18: PROCEEDINGS OF THE 9TH ACM INTERNATIONAL CONFERENCE ON FUTURE ENERGY SYSTEMS, pages 91–96. Backup Publisher: Assoc Comp Machinery;

ISSN: 1857-7881 (Print)
e-ISSN 1857-7431 (Online)

ACM SIGCOMM; Deutsche Forschungsgemeinschaft; ProCom; EnBW; TransnetBW.

41. Khan, A.-N., Iqbal, N., Rizwan, A., Ahmad, R., and Kim, D.-H. (2021). An ensemble energy consumption forecasting model based on spatial-temporal clustering analysis in residential buildings. ENERGIES, 14.0(11). Publisher: MDPI
42. Kim, J.-Y. and Cho, S.-B. (2019). Electric energy consumption prediction by deep learning with state explainable autoencoder. ENERGIES, 12.0(4). Publisher: MDPI.
43. Kiprijanovska, I., Stankoski, S., Ilievski, I., Jovanovski, S., Gams, M., and Gjoreski, H. (2020). Houseec: Day-ahead household electrical energy consumption forecasting using deep learning. ENERGIES, 13.0(10). Publisher: MDPI.
44. Kong, W., Dong, Z. Y., Hill, D. J., Luo, F., and Xu, Y. (2018). Short-term residential load forecasting based on resident behaviour learning. IEEE TRANSACTIONS ON POWER SYSTEMS, 33.0(1):1087–1088. Publisher: IEEE-INST ELECTRICAL ELECTRONICS ENGINEERS INC.
45. Kumaraswamy, S., Subathra, K., Dattathreya, Geeitha, S., Ramkumar, G., Metwally, A. S. M., and Ansari, M. Z. (2024). An ensemble neural network model for predicting the energy utility in individual houses. COMPUTERS & ELECTRICAL ENGINEERING, 114.0. Publisher: PERGAMON-ELSEVIER SCIENCE LTD.
46. Li, H., Heleno, M., Zhang, W., Garcia, L. R., and Hong, T. (2025). A cross-dimensional analysis of data-driven short-term load forecasting methods with large-scale smart meter data. ENERGY AND BUILDINGS, 344.0. Publisher: ELSEVIER SCIENCE SA.
47. Lin, W., Wu, D., and Jenkin, M. (2025). Electric load forecasting for individual households via spatial-temporal knowledge distillation. IEEE TRANSACTIONS ON POWER SYSTEMS, 40.0(1):572–584. Publisher: IEEE-INST ELECTRICAL ELECTRONICS ENGINEERS INC.
48. Lotfipoor, A., Patidar, S., and Jenkins, D. P. (2024). Deep neural network with empirical mode decomposition and bayesian optimisation for residential load forecasting. EXPERT SYSTEMS WITH APPLICATIONS, 237.0(A). Publisher: PERGAMON-ELSEVIER SCIENCE LTD
49. Lu, Y., Wang, G., and Huang, S. (2022). A short-term load forecasting model based on mixup and transfer learning. ELECTRIC POWER SYSTEMS RESEARCH, 207.0 Publisher: ELSEVIER SCIENCE SA.
50. Manandhar, P., Rafiq, H., Rodriguez-Ubinas, E., and Palpanas, T. (2024). New forecasting metrics evaluated in prophet, random forest,

ISSN: 1857-7881 (Print)
e-ISSN 1857-7431 (Online)

and long short-term memory models for load forecasting. ENERGIES, 17.0(23). Publisher: MDPI

51. Mansoor, H., Rauf, H., Mubashar, M., Khalid, M., and Arshad, N. (2021). Past vector similarity for short term electrical load forecasting at the individual household level. IEEE ACCESS, 9.0:42771–42785. Publisher: IEEE-INST ELECTRICAL ELECTRONICS ENGINEERS INC.
52. Masood, Z., Gantassi, R., Ardiansyah, and Choi, Y. (2022). A multi-step time-series clustering-based seq2seq lstm learning for a single household electricity load forecasting. ENERGIES, 15.0(7). Publisher: MDPI.
53. Massidda, L. and Marrocu, M. (2018). Smart meter forecasting from one minute to one year horizons. ENERGIES, 11.0(12). Publisher: MDPI.
54. Moldovan, D. and Slowik, A. (2021). Energy consumption prediction of appliances using machine learning and multi-objective binary grey wolf optimization for feature selection. APPLIED SOFT COMPUTING, 111.0 Publisher: ELSEVIER
55. Muqtadir, A., Li, B., Ying, Z., Songsong, C., and Kazmi, S. N. (2025). Nowcasting the next hour of residential load using boosting ensemble machines. SCIENTIFIC REPORTS, 15.0(1). Publisher: NATURE PORTFOLIO.
56. Nguyen, T. T. Q., Tran, T. P. T., Debusschere, V., Bobineau, C., and Rigo-Mariani, R. (2020). Comparing high accurate regression models for short-term load forecasting in smart buildings. IECON 2020: THE 46TH ANNUAL CONFERENCE OF THE IEEE INDUSTRIAL ELECTRONICS SOCIETY, pages 1962–1967. Backup Publisher: IEEE Ind Elect Soc and Nangyang Technol Univ and Inst Elect & Elect Engineers and Smart Grid Power Elect Consortium Singapore ISSN: 1553-572X
57. Ozcan, A., Catal, C., and Kasif, A. (2021). Energy load forecasting using a dualstage attention-based recurrent neural network. SENSORS, 21.0(21). Publisher: MDPI.
58. Ozdemir, S., Demir, Y., and Yildirim, O. (2025). The effect of input length on prediction accuracy in short-term multi-step electricity load forecasting: A cnnlstm approach. IEEE ACCESS, 13.0:28419–28432. Publisher: IEEE-INST ELECTRICAL ELECTRONICS ENGINEERS INC.
59. Page, M. J., McKenzie, J. E., Bossuyt, P. M., Boutron, I., Hoffmann, T. C., Mulrow, C. D., Shamseer, L., Tetzlaff, J. M., Akl, E. A., Brennan, S. E., et al. (2021). The prisma 2020 statement: an updated guideline for reporting systematic reviews. BMJ, 372:n71.

ISSN: 1857-7881 (Print)
e-ISSN 1857-7431 (Online)

60. Park, K.-J. and Son, S.-Y. (2023). Residential load forecasting using modified federated learning algorithm. IEEE ACCESS, 11.0:40675–40691. Publisher: IEEE-INST ELECTRICAL ELECTRONICS ENGINEERS INC.
61. Pla, E. and Jimenez Martinez, M. (2023). Dealing with change: Retraining strategies to improve load forecasting in individual households under covid-19 restrictions. ENERGY REPORTS, 9.0(11):82–89. Publisher: ELSEVIER
62. Qu, X., Guan, C., Xie, G., Tian, Z., Sood, K., Sun, C., and Cui, L. (2023). Personalized federated learning for heterogeneous residential load forecasting. BIG DATA MINING AND ANALYTICS, 6.0(4, SI):421–432. Publisher: TSINGHUA UNIV PRESS.
63. Razghandi, M., Zhou, H., Erol-Kantarci, M., and Turgut, D. (2021). Short-term load forecasting for smart home appliances with sequence-to-sequence learning. IEEE INTERNATIONAL CONFERENCE ON COMMUNICATIONS (ICC 2021). Backup Publisher: IEEE; Telus; Huawei; Ciena; Nokia; Samsung; Qualcomm; Cisco; Google Cloud ISSN: 1550-3607
64. Sajjad, M., Khan, Z. A., Ullah, A., Hussain, T., Ullah, W., Lee, M. Y., and Baik, S. W. (2020). A novel cnn-gru-based hybrid approach for short-term residential load forecasting. IEEE ACCESS, 8.0:143759–143768. Publisher: IEEE-INST ELECTRICAL ELECTRONICS ENGINEERS INC.
65. Sakib, M., Siddiqui, T., Mustajab, S., Alotaibi, R. M., Alshareef, N. M., and Khan, M. Z. (2025). An ensemble deep learning framework for energy demand forecasting using genetic algorithm-based feature selection. PLOS ONE, 20(1):e0310465.
66. Sakuma, Y. and Nishi, H. (2022). Hierarchical multiobjective distributed deep learning for residential short-term electric load forecasting. IEEE ACCESS, 10.0:69950– 69962. Publisher: IEEE-INST ELECTRICAL ELECTRONICS ENGINEERS INC
67. Shahsavari-Pour, N., Heydari, A., Keynia, F., Fekih, A., and Shahsavari-Pour, A. (2025). Building electrical consumption patterns forecasting based on a novel hybrid deep learning model. RESULTS IN ENGINEERING, 26.0. Publisher: ELSEVIER.
68. Shi, H., Xu, M., and Li, R. (2018). Deep learning for household load forecasting-a novel pooling deep rnn. IEEE TRANSACTIONS ON SMART GRID, 9.0(5):5271– 5280 Publisher: IEEE-INST ELECTRICAL ELECTRONICS ENGINEERS INC
69. Shi, J. and Wang, Z. (2022). A hybrid forecast model for household electric power by fusing landmark-based spectral clustering and deep learning. SUSTAINABILITY, 14.0(15). Publisher: MDPI.

ISSN: 1857-7881 (Print)
e-ISSN 1857-7431 (Online)

70. Shi, Y. and Xu, X. (2022). Deep federated adaptation: An adaptative residential load forecasting approach with federated learning. SENSORS, 22.0(9). Publisher: MDPI.
71. Sinha, A., Tayal, R., Vyas, A., Pandey, P., and Vyas, O. P. (2021). Forecasting electricity load with hybrid scalable model based on stacked non linear residual approach. FRONTIERS IN ENERGY RESEARCH, 9.0. Publisher: FRONTIERS MEDIA SA.
72. Sulaiman, S. M., Jeyanthy, P. A., Devaraj, D., and Shihabudheen, K., V. (2022). A novel hybrid short-term electricity forecasting technique for residential loads using empirical mode decomposition and extreme learning machines. COMPUTERS & ELECTRICAL ENGINEERING, 98.0. Publisher: PERGAMON-ELSEVIER SCIENCE LTD.
73. Taik, A. and Cherkaoui, S. (2020). Electrical load forecasting using edge computing and federated learning. ICC 2020 - 2020 IEEE INTERNATIONAL CONFERENCE ON COMMUNICATIONS (ICC). Backup Publisher: IEEE; Huawei; ZTE; Qualcomm ISSN: 1550-3607
74. Teperikidis, L., Boulmpou, A., Papadopoulos, C., and Biondi-Zoccai, G. (2024). Using chatgpt to perform a systematic review: a tutorial. Minerva cardiology and angiology, 72.
75. Tigo (2023). A solar powered future: Residential adoption on a global scale. Accessed: 2025-07-01.
76. Truong, L. H. M., Chow, K. H. K., Luevisadpaibul, R., Thirunavukkarasu, G. S., Seyedmahmoudian, M., Horan, B., Mekhilef, S., and Stojcevski, A. (2021). Accurate prediction of hourly energy consumption in a residential building based on the occupancy rate using machine learning approaches. APPLIED SCIENCES-BASEL, 11.0(5). Publisher: MDPI.
77. Ullah, F. U. M., Khan, N., Hussain, T., Lee, M. Y., and Baik, S. W. (2021). Diving deep into short-term electricity load forecasting: Comparative analysis and a novel framework. MATHEMATICS, 9.0(6). Publisher: MDPI.
78. Widmer, F., Nowak, S., Bowler, B., Huber, P., and Papaemmanouil, A. (2023). Datadriven comparison of federated learning and model personalization for electric load forecasting. ENERGY AND AI, 14.0. Publisher: ELSEVIER.
79. Xia, Z., Zhang, R., Ma, H., and Saha, T. K. (2024). Day-ahead electricity consumption prediction of individual household capturing peak consumption pattern. IEEE TRANSACTIONS ON SMART GRID, 15.0(3):2971–2984. Publisher: IEEE-INST ELECTRICAL ELECTRONICS ENGINEERS INC.

ISSN: 1857-7881 (Print)
e-ISSN 1857-7431 (Online)

80. Xu, C., Li, C., and Zhou, X. (2022). Interpretable lstm based on mixture attention mechanism for multi-step residential load forecasting. ELECTRONICS, 11.0(14). Publisher: MDPI.
81. Yang, W., Shi, J., Li, S., Song, Z., Zhang, Z., and Chen, Z. (2022). A combined deep learning load forecasting model of single household resident user considering multi-time scale electricity consumption behavior. APPLIED ENERGY, 307.0. Publisher: ELSEVIER SCI LTD.
82. Yousaf, A., Asif, R. M., Shakir, M., Rehman, A. U., and S. Adrees, M. (2021). An improved residential electricity load forecasting using a machine-learning-based feature selection approach and a proposed integration strategy. SUSTAINABILITY, 13.0(11). Publisher: MDPI.
83. Yuan, L., Ma, J., Gu, J., Wen, H., and Jin, Z. (2020). Featuring periodic correlations via dual granularity inputs structuredrnnsensemble load forecaster. INTERNATIONAL TRANSACTIONS ON ELECTRICAL ENERGY SYSTEMS, 30.0(11). Publisher: WILEY.
84. Zang, H., Xu, R., Cheng, L., Ding, T., Liu, L., Wei, Z., and Sun, G. (2021). Residential load forecasting based on lstm fusing self-attention mechanism with pooling. ENERGY, 229.0. Publisher: PERGAMON-ELSEVIER SCIENCE LTD
85. Zhang, X.-Y., Cordoba-Pachon, J.-R., Guo, P., Watkins, C., and Kuenzel, S. (2024). Privacy-preserving federated learning for value-added service model in advanced metering infrastructure. IEEE TRANSACTIONS ON COMPUTATIONAL SOCIAL SYSTEMS, 11.0(1):117–131. Publisher: IEEE-INST ELECTRICAL ELECTRONICS ENGINEERS INC.
86. Zhao, W., Li, T., Xu, D., and Wang, Z. (2024). A global forecasting method of heterogeneous household short-term load based on pre-trained autoencoder and deep-lstm model. ANNALS OF OPERATIONS RESEARCH, 339.0(1-2, SI):227–259. Publisher: SPRINGER.
87. Zhu, J., Miao, Y., Dong, H., Li, S., Chen, Z., and Zhang, D. (2024). Short-term residential load forecasting based on k-shape clustering and domain adversarial transfer network. JOURNAL OF MODERN POWER SYSTEMS AND CLEAN ENERGY, 12.0(4):1239–1249. Publisher: STATE GRID ELECTRIC POWER RESEARCH INST

ESJ Natural/Life/Medical Sciences Peer-reviewed

Design and Implementation of a Detection and Diagnostic System for Anomalies in a Grid-Connected Photovoltaic System

Ursula Vanelie Kani Mboyo
Aristide Mankiti Fati
Rene Evrard Josue Samba
National Higher Polytechnic School,
Marien Ngouabi University, Brazzaville, Republic of Congo

Doi:10.19044/esj.2026.v22n6p33

Submitted: 13 January 2026
Accepted: 24 February 2026
Published: 28 February 2026

Cite As:
Kani Mboyo, U.V., Mankiti Fati, A. & Samba, R.E.J. (2026). *Design and Implementation of a Detection and Diagnostic System for Anomalies in a Grid-Connected Photovoltaic System.* European Scientific Journal, ESJ, 22 (6), 33. https://doi.org/10.19044/esj.2026.v22n6p33

Abstract

This paper presents the design and implementation of a detection and diagnostic system for anomalies in a photovoltaic (PV) installation connected to the national EEC grid in Congo Brazzaville, under the framework of Denis SASSOU NGUESSO University. The main objective is to reduce maintenance costs and improve energy productivity, given that PV systems are inherently prone to operational failures. The study focuses on faults affecting the PV generator and proposes a method for detecting and precisely localizing anomalies that reduce energy output. The approach is based on analyzing the current–voltage (I–V) and power–voltage (P–V) characteristics of the PV generator under varying operating conditions. Results, summarized in tables for clarity, demonstrate that the Lambert W/numerical model accurately reproduces the module's electrical behavior, with a root mean square error (RMSE) of 0.1608 A for current (≈2 % of nominal current, 8 A) and 3.686 W for power (≈1.2 % of maximum power, 300 W). These low and unbiased errors validate the model for rapid performance drift detection, fault localization, and operating point optimization. The system provides a solid foundation for intelligent supervision and predictive maintenance, ensuring enhanced reliability, reduced downtime, and improved energy efficiency.

ISSN: 1857-7881 (Print)
e-ISSN 1857-7431 (Online)

Keywords: Photovoltaic generator, modeling, diagnostic, real-time simulation

Introduction

Background Review

In an effort to provide a scientific contribution to the challenges of photovoltaic (PV) systems in Africa in general, and in Congo Brazzaville in particular, this work focuses on the prevention of failures, malfunctions, and maintenance, whose costs remain particularly high. While several researchers are already engaged in this research area, our approach aims to provide a specific contribution anchored in the African context.

Over the past decade, the photovoltaic sector has experienced remarkable growth, driven by the progressive reduction in production costs and public policies promoting renewable energy (I.E. Al-Shetwi, 2025), (Photovoltaique.info). These developments have made PV installations increasingly attractive to both investors and end-users, due to a more favorable return on investment (Mikael, 2025).

However, like any industrial system, PV installations remain exposed to various faults and anomalies that can degrade performance or even cause complete system downtime (Benzagmout, 2021). Such malfunctions directly impact energy productivity, economic profitability, and associated maintenance costs (Djallel et al., 2020). In response to these challenges, the implementation of reliable and efficient diagnostic systems has become both an operational and strategic necessity (Bari, A. & Jarwar, 2025).

An effective diagnostic system must not only detect faults quickly but also locate them precisely, thereby reducing downtime and intervention costs (Achour, 2025). It is within this context that (Sepúlveda-Oviedo, 2023) was initiated, and the work presented in this thesis constitutes a direct contribution (Venkatakrishnan,2023). The primary objective is to design an integrated system capable of supervising, diagnosing, and optimizing the operation of PV installations, while remaining transparent to the end-user (Alosmani, 2023).

This research specifically focuses on the detection and localization of faults on the direct current (DC) side of the system, i.e., at the level of the PV generator. The adopted approach aims to minimize the number of required measurements, thereby respecting economic constraints while ensuring maximum efficiency (Benzagmout, 2021; Tahraoui, 2023). Currently, several monitoring systems measure power and energy output using voltage and current sensors (Guide Photovoltaïque, 2025). Some services go further by correlating production with meteorological data, such as satellite-measured solar irradiance (Tahraoui, M. et al, 2023). Although useful, these tools present

ISSN: 1857-7881 (Print)
e-ISSN 1857-7431 (Online)

notable limitations: they neither allow rapid detection nor precise localization of faults at their onset (Axiome energie, 2025).

In this context, we propose a methodology based on system modeling to characterize the current–voltage (I–V) and power–voltage (P–V) curves of the PV generator under different operating modes. Subsequently, a PV panel is simulated by integrating power failures, i.e., operational errors, and a corrective measure is proposed using the Lambert W model. This approach aims to strengthen diagnostic robustness and improve the overall reliability of the supervision system. In continuation of the research on photovoltaic systems, it was also essential to review the studies conducted by our predecessors in order to identify and refine the focus of our own investigation.

In the current context of energy transition, photovoltaic (PV) systems play a central role in renewable electricity generation. Their large-scale deployment is driven by undeniable advantages such as low operating cost, durability, modularity, and reduced environmental impact. However, despite their apparent reliability, PV installations remain vulnerable to various faults that can degrade performance. If not detected in time, these anomalies may lead to significant energy losses, service interruptions, or irreversible component damage. Consequently, research has intensified on advanced diagnostic methods aimed at improving the supervision, maintenance, and resilience of PV systems.

Several studies have proposed approaches based on electrical analysis of the PV generator, particularly through the current–voltage (I–V) characteristic. Benzagmout et al. (2021) developed a knowledge base linking each fault type to a specific I–V signature. Their discrete inference algorithm achieved more than 90% accuracy in anomaly detection and localization, which is highly relevant for grid-connected plants. However, the reliability of this method depends heavily on measurement quality, which can be difficult to obtain in real time without specialized instrumentation.

Djallel et al. (2020) adopted a comparative approach, evaluating different detection techniques through fault simulations. Neural network–based methods proved particularly effective for complex and nonlinear faults. Artificial intelligence enables automatic classification of symptoms and offers adaptability in dynamic environments, though it requires training on representative datasets, limiting applicability in poorly instrumented contexts.

Alosmani et al. (2023) proposed a hybrid approach combining thermal and electrical modeling with inference techniques. Their method improved energy yield by an average of 12% on tested sites, confirming the value of integrating physical data for refined diagnostics. Nevertheless, implementation remains complex and resource-intensive, which may hinder adoption in low-infrastructure settings.

ISSN: 1857-7881 (Print)
e-ISSN 1857-7431 (Online)

Spectral analysis of power curves was explored by Kouadri et al. (2022) to detect partial shading faults common in urban environments. This method achieved rapid detection with less than 5% error, useful for rooftop or dense-area installations. However, it is less effective for internal defects such as microcracks or cell degradation.

Achour et al (2024) developed low-cost monitoring systems using microcontrollers such as Arduino. These devices enable real-time data acquisition and local processing, reducing supervision costs. Pilot sites reported a 30% reduction in maintenance costs, demonstrating effectiveness for rural or domestic micro-installations. Yet, limited computational and storage capacity restricts their use in complex analyses or large-scale systems.

Tahraoui et al. (2022) analyzed transient responses of PV systems using MATLAB/Simulink simulations to localize faults with an error margin below two meters. This approach is relevant for large plants with extensive cabling but is sensitive to electromagnetic disturbances.

Khan et al. (2023) applied convolutional neural networks to thermal images, achieving fault recognition rates above 95%. This method is well-suited for drone-based inspections, enabling fast and non-intrusive monitoring. However, its effectiveness depends on image quality and lighting conditions.

Mikael et al. (2025) studied correlations between PV production and satellite meteorological data. By analyzing monthly deviations between expected irradiation and actual production, they identified hidden anomalies. This approach supports remote supervision of isolated installations, though the limited temporal resolution of satellite data restricts real-time diagnostics.

Overall, the reviewed studies highlight the diversity of approaches developed to enhance PV system reliability, ranging from electrical analysis and image processing to thermal modeling and artificial intelligence. Most methods face limitations related to implementation complexity, data dependency, or environmental conditions. Current trends point toward hybrid systems that combine multiple information sources and integrate intelligent algorithms capable of adapting diagnostics to real-world conditions. These works provide a solid foundation for advanced supervision solutions such as the DLDPV system presented in this thesis, which aims to deliver rapid, localized, and economically viable fault detection on the DC side.

Methodology

Review of fundamental concepts

Structure of a photovoltaic system

A photovoltaic (PV) system is responsible for converting solar photon energy into usable electrical energy for various applications. The system consists of a **PV cell** that produces direct current (DC), converters for adapting

ISSN: 1857-7881 (Print)
e-ISSN 1857-7431 (Online)

and conditioning the power, batteries for energy storage, and charge controllers to regulate and protect the system.

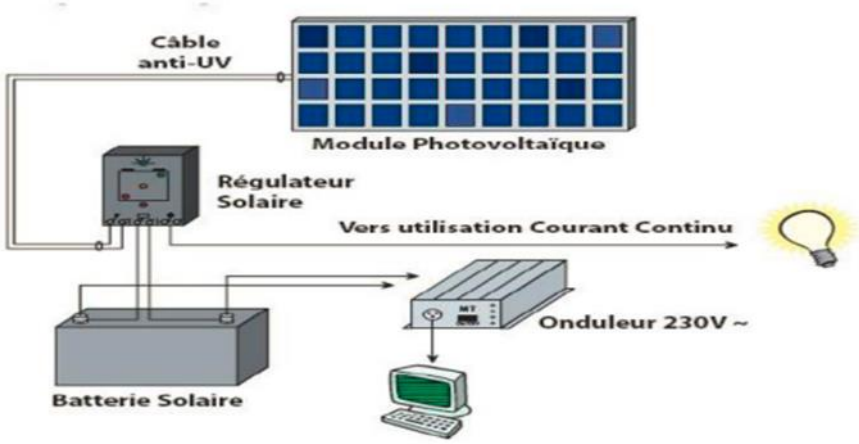

Figure 1: Structure of a Photovoltaic (PV) System

Photovoltaic generator

The photovoltaic (PV) **cell** is the unit responsible for producing electrical energy in the form of direct current (DC). The fundamental component that converts solar energy into electrical energy is the photovoltaic cell (A. Luque et al., 20211).

Photovoltaic cell

The photovoltaic cell is a semiconductor device, generally silicon-based, formed from two layers, one N-doped and the other P-doped, creating a PN junction (Bari, A. & Jarwar, 2025). It is the smallest constituent of a photovoltaic system, responsible for producing electricity from solar energy based on the principle of the photovoltaic effect.

Photovoltaic module

A single **PV cell produced** low power, insufficient for common applications. To produce usable power, multiple cells are interconnected either in series (to increase voltage at constant current) or in parallel (to increase current at constant voltage). A series grouping of these elementary components forms a PV module, which must be mechanically protected to withstand outdoor conditions. Since PV cells are fragile and sensitive to corrosion, the module ensures durability against humidity and temperature variations (Khaled Alosmani, 2023).

ISSN: 1857-7881 (Print)
e-ISSN 1857-7431 (Online)

Batteries

A solar battery stores electrical energy and releases it when demand exceeds PV production (e.g., at night or during insufficient sunlight). It ensures a quasi-continuous energy supply.

Charge controllers

The charge controller links the **PV cell** to the battery. It protects the battery against overcharging or deep discharging, making it essential for preserving battery lifetime (Bari, A. & Jarwar, 2025).

Conversion systems

An energy converter is installed either between the PV panel and the load (in systems without storage, using DC/DC converters) or between the battery and the load (using inverters or DC/AC converters) (Bari, A. & Jarwar, 2025).

DC/DC Converter

The DC/DC converter controls energy flow between the solar panel and the load. It adapts the apparent load impedance to the PV array impedance at the maximum power point. This adaptation system is commonly known as Maximum Power Point Tracking (MPPT) (Bari, A. & Jarwar, 2025).

DC/AC Converter (inverter)

The inverter is a key component of PV installations. It converts DC energy from PV modules into AC energy, either for local use or grid injection. In standalone systems (not connected to the public grid), inverters generate a 220 V, 50 Hz AC signal to create a local network. They can be combined with charge controllers and batteries to store energy for later use when PV production decreases (Bari, A. & Jarwar, 2025).

Grid-connected PV installation with surplus injection

This configuration allows users to produce their own electricity during sunny periods and feed surplus energy into the public grid, from which they can draw power when needed (Souaad Tahraoui, 2023).

ISSN: 1857-7881 (Print)
e-ISSN 1857-7431 (Online)

Figure 2: Grid-Connected Photovoltaic Installation with Surplus Energy Injection

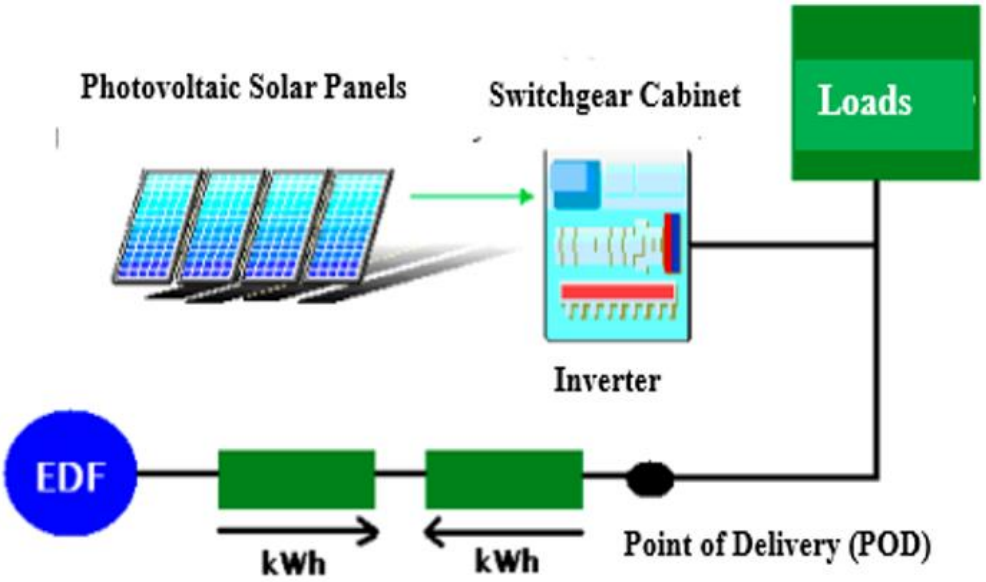

(Souaad Tahraoui, 2023)

Figure 2 illustrates the schematic of a grid-connected photovoltaic installation integrating a surplus injection mechanism. The system includes two distinct meters: the first records the amount of electricity purchased by the photovoltaic panel (PV) owner from the energy supplier, while the second measures the energy reinjected into the grid when production exceeds local consumption (Souaad Tahraoui,2023).

Defects in photovoltaic panels

During operation, a photovoltaic installation may be subject to various faults or abnormal operating conditions (A. Luque et al,20211). These anomalies can affect the overall performance of the system and compromise its energy reliability.

The most common and significant defects are classified according to the affected PV system component(A. Luque et al,20211):

- ✓ **PV array:** defects related to **PV cells**, such as microcracks, hot spots, or surface degradation;
- ✓ **junction Box:** anomalies affecting protection devices, particularly when multiple strings are connected in parallel;
- ✓ **cabling and Connectors:** insulation, connection, or continuity faults that may disrupt the series association of modules;
- ✓ **protection Diodes:** failures of bypass or blocking diodes, leading to power losses or overheating risks.

ISSN: 1857-7881 (Print)
e-ISSN 1857-7431 (Online)

Table 1: Origin of Faults and Anomalies in a Photovoltaic System

PV System Element	Origin of Faults and Anomalies
PV Generator	- Tree leaves, bird droppings, pollution, sand, snow, etc. - Cell deterioration, cracks, cell overheating - Moisture penetration, interconnection degradation, corrosion of cell links - Modules with different performance levels - Torn or broken module - Short-circuited or reversed modules
Junction Box	- Electrical circuit break - Electrical short circuit - Connection destruction - Corrosion of connections
Cabling and Connectors	- Open circuit - Short circuit - Incorrect wiring (reversed module) - Contact corrosion - Electrical circuit break
Protection Diodes (Bypass and Blocking Diodes)	- Diode destruction - Absence or malfunction of diodes - Incorrect polarity during installation, poorly connected diode

(Photovoltaique.info, 2025)

Table 2: Defects of PV Field Components

PV Field Component	Nature of Defects	Defect Classification
Cell	- Torn or broken module - Shading from pylons, chimneys, sand, snow, etc. - Cell overheating - Interconnection degradation - Cracks - Corrosion of cell links - Modules with different performance levels - Cell deterioration - Moisture penetration	Mismatch and shading defect
Cell Groups	- Diode destruction - Absence of diodes	Bypass diode defect

(J. Cubas et al, 2014)

This table highlights the main defects observed in photovoltaic modules, particularly at the cell and cell-group levels. Most anomalies originate from environmental factors (sand, snow, humidity, shading) or physical degradation (cracks, corrosion, overheating). These defects lead to performance losses, mismatches between cells, and failures in protection diodes, which can significantly affect the overall energy production of the PV system.

ISSN: 1857-7881 (Print)
e-ISSN 1857-7431 (Online)

Table 3: Classification of Defects in a Photovoltaic Field

PV System Component	Identified Defects	Defect Category
Diodes	- Polarity inversion - Incorrect connection - Short-circuited diode	Diode defect
Modules	- Short-circuited modules - Module polarity inversion - Shunted modules	Module defect
Strings	- Electrical circuit break - Connection destruction - Connection corrosion - Contact corrosion - Circuit short circuit - Disconnected module	Connectivity defect
PV Field	- Diode destruction - Absence of diodes - Diode inversion - Incorrect connection - Short-circuited diode	Anti-return diode defect

(J. Cubas et al, 2014)

This table presents the main defects observed in a photovoltaic field according to system components: diodes, modules, strings, and the PV field. The identified failures mainly involve polarity inversions, short circuits, poor connections, and corrosion. These defects can lead to performance degradation, loss of electrical continuity, or material damage. Such classification facilitates detection, diagnosis, and preventive maintenance of PV installations.

Diagnostic methods

In the analysis of photovoltaic (PV) installations, two essential diagnostic functions must be distinguished: **fault detection** and **fault localization**. Some methods are limited to identifying the presence of anomalies, while others allow precise localization of their origin. This distinction is fundamental for guiding maintenance interventions and optimizing system reliability. This section presents the main diagnostic methods used in the PV industry, as well as those proposed in scientific literature (A. Luque et al, 2021).

Infrared imaging method

Among diagnostic techniques applied to PV cells, several approaches identify defects such as cracks or internal degradation. Mechanical bending tests, photoluminescence imaging, and electroluminescence provide fine visualization of structural alterations. For PV modules, infrared imaging (thermal camera) is widely used. This method relies on the principle that all

ISSN: 1857-7881 (Print)
e-ISSN 1857-7431 (Online)

materials emit infrared radiation proportional to their temperature. By analyzing the thermal distribution on the module surface, localized anomalies can be detected. Defects identified through this technique include(Mikael,,2025):

- ✓ Leakage currents in cells;
- ✓ Increased resistance of cell interconnections;
- ✓ Abnormal heating due to internal defects;
- ✓ Unintended conduction of bypass diodes.

These results confirm the effectiveness of thermal imaging for rapid and non-intrusive localization of PV module defects.

Reflectometry

Reflectometry is a non-intrusive diagnostic method that injects a signal into a circuit and analyzes reflections caused by discontinuities or impedance variations. Applied to PV strings, it detects faults such as open circuits, short circuits, or impedance anomalies. Its experimental efficiency makes it a precise and rapid tool for fault localization, particularly useful in large-scale PV systems(Mikael, 2025).

Power and energy analysis

Analyzing the power and energy produced by a PV field enables fault detection and localization. The principle is to compare measured values with expected ones: significant deviations indicate anomalies. To refine localization, attributes of power or energy drops, such as duration, amplitude, frequency, and occurrence time, are studied. The defect whose calculated attributes best match observed ones is identified as the probable cause of failure(Mikael,2025).

Operating point analysis

Comparing measured maximum power points (current and voltage) with expected values provides additional information on PV system status. This binary analysis of currents and voltages identifies problems classified into four categories: defective modules within a string, defective strings, non-discriminable faults (shading, MPPT error, aging), and false alarms.

Static characteristic analysis

A PV field is characterized by its static current–voltage (I–V) curve under normal operation. Any modification of this characteristic may indicate a change in system state, either due to operating conditions (irradiance, temperature) or the appearance of one or more faults in the PV system (Mikael, 2025):

ISSN: 1857-7881 (Print)
e-ISSN 1857-7431 (Online)

Figure 3: Characteristic current–voltage (I–V)

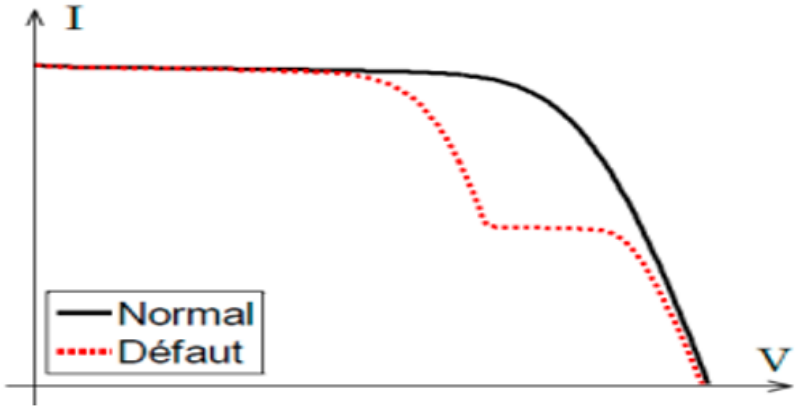

(Mikael, 2025)

Modeling of photovoltaic array

The modeling of photovoltaic (PV) cells involves two principal approaches:

- ✓ Single-diode model (simple exponential);
- ✓ Two-diode model (double exponential).

Modeling of the single-diode photovoltaic cell

The single-diode model provides a simplified representation of the electrical behavior of a photovoltaic cell. It is an empirical model that employs an ideal diode, parasitic resistances, and a current source to reproduce the current–voltage (I–V) characteristics of the cell. This approach captures the essential performance of PV devices while maintaining computational efficiency, making it widely adopted in both academic research and practical applications(A. Benzagmout, 2021).

Figure 4: Single-diode model schematic

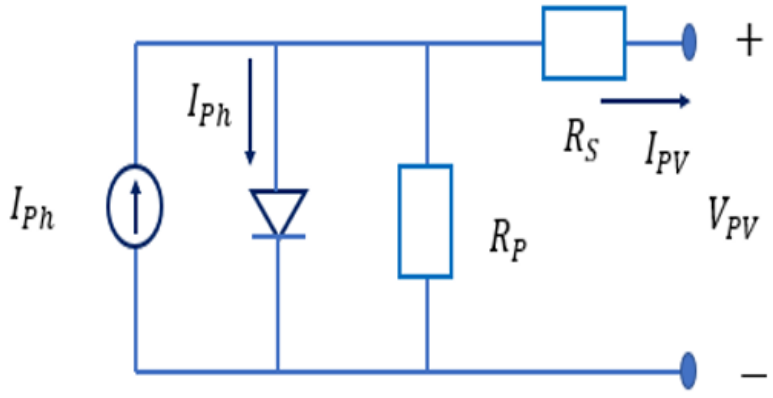

(A. Benzagmout, 2021)

ISSN: 1857-7881 (Print)
e-ISSN 1857-7431 (Online)

Single-diode model circuit representation

The schematic of the single-diode model (Figure 4) consists of the following elements (A. Benzagmout, 2021).:

Photocurrent Source (I_{Ph}): Represents the current generated by the photovoltaic effect within the cell. Its magnitude depends on the incident irradiance and the intrinsic characteristics of the cell.

Series Resistance (R_S): Accounts for internal Ohmic losses in the cell due to the resistivity of semiconductor materials and metallic contacts.

Shunt Resistance (R_{Sh}): Models parasitic leakage currents within the cell.

Ideal Diode (D): Represents the p–n junction of the cell. The current flowing through the diode (I_d) is expressed by the Shockley equation(A. Benzagmout,2021).:

$$\boldsymbol{I_d = I_0\left[exp\left(\frac{q(V_{PV}+R_S.I_{PV})}{nKT}\right)\right]} \quad \textbf{(1)}$$

$$\boldsymbol{I_d = I_{SC}\left[exp\left(\frac{V_{PV}}{V_t}\right) - 1\right]} \quad \textbf{(2)}$$

The single-diode photovoltaic model incorporates the following parameters:

- ✓ **Short-Circuit Current (I_{SC})**: Represents the current delivered by the cell when the output terminals are short-circuited.
- ✓ **Photovoltaic Voltage (V_{PV})**: Denotes the voltage across the terminals of the cell.
- ✓ **Thermal Voltage (V_t)**: Defined as the thermal potential of the cell, approximately 26 mV under ambient temperature conditions.
- ✓ **Parasitic Series Resistance (R_P)**: Models the internal resistive losses due to semiconductor material properties and contact resistances.
- ✓ **Parasitic Shunt Resistance (R_{Sh})**: Represents leakage paths within the cell that contribute to parasitic current losses.

I–V Velation of the single-diode model

The total current (I) flowing through the photovoltaic cell is given by the sum of the photocurrent source (I_{Ph}) and the diode current (I_d)(Z. Djallel et al, 2020):

$$I = I_{Ph} - I_d \quad (3)$$

ISSN: 1857-7881 (Print)
e-ISSN 1857-7431 (Online)

By substituting I_dWith its expression from the Shockley equation, the I–V relation of the single-diode model becomes:

$$I = I_{Ph} - I_{SC}\left[\exp\left(\frac{V_{PV}}{V_t}\right) - 1\right] + \frac{V}{R_P} - \frac{V_{PV}}{R_{Sh}} \tag{4}$$

This equation enables the simulation of the I–V curve of the photovoltaic cell under varying irradiance and temperature conditions.
The diode current (I_d) is expressed by the Shockley equation as:

$$I_d = I_0\left[\exp\left(\frac{q(V_{PV} + R_S I_{PV})}{nkT}\right) - 1\right] \tag{5}$$

where:

- ✓ $k = 1.380662 \times 10^{-23}$ J/(K)is Boltzmann's constant,
- ✓ $n$is the diode ideality factor (typically between 1 and 2),
- ✓ $q = 1.602 \times 10^{-19}$ Cis the electron charge.

The current through the parallel shunt resistance (R_{Sh}) is given by:

$$I_{sh} = \frac{V_{PV} + R_S I_{PV}}{R_{Sh}} \tag{6}$$

where:

- ✓ $R_S$is the series resistance of the cell,
- ✓ $R_{Sh}$is the shunt resistance of the cell,
- ✓ $V_{PV}$is the output voltage of the cell.

Finally, the four-parameter model of the photovoltaic cell is expressed as:

$$I_{PV} = I_{Ph} - I_0\left[\exp\left(\frac{q(V_{PV} + R_S I_{PV})}{nkT}\right) - 1\right] - \frac{V_{PV} + R_S I_{PV}}{R_{Sh}} \tag{7}$$

Four-parameter model

Figure 5 represents a four-parameter model.

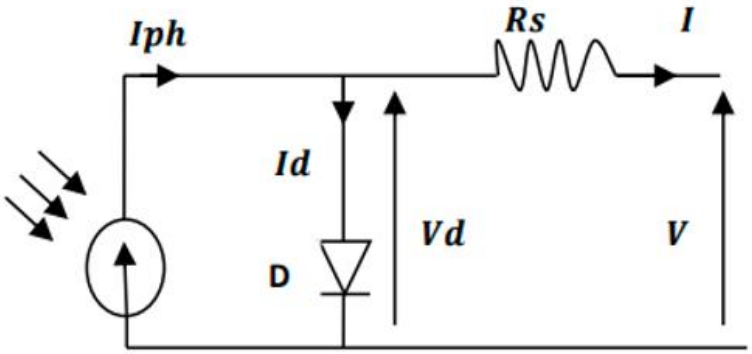

Figure 5: Four-Parameter Model [14]

ISSN: 1857-7881 (Print)
e-ISSN 1857-7431 (Online)

The series resistance $R_S$is added as the fourth parameter [14].

- ✓ R_S: Represents the resistance of the connections.
- ✓ The diode voltage is expressed as:

$$V_d - V + R_S I_{rs} = 0 \tag{8}$$

Thus, the current is given by:

$$I = I_{ph} - I_{sat}\left[\exp\left(\frac{V + IR_S}{nkT}\right) - 1\right] \tag{9}$$

Under standard test conditions (irradiance of 1000 W/m² and temperature of 25 °C):

$$\frac{kT}{q} \approx 26\,\text{mV}$$

with:

- ✓ $k = 1.38 \times 10^{-23}$ J\pK^{-1}(Boltzmann constant),
- ✓ $T = 25 + 273 = 298$ K,
- ✓ $q = 1.16 \times 10^{-19}$ C(electron charge).

Therefore, the relation becomes:

$$I = I_{ph} - I_{sat}\left[\exp\left(\frac{V + IR_S}{n \cdot 0.026}\right) - 1\right] \tag{10}$$

Two-diode model

We present the two-diode model to study the effect of partial shading on the energy production of photovoltaic (PV) panels. For this purpose, a comprehensive analysis of all available PV module configurations is carried out. The two-diode model is introduced as follows (A. Benzagmout et al. 2021):

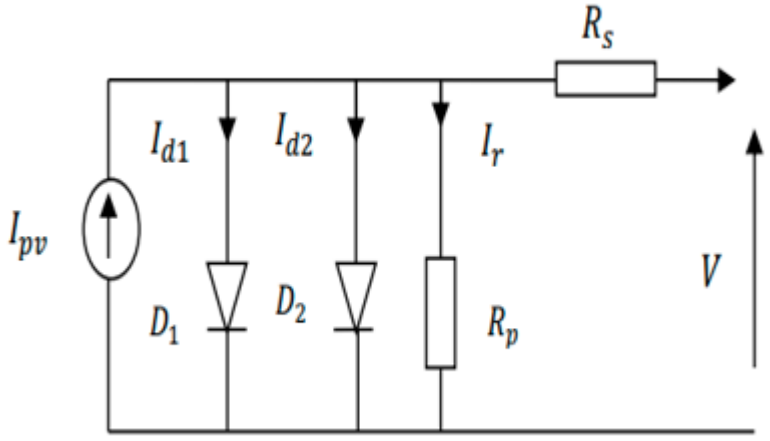

Figure 6: Equivalent Electrical Circuit of a Crystalline Silicon Cell – Two-Diode Model (2-D Rs)

ISSN: 1857-7881 (Print)
e-ISSN 1857-7431 (Online)

The following equation describes the output current of the photovoltaic cell for the two-diode model:

$$I_{PV} = I_{Ph} - I_{01}\left[-1 + \exp\left(\frac{V_{PV} + R_S.I_{PV}}{A_1.V_{t1}}\right)\right] - I_{02}\left[-1 + \exp\left(\frac{V_{PV} + R_S.I_{PV}}{A_1.V_{t2}}\right)\right] - \frac{V_{PV} + R_S.I_{PV}}{R_P} \quad (11)$$

where:

- ✓ I_{d1}: Reverse saturation current of diode D1.
- ✓ I_{d2}: Reverse saturation current of diode D2.
- ✓ V_{r1}: Thermodynamic potential of diode D1.
- ✓ V_{r2}: Thermodynamic potential of diode D2.
- ✓ A_1: Ideality factor of the junction of diode D1.
- ✓ A_2: Ideality factor of the junction of diode D2.

Modeling and simulation of PV cells using single- and two-diode models
Parameter estimation methods for PV modules

Several techniques have been developed to extract the characteristic parameters of photovoltaic modules. These can be grouped into three main categories(A. Benzagmout et al 2021),(K. Alosmani et al, 2023):

- ✓ Analytical methods ;
- ✓ Iterative methods ;
- ✓ Intelligent methods.

These approaches provide varying levels of accuracy depending on the models and application conditions. One example is the simple conductance method.
The optimization of solar panel model parameters is a complex problem, involving determining the optimal combination of parameters to achieve the best possible performance. Different optimization approaches, such as Genetic Algorithms (GA), Particle Swarm Optimization (PSO), and Artificial Neural Networks (ANN), can be employed to solve this type of problem.
In this study, we analyze the effectiveness of these three approaches by comparing them according to several criteria: their ability to converge to an optimal solution, their convergence speed, and their robustness under different experimental conditions. The results of this comparative analysis provide valuable insights for researchers and engineers seeking to optimize solar panel model parameters (Z. Djallel, 2020).
In the continuation of this work, each of these methods will be presented in detail, applied to the determination of the predicted current obtained from solving the nonlinear equation of the photovoltaic (PV) cell current.

ISSN: 1857-7881 (Print)
e-ISSN 1857-7431 (Online)

Since the I–V characteristic equation is inherently nonlinear, its resolution requires the application of numerical methods capable of providing either an exact solution vector or an approximate solution vector.
Several methods have been developed in recent years to solve this nonlinear equation, including (A. Luque et al,20211):

- ✓ Lambert-W function method ;
- ✓ Newton–Raphson method ;
- ✓ Simple conductance method.

In this study, we restrict ourselves to the application of the analytical method based on the Lambert-W function, which is used to determine the predictive current by explicitly solving the nonlinear equation characterizing the current delivered by the photovoltaic (PV) cell (A. Luque et al, 2011).

Figure 7. Real Photovoltaic Cell Model

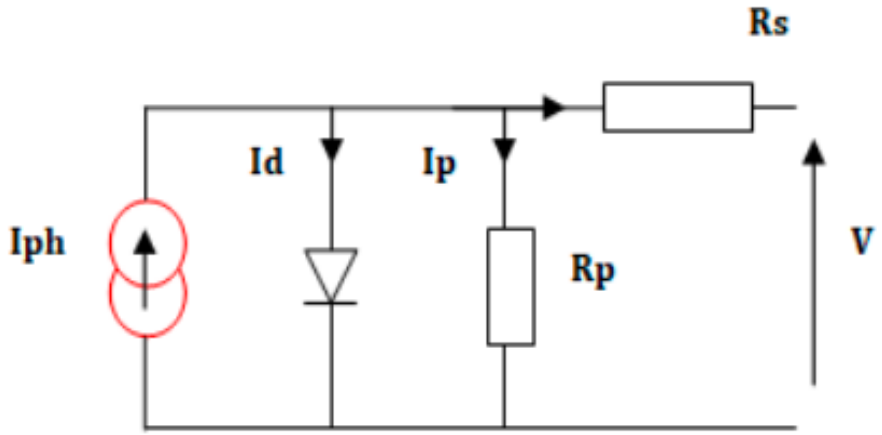

(Guide Photovoltaïque, 2025)

Analytical Method – Lambert-W Function

The Lambert-W function is defined as the function that satisfies the following relation:

$$Z = W(X) \cdot e^{W(X)} \tag{12}$$

where:

- ✓ Zrepresents the argument of the function W;
- ✓ $e$denotes the exponential function;
- ✓ $X$is a real or complex vector.

Consequently, the vector $X$is obtained in the following form:

$$X = W(Z)$$

The application of the Lambert-W function to the equation used to calculate the predicted current I_{PV}can be simplified as follows (Guide Photovoltaïque, 2025):

ISSN: 1857-7881 (Print)
e-ISSN 1857-7431 (Online)

$$(R_P + R_S)I_{PV} = R_P I_k - R_P I_0 \exp\left(\frac{V_{PV} + R_S I_{PV}}{AV_t}\right) - V_{PV} \tag{13}$$

where I_k is defined as:

$$I_k = I_{PV} + I_0$$

By multiplying both sides of (13) by the term $\frac{R_S}{R_P+R_S}$, we obtain:

$$R_S I_{PV} = \frac{R_S}{R_P + R_S}\left(R_P I_k - R_P I_0 \exp\left(\frac{V_{PV} + R_S I_{PV}}{AV_t}\right) - V_{PV}\right) \tag{14}$$

Equation (14) is further simplified, yielding:

$$\frac{V_{PV} + R_S I_{PV}}{AV_t} + \frac{R_S R_P I_0}{AV_t(R_P + R_S)} \exp\left(\frac{V_{PV} + R_S I_{PV}}{AV_t}\right) = \frac{R_S}{AV_t(R_P + R_S)}\left(R_P I_k + \frac{R_P V_{PV}}{R_S}\right) \tag{15}$$

$$\frac{R_S R_P I_0}{AV_t(R_P + R_S)} \exp\left[\frac{V_{PV} + R_S I_{PV}}{AV_t}\right] \exp\left[\frac{R_S R_P I_0}{AV_t(R_P + R_S)} exp\left(\frac{V_{PV} + R_S I_{PV}}{AV_t}\right)\right] = \frac{R_S R_P I_0}{AV_t(R_P + R_S)} \exp\left[\frac{R_S}{AV_t(R_P + R_S)}\right]\left(R_P I_k + \frac{R_p V_{PV}}{R_S}\right) \tag{16}$$

Equation (17) is further simplified, yielding:

$$\frac{R_S R_P I_0}{AV_t(R_P + R_S)} \exp\left[\frac{V_{PV} + R_S I_{PV}}{AV_t}\right] = LambertW\left(\frac{R_S R_P I_0}{AV_t(R_P + R_S)} \exp\left(\frac{R_S}{AV_t(R_P + R_S)}\left(R_P I_k + \frac{R_p V_{PV}}{R_S}\right)\right)\right) \tag{17}$$

Equation (17) is further simplified, yielding:

$$R_P I_0 \exp\left(\frac{V_{PV} + R_S I_{PV}}{AV_t}\right) = \frac{AV_t(R_P + R_S)}{R_S} ambertW\left(\frac{R_S R_P I_0}{AV_t(R_P + R_S)} \exp\left(\frac{R_S}{AV_t(R_P + R_S)}\left(R_P I_k + \frac{R_p V_{PV}}{R_S}\right)\right)\right) \tag{18}$$

ISSN: 1857-7881 (Print)
e-ISSN 1857-7431 (Online)

According to Equation (18), the term

$$R_P I_0 \exp\left(\frac{V_{PV} + R_S I_{PV}}{AV_t}\right)$$

is rewritten as:

$$R_P I_0 \exp\left(\frac{V_{PV} + R_S I_{PV}}{AV_t}\right) = R_P I_k - (R_P + R_S) - V_{PV} \quad (19)$$

Thus, the exact predicted output current is obtained by comparing Eq. (III.11) with Eq. (III.9), giving:

$$I_{PV} = \frac{R_P(I_{Ph} + I_0) - V_{PV}}{R_P + R_S} - \left(\frac{AV_t}{R_S} LambertW\left(\frac{R_S R_P I_0}{AV_t(R_P+R_S)} \exp\left(\frac{R_S}{AV_t(R_P+R_S)}\left(R_P I_k + \frac{R_p V_{PV}}{R_S}\right)\right)\right)\right) \quad (20)$$

Equation (20) therefore represents the exact solution of the nonlinear current equation of the photovoltaic cell.

Results and Discussion

The experimental study focused on analyzing the behavior of a photovoltaic module of type ISOFOTON I-50 PV. This module, composed of monocrystalline silicon cells, has a nominal power rating of 50 W and is commonly used in residential and commercial applications due to its reliability and stable performance.

The typical electrical characteristics of the ISOFOTON I-50 PV module are summarized in Table 4.

Table 4: Typical Electrical Characteristics of the ISOFOTON I-50 PV Module

Parameter	Value
Maximum Power P_{max}	39.10 W
Optimal Voltage V_m	14.9 V
Optimal Current I_m	2.62 A
Number of Cells	36

Influence of Different Parameters on Current and Power Characteristics

The I–V and P–V curves of solar panels provide valuable information about their electrical behavior and allow analysis of the influence of irradiance and temperature on performance. These insights are essential for the design, modeling, and optimization of photovoltaic systems.

Influence of Irradiance

Figures 8 and 9 present the I–V and P–V curves of a photovoltaic module under different irradiance conditions. The analysis of these curves shows that :

ISSN: 1857-7881 (Print)
e-ISSN 1857-7431 (Online)

- ✓ The current generated by the solar panel increases proportionally with irradiance. In other words, the higher the incident light, the greater the current produced.

The output voltage of the panel is less sensitive to irradiance variation compared to the current.

- ✓ However, a slight increase in voltage can be observed as irradiance rises.
- ✓ The delivered power, corresponding to the product $P = V \times I$, increases significantly with irradiance. This indicates an improvement in module efficiency under higher sunlight intensity.

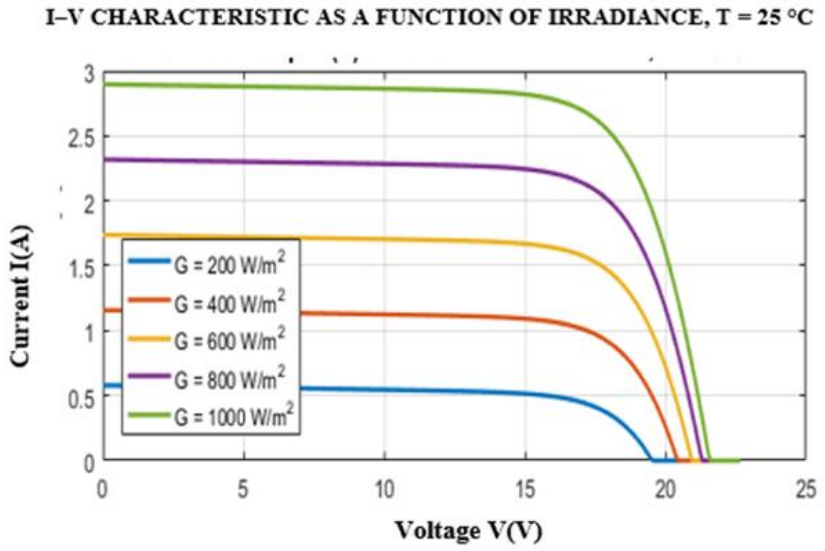

Figure 8: I–V Characteristic as a function of irradiance

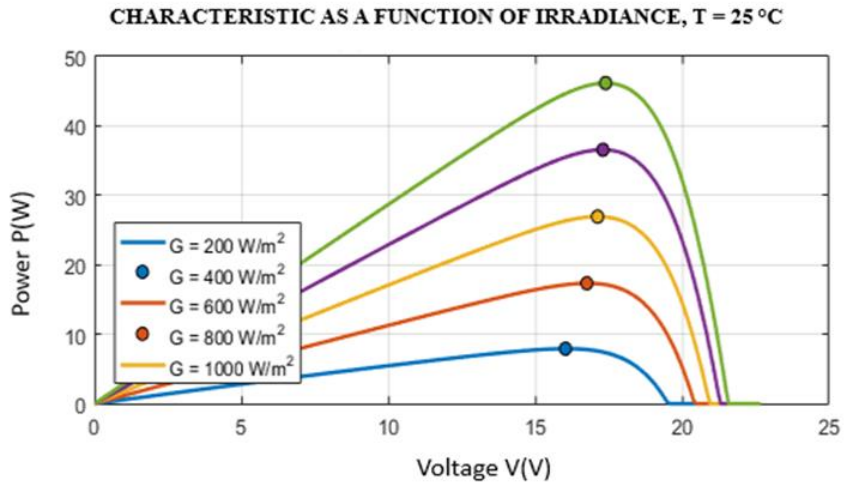

Figure 9: Characteristic $P = f(V)$as a Function of Irradiance

ISSN: 1857-7881 (Print)
e-ISSN 1857-7431 (Online)

Figures 10 and 11 present the I–V and P–V curves of a solar panel under different temperature conditions. It is observed that the short-circuit current increases slightly with temperature, while the open-circuit voltage decreases significantly. This voltage drop is associated with the increase in the saturation current of the panel's internal diode, a phenomenon that is accentuated by heat. Consequently, the shape of the I–V curves shifts toward lower voltages as temperature rises.

As a result, the maximum power produced by the solar panel decreases with increasing temperature. The optimal operating point (MPP) shifts toward lower voltages, indicating a loss of energy efficiency. In other words, even though the current increases slightly, the voltage drop dominates and leads to a reduction in the available power. Therefore, the solar panel exhibits reduced performance under high-temperature conditions.

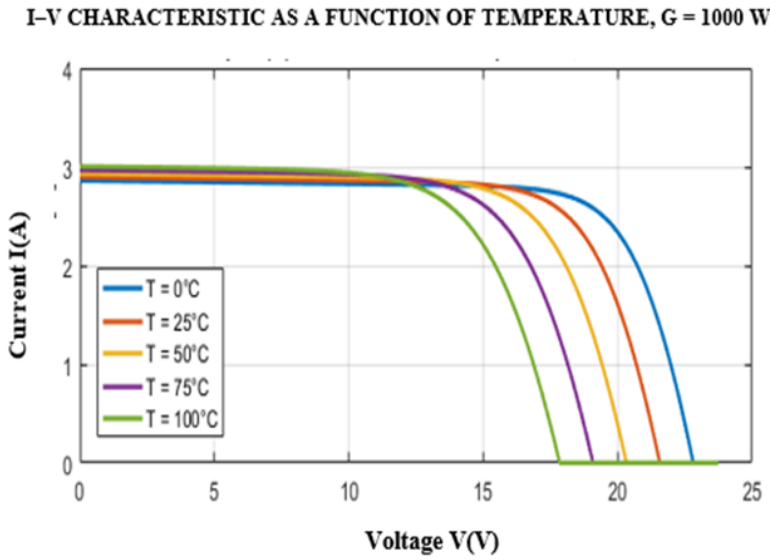

Figure 10: Characteristic $P = f(V)$as a Function of Temperature

ISSN: 1857-7881 (Print)
e-ISSN 1857-7431 (Online)

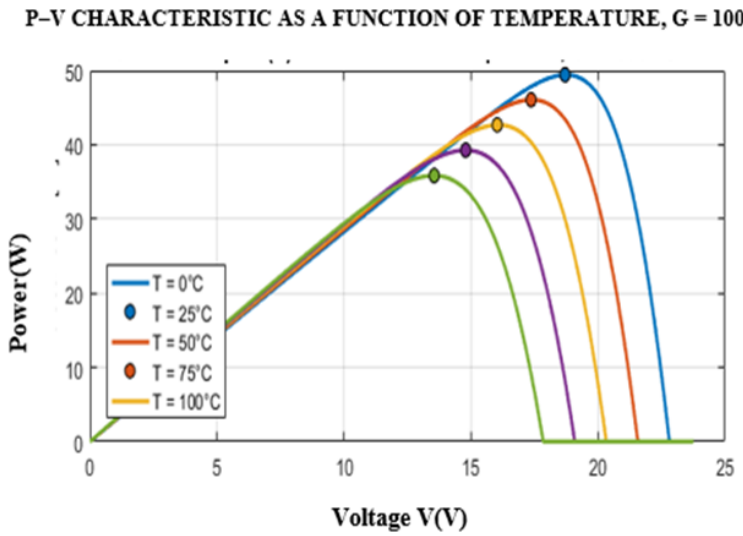

Figure 11: Characteristic $I = f(V)$as a Function of Temperature

Simulation of current–voltage (I–V) and power–voltage (P–V) characteristics

Figures 12 and 13 illustrate the current–voltage (I–V) and power–voltage (P–V) characteristic curves obtained from the numerical model of the photovoltaic module, compared with noisy simulated measurements. These results validate the consistency of the model and allow assessment of its accuracy in the context of photovoltaic system monitoring.

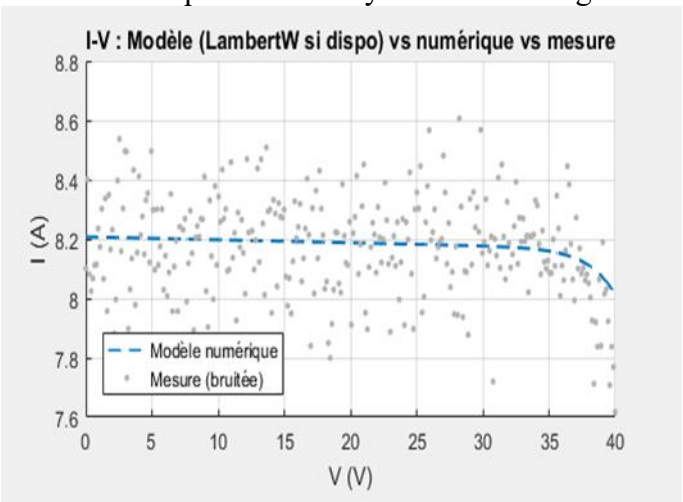

Figure 12: Current–Voltage (I–V) Characteristics

ISSN: 1857-7881 (Print)
e-ISSN 1857-7431 (Online)

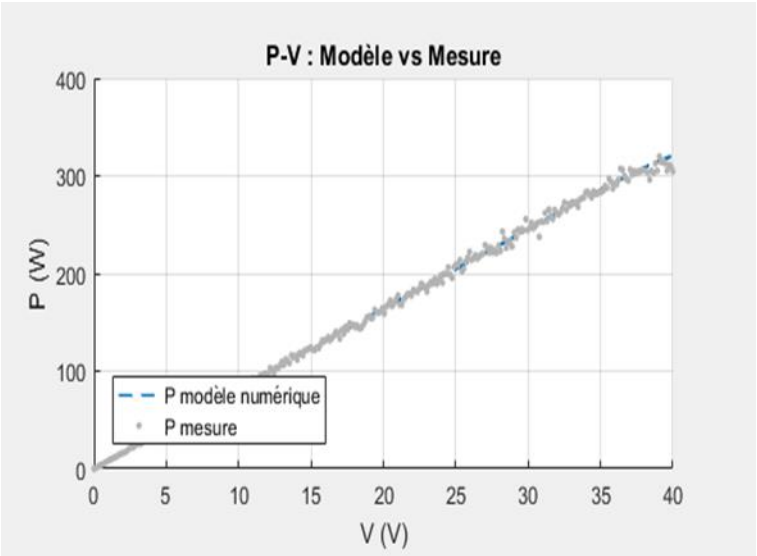

Figure 13: Characteristic P-V

Figure 12 shows that the numerical model curve (blue line) closely follows the general trend of the noisy measurement points (gray). The current remains nearly constant up to a voltage of approximately 35 V, after which it drops, a typical behavior of a photovoltaic generator. The slight fluctuations around the modeled curve originate from the added measurement noise, which simulates the inaccuracy of real sensors (thermal noise, temperature variation, electronic tolerances, etc.).

The obtained RMSE of the current (≈ 0.1608 A) corresponds to a relative error of less than 2% of the nominal current (≈ 8 A), indicating excellent agreement between the theoretical model and the measurements.

Figure 13 demonstrates an evolution consistent with theory: the power increases with voltage until reaching a maximum power point (MPP) around 33–35 V, then decreases beyond this value. The near-perfect overlap between the modeled curve and the noisy measurements confirms the validity of the numerical model for predicting the energy behavior of the module.

The obtained RMSE of the power (≈ 3.6860 W) is also very small compared to the maximum power (≈ 300 W), corresponding to a relative error of about 1.2%. This level of accuracy is more than sufficient for intelligent supervision applications, particularly for detecting efficiency drifts or operational faults.

Model errors and evaluation

Figures 14 and 15, respectively, present the deviations between the model and the measurements for current and power. The current error

ISSN: 1857-7881 (Print)
e-ISSN 1857-7431 (Online)

oscillates randomly around zero without systematic drift, indicating an unbiased and statistically reliable model.

The power deviations remain generally small but increase slightly in the high-voltage region, where the operating point sensitivity is maximal.

These observations confirm the robustness of the model against disturbances and parametric uncertainties (variations in R_s, R_p, I_0, etc.).

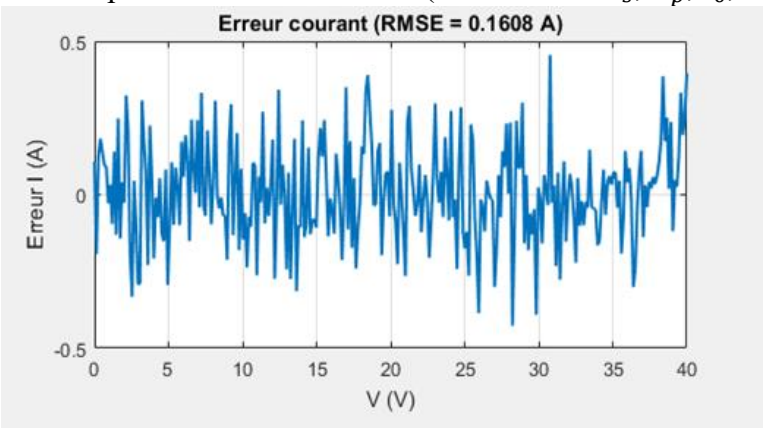

Figure 14: Current Error (RMSE = 0.1608 A)

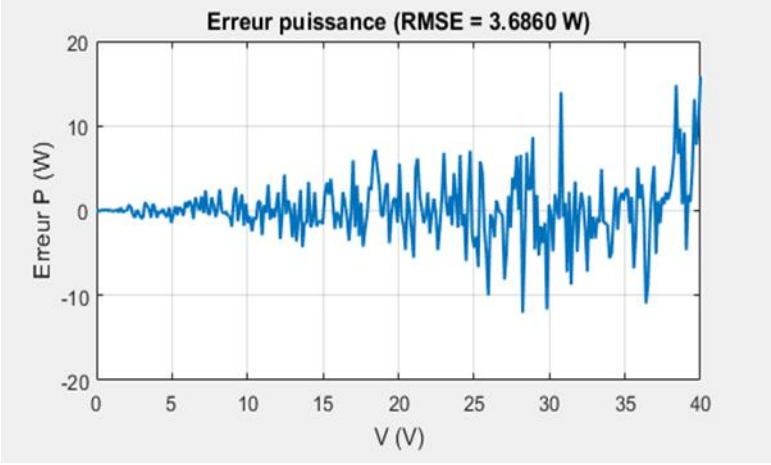

Figure 15: Power Error (RMSE = 3.6860 W)

The overall results demonstrate that the implemented PV model faithfully reproduces the electrical behavior of the photovoltaic module. The low RMSE values confirm the excellent accuracy of the Lambert-W/numerical model, enabling its use as a reliable reference for supervision.

In a real supervision architecture (e.g., via Zabbix or MQTT), this model can serve as a basis for:

- ✓ automatically detecting performance drifts,
- ✓ identifying losses due to soiling or interconnection faults, and

ISSN: 1857-7881 (Print)
e-ISSN 1857-7431 (Online)

- ✓ optimizing the operating point of the PV system.

This validation step, therefore, constitutes proof of the proper functioning of the supervision model and ensures its reliability for monitoring and predictive maintenance of the photovoltaic field.

Table 5 below presents a summary of the results related to the current–voltage and power–voltage characteristics, as well as the types of detected anomalies and the proposed solutions.

Table 5: Module Characteristics and Detection Performance

Parameter / Indicator	Value / Result	Remarks / Interpretation
PV Module	ISOFOTON I 50	Monocrystalline, 36 cells
Nominal Power (P_nom)	50 W	Standard residential capacity
Optimal Voltage (V_m)	14.9 V	Voltage at maximum power point (MPP)
Optimal Current (I_m)	2.62 A	Current at maximum power point (MPP)
Number of Cells	36	—
Current RMSE (I)	0.1608 A	Relative error < 2 %
Power RMSE (P)	3.686 W	Relative error ≈ 1.2 %
Anomaly Detection	Yes	Based on the Lambert W model / I–V measurements
Types of Errors Detected	Performance drift, losses due to soiling, and interconnection faults	Rapid detection and localization possible
Model Validity	Excellent	Agreement between simulated measurements and noisy data

Conclusion

This study provides a scientific contribution to improving the reliability and maintenance of photovoltaic (PV) systems, with a focus on the African and Congolese context. The analysis confirms that PV installations, despite their economic and energy advantages, remain susceptible to faults that can reduce performance and availability. The proposed methodology, based on modeling the I–V and P–V characteristics of the **PV cell** and applying the Lambert W model, enables precise simulation and analysis of operational failures. Results, summarized in Tables 1 and 3, show a root mean square error (RMSE) of 0.1608 A for current (≈2 % of nominal 8 A) and 3.686 W for power (≈1.2 % of maximum 300 W), validating the model's accuracy. These findings demonstrate the system's effectiveness for rapid fault detection, precise localization, and operating point optimization, providing a solid foundation for intelligent supervision and predictive maintenance, ultimately enhancing PV system reliability, efficiency, and energy productivity.

Conflict of Interest: The authors reported no conflict of interest.

Data Availability: All data are included in the content of the paper.

ISSN: 1857-7881 (Print)
e-ISSN 1857-7431 (Online)

Funding Statement: The authors did not obtain any funding for this research.

References:

1. I. E. Al-Shetwi and M. E. El-Hawary, "Performance driven energy costing: A novel analysis of solar photovoltaic cost performance and generation dynamics feeding hydrogen production," Energy Reports, vol. 13, pp. 5704–5730, Jun. 2025, doi: 10.1016/j.egyr.2025.02.053. :contentReference[oaicite:0]{index=0}
2. A. Luque and S. Hegedus, *Handbook of Photovoltaic Science and Engineering*, 2nd ed. Chichester, U.K.: Wiley, 2011.
3. Mikael, *Calculer la rentabilité d'une installation photovoltaïque en 2025 : guide complet*, Comparateur Panneau Solaire, avril 2025. [En ligne]. Disponible sur : https://www.comparateur-panneau-solaire.fr
4. A. Benzagmout, *Identification et détection de défauts dans les installations photovoltaïques*, Thèse de doctorat, PROMES, France, 2021. [En ligne]. Disponible sur : https://theses.hal.science/tel-04418470
5. Z. Djallel et Z. Zitouni, *Étude et détection de défauts dans un système photovoltaïque*, Université de Bordj Bou Arreridj, 2020. [En ligne]. Disponible sur : https://dspace.univ-bba.dz
6. Bari, A. & Jarwar, A.R. (2025). *PV Fault Diagnosis, Including Signal Acquisition, Signal Processing, and Fault Analysis*. Journal of Power and Energy Engineering, 13(7), 75–101.
7. K. Achour, *Calculer la rentabilité de son installation solaire*, Reonic, juillet 2025. [En ligne]. Disponible sur : https://reonic.com
8. Venkatakrishnan, G.R. et al. (2023). *Detection, location, and diagnosis of different faults in large solar PV systems—A review*. Int. J. of Low-Carbon Technologies, 18, 659–674.
9. Khaled Alosmani, *Optimisation des systèmes photovoltaïques : vers une meilleure efficacité et des performances sans défaut*, Thèse, LARIS, 2023. [En ligne]. Disponible sur : https://theses.hal.science/tel-04505262
10. A. Benzagmout, *Identification et détection de défauts côté DC dans les installations photovoltaïques*, PROMES, 2021. [En ligne]. Disponible sur : https://theses.hal.science/tel-04418470
11. Souaad Tahraoui, *Cours : Détection et localisation des défauts*, Université de Chlef, 2023. [En ligne]. Disponible sur : https://www.univ-chlef.dz
12. J. Cubas, S. Pindado, and M. Victoria, "On the analytical approach for modeling photovoltaic systems behavior," Solar Energy, vol. 105, pp. 199–206, Jul. 2014.

ISSN: 1857-7881 (Print)
e-ISSN 1857-7431 (Online)

13. Tahraoui, M. et al. (2023). *Performance analysis of PV systems based on meteorological data correlation*. Renewable Energy Journal.
14. Axiome Énergie, *Optimiser la production solaire avec des outils de monitoring*, 2025. [En ligne]. Disponible sur : https://www.axiome-energie.fr
15. A. Benzagmout et al., "Identification et détection de défauts dans les installations photovoltaïques," *IEEE Transactions on Sustainable Energy*, vol. 12, no. 3, pp. 1456–1464, 2021.
16. Z. Djallel and Z. Zitouni, "Comparative study of fault detection methods in PV systems," *Renewable Energy*, Elsevier, vol. 158, pp. 1123–1132, 2020.
17. K. Alosmani et al., "Hybrid diagnostic approach for PV systems using thermal and electrical modeling," *IEEE Journal of Photovoltaics*, vol. 13, no. 1, pp. 88–97, 2023.
18. M. Kouadri and D. Bouchafaa, "Spectral analysis for partial shading fault detection in PV modules," *Journal of Renewable Energy*, Hindawi, vol. 2022, Article ID 9876543.
19. A. Achour et al., "Low-cost embedded monitoring system for rural PV installations," *Energy Reports*, Elsevier, vol. 10, pp. 456–465, 2024.
20. S. Tahraoui et al., "Fault localization in PV fields using transient response analysis," *IEEE Access*, vol. 10, pp. 12345–12356, 2022.
21. M. Khan et al., "Thermal image-based fault classification in PV systems using CNN," *Journal of Sensors*, Hindawi, vol. 2023, Article ID 7654321.
22. J. Mikael et al., "Satellite-based performance monitoring of PV systems," *Solar Energy*, Elsevier, vol. 245, pp. 1021–1030, 2025.
23. Sepúlveda Oviedo, E.H. et al. (2023). *Fault diagnosis of photovoltaic systems using artificial intelligence: A bibliometric approach*. Heliyon, 9(11), e21491.

ESJ Natural/Life/Medical Sciences Peer-reviewed

Theophylline and Caffeine Content in Black Tea Produced in Burundi

Alice Ndayirukiye, PhD Student
Doctoral school, University of Burundi, Department of Chemistry,
Faculty of Sciences, CRSNE, Bujumbura, Burundi
Prof. Ferdinand Ndikuryayo
State Key Laboratory of Green Pesticide,
Guizhou University, Guiyang, P.R. China
Prof. Pierre Claver Mpawenayo
Dr. Jeremie Ngezahayo
Prof. Godefroid Gahungu
Department of Chemistry, Faculty of Sciences, CRSNE,
University of Burundi, Bujumbura, Burundi

Doi:10.19044/esj.2026.v22n6p59

Submitted: 17 December 2025
Accepted: 31 January 2026
Published: 28 February 2026

Cite As:
Ndayirukiye, A., Ndikuryayo, F., Mpawenayo, P.C., Ngezahayo, J. & Gahungu, G. (2026). *Theophylline and Caffeine Content in Black Tea Produced in Burundi*. European Scientific Journal, ESJ, 22 (6), 59. https://doi.org/10.19044/esj.2026.v22n6p59

Abstract

To date, the specific levels of theophylline in Burundian tea remain unknown, and scientific information regarding caffeine content is limited. This study aims to address this gap by determining the content of these methylxanthines in different grades of black tea produced across the six main tea-growing regions of Burundi. Using High-Performance Liquid Chromatography (HPLC) based on the reference NTC-ISO 20481 method, samples collected from a dry-season production by Office du Thé du Burundi (OTB) and Promotion pour la Théiculture à Mwaro (PROTHEM) were analyzed. The results revealed that the theophylline content ranged from 0.145% to 0.279%, while caffeine levels varied between 1.979% and 3.331%. The significant variations ($p < 0.05$) depending on both the region and the tea grade were also revealed. Generally, the PD and D1 grades were identified as the richest in methylxanthines, with OTB-produced teas showing higher concentrations than those from PROTHEM. These findings confirm that

ISSN: 1857-7881 (Print)
e-ISSN 1857-7431 (Online)

Burundian tea is comparable to premium East African teas and remains within safe limits for daily consumption. The results of this study should help consumers to control the amount of these methylxanthines according to their nutritional needs, while Burundian black tea companies could use them to better promote this product and better position themselves on the international market.

Keywords: Burundi tea, Caffeine, Theophylline, HPLC

Introduction

Tea, derived from the leaves of the plant Camellia *sinensis*, is the most widely consumed beverage in the world after water (Sajilata et al., 2008). It is one of the three most consumed non-alcoholic beverages globally (Rahman et al., 2013), and its consumption has increased considerably over the years. Considered healthier than coffee and cocoa, tea is strongly recommended by the World Health Organization (Dutta, 2017) and remains one of the most affordable beverages available (A. Hicks, 2009).

The health benefits of tea are largely attributed to biologically active ingredients, particularly a subgroup of alkaloids known as methylxanthines (Monteiro et al., 2016). These compounds, which include caffeine, theobromine, and theophylline, are chemically very similar (Figure 1) and are mainly found in foods such as coffee beans, cocoa beans, and tea leaves (Srdjenovic et al., 2008; Rodriguez et al., 2015). They play an important role in human health (Fernández et al., 2002) by sharing stimulatory effects on the central nervous system, as well as on the gastrointestinal, cardiovascular, renal, and respiratory systems (de Sena et al., 2011).

Among these, caffeine was first isolated from tea in the early 1820 (Ashihara et al., 2008). It acts as a mild stimulant and is metabolized in the liver into paraxanthine (80%), theobromine (11%), and theophylline (4%) (Londzin et al., 2021). Theophylline (1,3-dimethylxanthine) has been used for many years as a bronchodilator for chronic respiratory diseases like asthma (Jafari et al., 2011) and recently proposed as an adjuvant in COVID-19 treatment due to its immunomodulatory properties (Montaño et al., 2022). However, side effects such as nausea and dizziness can occur, necessitating dose moderation (B. Zhu et al., 2015).

ISSN: 1857-7881 (Print)
e-ISSN 1857-7431 (Online)

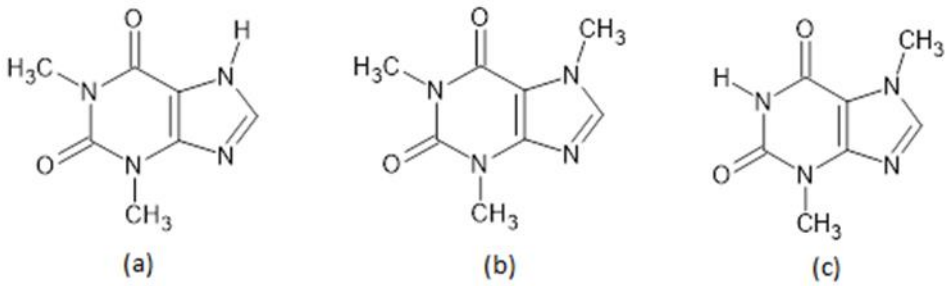

Figure 1: Chemical structures of (a) theophylline; (b) caffeine and (c) theobromine

Various factors, including soil, climate, plucking season, and processing methods, lead to variability in the methylxanthine content of tea (Dubuis et al., 2014 ; Turkmen & Velioglu, 2007 ; Baek et al., 2022).

In Burundi, the production and commercialization of tea across different grades are exclusively held by the Office du Thé du Burundi (OTB) and Promotion de la Théiculture à Mwaro (PROTHEM). Although Burundian tea is exported to many other countries??, currently, these organizations rely primarily on organoleptic tests to assess black tea quality before marketing. To the best of our knowledge, the specific levels of theophylline in Burundian tea remain unknown, and scientific information regarding caffeine content is limited. While it is established that content varies with the plucking season, determining these levels in dry-season production using High-Performance Liquid Chromatography (HPLC) would provide significant added value.

This work aims to determine the amounts of theophylline and caffeine in different grades of black tea produced in Burundi, considering both the grade and the production region. To achieve these objectives, a modified HPLC method (NTC-ISO 20481, 2008) was employed. This study expects to classify tea-growing regions based on their methylxanthine content. Ultimately, Burundian tea growers, industrialists, and consumers will benefit from understanding the levels of these compounds, allowing for better awareness, regulatory measures, and a clearer positioning of Burundian black tea quality.

Material and Methods

The sampling

The study was conducted on black tea samples collected from six major tea-growing regions in Burundi. The sampling sites and the corresponding processing factories managed by the OTB and PROTHEM are geographically illustrated in Figure 2.

ISSN: 1857-7881 (Print)
e-ISSN 1857-7431 (Online)

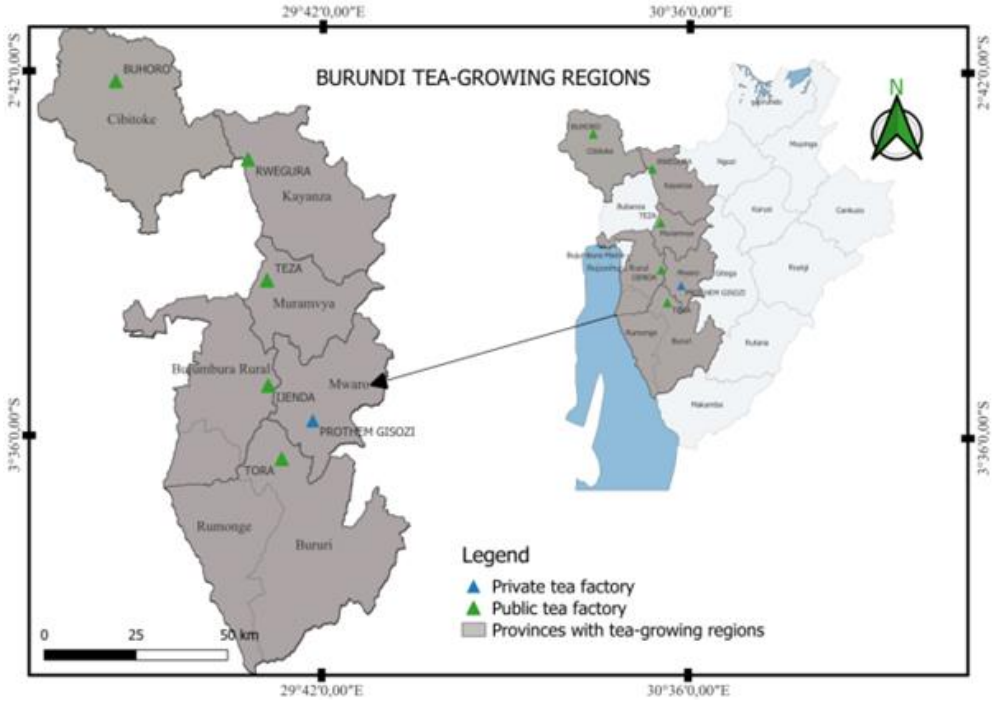

Figure 2: The location of tea processing factories in Burundi on map (the green triangles are used for the five OTB factories and the blue triangle for the PROTHEM factory).

Table 1: Distribution of samples by processing factories

Samples	TORA	TEZA	IJENDA	BUHORO	RWEGURA	GISOZI
PF1	+	+	+	+	+	+
BP1	+	+	+	+	+	+
PD	+	+	+	+	+	+
D1	+	+	+	+	+	+
D	-	+	+	+	-	+
F1	-	-	+	+	+	+
FS1	+	-	-	-	-	-
FS	+	+	-	+	-	-
BMF	+	+	+	+	+	-

The + and - signs indicate the availability and non availability of the tea grade at the factory at the time of sampling (PF1 = Pekoe Fannings One, BP1= Broken Pekoe One, PD = Pekoe Dust, D1 = Dust One, D = Dust, F1=Fannings, FS1= Fannings One, BMF = Broken Mixed Fannings).

A total of 41 samples were collected during the dry season production period, specifically between June and August 2022. The distribution of black tea grades varied based on factory availability at the time of sampling. The detailed distribution of samples across regions and grades is summarized in Table 1.

ISSN: 1857-7881 (Print)
e-ISSN 1857-7431 (Online)

Choice of method

The selection of High-Performance Liquid Chromatography (HPLC) was predicated on the requirement for a highly sensitive analytical method capable of simultaneously quantifying caffeine and theophylline, given that the latter typically occurs in trace amounts in tea (Baek et al., 2022).

Chemicals and reagents

The analytical standards used were pure theophylline (purity > 99%, SIGMA) and pure caffeine (Merck 2584, Germany). Reagents included analytical grade methanol and glacial acetic acid. Ultrapure water was obtained using a Puranity PU 15 UV/UF+ system.

Instrumentation and HPLC conditions

General laboratory equipment used for sample preparation included an analytical balance (SARTORIUS, QUINTIX35-1S, ®), a heated magnetic stirrer, centrifuge tubes, and a centrifuge (Eppendorf 5810R). Chromatographic analyses were conducted using an Agilent 1260 Infinity II UV HPLC system equipped with a Poroshell 120 EC-C18 column (4.6 × 100 mm) for separation. The mobile phase consisted of a mixture of water, methanol, and glacial acetic acid in a volumetric ratio of 79:20:1 (v/v/v), which was degassed in a Bransonic CPX3800 (CPX-952-818R) ultrasonic bath for 15 minutes prior to use. The optimized operating conditions included a flow rate of 0.9 mL/min, an injection volume of 10 µL, and a column temperature maintained at 40°C. Detection was performed via UV absorption at a wavelength of 272 nm, with a total run time set to 8 minutes per injection.

Preparation of standard solutions

Stock standard solutions (1000 ppm) of theophylline and caffeine were prepared by dissolving 0.10030 g and 0.10067 g of the respective pure standards in 100 mL of ultrapure water. From these stock solutions, a series of five diluted working standards were prepared to establish calibration curves (Table S1, Supporting Information: SI). The linearity of the method was verified by plotting peak areas against concentrations (Figure S1 and Table S2, SI).

Preparation of samples

The extraction protocol was based on the ISO method for caffeine determination (NTC-ISO 20481, 2008), with modification to the extraction time informed by existing literature (M. B. Hicks et al., 1996; López-Martínez et al., 2003a; X. Zhu et al., 2004). To optimize the solid-liquid extraction time for simultaneous determination, 5 g (± 0.01 mg) of a tea sample (Grade D1) and 5 g of magnesium oxide were added to 500 mL of distilled water in a flask.

ISSN: 1857-7881 (Print)
e-ISSN 1857-7431 (Online)

Three independent extraction runs were subsequently conducted under boiling conditions for durations of 30, 45, and 60 minutes, respectively. Upon completion, the solutions were cooled to room temperature, and a 50 mL aliquot from each run was centrifuged at 1510 rpm for 15 minutes. The resulting supernatant was filtered through a 0.20 μm microfilter into a vial for HPLC analysis, and the results of this preliminary optimization (Table S3, SI) indicated that 60 minutes was the optimal extraction time.

Sample analysis

Following optimization, all 41 tea samples were prepared using the protocol described above, with the solid-liquid extraction time fixed at one hour. Standards and samples were injected into the HPLC system under the conditions described in the instrumentation and HPLC conditions section. Compounds were identified by retention time and quantified using the best-fit linear regression equation from the calibration curves.

Statistical analysis

Statistical processing was carried out using SPSS software (*IBM SPSS Statistics for Windows*, 2020). An Analysis of Variance (ANOVA) was performed to assess the significance of differences between regions and grades. The Duncan multiple range test (Duncan, 1955) was applied to identify homogeneous groups and statistically significant differences ($p < 0.05$).

Results

Calibration and calculation of content

The linearity of the analytical method was confirmed through calibration curves for both analytes, which are displayed in Figure S1 (SI). The strong correlation observed allows for the direct determination of concentrations based on peak areas.

The final content of theophylline and caffeine in the tea samples was calculated using the following equation,

$$Content(\%) = \left[\frac{conc.(mg/L) \times V(L)}{m(g) \times 1000(mg)} \right] \times 100$$

where:

Conc. is the concentration (g/L) of theophylline or caffeine derived from the calibration curve;

V is the volume (L) of water used for the solid-liquid extraction;

m is the mass (g) of the tea sample.

ISSN: 1857-7881 (Print)
e-ISSN 1857-7431 (Online)

Average theophylline content

The quantitative results for theophylline across the 41 black tea samples are summarized in Table 2. Detailed statistical data, including the results of the Duncan multiple range test for significant differences, are provided in Table S4 (SI). To facilitate a visual comparison of the variations across different regions and grades, the trends in theophylline content are illustrated in Figure 3.

Average caffeine content

The average caffeine concentrations determined for the different grades of black tea produced in Burundi are presented in Table 3 and Table S5 (SI). Similar to theophylline, the distribution and specific trends of caffeine content across all tea-growing regions are depicted in Figure 4.

Comparative analysis of extraction method

To evaluate the influence of the preparation method, the methylxanthine content obtained via the standard ISO extraction was compared with the infusions prepared using tap water for five minutes. The raw data from these three comparative tests are listed in Table S6 (SI), while the aggregated average values are summarized in Table 4.

Table 2: Average theophylline content (% w/w) in different grades of tea from the same region

Grade	TORA	TEZA	IJENDA	MABAYI	RWEGURA	GISOZI
PF1	0.196 ± 0.011^{b}	0.207 ± 0.003^{c}	0.205 ± 0.007^{bc}	0.203 ± 0.003^{d}	0.188 ± 0.003^{c}	0.145 ± 0.009^{c}
BP1	0.201 ± 0.006^{b}	0.204 ± 0.005^{c}	0.189 ± 0.001^{d}	0.227 ± 0.003^{d}	0.206 ± 0.013^{b}	0.165 ± 0.003^{ab}
PD	0.202 ± 0.003^{ab}	0.230 ± 0.011^{ab}	0.214 ± 0.013^{ab}	0.279 ± 0.017^{a}	0.238 ± 0.014^{a}	0.169 ± 0.009^{ab}
D1	0.216 ± 0.002^{a}	0.220 ± 0.002^{b}	0.204 ± 0.003^{bc}	0.219 ± 0.021^{cd}	0.233 ± 0.004^{a}	0.177 ± 0.004^{a}
D	-	0.220 ± 0.011^{b}	0.199 ± 0.003^{cd}	0.257 ± 0.010^{b}	-	0.173 ± 0.003^{ab}
F1	-	-	0.206 ± 0.004^{bc}	0.220 ± 0.007^{cd}	0.203 ± 0.004^{b}	0.161 ± 0.009^{b}
FS	0.198 ± 0.003^{b}	0.241 ± 0.006^{a}	-	0.231 ± 0.002^{c}	-	-
FS1	0.213±0.001*	-	-	-	-	-
BMF	0.212 ± 0.006^{a}	0.205 ± 0.001^{c}	0.218 ± 0.001^{a}	0.170 ± 0.002^{e}	0.174 ± 0.003^{c}	-
P-Value	0.002	0.000	0.001	0.000	0.000	0.001

*The sign - indicates that the grade is not produced. In the same column, (a-e)the same superscripts for grades from the same region indicate that theophylline contents are statistically identical. *No comparison.*

ISSN: 1857-7881 (Print)
e-ISSN 1857-7431 (Online)

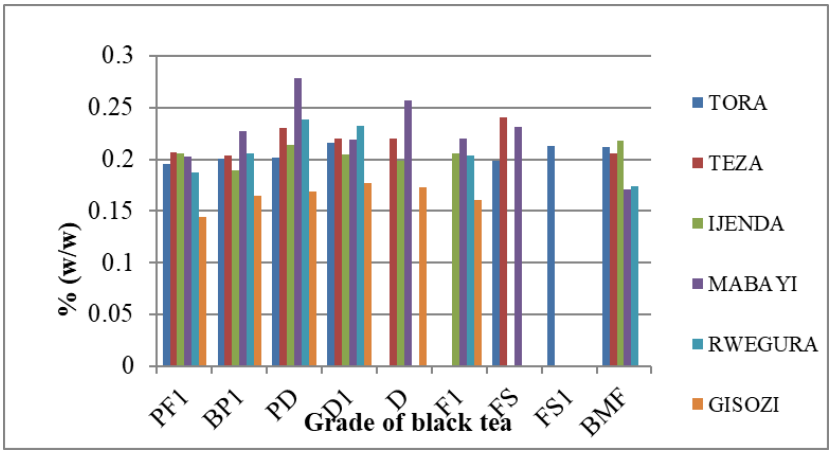

Figure 3: Theophylline content as a function of grade of black tea from the six regions

Table 3: Average caffeine content (% w/w) of different grades of tea from the same region

Grade	TORA	TEZA	IJENDA	MABAYI	RWEGURA	GISOZI
PF1	2.898±0.022^{c}	2.926±0.012^{ab}	2.627±0.018^{d}	3.004±0.026^{d}	2.397±0.017^{e}	2.528±0.021^{bc}
BP1	2.944±0.020^{b}	2.825±0.031^{bc}	2.687±0.018^{c}	2.923±0.039^{e}	2.443±0.023^{d}	2.509±0.021^{c}
PD	2.527±0.018^{f}	2.822±0.024^{bc}	2.756±0.021^{b}	3.331±0.055^{a}	3.213±0.034^{a}	2.703±0.023^{a}
D1	2.706±0.018^{e}	2.987±0.025^{a}	2.881±0.016^{a}	3.126±0.015^{b}	2.724±0.019^{c}	2.705±0.021^{a}
D	-	2.947±0.152^{a}	2.853±0.015^{a}	3.059±0.017^{c}	-	2.583±0.030^{b}
F1	-	-	2.672±0.019^{c}	2.774±0.026^{f}	3.006±0.020^{b}	2.460±0.014^{d}
FS	2.817±0.018^{d}	2.766±0.015^{c}	-	2.729±0.016^{f}	-	-
FS1	3.068±0.021*	-	-	-	-	-
BMF	2.921±0.018^{bc}	2.293±0.023^{d}	2.586±0.023^{e}	1.979±0.015^{g}	2.232±0.018^{f}	-
P-Value	0.000	0.000	0.000	0.000	0.000	0.000

*The sign - indicates that the grade is not produced. (a-g) in the same column, the same superscript (a-g) for grades from the same region indicate that theophylline contents are statistically identical. *No comparison.*

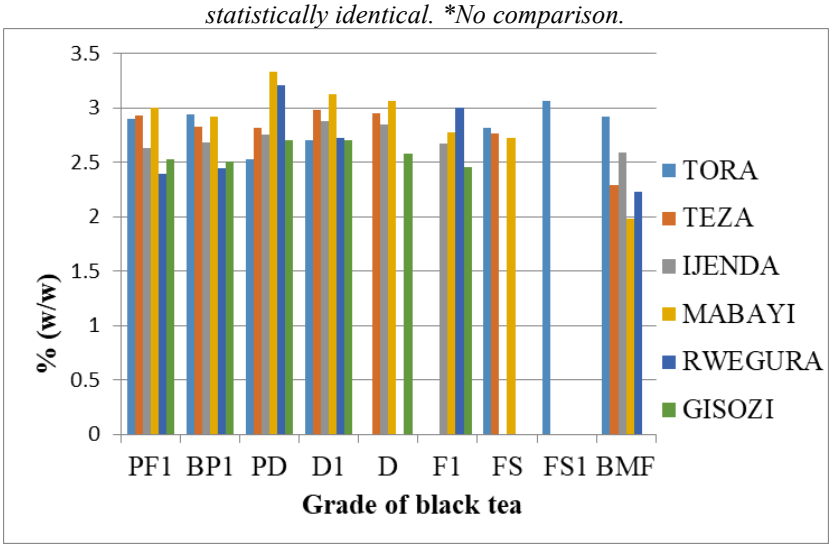

Figure 4: Caffeine content as a function of grade of black tea from the six regions

ISSN: 1857-7881 (Print)
e-ISSN 1857-7431 (Online)

Table 4: Average value of theophylline and caffeine content (% w/w) determined from tea infusions*

Sample	Theophylline	Caffeine
PD MABAYI	0.307±0.008 (0.279±0.017)[a]	3.034±0.017 (3.331±0.055)[b]
PF1 GISOZI	0.211±0.004 (0.145±0.009)[a]	2.334±0.001 (2.528±0.021)[b]

** Prepared using tap water infusion. a ISO 20481 based theophylline content value from this study and b ISO 20481 based caffeine content value from this study.*

Discussion

Method validation and linearity

The reliability of the analytical method was established prior to sample analysis. The calibration curves displayed in Figure S1 (SI) demonstrate excellent linearity, implying a strong correlation between peak area and concentration for the standard solutions ($R^2 = 0.99996$ for theophylline and $R^2 = 0.99998$ for caffeine).

Regarding extraction efficiency, the results of the theophylline extraction test yielded contents of 0.270%, 0.272%, and 0.282% for 30, 45, and 60 minutes, respectively. This aligns with previous studies indicating that the maximum extraction time of caffeine by water is one hour (Mourya et al., 2019). These results confirm that xanthines can be extracted and assayed simultaneously, in accordance with established protocols (de Sena et al., 2011 ; Horžić et al., 2009).

Theophylline content and variation

The results summarized in Tables 2 and S4 show that the average theophylline content of different grades of black tea produced in all tea-growing regions varies between 0.145% and 0.279%. Specifically, MABAYI black tea grade PD exhibits the highest theophylline content (0.279 ± 0.017%), while the lowest (0.145 ± 0.009%) is found in GISOZI black tea grade PF1.

Based on the average theophylline content, the classification of tea grades in ascending order for each region is as follows:

TORA: PF1 < FS < BP1 < PD < BMF < FS1 < D1
TEZA: BP1 < BMF < PF1 < D < D1 < PD < FS
IJENDA: BP1 < D < D1 < PF1 < F1 < PD < BMF
MABAYI: BMF < PF1 < D1 < F1 < BP1 < FS < D < PD
RWEGURA: BMF < PF1 < F1 < BP1 < D1 < PD
GISOZI: PF1 < F1 < BP1 < PD < D < D1

Analysis of variance (ANOVA) revealed very significant differences ($p < 0.05$) between the contents of tea grades within the same region and within the same grade across different regions. However, the Duncan post-hoc test indicates that PD and D1 grades have statistically identical contents in all tea-growing regions except for MABAYI.

ISSN: 1857-7881 (Print)
e-ISSN 1857-7431 (Online)

Overall, as summarized in Figure 3, the so-called "fibre-free first-line" grades found in all regions are generally rich in theophylline. Notably, the BMF grade (fibrous second-line) is also rich in theophylline across all regions. Furthermore, theophylline content of tea grades produced by OTB factories is generally higher than those produced by PROTHEM, with significant statistical differences.

The level of theophylline in Burundian black tea (0.145% to 0.279%) is relatively higher than data available in scientific literature, where reliable ranges are often 0.02–0.04% (Graham, H.N., 1984a ; Szymański et al., 2022) or as low as 0.00248% in South Korean tea (Baek et al., 2022). However, our results are comparable to Kenyan black tea (0.2331%) reported by Szymański et al. (2022). These variations can be ascribed to different manufacturing processes and processing methods (Turkmen & Velioglu, 2007).

Caffeine content and variation

As presented in Table 3 and S5 (SI), the average caffeine content varies between 1.979% and 3.331%. MABAYI PD grade black tea showed the highest caffeine content (3.331±0.055%), while the lowest was observed in the same region for BMF grade (1.979±0.015 %).

In general, the average caffeine content of the different grades allows us to establish a classification in ascending order for each of the six tea-growing regions:

TORA: PD < D1 < FS1 < PF1 < BMF < BP1
TEZA: BMF < FS < PD < BP1 < PF1 < D < D1
IJENDA: BMF < PF1 < F1 < BP1 < PD < D < D1
MABAYI: BMF < FS < F1 < BP1 < PF1 < D < D1 < PD
RWEGURA: BMF < PF1 < BP1 < D1 < F1 < PD
GISOZI: F1 < BP1 < PF1 < PD < D < D1

The results plotted in Figure 4 clearly show that, generally, PD and D1 grades are the richest in caffeine across most regions. The analysis of variance reveals a p-value much lower than 0.05, confirming that caffeine content varies significantly between grades in the same region. Nevertheless, the Duncan test identified some statistically identical contents, such as BP1 and PF1 exclusively in the TEZA and GISOZI regions. Similar to theophylline, OTB tea grades showed higher caffeine levels than PROTHEM grades.

The caffeine results are in line with global literature. Burundian tea levels (1.979%–3.331%) are comparable to teas consumed in Spain (1.8–3%) (Sanchez, 2017) and the UK (2.2–2.8%) (Khokhar & Magnusdottir, 2002) , as well as recent multi-country studies showing ranges of 2.37–3.3% (Szymański et al., 2022).

ISSN: 1857-7881 (Print)
e-ISSN 1857-7431 (Online)

Influence of preparation method and health implications

A comparison was made between the standard ISO 20481 method and a simple infusion (Table 4) using two samples (MABAYI PD and GISOZI PF1). The results show that theophylline content is higher in the infusion (0.211%–0.307%) than in the extract obtained using the ISO method (0.145%–0.279%).

This may be attributable to the nature of the water used. The acid-base properties of theophylline allow better extraction in slightly alkaline tap water compared to neutral distilled water (Bruneton, 2009). Mineral ions (Ca^{2+} and Mg^{2+}) in tap water promote the formation of water-soluble complexes by replacing the hydrogen on the N-7 position of the theophylline imidazole ring, whereas caffeine remains stable in pure water (Zareef et al., 2020; Astill et al., 2001).

Despite the extraction efficiency (Table S7, SI), the amount of theophylline per cup (250 ml) remains low (6.97 mg – 11.93 mg), which is well below the therapeutic doses of 13 mg/kg/24h for adults (Matte et al., 1982).

Regarding caffeine, concentrations range from 38.85 mg/cup for lighter varieties to 58.88 mg/cup for stronger ones. According to the European Food Safety Authority (EFSA Panel on Dietetic Products, Nutrition and Allergies (NDA, 2015), the safe daily intake for a healthy adult is 400 mg/day. This means consumers can safely enjoy up to 6 cups of the stronger Burundian tea or 10 cups of the lighter varieties daily. This aligns with UK consumption patterns (92–146 mg/day) (Khokhar & Magnusdottir, 2002), suggesting Burundian tea is a safe and flavorful source of methylxanthines.

Conclusion

This study successfully determined the theophylline and caffeine contents in various grades of black tea produced across the six main tea-growing regions of Burundi. Using a modified HPLC method (NTC-ISO 20481), we demonstrated that methylxanthine levels vary significantly depending on both the geographical region and the grade of tea.

Our findings reveal that Burundian black tea produced in dry season contains theophylline levels ranging from 0.145% to 0.279% and caffeine levels from 1.979% to 3.331%. Generally, the PD and D1 grades were identified as the richest in both compounds across most regions, while significant differences were observed between teas produced by OTB and PROTHEM. From a consumer perspective, we found that infusion with tap water extracts theophylline more efficiently than distilled water, likely due to mineral interactions. Furthermore, despite the robust methylxanthine content, Burundian black tea remains well within safe consumption limits established

ISSN: 1857-7881 (Print)
e-ISSN 1857-7431 (Online)

by the EFSA, allowing healthy adults to consume up to 6 cups of the strongest grades daily.

As a supplement to this study, an investigation was undertaken on other bioactive compounds acting on human health. By taking into account factors such as the geographical location, the picking period, and the soil conditions of Burundi's tea-growing sites, we will be able to quantify these compounds. Further studies could build upon this foundational work by exploring the specific agronomic and technological factors that influence these chemical profiles, ultimately contributing to the optimization of tea quality in Burundi.

Acknowledgements

Alice Ndayirukiye would like to express her gratitude to the two Burundian tea companies, OTB and PROTHEM, who allowed us to obtain the samples unconditionally. To the Burundian Bureau of Standardization and Quality Control for providing access to the chemical analysis laboratory.

Conflict of Interest: The authors reported no conflict of interest.

Data Availability: All data are included in the content of the paper.

Funding Statement: The authors did not obtain any funding for this research.

References:

1. Ashihara, H., Sano, H., & Crozier, A. (2008). Caffeine and related purine alkaloids : Biosynthesis, catabolism, function and genetic engineering. *Phytochemistry*, *69*(4), 841-856. https://doi.org/10.1016/j.phytochem.2007.10.029
2. Astill, C., Birch, M. R., Dacombe, C., Humphrey, P. G., & Martin, P. T. (2001). Factors Affecting the Caffeine and Polyphenol Contents of Black and Green Tea Infusions. *Journal of Agricultural and Food Chemistry*, *49*(11), 5340-5347. https://doi.org/10.1021/jf010759+
3. Baek, G.-H., Yang, S.-W., Yun, C.-I., Lee, J.-G., & Kim, Y.-J. (2022). Determination of methylxanthine contents and risk characterisation for various types of tea in Korea. *Food Control*, *132*, 108543. https://doi.org/10.1016/j.foodcont.2021.108543
4. Bruneton, J. (2009). *Pharmacognosie, phytochimie, plantes médicinales* ((4e éd.)). 75008 Paris.
5. de Sena, A. R., de Assis, S. A., & Branco, A. (2011). *Analysis of Theobromine and Related Compounds by Reversed Phase High-Performance Liquid Chromatography with Ultraviolet Detection : An Update (1992–2011)*.

ISSN: 1857-7881 (Print)
e-ISSN 1857-7431 (Online)

6. Dubuis, E., Wortley, M. A., Grace, M. S., Maher, S. A., Adcock, J. J., Birrell, M. A., & Belvisi, M. G. (2014). Theophylline inhibits the cough reflex through a novel mechanism of action. *Journal of Allergy and Clinical Immunology*, *133*(6), 1588-1598. https://doi.org/10.1016/j.jaci.2013.11.017
7. Duncan, D. B. (1955). *Multiple range and multiple F tests. Biometrics, 11(1), 1-42.* [Logiciel].
8. Dutta, P. (2017, septembre 11). *WHO Encourages Tea Drinking for a New Generation*. World Tea News. https://www.worldteanews.com/Features/who-encourages-tea-drinking-new-generation
9. EFSA Panel on Dietetic Products, Nutrition and Allergies (NDA). (2015). Scientific Opinion on the safety of caffeine. *EFSA Journal*, *13*(5). https://doi.org/10.2903/j.efsa.2015.4102
10. Fernández, P. L., Pablos, F., Martín, M. J., & González, A. G. (2002). Study of Catechin and Xanthine Tea Profiles as Geographical Tracers. *Journal of Agricultural and Food Chemistry*, *50*(7), 1833-1839. https://doi.org/10.1021/jf0114435
11. Graham, H.N. (1984a). *Tea : The plant and its manufacture; chemistry and consumption of the beverage. In : Spiller, G.A., ed., The Methylxanthine Beverages and Foods : Chemistry, Consumption and Health Effects, New York, Alan R. Liss, pp. 29–74).*
12. Hicks, A. (2009). *Current Status and Future Development of Global Tea Production and Tea Products*.*
13. Hicks, M. B., Hsieh, Y.-H. P., & Bell, L. N. (1996). Tea preparation and its influence on methylxanthine concentration. *Food Research International*, *29*(3-4), 325-330. https://doi.org/10.1016/0963-9969(96)00038-5
14. Horžić, D., Komes, D., Belščak, A., Ganić, K. K., Iveković, D., & Karlović, D. (2009). The composition of polyphenols and methylxanthines in teas and herbal infusions. *Food Chemistry*, *115*(2), 441-448. https://doi.org/10.1016/j.foodchem.2008.12.022
15. *IBM SPSS Statistics for Windows* (Version 27.0). (2020). [Logiciel]. IBM Corp.
16. Jafari, M. T., Rezaei, B., & Javaheri, M. (2011). A new method based on electrospray ionisation ion mobility spectrometry (ESI-IMS) for simultaneous determination of caffeine and theophylline. *Food Chemistry*, *126*(4), 1964-1970. https://doi.org/10.1016/j.foodchem.2010.12.054
17. Khokhar, S., & Magnusdottir, S. G. M. (2002). Total Phenol, Catechin, and Caffeine Contents of Teas Commonly Consumed in the United

ISSN: 1857-7881 (Print)
e-ISSN 1857-7431 (Online)

Kingdom. *Journal of Agricultural and Food Chemistry*, *50*(3), 565-570. https://doi.org/10.1021/jf010153l

18. Londzin, P., Zamora, M., Kąkol, B., Taborek, A., & Folwarczna, J. (2021). Potential of Caffeine in Alzheimer's Disease—A Review of Experimental Studies. *Nutrients*, *13*(2), 537. https://doi.org/10.3390/nu13020537
19. López-Martínez, L., López-de-Alba, P. L., García-Campos, R., & De León-Rodríguez, L. M. (2003). Simultaneous determination of methylxanthines in coffees and teas by UV-Vis spectrophotometry and partial least squares. *Analytica Chimica Acta*, *493*(1), 83-94. https://doi.org/10.1016/S0003-2670(03)00862-6
20. Matte, J., Lapointe, M., & LeBel, M. (1982). Guide posologique de la theophylline et ses sels. *Canadian Family Physician*, *28*, 111-115. https://www.ncbi.nlm.nih.gov/pmc/articles/PMC2306292/
21. Montaño, L. M., Sommer, B., Gomez-Verjan, J. C., Morales-Paoli, G. S., Ramírez-Salinas, G. L., Solís-Chagoyán, H., Sanchez-Florentino, Z. A., Calixto, E., Pérez-Figueroa, G. E., Carter, R., Jaimez-Melgoza, R., Romero-Martínez, B. S., & Flores-Soto, E. (2022). Theophylline : Old Drug in a New Light, Application in COVID-19 through Computational Studies. *International Journal of Molecular Sciences*, *23*(8), Article 8. https://doi.org/10.3390/ijms23084167
22. Monteiro, J. P., Alves, M. G., Oliveira, P. F., & Silva, B. M. (2016). Structure-Bioactivity Relationships of Methylxanthines : Trying to Make Sense of All the Promises and the Drawbacks. *Molecules*, *21*(8), Article 8. https://doi.org/10.3390/molecules21080974
23. Mourya, S., Bodla, R., Taurean, R., & Sharma, A. (2019). Simultaneous estimation of xanthine alkaloids (Theophylline, Theobromine and Caffeine) by High-Performance Liquid Chromatography. *International Journal of Drug Regulatory Affairs*, *7*(2), 35-41. https://doi.org/10.22270/ijdra.v7i2.315
24. NTC-ISO 20481. (2008). *Instituto Colombiano de Normas Técnicas y Certificación (ICONTEC) 2008 Café y Productos del Café Determinación del Contenido de Cafeína Usando Cromatografía Líquida de Alto Desempeño (HPLC), NTC-ISO 20481 (Colombia : Instituto Colombiano de Normas Técnicas y Certificación).*
25. Rahman, M. M., Kalam, M. A., Salam, M. A., & Rana, M. R. (2013). Aged leaves effect on essential components in green and oolong tea. *International Journal of Agricultural Research, Innovation and Technology*, *3*(2), Article 2. https://doi.org/10.3329/ijarit.v3i2.17845
26. Rodriguez, A., Costa-Bauza, A., Saez-Torres, C., Rodrigo, D., & Grases, F. (2015). HPLC method for urinary theobromine determination : Effect of consumption of cocoa products on

ISSN: 1857-7881 (Print)
e-ISSN 1857-7431 (Online)

theobromine urinary excretion in children. *Clinical Biochemistry*, *48*(16), 1138-1143. https://doi.org/10.1016/j.clinbiochem.2015.06.022

27. Sajilata, M. g., Bajaj, P. R., & Singhal, R. s. (2008). Tea Polyphenols as Nutraceuticals. *Comprehensive Reviews in Food Science and Food Safety*, *7*(3), 229-254. https://doi.org/10.1111/j.1541-4337.2008.00043.x
28. Sanchez, J. (2017). Methylxanthine Content in Commonly Consumed Foods in Spain and Determination of Its Intake during Consumption. *Foods*, *6*(12), 109. https://doi.org/10.3390/foods6120109
29. Srdjenovic, B., Djordjevic-Milic, V., Grujic, N., Injac, R., & Lepojevic, Z. (2008). Simultaneous HPLC Determination of Caffeine, Theobromine, and Theophylline in Food, Drinks, and Herbal Products. *Journal of Chromatographic Science*, *46*(2), 144-149. https://doi.org/10.1093/chromsci/46.2.144
30. Szymański, M., Korbas, J., & Szymański, A. (2022). Methylxanthines release from various teas during extraction with water. *Acta Poloniae Pharmaceutica*, *78*, 781-788. https://doi.org/10.32383/appdr/145572
31. Turkmen, N., & Velioglu, Y. S. (2007). Determination of alkaloids and phenolic compounds in black tea processed by two different methods in different plucking seasons. *Journal of the Science of Food and Agriculture*, *87*(7), 1408-1416. https://doi.org/10.1002/jsfa.2881
32. Zareef, M., Mehedi Hassan, M., Arslan, M., Ahmad, W., Ali, S., Ouyang, Q., Li, H., Wu, X., & Chen, Q. (2020). Rapid prediction of caffeine in tea based on surface-enhanced Raman spectroscopy coupled multivariate calibration. *Microchemical Journal*, *159*, 105431. https://doi.org/10.1016/j.microc.2020.105431
33. Zhu, B., Haghi, M., Goud, M., Young, P. M., & Traini, D. (2015). The formulation of a pressurized metered dose inhaler containing theophylline for inhalation. *European Journal of Pharmaceutical Sciences*, *76*, 68-72. https://doi.org/10.1016/j.ejps.2015.04.016
34. Zhu, X., Chen, B., Ma, M., Luo, X., Zhang, F., Yao, S., Wan, Z., Yang, D., & Hang, H. (2004). Simultaneous analysis of theanine, chlorogenic acid, purine alkaloids and catechins in tea samples with the help of multi-dimension information of on-line high performance liquid chromatography/electrospray–mass spectrometry. *Journal of Pharmaceutical and Biomedical Analysis*, *34*(3), 695-704. https://doi.org/10.1016/S0731-7085(03)00605-8

ESJ Natural/Life/Medical Sciences Peer-reviewed

Profile of Temporal Bone Computed Tomography Examinations at the University Hospital Center (CHU) Campus of Lomé

Judith Edwige Guiaba Kette Mokpondo
Department of Radiology, CHU-Campus Lomé, Lomé, Togo
Timothee Mobima
National Center for Medical Imaging, Bangui, Central African Republic
Aime Stephane Kouzou
Community Hospital Center of Bangui, Bangui, Central African Republic
Chrispin Euloge Tapiade
Francky Kouandongui Bangue Songrou
Christ Borel Tambala
National Center for Medical Imaging, Bangui, Central African Republic
Heritier Yannick Sombot Soule
Maman Elisabeth DOMITIEN Hospital Center, Bangui,
Central African Republic
Lantam Sonhaye
Victor Adjenou
Department of Radiology, CHU-Campus Lomé, Lomé, Togo

Doi:10.19044/esj.2026.v22n6p74

Submitted: 25 August 2025
Accepted: 15 February 2026
Published: 28 February 2026

Cite As:
Guiaba Kette Mokpondo, J.E., Mobima, T., Kouzou, A.S., Tapiade, C.E., Kouandongui Bangue Songrou, F., Tambala, C.B., Sombot Soule, H.Y., Sonhaye, L. & Adjenou, V. (2026). *Profile of Temporal Bone Computed Tomography Examinations at the University Hospital Center (CHU) Campus of Lomé.* European Scientific Journal, ESJ, 22 (6), 74. https://doi.org/10.19044/esj.2026.v22n6p74

Abstract

Introduction: The petrous bone is the inferior part of the temporal bone. It plays a crucial role in hearing and balance in the human body and is the site of a wide variety of pathologies, making it a public health concern. The aim of this study was to determine the profile of petrous bone computed tomography (CT) examinations.

ISSN: 1857-7881 (Print)
e-ISSN 1857-7431 (Online)

Methods: This was a prospective, descriptive study conducted over a 6-month period, involving 34 petrous bone CT examinations performed in the CT unit of the CHU-Campus in Lomé. The parameters analyzed included epidemiological data and lesions identified on CT imaging.

Results: Out of 6,328 CT examinations performed during the study period, 34 were petrous bone CT scans, representing 0.5%. All age groups were affected, with a predominance of the 31-40 year age group (23.5%). Males were predominant, with a sex ratio of 2.1. Drivers were the most represented occupational group (23.5%). The most frequent indication was petrous bone trauma (44.1%), with road traffic accidents being the leading cause (73.3%). In all cases, the examination was performed without contrast injection. CT findings were pathological in 70.6% of cases, mainly in trauma, conductive hearing loss, chronic otitis media, external auditory canal (EAC) stenosis, and pulsatile tinnitus. The main traumatic lesion identified was extra labyrinthine fractures (91.7%). Incudo-malleolar dislocation was the most common ossicular lesion (25%). Hemotympanum was observed in 83.3% of cases. CT scans were normal in 29.4% of cases, particularly in patients with vertigo/tinnitus, mixed hearing loss, conductive hearing loss associated with tinnitus, otalgia, and non-traumatic facial paralysis.

Keywords: Computed tomography, petrous bone, profile, trauma, hearing loss, Lomé

Introduction

The petrous bone is the inferior part of the temporal bone, located on each side of the skull. It has the shape of a quadrangular pyramid and forms the internal and horizontal portion of the temporal bone. The petrous bone contains the middle ear (the tympanic cavity and the ossicular chain) and is traversed by the facial nerve (Le Petit Larousse, 2017). It plays a crucial role in hearing and balance in the human body (Prades, 2010). It is the site of a wide polymorphism of pathologies (infectious, traumatic, tumoral, and malformative), for which specific monitoring must be instituted. Its complex composition and the presence of multiple adjacent structures make its evaluation difficult using conventional imaging (Grace, 2012; Ahmed, 2012). Computed tomography (CT), also known as scanography, is defined as a tomographic radiological system that measures the attenuation of an X-ray beam as it passes through an anatomical volume, with matrix-based reconstruction of a digitized image (Sonhaye, 2017; Masson, 2023). It remains one of the cross-sectional imaging modalities that plays an essential role in the exploration of the petrous bone. In high resolution, it allows detailed osseous assessment of the different compartments of the ear (Grace, 2012; Ahmed, 2012). When performed with iodinated contrast injection, it enables the

ISSN: 1857-7881 (Print)
e-ISSN 1857-7431 (Online)

evaluation of vascular and soft-tissue structures (Prades, 2010; Amy, 2018); moreover, it is widely available and accessible. Its limitations in otology, and more broadly in ENT practice, concern the evaluation of vertigo, balance disorders, and non-traumatic facial paralysis (Amy, 2018).

Methods

This was a prospective and descriptive study conducted over a six-month period from July 1 to December 31, 2022, at the University Hospital Center (CHU) Campus of Lomé, which is equipped with a General Electric (GE) Bright Speed Elite multi-slice CT scanner allowing the acquisition of 16 slices per 0.5-second rotation. This equipment has been in operation since 2010. The parameters used were those referred to as "petrous bone helical bone," as follows: field of view: 20 cm; matrix: 512^2; mAs: 220; kV: 140; reconstruction slice thickness: 0.6 mm; CTDI vol: 96.6 Gy. Strict patient immobilization was ensured.

Included in this study were patients who underwent a petrous bone CT examination, while those who presented for follow-up examinations were excluded. None of the patients received an iodinated contrast injection. Data were collected using a pre-established data collection form including the variables studied and were analyzed and processed using Epi Info software version 3.5.3. Data confidentiality was guaranteed. The names of patients and referring physicians do not appear in any document related to the results of this study.

Results

During the study period, 6,328 CT examinations were performed, including 34 petrous bone CT scans, corresponding to an overall frequency of 0.5%. Males were the most represented, accounting for 67.6% of cases. The mean age of patients was 37 years (range: 1 to 75 years), and the 31-40-year age group was the most represented, with 23.5% (Figure 1).

ISSN: 1857-7881 (Print)
e-ISSN 1857-7431 (Online)

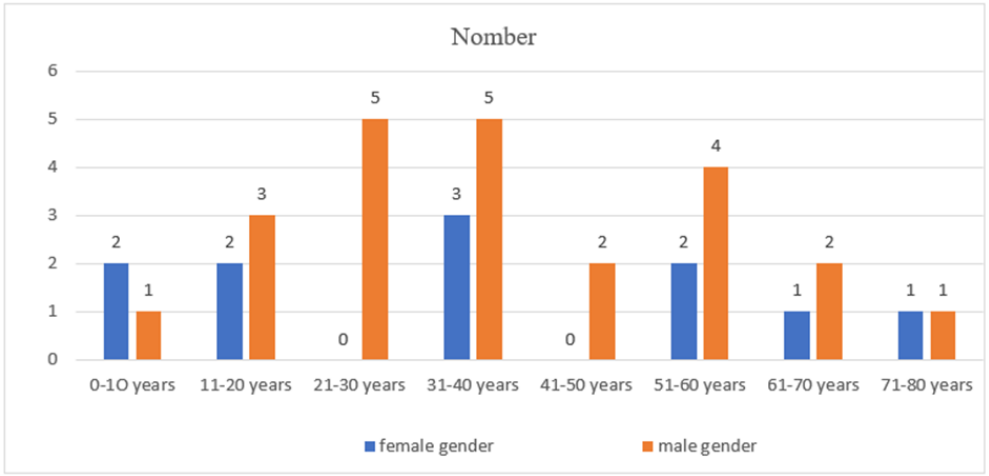

Figure 1: Distribution of patients according to age groups and sex

Regarding patients' professions and occupations, drivers were the most represented, accounting for 23.4%.

The majority of patients were referred from the Emergency Department (50%), and the main indication was trauma in 44.1% of cases (Table I).

Table I: distribution of patients according to the indication for petrous bone CT scans by referring department.

	Emergency Department n (%)	**ENT Department n (%)**	**Other Departments n (%)**	**Total n (%)**
Trauma	**12(35,3)**	**2(5,9)**	**1(2,9)**	**15(44,1)**
Conductive hearing loss	0(0,0)	5(14,9)	0(0,0)	5(14,9)
EAC* stenosis	2(5,9)	2(5,9)	0(0,0)	4(11,8)
Chronic otitis media	2(5,9)	2(5,9)	0(0,0)	4(11,8)
Otalgia	0(0,0)	0(0,0)	1(2,9)	1(2,9)
Mixed hearing loss	0(0,0)	1(2,9)	0(0,0)	1(2,9)
Sensorineural hearing loss / tinnitus	0(0,0)	1(2,9)	0(0,0)	1(2,9)
Pulsatile tinnitus	0(0,0)	1(2,9)	0(0,0)	1(2,9)
Tinnitus / vertigo	0(0,0)	0(0,0)	0(0,0)	1(2,9)
Facial paralysis / otalgia	1(2,9)	0(0,0)	1(2,9)	1(2,9)
Total	**17(50)**	**14(41,3)**	**3(8,7)**	**34(100)**

n (%): number (percentage)
***EAC*:** External Auditory Canal
***ENT*:** Otorhinolaryngology

ISSN: 1857-7881 (Print)
e-ISSN 1857-7431 (Online)

Other departments: Other university hospital departments, private practices, and clinics.

Regarding prescribers, interns or resident physicians (DES) were the main prescribers, accounting for 58.8%.

The techniques used for petrous bone CT examinations were dominated by craniocerebral CT, which accounted for 55.8% of cases.

Regarding the results of petrous bone CT examinations, 70.6% of cases were pathological across the different indications, as shown in Table II.

Table II: Distribution of patients according to petrous bone CT findings by indication

	Normal CT n (%)	**Pathological n (%)**	**Total n (%)**
Trauma	**3(8,8)**	**12(35,3)**	**15(44,1)**
Conductive hearing loss	2(5,9)	3(8,8)	5(14,7)
EAC* stenosis	0(0,0)	4(11,8)	4(11,8)
Chronic otitis media	0(0,0)	4(11,8)	4(11,8)
Otalgia	1(2,9)	0(0,0)	1(2,9)
Mixed hearing loss	1(2,9)	0(0,0)	1(2,9)
Sensorineural hearing loss / tinnitus	0(0,0)	1(2,9)	1(2,9)
Pulsatile tinnitus	1(2,9)	0(0,0)	1(2,9)
Tinnitus / vertigo	1(2,9)	0(0,0)	1(2,9)
Facial paralysis / otalgia	1(2,9)	0(0,0)	1(2,9)
Total	**10(29,4)**	**24(70,6)**	**34(100)**

Hemotympanum was the most frequently observed lesion (83.3%), followed by fracture of the temporal squama in 75% of cases (Table III).

Table III: Traumatic lesions observed

Traumatic lesions	**Number (n)**	**Percentage (%)**
Hemotympanum	**10**	**83,3**
Temporal squama fracture	9	75
Mastoid air cell opacification	8	66,7
Tympanic bone fracture	7	58,3
Mastoid fracture	5	41,7
Ossicular lesions	3	25
Tegmen tympani fracture	1	8,8
Fracture of the medial wall of the middle ear	1	8,8

n (%): number (percentage)
EAC = External Auditory Canal

ISSN: 1857-7881 (Print)
e-ISSN 1857-7431 (Online)

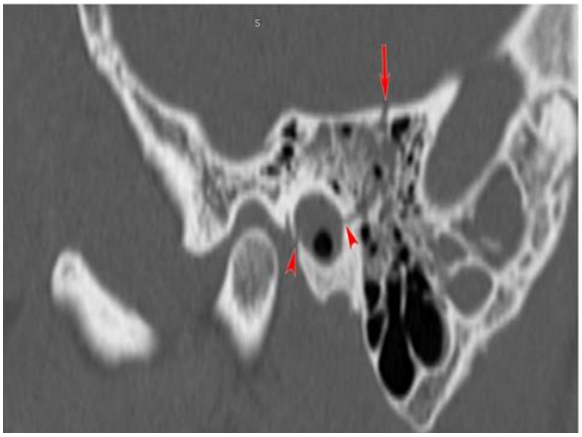

Figure 2: CHU-Campus Image (Lomé)

A 22-year-old male patient with head trauma associated with otorrhagia. Sagittal CT reconstruction of the left petrous bone showing a disruption of the left temporal squama, consistent with an extra labyrinthine fracture (arrowhead), associated with opacification of the tympanic cavity consistent with hemotympanum, and a discontinuity of the tegmen tympani (arrow).

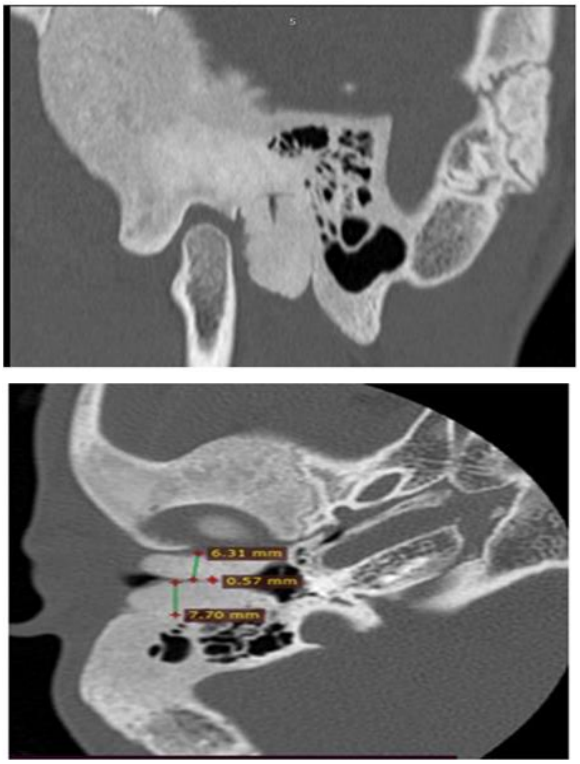

Figure 3a, b: CHU-Campus Image (Lomé)

ISSN: 1857-7881 (Print)
e-ISSN 1857-7431 (Online)

A 40-year-old male patient presenting with stenosis of the right external auditory canal. Sagittal reconstruction (a) and axial CT slice (b) of the right petrous bone show a ground-glass appearance of the bone marrow involving the medullary bone of the outer third of the petrous portion of the temporal bone, associated with cortical expansion and cortical thinning without bone lysis, resulting in stenosis of the right external auditory canal.

Discussion

This study is the first of its kind conducted at the CHU-Campus of Lomé. One of its strengths lies in the availability of complete information and all the necessary data. No major difficulties were encountered during the study. During the study period, 6,328 patients underwent CT examinations, including 34 petrous bone CT scans, corresponding to an overall frequency of 0.5%. This indicates that requests for petrous bone CT examinations remain low in our setting.

The mean age was 37 years, with extremes ranging from 1 to 75 years. A marked predominance of the 21-40-year age group (38.2%) was observed, compared with 23.3% for the 0–20-year age group. In accordance with the indications for petrous bone CT (Prades, 2010), all age groups were concerned, with a predominance among young adults. Males were more frequently represented (67.6%) than females (32.3%), with a sex ratio of 2.1. This may be explained by the high frequency of traumatic petrous bone CT examinations in this study (44.1%) (Table II). This male predominance among young adults undergoing CT for traumatic petrous bone injuries has also been reported by Sonhaye et al. (Sonhaye, 2017), who found 57.7% in the 20–40-year age group and a male predominance of 77.4% versus 22.6% for females, corresponding to a sex ratio of 3.42. Similarly, Hiroual et al. (Hiroual, 2010) reported a marked male predominance with a ratio of 16 men for one woman. This male predominance, observed both in the literature and in the present series, may be explained by the fact that trauma predominantly affects men.

Anyone, regardless of profession, may develop petrous bone pathology. Road traffic accidents involving two-wheeled vehicles are a frequent cause of more than 50% of deaths among young adults aged 15-44 years (WHO, 2015).

In this series, petrous bone trauma accounted for 44.1% of cases among young adults aged 21-40 years. This result is comparable to that reported by Issa et al. (Issa, 2020), who found a proportion of 42.9%. Among the 15 petrous bone CT requests for trauma, vehicle drivers were the most represented (53.3%), including 75% two-wheeled vehicle drivers and 25% four-wheeled vehicle drivers. Drivers of two-wheeled vehicles were therefore particularly exposed to petrous bone trauma.

ISSN: 1857-7881 (Print)
e-ISSN 1857-7431 (Online)

The main indication for petrous bone CT was trauma (44.1%), followed by conductive hearing loss (14.7%), and, with equal proportions of 11.8%, chronic otitis media and external auditory canal stenosis. Otalgia, mixed hearing loss, sensorineural hearing loss/tinnitus, pulsatile tinnitus, tinnitus/vertigo, and facial paralysis/otalgia each accounted for 2.9%. These findings are consistent with those of Amy et al. (Amy, 2018), who reported that CT remains the first-line imaging modality for the evaluation of petrous bone trauma and conductive hearing loss with a normal tympanic membrane.

However, CT is often complemented or replaced by MRI when evaluating facial paralysis, tinnitus, and vertigo (Masson, 2013). Nevertheless, CT is indicated in chronic otitis media only for preoperative assessment when surgical treatment is considered because of significant conductive hearing loss (WHO, 2015). CT also retains its role in the evaluation of otalgia with positive otoscopy, particularly in necrotizing or complicated external otitis, or in otalgia secondary to tumors of the external auditory canal or middle ear (Prades, 2010).

Petrous bone CT examinations were mainly requested by interns and resident physicians on call, accounting for 58.8%, followed by ENT specialists (32.3%), while other physicians accounted for 8.8%. Similarly, the main referring departments were the surgical emergency department (50%) and ENT departments (41.2%). These findings are consistent with those reported in the literature (Sonhaye, 2017). This may be explained, on the one hand, by the predominance of traumatic petrous bone injuries in this study and, on the other hand, by the fact that in Lomé both university hospitals had surgical emergency departments, but only the CT unit of CHU-Campus was operational. Outside trauma, the main indications for petrous bone CT fall within the ENT specialty (hearing loss, chronic otitis media, EAC stenosis, otalgia, pulsatile tinnitus, tinnitus/vertigo, and facial paralysis/otalgia).

The most frequently performed technique was craniocerebral CT followed by petrous bone CT using the “helical bone” protocol, accounting for 55.9%, mainly in patients evaluated for petrous bone CT in the context of acute head trauma with suspected petrous bone fracture. Saraiya (Saraiya, 2009) justified this approach by highlighting the inadequacy of conventional brain CT with thin-slice bone window reconstruction of the petrous bone, which may lead to imprecise lesion assessment, with nearly one-third of petrous bone fractures remaining undetected. Furthermore, Amy et al. (Amy, 2018) reported that 18-22% of skull fractures involve the temporal bone, and Sun et al. (Sun, 2011) noted that 90% of patients with petrous bone trauma present with associated brain injury. This underscores the need to complement craniocerebral CT with dedicated petrous bone CT in such contexts. In this series, direct performance of petrous bone CT using the “helical bone” protocol accounted for 32.3%, mainly in patients examined at a distance from

ISSN: 1857-7881 (Print)
e-ISSN 1857-7431 (Online)

the trauma who had already undergone brain CT, and in other indications, particularly conductive hearing loss with suspected otosclerosis. This technique allows better assessment of ossicular lesions due to resorption of hemotympanum in the days following trauma (Amy, 2018). In patients with conductive hearing loss and suspected otosclerosis, petrous bone CT using the "helical otosclerosis" protocol accounted for 11.8% in this series. It should be noted that focused centering on the tympanic cavities, labyrinthine capsule, and internal auditory canal provides a "magnification effect" compared with conventional axial slices. All examinations were performed without iodinated contrast injection. Contrast administration is indicated only in cases of suspected expansive lesions or malignant external otitis.

Petrous bone CT findings were pathological in 70.6% of cases and normal in 29.4%. The high rate of pathological findings was mainly observed in trauma, chronic otitis media, and EAC stenosis. This can be explained by the excellent natural contrast between air and ossicles, facilitating CT evaluation of the middle ear, and by the high sensitivity of CT in detecting bone lesions, particularly petrous bone fractures, as reported by Darrouzet et al. (Darrouzet, 2010).

Extra labyrinthine fractures were the most frequent (91.7%), followed by mixed fractures (8.3%). These results are consistent with those reported in the literature (Sonhaye, 2017). Barreau (Barreau, 2011) reported that extra labyrinthine fractures account for more than 90% of petrous bone fractures, and Amy et al. (Amy, 2018) reported proportions ranging from 94% to 97%. In contrast, Traoré et al. (Traoré, 2022) found a lower proportion of 79.3%.

Several lesions were associated with fractures, mainly hemotympanum (83.3%), followed by hemorrhagic opacification of mastoid air cells (66.7%). These proportions are lower than those reported by Sonhaye et al. (Sonhaye, 2017), who found 96.7% for hemotympanum and 80.3% for mastoid air cell opacification. Conversely, Traoré et al. (Traoré, 2022) reported lower rates, with 72.4% for hemotympanum and 55.2% for mastoid air cell opacification. The high sensitivity of CT in detecting hemotympanum may explain these elevated rates.

Ossicular lesions were identified in 25% of cases, a proportion higher than that reported by Melaine et al. (Melaine, 2020), who found 19.4%, and comparable to the 26.7% and 28.9% reported by Sonhaye et al. and Hiroual et al., respectively (Sonhaye, 2017; Hiroual, 2010). These lesions mainly consisted of Incudo-malleolar dislocations. In accordance with the literature (Amy, 2018), dislocations remain the most frequent ossicular lesions and may be associated with one another.

All four CT examinations requested for chronic otitis media were positive (100%). All patients showed opacification of the mastoid air cells and tympanic cavity, associated with mastoid cortical osteolysis and/or

ISSN: 1857-7881 (Print)
e-ISSN 1857-7431 (Online)

osteosclerosis; only one patient had ossicular erosion. These findings are consistent with data from the literature (Varoqueux, 2010; Amy, 2015; Shekhrajika, 2019). CT commonly shows opacification and sclerosis of the mastoid air cells. Other lesions should be sought to explain conductive hearing loss, including tympanic membrane perforation, middle ear cavity opacification, or post-inflammatory ossicular erosion (sequelae otitis) (Varoqueux, 2010). Secondary cholesteatoma is a major complication of chronic otitis media (Amy, 2015), accounting for one-third of chronic otitis media with a perforated tympanic membrane and occurring at any age. At an early stage, CT shows a small, round opacity with convex margins located in the external attic or "Prussak's space." Erosion of the inferior angle of the scutum is an important diagnostic sign (Varoqueux, 2010). At a more advanced stage, it may appear as a larger convex opacity eroding adjacent bony structures or as complete opacification of the attic or tympanic cavity. Finally, it may be evacuated spontaneously or by the clinician during examination. In such cases, CT may appear almost normal, sometimes revealing only residual signs left by the evacuated cholesteatoma, such as marked widening of the external attic with blunting of the scutum tip, destruction of the supra meatal squama, ossicular destruction, or tegmen tympani dehiscence (Varoqueux, 2010). Middle ear cholesteatoma is considered a dangerous form of chronic otitis because of its progressive nature and potentially life-threatening complications. Its evolution differs significantly between adults and children.

External auditory canal stenosis can occur at any age and has a wide range of etiologies. In this study, 11.7% of petrous bone CT requests were for EAC stenosis, and all results were pathological. Among these patients, the first two were infants aged 1 and 2 years, and the other two were aged 39 and 40 years. Three of them (75%) presented with soft-tissue opacification of the EAC, with or without associated findings. The first patient, aged 1 year, showed near-total soft-tissue opacification of the right EAC and partial opacification on the left, associated with bilateral ossicular fixation. The second patient, aged 2 years, showed near-total soft-tissue opacification of the right EAC. In the third patient, aged 39 years, CT demonstrated soft-tissue opacification of both EACs with more marked bony erosions on the left. According to the literature (Bensimon, 2010; Varsha, 2012; Charfeddine, 2016), EAC pathologies may have similar clinical presentations, and soft-tissue opacification on CT may suggest several diagnoses, including epidermoid pathologies (cholesteatoma, epidermoid cyst, cholesterol granuloma) and neural pathologies (meningioma, schwannoma) (Benson et al., 2022). In the fourth patient, aged 40 years, CT showed a ground-glass appearance of the medullary bone involving the outer third of the petrous portion of the temporal bone, with cortical expansion and thinning without

ISSN: 1857-7881 (Print)
e-ISSN 1857-7431 (Online)

bone lysis, resulting in right EAC stenosis secondary to fibrous dysplasia of the temporal bone. These classic CT features have been described in the literature (Mahoudeau, 2022). Fibrous dysplasia is a rare disease that can involve any bone, particularly those of the face. In the craniofacial region, the maxilla, zygoma, frontal bone, ethmoid, and mandible are most frequently affected, whereas temporal bone involvement is rare, accounting for only 11–12% of craniofacial fibrous dysplasia cases (Benson, 2022). CT also allows detection of possible stenoses of the skull base foramina.

In this study, conductive hearing loss accounted for 14.3% of petrous bone CT requests, including one case of ossicular chain malformation with an inverted (downward-oriented) Incudo-malleolar joint. Other minor forms of ossicular chain malformations have been described in the literature. According to the literature, 50% of pediatric sensorineural hearing loss cases are of genetic origin, while environmental causes include cytomegalovirus infection, neonatal distress, and meningitis. Genetic causes are most often isolated but may be syndromic in 30% of cases (Veillon, 2010).

Conclusion

This study shows that petrous bone CT remains the primary imaging modality, although its utilization remains low and is mainly requested by interns, resident physicians in surgical emergency departments, and ENT specialists. Both sexes were affected, with a male predominance, and the 31-40-year age group was the most represented. The most frequent indication remains petrous bone trauma, in which computed tomography plays a central role, followed by conductive hearing loss, external auditory canal stenosis, and chronic otitis media. In contrast, CT has a limited role in the evaluation of vertigo/tinnitus and non-traumatic facial paralysis. Ear pathology represents a public health issue and has a negative impact on interpersonal relationships.

Conflict of Interest: The authors reported no conflict of interest.

Data Availability: All data are included in the content of the paper.

Funding Statement: The authors did not obtain any funding for this research.

Declaration for Human Participants: This research followed the Ministry of Higher Education and Scientific Research in Togo and its guidelines for research ethics involving human subjects, and the Science Council of Togo's Code of Conduct for Scientists. The research was approved by the institutional review board at the Faculty of Health Sciences at the University of Lomé, Togo.

ISSN: 1857-7881 (Print)
e-ISSN 1857-7431 (Online)

References:

1. Ahmed AR, Benj0*amin Y. 2012. Lesions of the Petrous Apex: Classification and Findings at CT and MR Imaging. Radiographics; 32:151-173.
2. Amy FJ, Daniel TG, Gul M. 2015. Imaging Review of the Temporal Bone: Part II. Traumatic, Postoperative, and Non-inflammatory Non-neoplastic Conditions. Radiology; 276(3):655–672.
3. Amy F, Juliano I. 2018. Cross-sectional imaging of the ear and temporal bone. Head and Neck Pathology; 12(3):302-320.
4. Barreau X. 2011. Imaging of temporal bone fractures. Journal de Radiologie; 92:958-966.
5. Benson JC, Lane IL. 2022. Temporal bone anatomy. Neuroimaging Clinics of North America; 32(4):763-775.
6. Charfeddine S, Chahed H, Besbes G, Dziri S. 2016. Severe to profound bilateral hearing loss in adults: etiologies and therapeutic indications. Journal of Medical Rehabilitation: Practice and Training in Physical and Rehabilitation Medicine; 36(4):173-184.
7. Darrouzet V, Merriot P, Veillon F. 2010. Temporal bone trauma. In: Imaging of the Ear; pp. 321-334.
8. Grace SP, Sung ELG, Michael R, Yoshimi A. 2012. Interactive Web-based Learning Module on CT of the Temporal Bone: Anatomy and Pathology. Radiographics; 32:E85-E105.
9. Hiroual MR, Zougarhi A, Cherif Idrissi El Ganouni N, Essadki O, Ousehal A, Tijani Adil O, et al. 2010. Contribution of CT in temporal bone trauma: a series of 38 cases. Journal de Radiologie; 91:53–58.
10. Issa, Konaté, Lambert, Yao B, Kouassi K, Bravo T, Emile AB, Maru VK, D'dri K. 2020. Epidemiological, clinical, and CT features of cranio-encephalic injuries in road traffic accident victims involving two-wheeled vehicles in Bouaké (Côte d'Ivoire). Journal Africain d'Imagerie Médicale; 12-2.
11. Le Petit Larousse de la Médecine. 2017. However, CT of the temporal bone remains limited in the exploration of vertigo/tinnitus and non-traumatic facial paralysis. Scanner: 1152-853.
12. Mahoudeau P, Tringali S, Fieux M. 2022. External auditory canal stenosis. Annales Françaises d'Oto-Rhino-Laryngologie et de Pathologie Cervico-Faciale; 139(1):50-53.
13. Masson F, Dangin X, Baudin P. 2013. Computed tomography: principles and image formation. In: CT Scanner and X-ray. Elsevier Masson:119-174.
14. World Health Organization (WHO), Geneva. 2011. Global Plan for the Decade of Action for Road Safety 2011-2022. Available at: www.who.int (accessed August 20, 2015).

ISSN: 1857-7881 (Print)
e-ISSN 1857-7431 (Online)

15. Prades JM, Veyret CH, Saliou G, Lescanne E, Christian M. 2010. Anatomy and normal imaging of the human temporal bone. In: Christian M, editor. Imaging of the Ear and Temporal Bone. SFORL-SFR-CIREOL:37-73.
16. Saraiya A. 2009. Temporal bone fractures. American Journal of Emergency Radiology; 16:255-260.
17. Shekhrajika N, Moonis G. 2019. Imaging of non-traumatic temporal bone emergencies. Seminars in Ultrasound, CT and MRI; 40(2):116–124.
18. Sonhaye L, Bah OA, Kolou B, Amadou A, Adambounou K, Tchaou M, Bah MO, Adjenou KV, N'dakena K. 2017. Temporal bone trauma: CT findings in 60 cases in Lomé. Revue CAMES Santé; 5(1):57-61.
19. Sun GH, Shoman NM, Samy RN, Cornelius RS, Koch BL, Pensak ML. 2011. Contemporary temporal bone fracture classification systems reflect concurrent intra crânial and cervical spine injuries. Laryngoscope; 121(5):929-932.
20. Traoré O, Guindo I, Wakrim S, Dembele M, Cisse I, Dackouo M, Keita AD. 2022. Role of helical CT in temporal bone trauma: a series of 12 cases at Ibn Rochd University Hospital, Casablanca. Pan African Medical Journal; 41-1.
21. Bensimon JL. 2010. Otalgia. In: Christian M, editor. Imaging of the Ear and Temporal Bone. SFORL-SFR-CIREOL:277-296.
22. Varsha MJ, Shantanu KN, Ravi KG, Jitender RK, Vinay KEC. 2012. CT and MR Imaging of the Inner Ear and Brain in Children with Congenital Sensorineural Hearing Loss. Radiographics; 32:683-698.
23. Varoquaux A, Cassagneau P, Jacquier A, Louis G, Champsaur P, Bartoli JM, et al. 2010. Radio-anatomy of the ear. In: Dubrulle F, Martin-Duverneuil N, Moulin G, editors. ENT Imaging. Elsevier Masson:251-271.
24. Veillon F, Fraysse B, Escudé B, Deguinne O, Robier A. 2010. Conductive and mixed hearing loss with normal tympanic membrane in adults. In: Christian M, editor. Imaging of the Ear and Temporal Bone. SFORL-SFR-CIREOL:95-137.

ESJ Natural/Life/Medical Sciences Peer-reviewed

Contribution to the Systematic Study of the Ornamental Flora of Gorée Island (Dakar-Senegal)

Dieng Birane
Gueye Fatou Kine
Sagna Gnima
Diouf Jules
Diouf Ndongo
Gaye Alioune
Fall Ndeye Fatou Dieng
Lo Penda
KA Samba Laha
Diouf Alassane
Noba Kandioura
Mbaye Mame Samba
Laboratory of Botany and Biodiversity,
Department of Plant Biology, Faculty of Science and Technology,
Cheikh Anta DIOP University, Dakar-Fann, Senegal

Doi:10.19044/esj.2026.v22n6p87

Submitted: 13 January 2026
Accepted: 21 February 2026
Published: 28 February 2026

Cite As:
Dieng, B., Gueye, F. K., Sagna, G., Diouf, J., Diouf, N., Gaye, A., Fall, N. F. D., Lo, P., KA, S. L., Diouf, A., Noba, K. & Mbaye, M. S. (2026). *Caractérisation.* European Scientific Journal, ESJ, 22 (6), 87. https://doi.org/10.19044/esj.2026.v22n6p87

Abstract

Gorée Island, located approximately 4.5 km off the coast of Dakar, is both an island in the North Atlantic Ocean and one of the 19 boroughs of Senegal's capital city. This emblematic site has been widely studied in fields such as archaeology, geology, history, and tourism. However, its ornamental flora has received very little scientific attention. This is particularly concerning given that recent decades have been marked by the depletion of its natural resources due to numerous human activities combined with urban expansion and climate change. It is therefore crucial to improve scientific knowledge of Gorée Island's ornamental flora to support sustainable and participatory management. This study, conducted in September 2021, aims to

ISSN: 1857-7881 (Print)
e-ISSN 1857-7431 (Online)

contribute to a broader understanding of Gorée's ornamental flora. More specifically, this study aims to establish the taxonomic, biological, and chorological profiles of the ornamental flora of Gorée. The methodological approach consisted of conducting a field survey in the three gardens (Canary Garden, Public Garden, and Succulent Plant Garden) and the flowerbeds of the municipality. The results showed that 55 plant species belonging to 49 genera, grouped into 31 families, were identified. Of these species, 36 are already listed in the flora of Senegal, while the remaining 13 have not been recorded and could be introduced to Senegal. This flora is composed exclusively of angiosperms, with three dominant families: Apocynaceae (9.09%), Acanthaceae (7.27%), and Asparagaceae (7.2%). In terms of biological types, Phanerophytes are the most represented (50.91%), followed by Chamaephytes (20%). Chorologically, the flora is dominated by pantropical species, which account for 34.55% of the species mentioned, compared to 21.82% for other African-American species.

Conclusion and application: This work has allowed us to characterize the ornamental flora of Gorée Island. Indeed, the structure of the flora, as well as its taxonomic, biological, and chorological spectra, has been determined. The results of this study can be used to develop tools for taxon identification (identification key).

Keywords: Flora, Ornamental, Characterization, Management, Gorée

Introduction

Gorée Island, located about 4.5 km off the coast of Dakar, is both an island in the North Atlantic Ocean and one of the 19 municipal districts of Senegal's capital city. It is a symbolic site of remembrance of the transatlantic slave trade in Africa. The island was designated a historic site in 1944, with protective measures implemented in 1951 (during the colonial era). It was subsequently inscribed on the national heritage list in 1975 (Decree No. 012771 of November 17, 1975) and on the UNESCO World Heritage List in 1978 (DEEC, 2022).

This iconic Senegalese territory has been the focus of numerous studies spanning archaeology, history, and tourism. Furthermore, despite centuries of conquest, pillaging, and urban redevelopment (the 18th century), the area currently occupied by the Adanson Public Garden has remained largely intact. This garden has nonetheless evolved, adapting to different configurations and functions throughout over three and a half centuries of documented urban development on Gorée Island.

However, the ornamental flora of Gorée Island has received little scientific investigation. Recent decades have been characterized by the depletion of its natural resources due to numerous human activities combined

ISSN: 1857-7881 (Print)
e-ISSN 1857-7431 (Online)

with urban expansion and climate change (MEED, 2014). The impact of these constraints is clearly visible today, especially as a result of climate change. Thus, the quality of the living environment is now recognized as crucial to the physical and psychological well-being of populations, which highlights the importance of ornamental plants as they also play a significant role in improving the living environment. It is therefore essential to enhance scientific knowledge about the ornamental flora of Gorée Island in order to support sustainable and participatory management.

This study was undertaken to enhance the overall understanding of the ornamental flora of Gorée Island. Specifically, it aims to characterize its taxonomic, biological, and chorological composition.

Materials and Methods

Presentation of the study area

The studies were conducted in three gardens (the Canary Garden, the Public Garden, and the Succulent Garden) as well as along other pathways on Gorée Island, located in the Bay of Dakar. These themed gardens contribute to the beautification of the living environment and also provide spaces for recreation and community gatherings. Gorée is one of the 19 boroughs of the capital of Senegal. It is a symbolic site of remembrance of the transatlantic slave trade in Africa, officially recognized by the United Nations (UN) in 1978. Gorée, the "memory island" of this tragedy, was thus one of the very first sites to be inscribed on UNESCO's World Heritage List.

ISSN: 1857-7881 (Print)
e-ISSN 1857-7431 (Online)

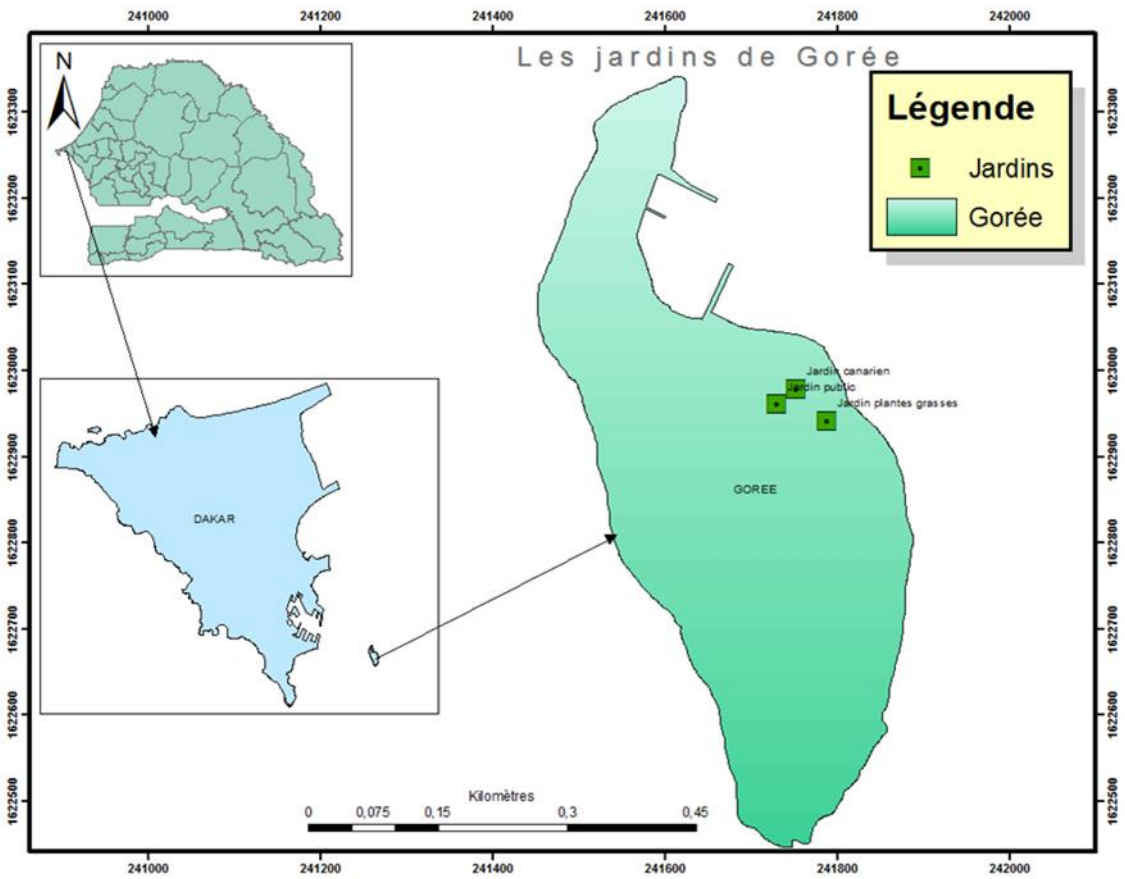

Figure 1: Map showing the location of the Canary Garden, the Public Garden, and the Succulent Garden

Methods

Equipment

The following equipment was required to complete this work:

- A GPS device to obtain the geographical coordinates of the gardens;
- Floristic inventory sheets to record the present species in the different gardens;
- Notebooks, pencils and erasers for taking notes;
- Pruning shears for collecting samples;
- A press for preserving and drying samples;
- A digital camera for taking pictures of ornamental plants

The following books and websites were used for species identification:

- Flora of Senegal (Berhaut, 1967),
- Flora of West Tropical Africa (Hutchinson & Dalziel, 1954, 1958, 1963, 1968, 1972)

ISSN: 1857-7881 (Print)
e-ISSN 1857-7431 (Online)

- Catalogue of vascular plants of Burkina Faso (Thiombiano et *al*., 2012).
- Master's and PhD theses from the Laboratory of Botany and Biodiversity: Photo libraries of Dieng (2014 and 2019).

Data Collection

The floral inventory

The inventory was conducted through a field survey, which consisted of traversing the area in all directions, recording all plant species encountered. For each plant, its botanical characteristics were described on site and its common name was recorded. Once at the laboratory, the botanical characteristics of each plant were compared with those described in the available documentation. After identification, each species was assigned its scientific name, and the description of its botanical characteristics was finalized.

Data Processing

Analysis of the flora structure

To analyze the structure of the ornamental flora of Gorée Island, taxonomic, biological and chorological composition were examined.

Taxonomic spectrum

After compiling the floristic list, the taxonomic spectrum shows the distribution of species across different taxonomic ranks (genus, family, class, etc.). Determining the taxonomic spectrum made it possible to establish the number of species, genera, and families recorded and to identify the dominant taxa at each taxonomic rank.

The nomenclature used follows the database managed by the Conservatory and Botanical Garden (CJB) of Geneva; this database is based on the seminal work of Lebrun and Stork (1991-1997) and is accessible on the following regularly updated website:
http://www.ville-ge.ch/musinfo/bd/cjb/africa/index.php?langue=fr
The taxonomic classification used is that of APG III (2009).

Biological spectrum

The biological spectrum shows the distribution of species among different biological forms. These forms refer to "the set of morphological characteristics that play a role in resistance to adverse conditions, and therefore in the localization of plant species" (Serge et *al*., 2015). Raunkier's (1934) biological types are adapted to the intertropical zone where the

ISSN: 1857-7881 (Print)
e-ISSN 1857-7431 (Online)

unfavorable season corresponds to the dry season (Lebrun, 1966). This classification distinguishes eight biological forms, which are:

- phanerophytes (Ph): woody plants whose buds are located more than 50 cm above the ground;
- chamaephytes (C): perennial woody or herbaceous plants, rooted, whose regenerative buds are located near the ground, below 50 cm;
- hemicryptophytes (He): rooted plants whose bud is located on the surface of the soil, and whose aerial part dies during the unfavorable season;
- geophytes (Ge): plants whose bud is well buried in the soil;
- therophytes (Th): plants that survive the unfavorable season in the form of seeds;
- Parasites (Par): plants that draw water, mineral salts and/or photosynthates from other plants (functional parasitism).

The distribution of the recorded species according to Raunkier's (1934) biological types was based on a synthesis of information on species biological types from the work of Berhaut (1971; 1988), Hutchinson et *al*., (2014), and Thiombiano et *al*., (2012). Thus, the biological spectrum was first established at the overall level, without distinguishing individual sites, and was then determined separately for each site.

For the evaluation and interpretation of the results, the percentage of each biological type was calculated using the following formula:

$$\text{Frequency of a given biological type (\%):} \quad \frac{\text{Number of species of the biological type in question}}{\text{Total number of species}} \text{ X 100}$$

Chorological spectrum

The chorological spectrum shows the distribution of recorded species across the various regions of the biosphere. To establish it, each species was assigned to a phytogeographical type based on the regions where it was recorded. The phytogeographical types used are based on the major chorological subdivisions established for Africa by White (1986), the main ones are:

- Cosmopolitans (Cos): species found in both tropical and non-tropical regions;
- Pantropical (Pt): species widespread in Africa, America, tropical Asia and Australia (intertropical regions);
- Paleotropical (Pal): species found in Africa and tropical Asia as well as in Madagascar and Australia (tropical zones of the Old World);
- African American (Am): species found in Africa and tropical America;

ISSN: 1857-7881 (Print)
e-ISSN 1857-7431 (Online)

- African American and Australian (Amu);
- Afro-Asians (As);
- Afro-Asian and Subtropical (AsT);
- Afro-tropical (AT): species distributed throughout tropical Africa;
- Pantropical and Mediterranean (Pt-Me);
- Afro-Malagasy (AM): species distributed in Africa and Madagascar;
- Afro-Malagasy and Asian (Mas);

The phytogeographic distribution of the species identified was synthesized from the chorological information provided in the work of Berhaut (1971-1988), Hutchinson et *al*., (2014) and Thiombiano et *al*., (2012). It was established using the following formula.

$$\text{Frequency of a given phytogeographical type (\%)} = \frac{\text{Number of species of the phytogeographical type in question}}{\text{Total number of species}} \times 100$$

Results and Discussion

Qualitative Analysis

Overall structure of the flora

Table 1 summarizes the results on the list of species inventoried in the three (3) gardens. For each species, its presence or absence in the flora of Senegal, its geographical distribution, and its biological type were noted.

Fifty-five (55) species belonging to 49 genera grouped into 31 families were recorded in the gardens of Gorée Island. Among these ornamental species, 36 have already been cited in the flora of Senegal, while the remaining 19 have not been listed and could be introduced to Senegal.

Table 1: List of species inventoried on Gorée Island

Family	Sub-family	NG	NS	*Espèces*	FS	BT	GR
Acanthaceae (D)		3	4	*Pseuderanthemum carruthersii* (Seem.) Guillaumin	-	C	As
				Pseuderanthemum carruthersii var. reticulatum (W.Bull) Fosberg	-	C	Pt
				Ruellia tuberosa L.	-	C	Am
				Asystasia gangetica (L.) T. Anderson	+	C	Amu
Agavaceae (M)		1	1	*Agave sisalana* L.	+	P	Pt
Aloeaceae (M)		1	1	*Aloe vera* (L.) Burm.f	+	H	Cosm
Amaranthaceae (D)		1	1	*Alternanthera brasiliana* (L.) Kuntze	-	C	Pt
Amaryllidaceae (M)		2	2	*Crinum amabile* Donn ex Kew Gawler.	-	G	Pt

ISSN: 1857-7881 (Print)
e-ISSN 1857-7431 (Online)

Family	Sub-family	NG	NS	*Espèces*	FS	BT	GR
				Hymenocallis speciosa (L. f. ex Salisb.) Salisb.	-	G	As
Apocynaceae (D)	Apocynoideae	4	4	*Catharanthus roseus* (L.) G. Don	+	C	Pt
				Nerium oleander L.	+	P	Pt
				Saba senegalensis (A. DC.) Pichon	+	P	Af
				Thevetia neriifolia Juss. Ex Steud.	+	P	Pt
	Asclepioideae	1	1	*Calotropis procera* Ait	+	P	Pt
Araceae (D)		1	1	*Philodendron lacerrum* (Jacq.) Schott.	-	Np	Am
Araliaceae (D)		1	3	*Polyscias balfouriana* (André) L.H.Bailey	-	Np	Mas
				Polyscias guilfoylei Cogn.et March.	+	P	Pt
				Polyscias guilfoylei. Var.laciniata L.H. Bailey.	+	P	Mas
Arecaceae (M)		3	3	*Phoenix dactylifera* L.	+	P	As-T
				Pritchardia pacifica Seem. Et Wendl.	+	P	Af-Poly
				Washingtonia filifera (Linden ex André) H.Wendl.	+	P	Am
Asparagaceae (M)		2	4	*Sansevieria cylindrica* W.B	-	G	Af
				Sansevieria trifasciata Prain.	-	G	Af
				Sansevieria trifasciata (De Wild.) NEBr. *Var laurentii*	-	G	Af
				Yucca elephantipes Lem.	-	P	Am
Boraginaceae (D)		1	1	*Cordia sebestena* L.	-	P	Pt
Cacataceae (D)		3	3	*Echinocactus grusonii* Hildm.	-	Np	Am
				Nopalea cochenillifera (L.) Salm -Dyck	+	C	Am
				Opuntia tuna (L.) Mill	+	P	Amu
Casuarinaceae (D)		1	1	*Casuarina equisetifolia* L.	+	P	Pt
Combretaceae (D)		1	1	*Terminalia catapa* L.	+	P	Pt
Commelinaceae (M)		2	2	*Tradescantia pallida* (Rose) D.R. Hunt	-	C	Am
				Tradescantia spathacea SW.	+	C	Am
Cyperaceae (M)		1	1	*Cyperus alternifolius* L	+	G	Cosm

ISSN: 1857-7881 (Print)
e-ISSN 1857-7431 (Online)

Family	Sub-family	NG	NS	*Espèces*	FS	BT	GR
Euphorbiaceae (D)		3	3	*Elaephorbia drupifera* (Thonn.) Stapf	+	P	Af
				Euphorbia lactea Haw	+	Np	As
				Pedilanthus tithymaloides (Linn.) Poit.	+	C	Am
Heliconiaceae (D)		1	1	*Heliconia bihai* (L) L.	-	P	Am
Lamiaceae D)		2	2	*Ocimum basilicum* L.	+	T	Cosm
				Volkameria inermis L.	-	Np	As
Lythraceae (D)		1	1	*Punica granatum* L.	-	P	Pt-Me
Malvaceae (D)	Bombacoideae	1	1	*Adansonia digitata* L.	+	P	Ma
	Malvoideae	1	1	*Hibiscus Rosa sinensis* L.	+	P	Ma
Meliaceae (D)		1	1	*Azadirachta indica* L.	+	P	Pt
Moraceae (D)		1	1	*Ficus retusa* L.	+	P	Pt
Moringaceae (D)		1	1	*Moringa oleifera* Lam.	+	Np	Pt
Nyctaginaceae (D)		2	3	*Bougainvillea glabra* Choisy.	+	P	Pt
				Bougainvillea spectabilis Willd.	+	P	Pt
				Mirabilis jalapa L.	+	T	Cosm
Oleaceae (D)		1	1	*Jasminum sambac* (Linn.), Aiton	+	P	AsT
Passifloraceae (D)		1	1	*Turnera ulmifolia* L.	-	C	Pt
Plumbaginaceae (D)		1	1	*Plumbago auriculata* Thunb.	+	H	Pt
Polygonaceae (D)		1	1	*Coccoloba uvifera* (L.) L.	+	P	As-Am
Sapotaceae (D)		1	1	*Manilkara zapota* (L.) P. Royen	+	P	Am
Strelitziaceae (M)		1	1	*Ravenala madagascariensis* Gmel. J.F.	+	P	Ma
Total		**49**	**55**				

Legend: NG (Number of genera), NE (Number of species), FS (Flora of Senegal), + (presence) and - (absence), D (dicotyledons), M (monocotyledons); BT: Phanerophytes (P), Nanophanerophytes (Np), Chamaephytes (C), Hemicryptophytes (H), Geophytes (G), Therophytes (T); GR (Geographic Distribution), African (Af), African American (Am), American (Am), African American and Asian (Am As), Afro-Asian (As), Afro-Malagasy and Asian (Mas), and Pantropical (Pt). TB (Biological type), P (Phanerophytes), G (Geophytes), C (Chamaephytes), H (Hemicryptophytes), T (Therophytes)

Taxonomic spectrum

Table 2 provides information on the taxonomic spectrum of the ornamental flora of Gorée Island.

ISSN: 1857-7881 (Print)
e-ISSN 1857-7431 (Online)

This flora is 100% dominated by angiosperms (Table 2). Among these angiosperms, dicotyledons are dominant with 70.97% of families, 75.51% of genera and 72.73% of species.

Table 2: Taxonomic spectrum

Taxonomic Groups	Families		Genres		Species	
	Nb	Proportion (%)	Nb	Proportion (%)	Nb	Proportion (%)
Dicotyledons	22	70.97	37	75.51	40	72.73
Monocotyledons	9	29.03	12	24.49	15	27.27
TOTAL	**31**	**100.00**	**49**	**100.00**	**55**	**100.00**

Nb = number

Table 3 shows the distribution of the species inventoried by family in the three (3) gardens of Gorée Island.

The analysis reveals that this flora is dominated by three families: Apocynaceae (9.09%), followed by Acanthaceae (7.27%) and Asparagaceae (7.27%), which together account for 23.64% of the flora. However, five other families are also relatively well represented, each accounting for 5.45%: Araliaceae, Arecaceae, Cacataceae, Euphorbiaceae, and Nyctaginaceae (Table 3). The remaining 23 families comprise 49.09% of the flora.

Table 3: Distribution of species by ornamental family

Familles	Nombre d'espèces	Proportion (%)
Apocynaceae (D)	5	9,09
Acanthaceae (D)	4	7,27
Asparagaceae (M)	4	7,27
Araliaceae (D)	3	5,45
Arecaceae (M)	3	5,45
Cacataceae (D)	3	5,45
Euphorbiaceae (D)	3	5,45
Nyctaginaceae (D)	3	5,45
Amaryllidaceae (M)	2	3,64
Commelinaceae (M)	2	3,64
Lamiaceae D)	2	3,64
Malvaceae (D)	2	3,64
Agavaceae (M)	1	1,82
Aloeaceae (M)	1	1,82
Amaranthaceae (D)	1	1,82
Araceae (D)	1	1,82
Boraginaceae (D)	1	1,82
Casuarinaceae (D)	1	1,82
Combretaceae (D)	1	1,82
Cyperaceae (M)	1	1,82
Heliconiaceae (D)	1	1,82
Lythraceae (D)	1	1,82
Meliaceae (D)	1	1,82
Moraceae (D)	1	1,82
Moringaceae (D)	1	1,82
Oleaceae (D)	1	1,82

ISSN: 1857-7881 (Print)
e-ISSN 1857-7431 (Online)

Familles	Nombre d'espèces	Proportion (%)
Passifloraceae (D)	1	1,82
Plumbaginaceae (D)	1	1,82
Polygonaceae (D)	1	1,82
Sapotaceae (D)	1	1,82
Strelitziaceae (M)	1	1,82
TOTAL	**55**	**100,00**

Biological Spectrum

Figure 2 presents the biological types of species in the three gardens on Gorée Island. Analysis of Figure 2 shows that Phanerophytes are the most represented, accounting for 50.91% of the flora, followed by Chamaephytes (20%). Geophytes and Nanophanerophytes each account for 10.91%. Hemicryptophytes and Therophytes each represent 3.64% of the recorded species.

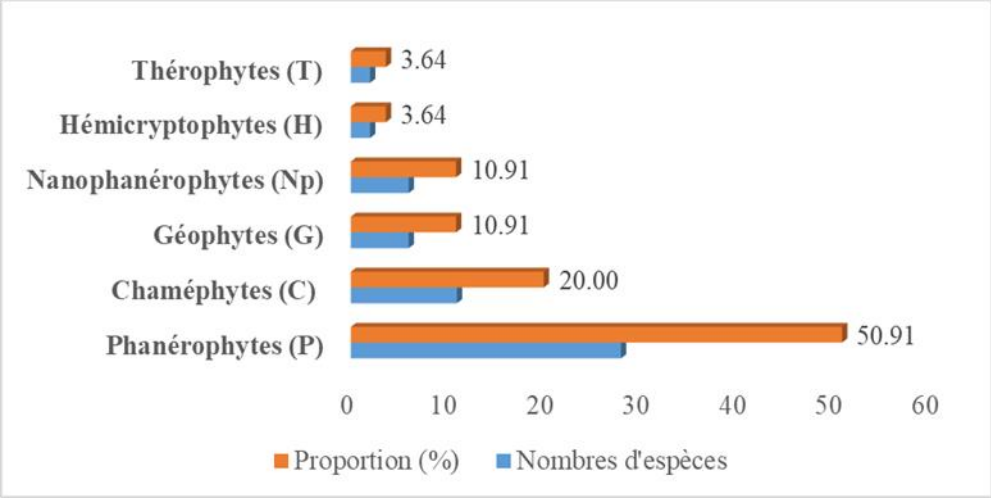

Figure 2 : Biological types of species

Chorological spectrum

Data on the distribution of species according to their geographical affinities are recorded in Table 4. This ornamental flora is dominated by pantropical species, which account for 34.55% of the species listed. These are followed by Afro-American and African species, accounting for 21.82% and 9.09%, respectively. In contrast, the Afro-Asian and cosmopolitan species are relatively well represented, each accounting for 7.27% of the flora.

ISSN: 1857-7881 (Print)
e-ISSN 1857-7431 (Online)

Table 4 : Chorological spectrum

Biogeographical affinities	Number of species	Proportion (%)
Pantropical species (Pt)	19	34.55
African American (Am) species	12	21.82
African species (Af)	5	9.09
Afro-Asian species (As)	4	7.27
Cosmopolitan species (Cosm)	4	7.27
Afro-Malagasy species (Ma)	3	5.45
Tropical Afro-Asian Species (AsT)	2	3.64
Afro-Malagasy and Asian species (Mas)	2	3.64
African and Polynesian (Af-Poly) species	1	1.82
Pantropical and Mediterranean (Pt-Me) species	1	1.82
African American and Australian (Amu) species	1	1.82
Afro-Asian and American (As Am) species	1	1.82
TOTAL	**55**	**100.00**

Discussion

The species diversity of the gardens and pathways of Gorée includes 55 species. This figure is lower than that of Dieng (2019) and Sagna (2019), who recorded 225 and 160 ornamental species, respectively, in Dakar and Mbour. This difference in floristic richness can be explained by the fact that the 2019 inventory was conducted in 84 horticultural sites in the Dakar region, whereas for this study, only three gardens and the small pathways of the Gorée municipality were visited. Furthermore, Dakar and Mbour are the main cities where floral activity has been rising in recent years. However, this figure is higher than that of Fall (2023), who recorded 44 species in the green spaces of Gorée. Moreover, 34.54% of these ornamental species are not present in the vascular and illustrated flora of Senegal. This could be explained by the fact that floriculture is one of the main drivers of the introduction of invasive plants throughout the world (Reichard et *al*., 2001; Bell et *al*., 2003; Dehnen-Schmutz et *al*., 2007; Burt et *al*., 2007).

From a taxonomic diversity perspective, the ornamental flora of the Gorée commune is dominated by dicotyledons (70.97%) and monocotyledons (29.03%). These angiosperms comprise 49 genera belonging to 31 families. These results corroborate those of Dieng (2019), Sagna (2019), and Gaye (2018), who also noted a dominance of dicotyledons of 63.11%, 65.63% and 78.94%. Furthermore, it should be noted that perennial species are by far the most common, representing 96.36% of the ornamental flora. Annual species, on the other hand, account for only 3.64% of the species recorded. These results are similar to those of Dieng (2019) and Sagna (2019), who also showed that perennial species are by far the most prevalent, at 93.33% and 94.38%, respectively. This similarity could be explained by the fact that these perennial species are better adapted to local climatic conditions or better suited to landscaping needs. Moreover, seasonal ornamental plants are not widely

ISSN: 1857-7881 (Print)
e-ISSN 1857-7431 (Online)

cultivated by Senegalese nursery growers due to their high maintenance costs. Municipalities, hotels, and private clients also seek perennial ornamental species that offer year-round greenery and do not require seasonal maintenance.

Regarding biogeographical affinities, the ornamental flora of Gorée, like that of most Senegalese cities (Dakar, Mbour) and other African cities, is dominated by exotic taxa. Only 9.09% of the recorded species originate from the African continent, and approximately 36 species are reported in the flora of Senegal. The remaining 19 have not been recorded and can therefore be considered newly introduced species to Senegal through floriculture. The increased importance of pantropical species seems linked to Senegal's more westerly and oceanic geographical position (Dieng, 2014; Dieng, 2019). It is likely that these species are better adapted to Senegal's bioclimatic conditions than some strictly African species.

Conclusion

This study aimed to contribute to a better understanding of the ornamental flora of Gorée Island and identified 55 species belonging to 49 genera of 31 families. This flora is entirely dominated by angiosperms, with dicotyledons representing the majority (70.97% of families, 75.51% of genera, and 72.73% of species). It is characterized by the predominance of three families: Apocynaceae (9.09%), Acanthaceae (7.27%), and Asparagaceae (7.27%), accounting for 23.64% of the flora. Biologically, Phanerophytes clearly dominate the flora, accounting for 50.91% of the identified species, followed by Chamaephytes (20%). Regarding geographical distribution, pantropical species dominate, accounting 34.55% of the species cited, followed by Afro-American and African species with 21.82% and 9.09%, respectively. This work has allowed us to characterize the ornamental flora of Gorée Island. Indeed, the structure of the flora, as well as its taxonomic, biological, and chorological spectra, has been determined.The results of this study can be used to develop tools for identifying taxa (identification keys).

Conflict of Interest: The authors reported no conflict of interest.

Data Availability: All data are included in the content of the paper.

Funding Statement: The authors did not obtain any funding for this research.

References:

1. Adjima T., Marco S., Stefan D., Amadé O., Karen H., Georg Z.- Catalogue of vascular plants of Burkina Faso- 2012- Edition of the

ISSN: 1857-7881 (Print)
e-ISSN 1857-7431 (Online)

conservatories and botanical gardens of the City of Geneva; Volume 65; ISSN: 0373-2975 65 1-391 (2012)
2. Angiosperm Phylogeny Group, 2009. An update of the Angiosperm Phylogeny Group classification for the orders and families of flowering plants: APG III. Botanical Journal of the Linnean Society 161: 105-121.
3. Bell C.E., Wilen C.A., Stanton A.E., 2003. Invasive plants of horticultural origin. Hortscience, 38:14-16.
4. Berhaut J., 1967 - Flora of Senegal. Dakar. 2nd Ed. Clairafrique.
5. Berhaut J., 1971 - Illustrated Flora of Senegal, Dicotyledons, Volume I, Acanthaceae to Avicenniaceae. Senegal. Government of Senegal, Ministry of Rural Development, Directorate of Water and Forests.
6. Berhaut J., 1974 - Illustrated Flora of Senegal, Dicotyledons, Volume II, Balanophoraceae to Compositae. Senegal. Government of Senegal, Ministry of Rural Development, Directorate of Water and Forests.
7. Berhaut J., 1975 - Illustrated Flora of Senegal, Dicotyledons, Volume III, Connaraceae to Euphorbiaceae. Senegal. Government of Senegal, Ministry of Rural Development, Directorate of Water and Forests. 8. Berhaut J., 1975 - Illustrated Flora of Senegal, Dicotyledons, Volume IV, Ficoideae to Leguminosae. Senegal. Government of Senegal, Ministry of Rural Development, Directorate of Water and Forests.
8. Berhaut J., 1976 - Illustrated Flora of Senegal, Dicotyledons, Volume V, Papilionaceous Legumes. Senegal. Government of Senegal, Ministry of Rural Development, Directorate of Water and Forests. 43
9. Berhaut J., 1979 - Illustrated Flora of Senegal, Dicotyledons, Volume IV, Linaceae to Nymphaeaceae. Senegal. Government of Senegal, Ministry of Rural Development, Directorate of Water and Forests.
10. Dehnen-Schmutz K., Touza J., Perrings C., Williamson M., 2007. The horticultural trade and ornamental plant invasions in Britain. Conservation Biology, 21: 224-231.
11. Dieng B. (2014) – Ornamental plants of the city of Dakar: Characterization of the flora, Key to the identification of taxa and Photo Library. Master's thesis in Taxonomy, Biodiversity, Ethnobotany and Conservation of Natural Resources, UCAD, 162.
12. Dieng B. (2019) – Floriculture in Dakar (Senegal): Diagnosis of farms, Characterization of taxa and Valorization. Cheikh Anta Diop University, Dakar (Senegal), 266.
13. Fall N.F.D. (2023) – Green spaces of Gorée (Dakar-Senegal): Characterization of the flora and valorization of plant potential; Master's thesis; Department of Plant Biology; Cheikh Anta Diop University, Dakar (Senegal). P 59.

ISSN: 1857-7881 (Print)
e-ISSN 1857-7431 (Online)

14. Gaye A. (2018) – Medicinal ornamental plants of Dakar (Senegal): characterization of taxa and therapeutic values. Master's thesis in Taxonomy, Biodiversity, Ethnobotany and Natural Resource Conservation, UCAD, 53.
15. Hutchinson J., Dalziel J.M. (1954) – Flora of West Tropical Africa, vol. I, part 1. London: Millbank, s.w.1.
16. Hutchinson J., Dalziel J.M. (1958) – Flora of West Tropical Africa, vol. I, part 2. London: Millbank, s.w.1.
17. Hutchinson J., Dalziel J.M. (1963) – Flora of West Tropical Africa, vol. II. London: Millbank, s.w.1.
18. Hutchinson J., Dalziel J.M. (1968) – Flora of West Tropical Africa, vol. III, part 1. London: Millbank, s.w.1.
19. Hutchinson J., Dalziel J.M. (1972) – Flora of West Tropical Africa, vol. III, part 2. London: Millbank, s.w.1.
20. MEED (2014) – Fifth National Report on the Implementation of the Convention on Biological Diversity.
21. Radji A.R., Kokou K., Akpagana K. (2010) – Diagnostic study of the ornamental flora of Togo. Int. J. Biol. Chem. Sci. 4(20, pp. 491-508.
22. Sagna G. (2019) – Floriculture in Mbour (Senegal): Diagnostic Study and Characterization of Ornamental Flora. Master's Thesis in Taxonomy, Biodiversity, Ethnobotany and Conservation of Natural Resources, UCAD, p. 84.
23. Thiombiano A., Schmidt M., Dressler S., Ouédraogo A., Hahn K., Zizka G. (2012) - CATALOGUE OF VASCULAR PLANTS OF BURKINA FASO, Botanical Conservatory and Garden Publishing ; ISSN: 0373-2975 65 1-391 (2012)

ESJ Natural/Life/Medical Sciences Peer-reviewed

Contribution to Hydrogeological Knowledge of the Turonian-Coniacian Aquifer Exploited in the Coastal Sedimentary Basin of Benin-Togo

Glessougbe Cherguie Mellone Extraila
Laboratory of Applied Hydrology (LHA), National Water Institute (INE), University of Abomey-Calavi (UAC), Cotonou, Benin
International Chair in Mathematical Physics and Applications (ICMPA – UNESCO Chair), Cotonou, Benin
Alassane Abdoukarim
Kodjo Apelete Raoul Kpegli
Laboratory of Applied Hydrology (LHA), National Water Institute (INE), University of Abomey-Calavi (UAC), Cotonou, Benin
Gnandi Kissao
Waste Management, Treatment and Recovery Laboratory, Faculty of Sciences, University of Lomé, Lomé, Togo
Bio Guidah Chabi
Alassane Zakari Aoulatou
Laboratory of Applied Hydrology (LHA), National Water Institute (INE), University of Abomey-Calavi (UAC), Cotonou, Benin
International Chair in Mathematical Physics and Applications (ICMPA – UNESCO Chair), Cotonou, Benin
Daouda Mama
Moussa Boukari
Laboratory of Applied Hydrology (LHA), National Water Institute (INE), University of Abomey-Calavi (UAC), Cotonou, Benin

Doi:10.19044/esj.2026.v22n6p102

Submitted: 22 September 2025
Accepted: 12 February 2026
Published: 28 February 2026

Cite As:
Glessougbe, C. M. E., Abdoukarim, A., Kpegli, K. A. R., Kissao, G., Chabi, B. G., Aoulatou, A. Z., Mama, D., & Boukari, M. (2026). *Contribution to Hydrogeological Knowledge of the Turonian-Coniacian Aquifer Exploited in the Coastal Sedimentary Basin of Benin-Togo.* European Scientific Journal, ESJ, 22 (6), 102. https://doi.org/10.19044/esj.2026.v22n6p102

ISSN: 1857-7881 (Print)
e-ISSN 1857-7431 (Online)

Abstract

Our article contributes to improving hydrogeological knowledge of the Turonian-Coniacian aquifer in the Benin-Togo coastal sedimentary basin by determining the geometry, structure, and piezometry of this aquifer in the northern part of the Benin-Togo coastal sedimentary basin. The structure of the Turonian-Coniacian aquifer was determined through geological and hydrogeological correlation of existing logs from thirty-three boreholes on the northern plateaus of the Benin-Togo coastal sedimentary basin. Three cross-sections were created (in Benin and Togo) using the traditional method, combining topographic maps, graph paper, and QGIS 2.18.15. Piezometry was then carried out in three stages: determination of the altitudes of the measurement points (56 wells), calculation of the piezometric levels, and interpolation of the calculated piezometric levels. The piezometric map was produced successively using Excel, Surfer 11, and QGIS 2.18.15.

A total of five layers were identified following the hydrogeological sections carried out. These are the lateritic layer (2 to 15 m from north to south); the sandy layer (extending up to 25 m); the very thick clay layer (60 m in the south, 200 m in the Lama depression, and almost absent in the north); the clayey-sandy layer (varying from 4 to 25 m in some areas); and the limestone layer (embedded in the clay layer, reaching up to 20 m in thickness). The Coniacian-Turonian aquifer outcrops north of the northern plateaus of the Benin-Togo coastal sedimentary basin. As the flow direction is mainly north-south, it can be deduced that the aquifer is recharged by rainwater infiltration in its outcrop areas.

Although the resource is natural, as is its renewal, it is important that the nations that exploit it, including Benin and Togo, reach a consensus on its efficient use in order to avoid any conflict in the future.

Keywords: Turonian-Coniacian, coastal sedimentary basin, groundwater flow, kriging, SRTM

Introduction

Globally, the issue of water supply is becoming increasingly worrying. Groundwater constitutes the largest reserve of liquid drinking water on the planet and has an annually renewable volume through precipitation infiltration of approximately 8 to 10 million km3, or 98 to 99% of the total (Margat, 1989). In recent decades, this freshwater resource has been affected by phenomena linked to climate change (Holman et al., 2012; Seguin et al., 2019) and socio-economic developments (Mérino, 2009), leading to an explosion in water consumption and, inevitably, a deterioration in its quality. In many regions of Africa, such as Benin and Togo, groundwater is the only reliable source of water. Up to 75% of the population uses groundwater as their main source of

ISSN: 1857-7881 (Print)
e-ISSN 1857-7431 (Online)

drinking water, which is accessible at low cost (Nijsten, 2018; Mérino, 2009; Penant, 2016). It is also a vital source of fresh water in all tropical regions, providing access to safe water for domestic, agricultural, and industrial purposes close to the point of demand (Kotchoni et al., 2019).

Translated with DeepL.com (free version)Benin and Togo mainly use groundwater to supply drinking water to their populations, as it is generally of better quality than surface water. However, limited knowledge of the hydrogeological characteristics of the land could seriously jeopardise the preservation of these water resources for future generations (Orou-Pété et al., 2021). The Turonian-Coniacian is one of the four major aquifer units in the Coastal Sedimentary Basin (BSC) and is the deepest. It is tapped in the north of the BSC (where it outcrops) with large-diameter wells; in the Lama depression, it is artesian in nature, and in the south of the BSC. With the uncontrolled spread of urban populations linked to demographic growth, it is urgent to control the reservoir in order to manage it efficiently. The objective is to ensure sustainable management of the resource. Management of this deep aquifer inevitably requires hydrogeological characterization.

The objective of the work is to determine the structure, geometry, and piezometry of the Turonian-Coniacian aquifer.

To achieve our objectives, we asked ourselves the following questions/hypotheses:

- The Turonian-Coniacian aquifer is a continuous layer, regardless of the influence of the dip of the plateaus from Benin to Togo.
- What are the likely areas of renewal for this aquifer?
- How does underground flow occur in the Turonian-Coniacian aquifer?
- Is the Turonian-Coniacian aquifer confined or unconfined?

Study area

Location, Climate, Vegetation, and Soils

The Keta Basin in Benin and Togo is located in the tropical zone between the equator and the Tropic of Cancer, between parallels 6° 10' and 7° 75' north latitude and meridians 1° 0' and 2° 48' east longitude. The study area occupies the southern tip of the two countries, with the Mono River forming the border. Known in Togo as the Togolese Coastal Sedimentary Basin, it covers an area of approximately 3,300 km2, or 6% of the national territory (Gnazou et al., 2015). In Benin, it is known as the Benin Coastal Sedimentary Basin and covers an area of approximately 11,476 km2, or 10% of the national territory (Glodji et al., 2019). The Benin-Togo Coastal Sedimentary Basin (BSCB-T) covers a total area of approximately 14,776 km2 and is bounded to the north by the outcrops of its substrate (Panafrican crystalline basement) and extends southwards into the offshore portion under the Atlantic Ocean,

ISSN: 1857-7881 (Print)
e-ISSN 1857-7431 (Online)

widening from west to east, from the border between Ghana and Togo to that between Benin and Nigeria.

The Turonian-Coniacian aquifer that is the subject of our study outcrops north of the BSC Benin and Togo on the four northern plateaus of Benin (Kétou, Zagnanado, Abomey and Aplahoué) and the three in Togo (Kouvé, Tchévié and Fogbé).

The region, which has a subequatorial climate, is characterised by two distinct rainy seasons linked to the movement of the Intertropical Front (a longer rainy season from mid-March to July and a shorter rainy season from mid-September to November) and two dry seasons from August to mid-September and from December to mid-March, respectively (Achidi et al., 2012).

The average annual rainfall recorded at the Bohicon weather station in Benin (from 1922 to 2009) is 1,197 mm, with potential evapotranspiration of approximately 1,500 mm/year (Achidi et al., 2012; Amoussou, 2005) cited by (Kpegli et al., 2018).

Rainfall across the basin is not uniform; it decreases significantly from the northeast (1,445 mm in Tabligbo) to the southwest (864 mm in Lomé). The average monthly temperature varies between 25 and 29 °C in Lomé (Gnazou, 2008). Similarly, rainfall gradients vary from west to east between 900 and 1450 mm in southern Benin (Alassane, 2004). Relative humidity is high, ranging between 65% and the average annual temperature is 27°C but can reach 38°C in the dry season and drop to 19°C in the rainy season (Kpegli et al., 2018).

The original vegetation of the study area (in Benin) is characterised by a mosaic of forests and savannahs, but has been largely replaced by secondary grasslands or savannahs due to human intervention. However, isolated tropical forests (original vegetation), most of which are protected for religious reasons, still exist (Adjakidje, 1984); (Adjanohoun, 1989; Houndagba, 2015) cited by (Kpegli et al., 2018). In Togo, it is mostly covered by wooded savannah (Alassane, 2004). The Togolese portion of the study area extends over an ecological zone characterised by Guinean humid savannahs with patches of humid forests.

According to (Volkoff, 1970) and (Lamouroux, 1966), cited respectively by (Alassane, 2004) and (Gnazou, 2008), the soils of the entire Benin-Togo coastal sedimentary basin include ferralitic soils. These are either ferruginous sesquioxide soils or leached soils with concretions on clayey-sandy or sandy-clayey sediments, or vertisols on clayey sediments. The coastal and alluvial zone is covered with either hydromorphic soils, halomorphic soils leached with alkalis, or poorly developed soils on coastal or alluvial sands. They also include tropical ferruginous soils leached at shallow depths.

ISSN: 1857-7881 (Print)
e-ISSN 1857-7431 (Online)

The population of the Togo Sedimentary Basin (BSCT) is approximately 1,164,500 inhabitants, according to data from the National Institute of Statistics and Economic and Demographic Studies (INSEED) on the 2010 general population and housing census. The population of the Benin Sedimentary Basin (BSCB) is estimated based on the populations of the various districts covered by the basin. According to the National Institute of Statistics and Economic Analysis (INSAE), it is approximately 5,271,802 inhabitants, RGPH4-2013. The population of the Benin-Togo Coastal Sedimentary Basin (BSCB-T) is around 6,436,300 inhabitants. Economic activities in the basin are dominated by rain-fed agriculture, crafts and trade. Food crops such as maize and cassava are widely grown. Irrigated rice cultivation is also practised in the Kovié, Mission-Tové, Hon, Yovotonou and Ouinhi areas. The BSCB-T is mainly populated by the Evé, Ouatchi, Fon, Goun, Kotafon, Aïzo, Adja, Mina and Xwla peoples, and a few minority groups such as the Yoruba, Haousa and Nago.

Geomorphologically, the Benin-Togo coastal sedimentary basin is organised on either side of the Lama depression, which runs north-northeast to south-southwest, into a series of sloping plateaus cut by river valleys. This basin is drained by the main rivers of the Zio, Haho, Mono, Couffo, Zou and Ouémé.

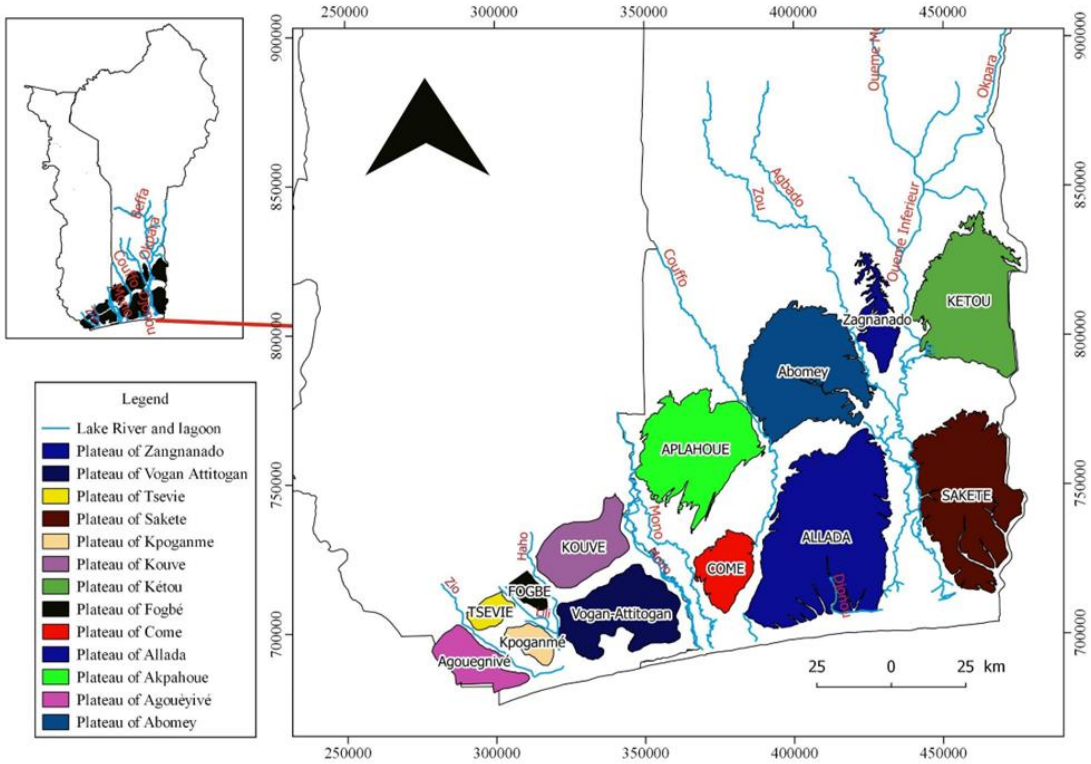

Figure 1: Location of the study area

ISSN: 1857-7881 (Print)
e-ISSN 1857-7431 (Online)

Geology and hydrogeology of the Benin and Togo Coastal Sedimentary Basin

From a geological point of view, according to the synthesis of previous studies on the stratigraphy and geology of this basin, reconstructed using seismic, lithological, structural and sedimentological data, as well as numerous hydraulic and petroleum surveys and mineral deposits (Monciardini et al., 1986); (Sylvain et al., 1986); (Johnson, 1987); (Breda, 1987); (Kaki et al., 2001); (Da Costa et al., 2005) and (Oyédé et al., 2006)), the Kéta Basin, which covers Benin and Togo, comprises sedimentary formations (sand, gravel, sandy clay, clay, marl, limestone) dating from the Cretaceous to the Quaternary periods, which have a monoclinal appearance characterised by differential subsidence, increasing towards the south-southeast (Slansky, 1962); (Gnazou, 2015). The sedimentary aquifers of the coastal basin (Kéta Basin) are multi-layer aquifers, which generally have high productivity (Boukari et al., 1994); (Boukari, 1998).

From a hydrogeological perspective, the Coastal Sedimentary Basin contains four aquifers separated by thick aquicludes with low permeability. These are the Quaternary sand aquifer, the Miocene-Pliocene sand aquifer, the Palaeocene limestone aquifer and the Upper Cretaceous (Turonian-Coniacian) sand aquifer. The Quaternary and Miocene-Pliocene aquifers are shallow and can be tapped with large-diameter wells. The Palaeocene and Upper Cretaceous aquifers are deep, but the Upper Cretaceous aquifer (the subject of our study) has the particularity of outcropping in the northern part of the Coastal Sedimentary Basin, where it is recharged.

The Upper Cretaceous aquifer layer resting on the bedrock, fragmented by longitudinal and transverse faults represented by alternating sandy layers of varying thickness, is free-flowing north of the Lama depression (on the northern plateaus) and confined to the south. Its thickness gradually increases from 50 to 60 m in the north to more than 800 m near the coast (Maliki, 1993, cited by Alassane, 2004). In Togo, its thickness varies between 5 and 25 m and is clayey or sandy-clayey in nature. The depth varies between 50 and 120 m in places (Gnazou, 2008).

ISSN: 1857-7881 (Print)
e-ISSN 1857-7431 (Online)

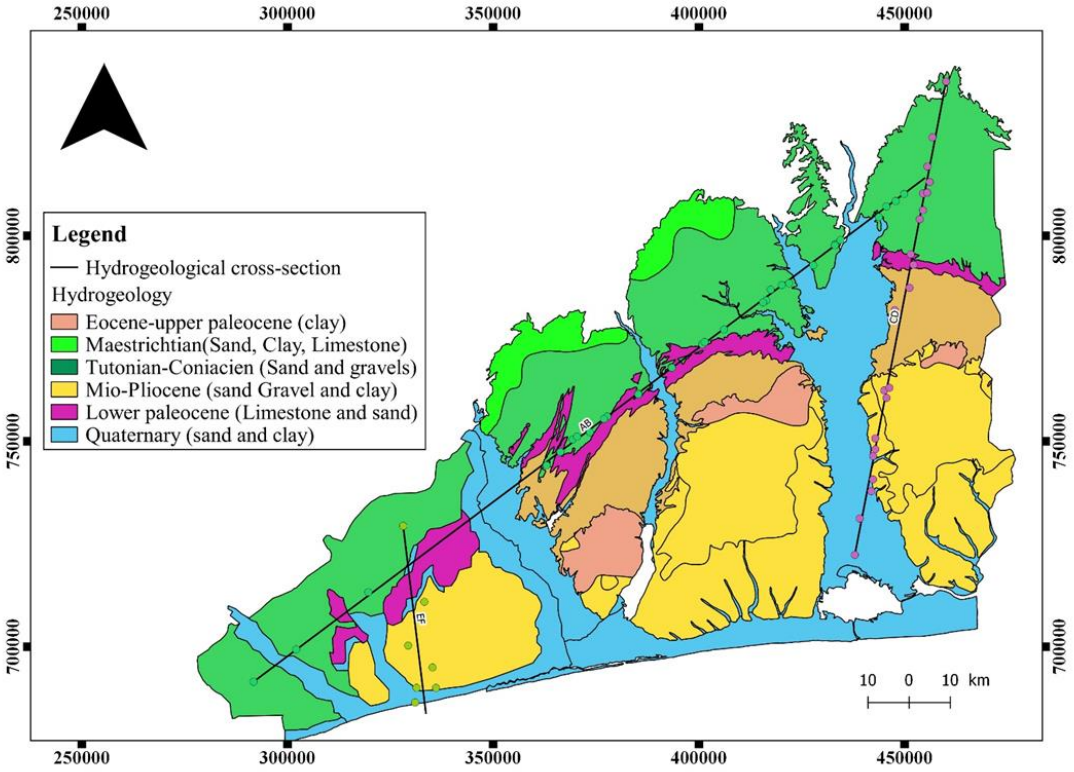

Figure 2: Geology of the Benin-Togo Sedimentary Basin showing the sections to be cut

The Benin and Togo coastal sedimentary basins have been the subject of several geological and hydrogeological investigations. The four aquifer units have been studied by several authors. According to (Dray et al., 1989), it is preferable to exploit the deep, high-quality, well-protected Coniacian Turonian aquifer rather than the surface aquifers, which are prone to frequent contamination problems.

Is this aquifer not being renewed? Where is it recharged? Is it through outcrops or lateral flow?

Our study consists of observing the current behavior of the aquifer, specifying its structure and geometry, and searching for likely areas of resource renewal and its direction of underground flow.

Materials and methods

Data collected and materials used

The data collected initially concerned stratigraphic logs (from boreholes and piezometers), from which those used to produce hydrogeological cross-sections were selected. We then collected topographical maps of the terrain in Benin and Togo from the National

ISSN: 1857-7881 (Print)
e-ISSN 1857-7431 (Online)

Geographic Institute (IGN) and the Directorate General of Cartography (DGC) in Lomé, respectively.

We then carried out a field campaign consisting of measuring static levels in 58 large-diameter wells during the high water period (July 2023) in Benin and eight wells in Togo (insignificant for producing a piezometric map) during the same period (July 2023). This piezometric study campaign was carried out over a one-week period to ensure that groundwater levels were comparable. These static levels were used to produce the piezometric map of the aquifer system, which is presented and analyzed below.

During our site work, we used a Garmin GPS (Global Positioning System) to record geographic coordinates in the field, a piezometric probe to measure static levels, Grapher 15 and Excel software for data processing, QGIS 2.18.15 to organize scanned images of lithostratigraphic correlations and hydrogeological sections produced on graph paper, and QGIS and Surfer 11 for map creation and a digital camera for instant photographs.

Méthods

Hydrogeological cross-sections

To determine the structure and geometry of the aquifer captured by the exploitation works, we first carried out a geological identification by creating three (03) cross sections. These are the Benin-Togo (AB), Kouvé-Attitogan (EF), and Kétou Sakété (CD) cross sections (NNE-SSW direction). To produce these sections, the stratigraphic logs from the boreholes were projected in QGIS 2.8.15. Thirty-three (33) drilling logs were used for the three sections: eighteen (18) logs for the Benin-Togo (AB) section, five (05) for the Kouvé-Attitogan section, and ten (10) for the Kétou-Sakété section. To select them, we first sorted the boreholes capturing the Coniacian Turonian in the database of the Directorate General of Water (DGEau), then used those located on or near our various cross-cutting lines from this selection. Next, the topographic profiles and lithostratigraphic correlations between the various stratigraphic logs of the boreholes were drawn on graph paper using the topographic maps mentioned above. The static levels (measured during drilling) were then transferred to the vicinity of the boreholes and, finally, these levels were correlated to obtain the piezometric line of the captured horizon; the sections obtained were scanned, organized, and digitized in QGIS 2.8.15 to be exported as images.

Piezometric surveys

To identify the measuring wells, we started from the data provided by the Directorate General for Water, identifying the wells that capture the Turonian-Coniacian aquifer. Statistical levels (NS) were measured in 56 (fifty-six) wells (large diameter) by first measuring the depth of the water relative to

ISSN: 1857-7881 (Print)
e-ISSN 1857-7431 (Online)

the well coping using a piezometric probe, then subtracting the height of the rim. Next, the geographical coordinates (X and Y) were recorded at each well using a GPS device.

The piezometric map were created in three stages: determining the altitudes of the measurement points, calculating the piezometric levels, and interpolating the calculated piezometric levels. We began by determining the altitudes of the measurement points.

The piezometric level is the static level relative to mean sea level (0). As we were unable to level all our measurement points and could not rely on the low accuracy of the Z altitudes recorded by GPS in the field, we determined them using an equation (3) that was established through a correlation between the altitude values of the IGN Benin geodetic markers located within and near the study area, and the altitude values of these geodetic benchmarks extracted from a global 1-arc second SRTM Digital Terrain Model (DTM) (DTM with a spatial resolution of 30m x 30m, downloaded from the website https://ers.cr.usgs.gov/ already mentioned above).

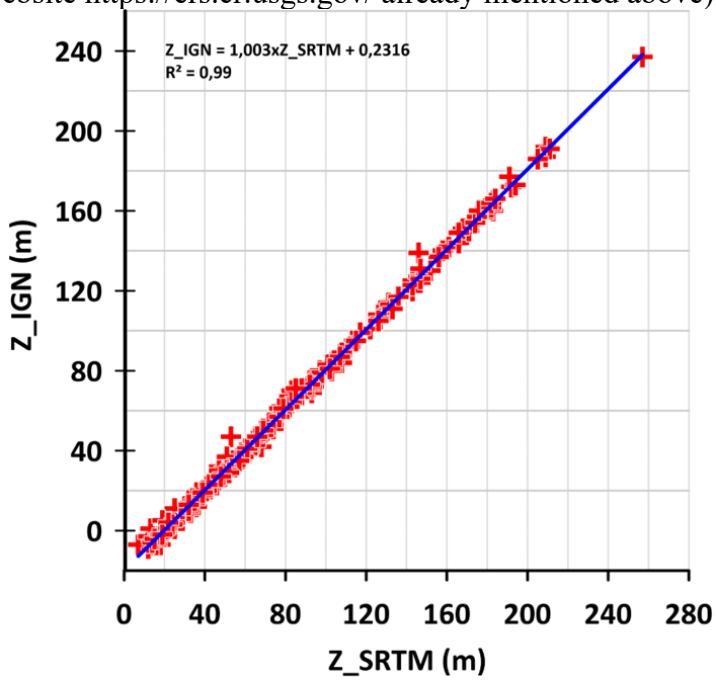

Figure 3: Correlation line between IGN altitudes and SRTM altitudes

We then calculated the piezometric levels (Np) using the formula

Np= Z-Ns/sol

Equation (1)

Replacing Z with its value in equation (1), we obtained:

Np= (1.003*Z_MNT+0.2316) –Ns/sol

Equation (2)

ISSN: 1857-7881 (Print)
e-ISSN 1857-7431 (Online)

With NP (m): the piezometric level, Z: the estimated altitude of the measurement point; Z_MNT: the altitude of the point from the SRTM 1Arc global DTM source at https://ers.cr.usgs.gov/ and NS: the static level measured relative to the ground.

The advantage of RSR is that it normalizes the root mean square error (RMSE) by the standard deviation of the components concerned (Moriasi et al., 2007). The values of the comparison criteria between the experimental variogram and the modeled variogram are presented in Table 1.

Table 1: Values of parameters for comparing measured piezometric levels and those estimated from the DTM

MNT	NSE	RSR	R^2	Taux de performance du NSE	Taux de performance du RSR
SRTM	0,9978	0,046	0,9982	Satisfaisant	très bien
CGIAR	0,3147	0,82	0,4912	Insatisfaisant	mauvais
GTOPO30	0,8148	0,43	0,22	Satisfaisant	bien

For plotting the iso-value curves, the interpolation method chosen is kriging, as the results can be checked using distance variograms, (Orou pété et al., 2021). According to (Matheron, 1965), cited in (Orou pété et al.,2021), the theoretical variogram is only representative of the empirical variogram in the vicinity of the origin. The power model is the one that best fits our piezometric level values.

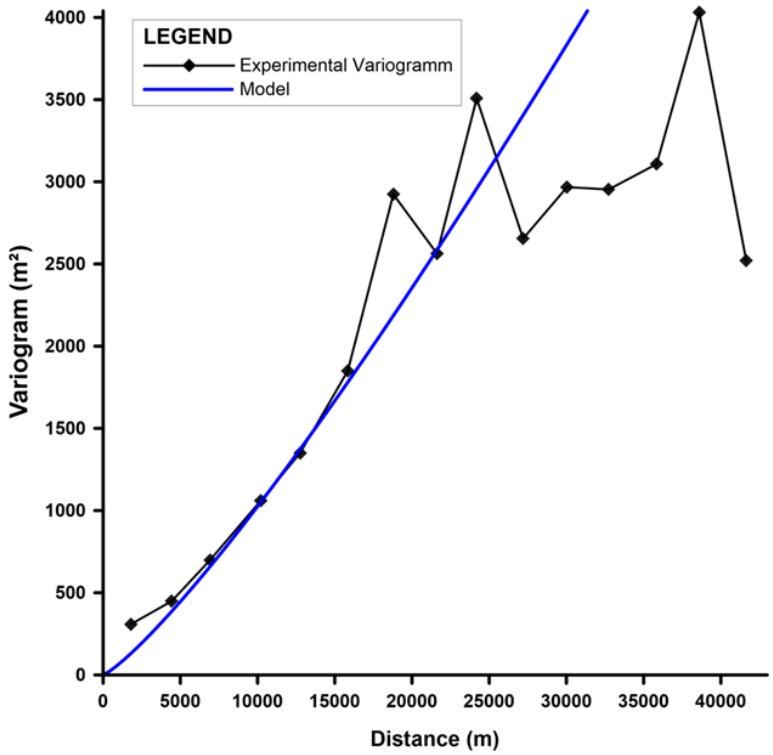

Figure 4: Adjusted distance variograms for piezometric levels

ISSN: 1857-7881 (Print)
e-ISSN 1857-7431 (Online)

The formula for the power adjustment model is as follows:

$$\gamma(h) = 1{,}5+bh^{1{,}99} \text{ with b: the slope of the straight line.}$$

In Togo, this approach could have been applied if we had not been limited by the availability of functional wells. Piezometry was only possible in Benin in this case. Nevertheless, (Gnazou, 2015) addressed the piezometry of the Paleocene aquifer, which seems to reflect, given the relief and dip of the plateaus, the flow of water over the coastal sedimentary basin of Togo.

Results

Geological and hydrogeological identification of the aquifer being exploited

Based on the lithological cross-sections collected from boreholes, three hydrogeological cross-sections were produced in the following directions: South-West to North-East (Togo-Benin); North-North-West to South-South-East (Kouvé-Atitogan); NN East–SS West (Kétou-Sakété). The hydrogeological sections obtained are shown in Figures 5, 6 and 7.

Five (05) more or less continuous layers of different lithology are crossed by the correlated boreholes. They consist of a surface layer of laterite (1 to 7 m), a clay layer dating from the Maastrichtian, sandy layers, a clay-sandy layer, and limestone. The thickness of the layers varies depending on the location of the sections. In the section leaving Benin, the lateritic layer is superficial, ranging from 1 to 7 m, while the clay layer, which gradually thickens in the Lama depression in Benin, narrows north of Kétou and varies between 3 m and 35 m. The sandy layer varies between 3 and 20 m in Togo, 5 to 10 m in the Lama depression in Benin, and outcrops north of Kétou.

For the Kouvé-Atitogan and Kétou-Sakété sections, the clayey-sandy layer is 4 to 25 m thick, the sand up to 10 m, and two limestone levels are encountered (2 to 20 m each). The clay layer reaches a thickness of 150 to 200 m in the south (in the Lama depression) and decreases until it disappears in the north.

The sandy layer (which appears to have two levels in Togo) is a Turonian-Coniacian formation (Cretaceous sand), while the limestone layer between the thick clay layers is a Palaeocene formation.(Monciardini et al., 1986). The sandy layer has a section that outcrops (and is therefore unconfined) to the north of the plateaus and gradually sinks towards the south until it disappears completely under the thick clay layers, making the aquifer confined. The Palaeocene limestone aquifer is confined from south to north of the Coastal Sedimentary Basin.

ISSN: 1857-7881 (Print)
e-ISSN 1857-7431 (Online)

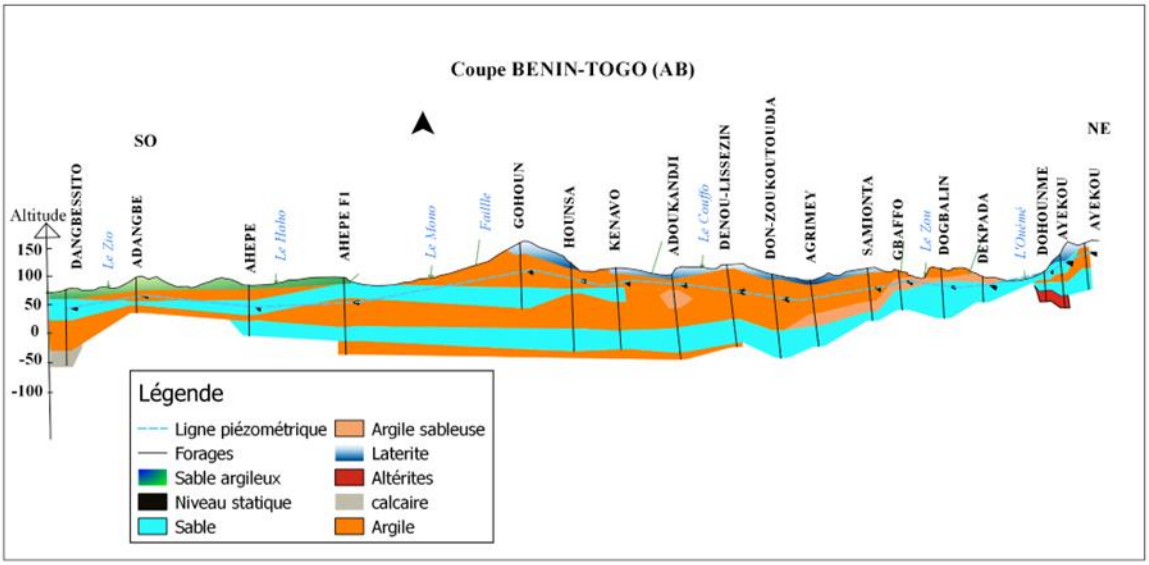

Figure 5: Hydrogeological cross-section of Benin-Togo

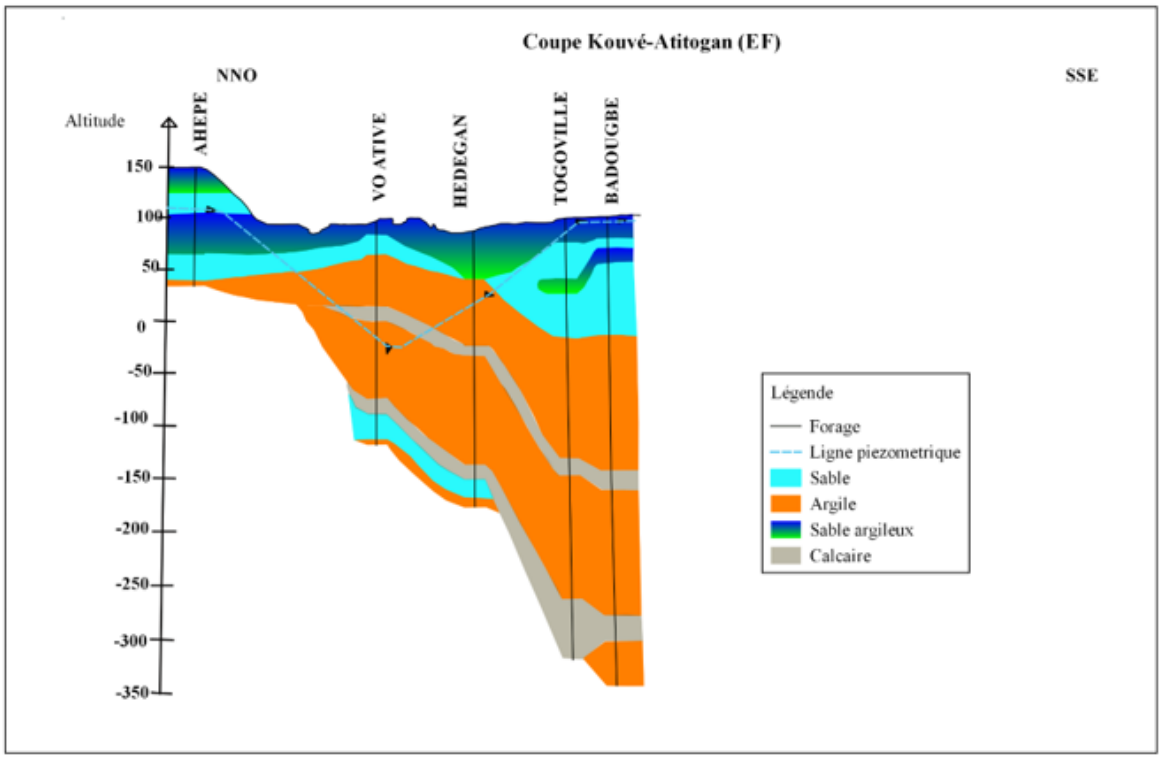

Figure 6: Hydrogeological cross-section of Kouvé-Atitogan

ISSN: 1857-7881 (Print)
e-ISSN 1857-7431 (Online)

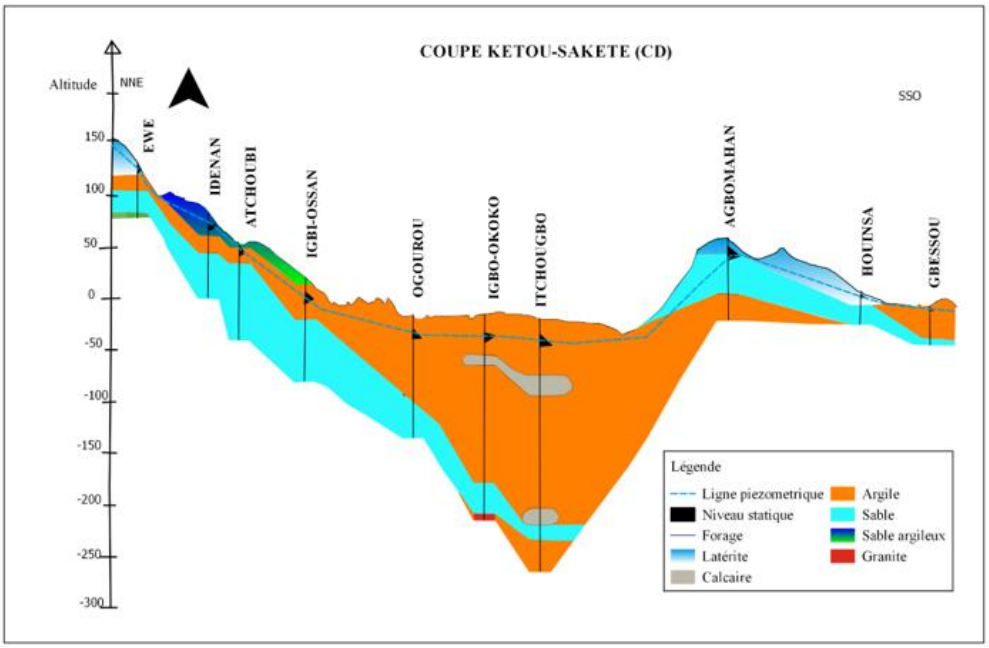

Figure 7: Hydrogeological cross-section of Kétou-Sakété

Piezometry

Piezometric surveys of the aquifer (Figure 8) were only possible for the Beninese part, given the unrepresentative nature of the wells due to their virtual absence in our study area in Togo. The flow directions are multidirectional and differ from one plateau to another. We have a first recharge zone located north of the study area (north of the Kétou plateau) at an altitude of approximately 120 m and a second recharge zone located on the Zagnanado plateau, from where groundwater flows mainly southward. The highest altitude on this plateau is 180 m, compared to 40 m in the depression zone. Observing the direction of flow, groundwater diverges locally on this central plateau towards the Zou and Ouémé river valleys. A recharge zone located northwest of the northern plateau of Abomey, from where groundwater generally flows towards the southeast. The fourth recharge zone is located to the northeast, on the Aplahoué plateau (Kpégli et al., 2018). On these last two plateaus, the highest point is 200 m above sea level.

ISSN: 1857-7881 (Print)
e-ISSN 1857-7431 (Online)

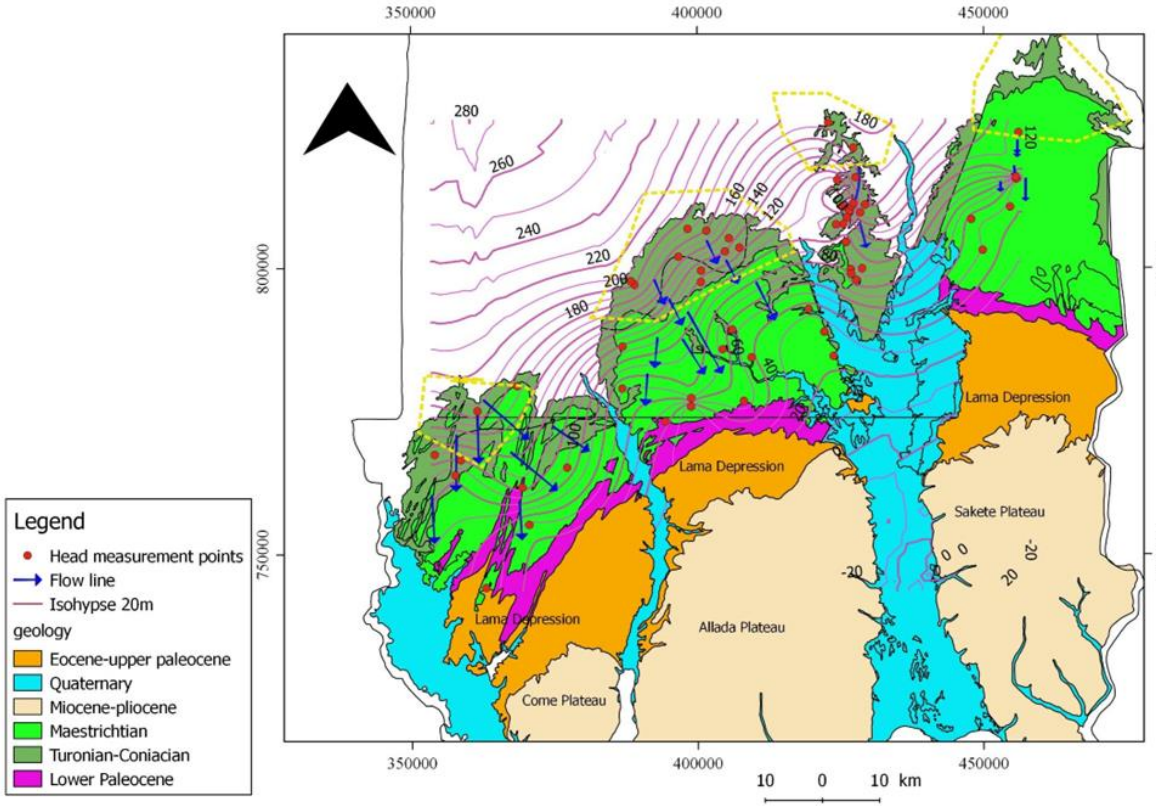

Figure 8: Piezometric map of Turonien Coniacien in Bénin

In the absence of a piezometric map of the Turonian-Coniacian in Togo, the author (Gnazou, 2005) highlighted the direction of underground flow through his study of the Paleocene limestone aquifer (Figure 09). Flow generally occurs from north to south.

ISSN: 1857-7881 (Print)
e-ISSN 1857-7431 (Online)

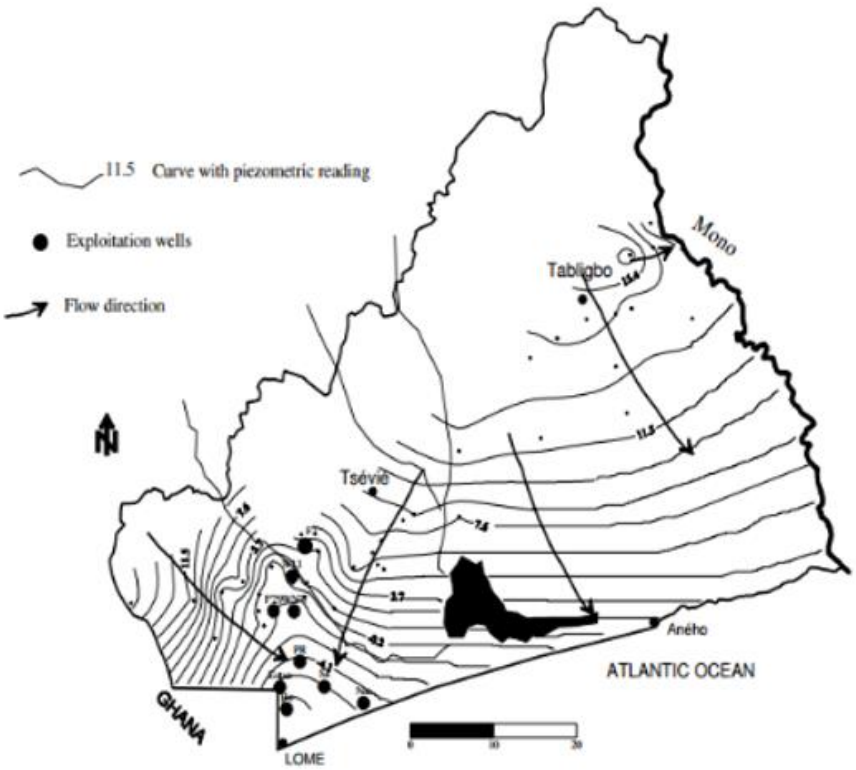

Figure 9: Piezometric map produced by Gnazou in March 2005 showing the general direction of flow in the coastal sedimentary basin in Togo

Discussions

Previous studies, such as those by Slansky (1962), have contributed to the geological study of the Benin-Togo coastal sedimentary basin and show how the layers and facies are structured. Lithostratigraphically, the deposits studied consist mainly of fluvial to marine detrital facies (sandstone, various sands) and sandstone-carbonate rocks (calcareous sandstone, calcareous siltstone). They show several lateral variations in facies and a thickening of all formations from the northern edge towards the center of the basin (Da Costa et al., 2013). The formations in the basin have a slightly inclined structure, marked by a slight dip of 1 to 2° towards the southeast due to plate tectonics (Da Costa et al., 2013).

The Kouvé-Attitogan (Fig. 6) and Kétou-Sakété (Fig. 7) sections crossing the Lama depression reveal the presence of limestone (Paleocene) trapped between thick layers of clay 15 to 30 m thick in boreholes 50 m to over 250 m deep (Gnandi et al., 2009). This zone promotes artesianism, whether gushing or not. In Benin (Fig. 7), Paleocene limestones are found at depths of 150 to 200 m in the north and 300 m in the south (Boukari, 2002).

ISSN: 1857-7881 (Print)
e-ISSN 1857-7431 (Online)

Located above the bedrock, the Upper Cretaceous is represented in Togo (Fig. 5 and Fig. 6) by alternating sandy layers of varying thickness and clayey or sandy-clayey layers (Gnandi et al., 2009; Da Costa et al., 2005). The sandy layers, which are the most productive, are often found at depths greater than 50 m in the north (Ahépé). Further south, they are found at depths greater than 200 m in the Vo-Ativé and Hedegan regions (Gnandi et al., 2009). In Benin, its depth varies across the territory, as does its thickness (Kpégli et al., 2018). In the northern region (northern Abomey plateau, Zagnanado plateau, and northern Kétou plateau), hand-dug wells (up to 70 m deep) extend into this main aquifer. In the south, it is impossible to exploit the Upper Cretaceous aquifer using hand-dug wells due to the thick clayey materials covering it and the artesian conditions that prevail for this aquifer in the south. Thus, only deep boreholes exploiting the Upper Cretaceous aquifer are present in the south (Kpégli et al., 2018).

By examining the piezometry, four flow directions are identified (each northern plateau of Benin) (Kpégli et al., 2018). On the BSC in Togo and Benin, water generally flows from north to south. The probable recharge area of the Cretaceous is located north of the northern plateaus of the BSC ((Gnazou 2005) and (Kpégli et al., 2018)).

The piezometric map produced by (Kpégli et al., 2018) from piezometric data from November 2015 reveals flow directions and piezometric values similar to those we obtained with data from July 2023.

Conclusion

Five (05) more or less continuous layers, differing in lithology, are traversed by the correlated boreholes. These consist of a surface layer of laterite, a clayey layer dating from the Maastrichtian, sandy layers, a clayey-sandy layer and limestone.

Limestone (Paleocene) is trapped between thick layers of clay with a thickness of 15 to 30 m in boreholes ranging from 50 m to over 250 m deep (Gnandi et al., 2009). In Benin (Fig. 7), Paleocene limestone is found at depths of 150 to 200 m in the north and 300 m in the south (Boukari, 2002), with a thickness of 10 to 30 m.

The most productive Upper Cretaceous sands in Togo are found at depths of over 50 m in the north and over 200 m in the south. In Benin, its depth varies across the territory, as does its thickness. On the northern plateaus of the Coastal Sedimentary Basin, this aquifer can be tapped with large-diameter wells and can reach depths of up to 70 m. In the south, the impermeable formations that form its roof do not allow it to be captured by wells. It can reach depths of up to 600 m in the south (Boukari, 2002). Its thickness ranges from 50 to 150 m (Géohydraulique, 1985). The dense clay formations in the south of the Lama depression, which cover the Turonian-

ISSN: 1857-7881 (Print)
e-ISSN 1857-7431 (Online)

Coniacian and Paleocene aquifers, promote atesianism, whether or not it springs from the boreholes that capture these aquifers.

From piezometric studies, water generally flows from north to south. This leads us to conclude that the aquifer is fed by rainwater infiltration in the outcrop areas north of the northern plateaus of the coastal sedimentary basin. In Togo, most wells have been abandoned and are used as garbage dumps, while others have been motorized to facilitate exploitation of the resource on the northern plateaus. We suggest that a considerable number of wells be constructed to enable stricter monitoring of the water table. The hydrodynamic aspects (estimation of transmissivity, storage coefficient; recharge in terms of quality and quantity) of the Upper Cretaceous should be considered in order to update the available data and thereby contribute more effectively to resource management.

The northern part of the northern plateaus, which constitute the recharge points for the Coniacian Turonian, should be subject to extensive protection. Units to regulate population growth and control activities carried out in these areas must be essential points of reflection for the Beninese and Togolese authorities in order to avoid possible pollution of the aquifer.

Conflict of Interest: The authors reported no conflict of interest.

Data Availability: All data are included in the content of the paper.

Funding Statement: This research was carried out as part of the Africa Water and Sanitation Excellence Center (C2EA) project funded by the World Bank, the French Development Agency (AFD), and the Beninese government.

References:

1. Achidi J., Bourguet L., Elsaesser R., Legier A., Paulve E., Tribouillard N., (2012). Notice explicative de la carte hydrogeologique du Benin : carte du bassin sedimentaire de Kandi a l'echelle 1/200 000. Technical report. DGEau, Cotonou, Benin, p. 45.
2. Adjakidje V. (1984). Contribution à l'étude botanique des savanes guineennes de la République Populaire du Bénin. Thèse de doctorat. Université de Bordeaux III, Bordeaux 284p.
3. Adjanohoun E. (1989). Contribution aux études ethnobotaniques et floristiques en République Populaire du Bénin. Agence de Coopération Culturelle et Technique, Paris c, 895 p.
4. Akiti T.T. (1980) Etude Géochimique et Isotopique de quelques aquifères au Ghana: gneiss de la Plaine d'Accra, calcaire de la Plaine SE de la Volta, granite de la Haute Région [Geochemical and isotopic study of several aquifers in Ghana: Accra plain gneiss, SE Volta plain

ISSN: 1857-7881 (Print)
e-ISSN 1857-7431 (Online)

limestone, High Region granite] PhD Thesis, Université Paris-Sud, Orsay France, 345pp

5. Akouvi A. (2005) Etude géochimique et hydrogéologique des eaux souterraines d'un bassin sédimentaire côtier en zone tropicale. Implications sur la gestion, la protection et la préservation des ressources en eau du Togo (Afrique de l'Ouest) [Geochemical and hydrogeological study of groundwater from the coastal sedimentary basin in the tropical zone: implication for management, protection and preservation of the water resources of Togo (West Africa)]. PhD Thesis, Université Pierre et Marie Curie, Paris VI, Paris, France, 163 pp
6. Alassane A. (2004). Etude hydrogéologique du continental terminal et des formations de la plaine littorale dans la région de Porto novo (sud du Benin) : Identification des aquifères et vulnérabilité de la nappe superficielle. [Thèse De Doctorat de Troisième Cycle]. Université Cheikh Anta Diop De Dakar Faculté Des Sciences Et Techniques.
7. Amoussou H.S. (2005). Morpho Dynamique du delta de la Sô, Mémoire de Maîtrise. DGAT, FLASH, UAC 108 p
8. Breda (1989). Notice explicative de la carte géologique à 1/200000, Feuille Pira -Savè, Abomey -Zagnanado et Lokossa-Porto Novo, mémoire n°3, 1ere édition, 77 p. 6. DGH (2000). Politique nationale de gestion des ouvrages hydrauliques. Rapport, Cotonou, 39 p. *1e édition*. 64p + 2 annexes.
9. Boukari M. (1998). Fonctionnement du système aquifère exploité pour l'approvisionnement en eau de la ville de Cotonou sur le littoral Béninois. Impact du développement urbain sur la qualité des ressources. Université Cheikh Anta Diop, Dakar, Sénégal, 254p + annexe
10. Boukari M. (2002). Réactualisation des connaissances hydrogéologiques relatives au Bassin Sédimentaire Côtier du Bénin.
11. Boukari M., Oyédé M., Alidou S., Gaye G. B. et Maliki R. (1994). Identification des aquifères de la zone littorale du Bénin (Afrique de l'Ouest) : hydrodynamique, hydrochimie et problèmes d'alimentation en eau de la ville de COTONOU. Africa Géoscience Review, Vol. 2, No.1, p121-139.
12. Da Costa Pauline Y.D. (2005). Biostratigraphie et Paléogéographie du bassin sédimentaire du Togo. *Thèse de Doctorat, Université de Lomé*, 2 tomes, 476p.
13. Da Costa Pauline Y. D., Ampah K. C. Johnson et Pascal Affaton. (2013). Les terrains paléozoïques et mésozoïques du basin côtier togolais : Stratigraphie et Paléogéographie

ISSN: 1857-7881 (Print)
e-ISSN 1857-7431 (Online)

14. DE A. G. D. E. Z., & Cristallin S. (1992). Comite interafricain d'études hydrauliques (CIEH).
15. Dray M., Giachello L., Lazzarotto V., Mancini M., Roman E., Zuppi G.M. (1989). Etude isotopique de l'aquifère crétacé du bassin béninois [Isotopic study of the Cretaceous aquifer of the Benin basin]. Hydrogéologie 3:167–177
16. Gallo G. (1979). Complementary use of environmental isotopes and water chemistry for the hydrogeological study of the Ribeirao Preto groundwater, Brazil. In Isotope hydrology 1978.
17. Géohydraulique, (1985). Notice explicative de la carte hydrogéologique à l'échelle 1/200 000 du Bassin Sédimentaire Côtier du Bénin. Reportage. 23p. Direction générale de l'Hydraulique, Cotonou, Bénin
18. Glodji L. A., Alassane A., Dossou P. M., Zogo A., Ahossi A., & Gbewezoun V. (2019). Influence de la Réactivation de la Faille de Kandi sur l'artésianisme dans le Bassin Versant du Fleuve Mono au Sud-ouest du Bassin Sédimentaire Côtier du Bénin (Afrique de l'Ouest). *European Scientific Journal ESJ*, *15*(24). https://doi.org/10.19044/esj.2019.v15n24p346.
19. Gnandi K., Fussi F., Asplund F., (2009). Etude de faisabilité des forages manuels au togo**. I**dentification des zones potentiellement favorables
20. Gnazou M.D-T. (2008). Etude hydrodynamique, hydrochimique, isotopique et modélisation de l'aquifère du bassin sédimentaire côtier du Togo. *Thèse Univ. Lom*é. 204p.
21. Gnazou M.D.T, Sabi B. E, Togbe K.A, Da Costa Pauline Y.D., (2015). Actualisation structurale de l'aquifère du paléocène dans le bassin Côtier du Togo. 22p.
22. Houndagba J.C. (2015). Dynamique des paysages naturels dans le centre du Bénin. Thèse de doctorat. Université d'Abomey Calavi, Abomey Calavi 349p.
23. Holman I. P., Allen D. M., Cuthbert M. O., & Goderniaux P. (2012). Towards best practice for assessing the impacts of climate change on groundwater. Hydrogeology Journal, 20(1), 1-4. https://doi.org/10.1007/s10040-011-0805-3
24. Idder T., Idder A., Cheloufi H., Benzida A., Khemis R., & Moguedet G. (2013). La surexploitation des ressources hydriques au Sahara algérien et ses conséquences sur l'environnement-Un cas typique : L'oasis de Ouargla (Sahara septentrional). Techniques Sciences Méthodes, 5, 31-39.
25. Johnson A.K.C. (1987). Le bassin côtier à phosphates du Togo (Maastrichtien-Eocène moyen) [The coastal phosphatic basin of Togo

ISSN: 1857-7881 (Print)
e-ISSN 1857-7431 (Online)

(Maastrichtian-Middle Eocene)]. PhD Thesis, Université de Bourgogne et Université du Bénin (Togo), Dijon, France, and Lomé, Togo, 360 pp.

26. Kaki C., Oyédé L.M., & Yessoufou S. (2001). Dynamique sédimentaire et environnement côtier béninois à l'Est de l'embouchure du fleuve Mono. Rech. Sci. Univ. Lomé (Togo), 5 (2), 247-261.
27. Kpegli K. A. R., Alassane A., van der Zee S. E. A. T. M., Boukari M., & Mama D. (2018). Development of a conceptual groundwater flow model using a combined hydrogeological, hydrochemical and isotopic approach : A case study from southern Benin. *Journal of Hydrology: Regional Studies*, *18*, 50-67. https://doi.org/10.1016/j.ejrh.2018.06.002
28. Kotchoni D. O. V., Vouillamoz J.-M., Lawson F. M. A., Adjomayi P., Boukari M., & Taylor R. G. (2019). Relationships between rainfall and groundwater recharge in seasonally humid Benin: A comparative analysis of long-term hydrographs in sedimentary and crystalline aquifers. Hydrogeology Journal, 27(2), 447-457. https://doi.org/10.1007/s10040-018-1806-2
29. Lamouroux M. (1966). Carte Pédologique à l'échelle 1/1000000.Ed. ORSOM.Lomé.
30. MALIKI A.R. (1993). Etude hydrogéologique du littoral béninois dans la région de Cotonou et ses environs. Thèse de Doctorat de 3ème cycle, Université Cheikh Anta Diop de Dakar, Sénégal, p164+ Annexes.
31. Margat J. (1989). Sécheresse et eaux souterraines. La Houille Blanche, 7-8, Article 7-8. https://doi.org/10.1051/lhb/1989049
32. Mérino M. (2009). La maîtrise de l'eau en Afrique de l'Est : Tensions et territoires. Sécurité globale, 9(3), 69-78. Cairn.info. https://doi.org/10.3917/secug.009.0069
33. Monciardini C., Tchota K., Slansky M., Podevin G. Marteau P., Le Nidre Y., Farjanel G., Chateauneuf J.J., Castaing C., Carbonel G., Blondeau A. & Andreiff P. (1986) Synthèse géologique du bassin côtier Crétacé Supérieur – Tertiaire du Togo – Recherche de tourbe, lignite, charbon et autres substances industrielles. *Rapport BRGM 86 TGO.*
34. Nijsten G.-J. (2018). Transboundary aquifers of Africa_ Review of the current state of knowledge and progress towards sustainable development and management. Journal of Hydrology.
35. Oyédé L.M., Tossou M.G., Kaki C., Laibi R .A. & Lang, J . (2006). Phénomènes enregistrables, milieu enregistreur et messages enregistrés : application aux séquences biosédimentaires du quaternaire récent dans le géosystème margino -littoral béninois (Afrique de l'Ouest). Africa Géoscience Review, 13 (3), 395-408

ISSN: 1857-7881 (Print)
e-ISSN 1857-7431 (Online)

36. Penant P. (2016). Caractérisation des sources de nitrate dans les aquifères cristallins du Centre du Bénin. Univèrsité de Liége.
37. Salifou G.O.P.A.., Gbewezoun H.G.V., Alassane A. Z., Alassane A., Lawin A.E., Daouda M. et Moussa B. (2021). Caractérisation de l'aquifère superficiel du Bassin Sédimentaire de Kandi (Nord-Est Bénin, Afrique Ouest): nature et structure du réservoir, Hydrodynamique. European Scientific Journal, ESJ. January 2021 edition Vol.17, No.3 ; www.eujournal.org
38. Seguin J.-J., Allier D., & Manceau J.-C. (2019). Contribution d'un index piézométrique standardisé à l'analyse de l'impact des sécheresses sur les ressources en eau souterraine. Géologues. https://hal.archives-ouvertes.fr/hal-03219172
39. Slansky M. (1962) Contribution à l'étude géologique du bassin sédimentaire côtier du Dahomey et du Togo. *Thèse Univ. Nancy, Mém. BRGM n°11,* 270p.
40. Sylvain J.P., Aregba A., Assih-Edeou P., Castaing C., Chevremont J., Collart J., Monciardini C., Marteau P., Ouasane I. & Tchota. (1986). Notice explicative de la carte géologique à 1/200000. Feuille de Lomé. *Mémoire n° 5* DGMG/BNRM.
41. VOLKOFF B. et WILLAIME P. (1976). Notice explicative de la carte pédologique de reconnaissance de la République Populaire du Bénin au 1/200.000 feuille de ABOMEY (2). ORSTOM 1976 ISBN 2-7099-0423-3, ISBN 2-7099-0425-X.

ESJ Natural/Life/Medical Sciences Peer-reviewed

Morphological Characterization of Amaranth (*Amaranthus hybridus* L.) Accessions from Urban and Peri-Urban Market Gardening of Abidjan and Yamoussoukro

Jean-Claude N'zi, PhD
Unit of Training and Research of Biosciences, University Felix Houphouët-Boigny, Côte d'Ivoire / ICRAF-World Agroforestry, Côte d'Ivoire
Christophe Kouame, PhD
ICRAF-World Agroforestry, Côte d'Ivoire
Kabre Vonogo Nikodeme, PhD
Université Joseph Ki-Zerbo, Burkina Faso
Fondio Lassina, PhD
Centre National de Recherche Agronomique, Côte d'Ivoire
Agbo Edith, PhD
UFR Nutrition, Université Nangui-Abrogoua, Côte d'Ivoire
Mahyao Adolphe, PhD
Centre National de Recherche Agronomique, Côte d'Ivoire

Doi:10.19044/esj.2026.v22n6p123

Submitted: 12 September 2025
Accepted: 19 February 2026
Published: 28 February 2026

Cite As:
N'zi, J.-C., Kouame, C., Kabre, V.N., Fondio, L., Agbo, E., & Mahyao, A. (2026). *Morphological Characterization of Amaranth (Amaranthus hybridus L.) Accessions from Urban and Peri-Urban Market Gardening of Abidjan and Yamoussoukro*. European Scientific Journal, ESJ, 22 (6), 123. https://doi.org/10.19044/esj.2026.v22n6p123

Abstract

This work focuses on the morphological characterization of eighteen amaranth (*Amaranthus hybridus*) accessions collected in urban and peri-urban market gardening of Abidjan and Yamoussoukro in Côte d'Ivoire. These accessions were regenerated and multiplied at the Experimental and Production Station of the National Center for Agronomic Research in Anguédédou. This study was conducted using a Fisher block design with three replicates. Quantitative and qualitative variables were observed and measured for each of these accessions. Collected data were submitted to analysis of variances and multivariate analyses (PCA) to discriminate variables. Results showed a high variability for each of the nine (09) quantitative variables and

ISSN: 1857-7881 (Print)
e-ISSN 1857-7431 (Online)

for some of the fifteen (15) qualitative variables studied. The green morphotypes showed the strongest performance in terms of leaf biomass (29 leaves per plant), stem diameter (5.9 cm), plant height (137 cm) and panicle length (48.7 cm). These data confirm morphological variability within the population of *A. hybridus* studied could be used in a selection program for the improvement and sustainable cultivation of this foodstuff in Côte d'Ivoire.

Keywords: *Amaranthus hybridus*, diversity, accessions, variables, urban and peri-urban market gardening

Introduction

Market gardening is a growing activity that generates income for the populations in large cities and their surroundings due to the increase in food needs. Among these dietary needs are leafy vegetables, including amaranth (*Amaranthus spp.*), a leafy vegetable rich in vitamins and essential minerals. Indeed, according to Fondio et al. (2011), amaranth leaves are rich in vitamins A, C and B9, iron, calcium and sulphur amino acids such as methionine, lysine and cysteine. Amaranth is a popular vegetable plant on many global vegetable farms whose leaves and seeds are consumed in various forms (Písaříková et al., 2005; Fondio et al., 2012; Mburu et al., 2012) thus constituting a good food supplement to starchy foods such as cereals and tubers.

The cultivation of this species provides considerable income to farmers through the marketing of its leaves and seeds (National Research Council, 2006; Fondio et al., 2012). However, very little agronomic data exist on this species of traditional leafy vegetable in Côte d'Ivoire. The only information available is the work of Terrible (1983) on the census of vegetable plants grown in Côte d'Ivoire, Ondo (1992) who reported on the inventory of cultivated plants in the botanical garden of the University Felix Houphouët-Boigny and Fondio et al. (2011; 2012) on the technical itinerary of this species in Côte d'Ivoire and on good agricultural practices for the production of underutilized vegetables in sub-Saharan Africa. To help mitigate this situation, a study was undertaken to determine the morphological variability of some accessions in urban and peri-urban market gardening in Abidjan and Yamoussoukro for a better knowledge of *A. hybridus* L. The specific objectives were (i) to collect the accessions grown by the producers, (ii) to evaluate the agronomic performance of the accessions through morphological markers and (iii) to establish the link between the different traits expressed by the individuals of *Amaranthus hybridus* studied.

ISSN: 1857-7881 (Print)
e-ISSN 1857-7431 (Online)

Material & Methods

Plant material

The plant material consists of eighteen (18) accessions of *Amaranthus hybridus* collected from Abidjan and Yamoussoukro. The choice of these cities is due to their high supply of production and consumption of *A. hybridus*. The exhaustive collection technique was used by surveying all the producers in each city surveyed, so that the number varies greatly from one city to another. Each accession was represented by seeds and accompanied by a collection sheet containing information on the geographical origin of the accession, the farmer descriptors, the cultivation practices, and the accession code.

Experimental site

This study was conducted in 2008 at the Experimentation and Production Station of the National Center for Agronomic Research (CNRA) in Anguédédou, a locality located thirty kilometers from Abidjan in the southwest of Côte d'Ivoire with the geographical coordinates of 5°22 N, 4°8W, and 95 m altitude. The climate of the study area is bimodal with two rainy seasons (March-June and September-November) and two dry seasons (July-August and December-February) as shown in Figure 1 (N'zi et al., 2015). During the period of the trial, minimum and maximum temperature averages ranged between 20 and 25°C, and 29 and 35°C, respectively (Figure 2). The monthly humidity average was 79%. The soil of the experimental plot was ferralitic and sandy-textured, highly acidic with a well-decomposed organic matter content (pH = 4.5 and C/N = 10.5) according to Fondio et al. (2015).

Methods

Experimental set-up and cultural practices

The experimental design used was a Fisher block with 3 repetitions with an elementary plot of 2 x 5 m. Before transplanting, the soil was deeply disturbed and levelled, followed by organic fertilization with chicken droppings, maintenance, and regular irrigation of the plots. The seeds were then placed in nurseries on boards set up for this purpose. Twenty-one days after sowing, the plants were transplanted on ridges. Each ridge constituted an elementary plot which included 7 plants arranged in a line with 20 cm between the rows and 20 cm between plants in the same line. Phytosanitary treatments were carried out on request.

ISSN: 1857-7881 (Print)
e-ISSN 1857-7431 (Online)

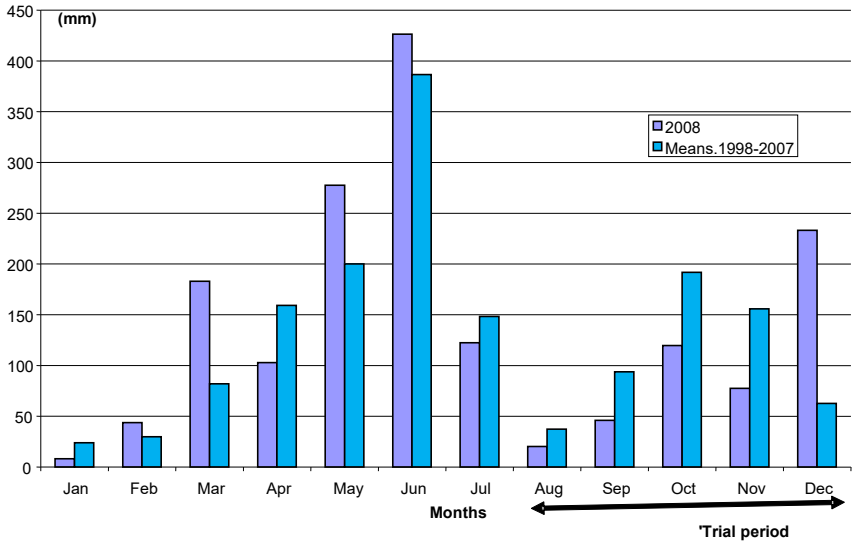

Figure 1: Monthly average rainfall recorded in 2008 and athe verage over the period of 1998-2007

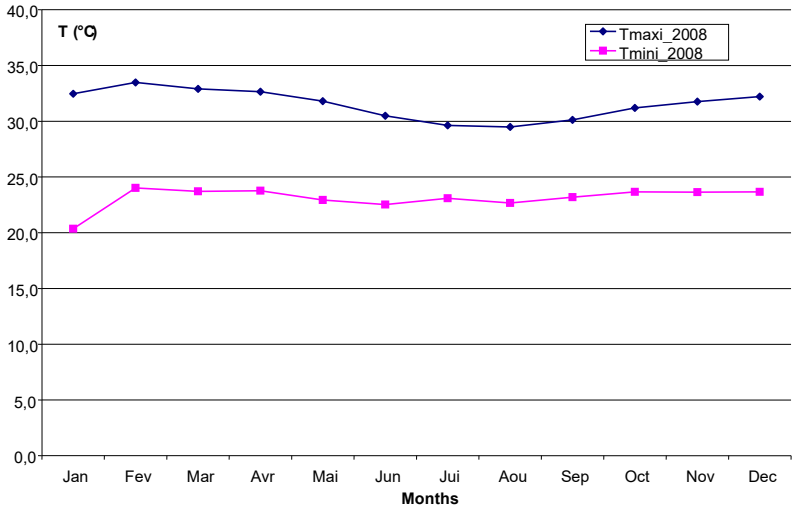

Figure 2: Maximum and minimum temperatures recorded in 2008

Data collection

Data on fifteen (15) qualitative variables and nine (09) quantitative variables were observed and measured on three plants per line out of seven (07) plants, randomly marked. For this characterization, the IPGRI descriptor for amaranth was used for the choice of variables or characters (Grubben, 1975; Grubben & van Sloten, 1981). Thus, the date of emergence (DLEV), the date of flowering (DFLO), the plant height (LONGTIG), the stem diameter (LARTIG), the petiole length (LONGPET), the blade length (LONGLIM), the leaf blade width (LARGLIM), the number of leaves (NFEUIL), and the

ISSN: 1857-7881 (Print)
e-ISSN 1857-7431 (Online)

panicle length (LONGPAN) were observed, described and measured likewise the spinosity of the plant (SPINOS), the phyllotaxis of the plant (PHYTAX), the shape of the tip of the blade (BOSLIM), the shape of the base of the blade (BASLIM), the shape of the blade (FORLIM), the margin of leaves (BFEUIL), the prominence of veins (PROENER), the type of inflorescence (TYPINFL), the inflorescence colour (COULINF), the stem colour (COULTIG), the colour of the blade (COULLIM), the petiole colour (COULPET), the veins colour (COULNER), the inflorescence position (POSINF), and the root type (TYPRACI). The date of emergence is expressed in days after sowing and corresponds to the number of days that separate the sowing and the emergence of 50% of the seeds, as well as the date of flowering, corresponding to the number of days from sowing to the appearance of the first flower. The seeds of the panicles were harvested when they were completely dry.

Data analysis

All data collected were analyzed using the SAS software. Analysis of variance was performed to determine the significance of the block and the variety effects. The separation of the means was performed according to the Duncan test at 5% threshold. Multivariate analyses (PCA) were done discriminate the studied variables.

Results and Discussion

Results

Morphological diversity related to the qualitative variables of *Amaranthus hybridus* L.

The analysis of the qualitative variables showed the existence of morphological variability, especially in the colour of the organs within the *Amaranthus hybridus* L. accessions studied (Table 1). Based on the coloration of the stem and inflorescence, three (03) morphotypes stand out with a clear predominance of the green morphotype, which represented 67% of the collection. This morphotype, in addition to the green colouration of the stem and inflorescence, also had a uniform green colour of the flower petals, leaf blades, and leaf veins (Figure 3). The green-purple (Spr-green) or purple-green (Prp-green) morphotypes represented 28% of the collection. This morphotype retained the same colouration for the leaves and flowers in addition to that of the stem and inflorescence. The purple morphotype represented 5% of the collection. This morphotype also retained the same purple coloration for the leaves and flowers. At the level of the inflorescence, one form was observed, the panicle.

ISSN: 1857-7881 (Print)
e-ISSN 1857-7431 (Online)

Morphological diversity related to quantitative variables of *Amaranthus hybridus*

Analysis of the variability of quantitative variables of Amaranthus hybridus

The analysis of the comparative average performance of *Amaranthus hybridus* accessions showed relatively low values of the coefficients of variation (CV<30%) for the variables studied, thus reflecting a low heterogeneity of the plant material for these different traits. Indeed, the values of the coefficient of variation varied from 4.98% to 24.84%. Accessions of *A. hybridus* flowered between 38 and 60 days after sowing at an average height of 108.4 cm with stems of 4.1 cm in diameter. Most accessions had leaves with long petioles (10.1 cm) and a long, wide blade of 14.9 cm and 6.7 cm, respectively. All accessions of *A. hybridus* had panicles ranged from 36 cm to 48.7 cm long. In summary, the results of the analysis of variance showed that the characteristic features discriminating the different accessions of *A. hybridus* are, among others, the height of the plant, the diameter of the stem, the length of the petiole and the number of leaves, whose values of the coefficient of variation varied between approximately 20 and 25% (Table 2). The analysis of the probability levels of the quantitative variables studied showed significant differences observed at the 1 and 5% thresholds for some of the quantitative variables studied. Thus, variables such as emergence date corresponding to the number of days after sowing, flowering date and number of leaves showed a very significant difference at the 1% threshold. Variables such as plant height and leaf blade width showed a significant difference at the 5% threshold. The other four (04) variables, stem diameter, petiole length, blade length and panicle length, showed no significant differences at the 1% and 5% levels (Table 3).

ISSN: 1857-7881 (Print)
e-ISSN 1857-7431 (Online)

Table 1: Qualitative variables of the different accessions of Amaranthus hybridus observed in the experimental station

ACCESSIONS	SPINOS	PHYTAX	BOSLIM	BASLIM	FORLIM	BFEUIL	PROENER	TYPINFL	COULINF	COULTIG	COULLIM	COULPET	COULNER	POSINF	TYPRACI
TATROK	0 thorn	Couplet	Sharp	Sharp	Lanceolate	Whole	Few	Panicle	Green	Green	Green	Green	Green	Terminal	Pivot
AMPT08	0 thorn	Couplet	Sharp	Sharp	Lanceolate	Whole	Few	Panicle	Green	Green	Green	Green	Green	Terminal	Pivot
YQB06	0 thorn	Couplet	Sharp	Sharp	Lanceolate	Whole	Few	Panicle	Purple	Purple	Purple	Purple	Purple	Terminal	Pivot
ABAN04	0 thorn	Couplet	Sharp	Sharp	Lanceolate	Whole	Few	Panicle	Green	Green	Green	Green	Green	Terminal	Pivot
YKO07	0 thorn	Couplet	Sharp	Sharp	Lanceolate	Whole	Few	Panicle	Green	Green	Green	Green	Green	Terminal	Pivot
AKSSI07	0 thorn	Couplet	Sharp	Sharp	Lanceolate	Whole	Few	Panicle	Green	Green	Green	Green	Green	Terminal	Pivot
YQB06	0 thorn	Couplet	Sharp	Sharp	Lanceolate	Whole	Few	Panicle	Green	Green	Green	Green	Green	Terminal	Pivot
YFON01	0 thorn	Couplet	Sharp	Sharp	Lanceolate	Whole	Few	Panicle	Green	Green	Green	Green	Green	Terminal	Pivot
APB09	0 thorn	Couplet	Sharp	Sharp	Lanceolate	Whole	Few	Panicle	Prp-green	Prp-green	Green	Prp-green	Green	Terminal	Pivot
KNYA	0 thorn	Couplet	Sharp	Sharp	Lanceolate	Whole	Few	Panicle	Prp-green	Prp-green	Green	Green	Green	Terminal	Pivot
YQB05	0 thorn	Couplet	Sharp	Sharp	Lanceolate	Whole	Few	Panicle	Green-prp	Green-prp	Green	Green	Green	Terminal	Pivot
YMIL02	0 thorn	Couplet	Sharp	Sharp	Lanceolate	Whole	Few	Panicle	Prp-green	Prp-green	Green	Green	Green	Terminal	Pivot
AMPT02	0 thorn	Couplet	Sharp	Sharp	Lanceolate	Whole	Few	Panicle	Green-prp	Green-prp	Green-prp	Green-prp	Green-prp	Terminal	Pivot
YFON04	0 thorn	Couplet	Sharp	Sharp	Lanceolate	Whole	Few	Panicle	Green	Green	Green	Green	Green	Terminal	Pivot
YQR04	0 thorn	Couplet	Sharp	Sharp	Lanceolate	Whole	Few	Panicle	Green	Green	Green	Green	Green	Terminal	Pivot
YGK05	0 thorn	Couplet	Sharp	Sharp	Lanceolate	Whole	Few	Panicle	Green	Green	Green	Green	Green	Terminal	Pivot
YQB08	0 thorn	Couplet	Sharp	Sharp	Lanceolate	Whole	Few	Panicle	Green	Green	Green	Green	Green	Terminal	Pivot
ABAN17	0 thorn	Couplet	Sharp	Sharp	Lanceolate	Whole	Few	Panicle	Green	Green	Green	Green	Green	Terminal	Pivot

SPINOS: Spinosity; **PHYTAX:** Phyllotaxis; **BOSLIM:** Shape of the tip of the blade; **BASLIM:** Shape of the base of the blade; **FORLIM:** Shape of the blade; **BFEUIL:** Leaf margin; **PROENER:** Vein prominence; **TYPINFL:** Inflorescence type; **COULINF:** Inflorescence colour; **COULTIG:** Stem colour; **COULLIM:** Blade colour; **COULPET:** Petiole colour; **COULNER:** Vein colour; **POSINF:** Inflorescence position; **TYPRACI:** Root type. Green-prp: Greenish purple; Prp-green: Purple green; Pivot: Taproot; 0 thorn: Spineless.

ISSN: 1857-7881 (Print)
e-ISSN 1857-7431 (Online)

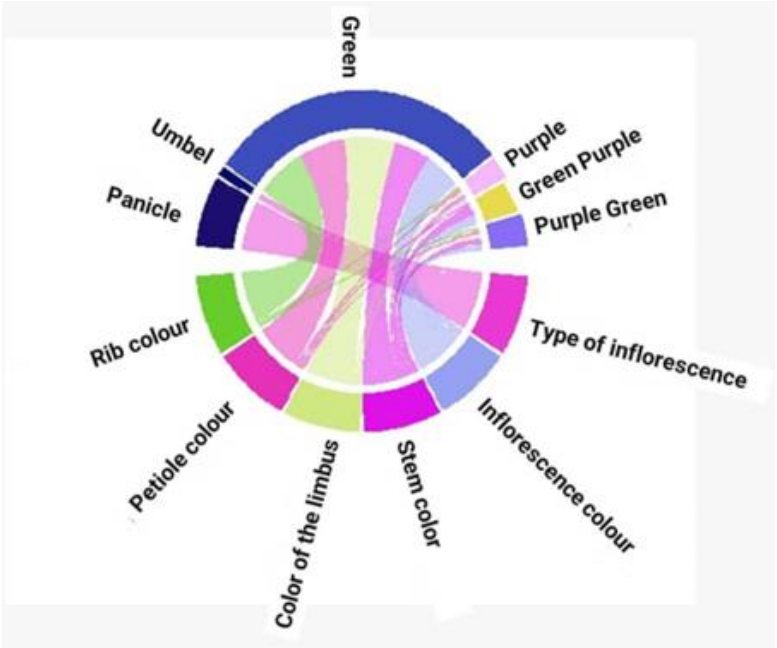

Figure 3: Pie diagram linking the different qualitative variables discriminating between *Amaranthus hybridus accessions*

Analysis of the relationships between quantitative variables of Amaranthus hybridus

The study of the relationships between the quantitative and qualitative variables measured revealed several correlations at the 5% threshold (Table 4). Positive and significant correlations are observed between the height of the plant and each of the variables, number of leaves (0.746); width of the blade (0.688); stem diameter (r = 0.681) and petiole length (r = 0.583). Positive and significant correlations were also observed between inflorescence colour and each of the variables, stem colour (r = 1); petiole colour (r = 0.739); blade colour and vein (r = 0.620); between the date of emergence and each of the variables blade width (r = 0.567) and vein prominence (r = 0.998). A positive and significant correlation was observed between petiole length and each of the variables blade length (r = 0.611) and blade width (r = 0.541). On the other hand, the most important negative and significant correlations were observed between the emergence date and the flowering date (r = -0.668); between the flowering date and each of the variables blade width (r = - 0.507) and vein prominence (r = - 0.676).

Organization of the variability of *Amaranthus hybridus*

The results of the principal component analysis (PCA) of the quantitative descriptors showed that the first 3 components with eigenvalues

ISSN: 1857-7881 (Print)
e-ISSN 1857-7431 (Online)

of 5.31, 3.58, and 3.08, respectively, expressed 70.49% of the total variability observed. The analysis of eigenvalues showed that the variables studied had different performances (Table 5). The variables plant height, leaf blade width, leaf number, leaf blade color, stem color, inflorescence color, petiole color, and vein color are correlated with axis 1 and explain 31.28% of the total variance. These variables defined this axis, which thus represented the productivity and color axis. The variables stem width, petiole length and blade length are correlated with axis 2 and expressed 21.08% of the total variance. This is the axis of biometric diversity. The variables, vein prominence, flowering date, panicle length, inflorescence type, and root type, were strongly correlated with axis 3 and expressed 18.13% of the total variance. This is the axis of flowering. In total, 11 descriptors plant height, leaf blade width, leaf number, leaf blade colour, stem colour, inflorescence colour, petiole colour, vein colour, stem diameter, petiole length and leaf blade length contributed to more than 52% of the total variability.

ISSN: 1857-7881 (Print)
e-ISSN 1857-7431 (Online)

Table 2: Quantitative variables of the different accessions of *Amaranthus hybridus* measured in the experimental station

Accessions	DLEV (das)	DFLO (das)	LONGTIG (cm)	LARTIG (cm)	LONGPET (cm)	LONGLIM (cm)	LARGLIM (cm)	NFEUIL	LONGPAN (cm)
ABAN04	3 a	45 efgh	78.3 d	2.9 b	6.9 b	13.3 b	5.4 cd	19 cdef	38.5 abc
ABAN17	3 a	42 ghij	137 a	5.9 a	13.8 a	18.3 d	8.8 a	29 ab	41.2 abc
AKSSI07	3 a	48 bcde	99 abcd	3.1 b	10.2 ab	14.2 ab	6.4 bc	16 ef	35.9 c
AMPT02	3 a	41 hij	92.8 bcd	4.4 ab	9.8 ab	13.9 ab	6.5 bc	22 abdef	39.3 abc
YMIL02	3 a	38 k	126 abc	4.5 ab	12.3 a	15.8 ab	7.5 abc	28 abc	48 ab
APB09	3 a	38 jk	117.5 abcd	4.1 ab	9.8 ab	14.4 ab	7.2 abc	31 a	39 abc
YQB06	3 a	45 defgh	127,2 abc	4 ab	9.3 ab	15.5 ab	7.5 abc	28 abc	40.8 abc
YQB06	3 a	46 cdefg	101 abcd	2.9 b	7 b	6.1 bc	6.1 bc	20 bcdef	42.8 abc
YFON01	3 a	40 ijk	104 abcd	4.3 ab	9.7 ab	14.7 ab	6.7 abc	15 f	42.8 abc
YFON04	3 a	44 fghi	96.8 abcd	3.7 b	9.1 ab	14.5 ab	6.4 bc	18 ef	39.3 abc
YGK05	3 a	46 cdefg	106.3 abcd	4 ab	12.5 a	16.5 ab	7 abc	19 cdef	44.8 ab
YKO07	3 a	49 bc	134.2 ab	4.4 ab	10.3 ab	15.7 ab	8.1 ab	25 abcdef	44 abc
YQB08	3 a	47 cdef	114.8 abcd	4.3 ab	11.2 ab	14 ab	6.7 abc	21 bcdef	36 bc
YQB05	3 a	46 cdefg	132.5 ab	4.8 ab	10.6 ab	12.9 ab	6.2 bc	27 abc	44.5 abc
YQR04	3 a	44 fghi	93.2 bcd	3.9 b	10.4 ab	15.4 ab	6.8 abc	18 def	37 abc
AMPT08	3 a	49 bcd	105.8 abcd	4 ab	9 ab	16.8 ab	6.7 abc	26 abcd	39.2 abc
TATRO	2,3 b	52 b	97.7 abcd	4.1 ab	10.2 a	15.9 ab	4.1 d	22 abcdef	48.7 a
KNYA	2 c	60 a	87.5 cd	4.1 ab	9.5 ab	12;9 b	6.3 bc	17 def	43 abc
Averages	**3**	**45**	**108.4**	**4.1**	**10.1**	**14.9**	**6.7**	**22**	**41.4**
C.V.	**6.85**	**4.98**	**19.59**	**24.84**	**23.95**	**16.3**	**16.99**	**21.6**	**14.5**

DLEV: Date of emergence; **DFLO:** Date of flowering; **LONGTIG:** Plant height; **LARTIG:** Stem diameter; **LONGPET:** Petiole length; **LONGLIM:** Blade length; **LARGLIM:** Leaf blade width; **NFEUIL:** Number of leaves; **LONGPAN:** Panicle length.
Numbers followed by the same letter are not significantly different at the 5% level. ***C.V.:*** *Coefficient of variation;* ***DAS:*** *Days after sowing.*

ISSN: 1857-7881 (Print)
e-ISSN 1857-7431 (Online)

Table 3: Probability levels of quantitative variables studied for *Amaranthus hybridus*

Accessions	DLEV (das)	DFLO (das)	LONGTIG (cm)	LARTIG (cm)	LONGPET (cm)	LONGLIM (cm)	LARGLIM (cm)	NFEUIL	LONGPAN (cm)
Repetition	-	0.8548	0.3748	0.1893	0.0167	0.0060	0.0321	0.2545	0.0663
Accessions	0.0001	0.0001	0.0431	0.1734	0.1654	0.4048	0.0156	0.0015	0.3531
Averages	**3**	**45**	**108.4**	**4.1**	**10.1**	**14.9**	**6.7**	**22**	**41.4**
C.V.	**6.85**	**4.98**	**19.59**	**24.84**	**23.95**	**16.3**	**16.99**	**21.6**	**14.5**

DLEV: Date of emergence; **DFLO:** Date of flowering; **LONGTIG:** Plant height; **LARTIG:** Stem diameter; **LONGPET:** Petiole length; **LONGLIM:** Blade length; **LARGLIM:** Leaf blade width; **NFEUIL:** Number of leaves; **LONGPAN:** Panicle length. *Numbers followed by the same letter are not significantly different at the 5% level.* ***C.V.:*** *Coefficient of variation;* ***DAS:*** *Days after sowing.*

Table 4: Correlation matrix of quantitative and qualitative variables

VAR.	DLEV	DFLO	LONGTIG	LARTIG	LONGPET	LONGLIM	LARGLIM	NFEUIL	LONGPAN	PROENER	TYPINFL	COULINF	COULTIG	COULLIM	COULPET	COULNER	TYPRACI
DLEV	-																
DFLO	**-0.668**	-															
LONGTIG	0.157	-0.355	-														
LARTIG	0.007	-0.271	**0.681**	-													
LONGPET	0.067	-0.192	**0.583**	**0.781**	-												
LONGLIM	-0.318	0.080	0.439	**0.507**	**0.611**	-											
LARGLIM	**0.567**	**-0.507**	**0.688**	**0.557**	**0.541**	**0.493**	-										
NFEUIL	-0.097	-0.316	**0.746**	**0.537**	0.313	0.378	0.457	-									
LONGPAN	-0.362	0.109	0.293	0.291	0.251	0.205	-0.127	0.227	-								
PROENER	**0.998**	**-0.676**	0.159	0.005	0.058	-0.306	**0.584**	-0.086	-0.382	-							
TYPINFL	0.082	0.303	-0.301	0.008	-0.086	-0.343	-0.096	-0.242	0.108	0.081	-						
COULINF	0.218	-0.311	0.265	0.151	0.018	-0.182	0.215	**0.482**	0.176	0.214	0.354	-					
COULTIG	0.218	-0.311	0.265	0.151	0.018	-0.182	0.215	**0.482**	0.176	0.214	0.354	**1,.00**	-				
COULLIM	0.106	-0.059	0.189	0.010	-0.125	0.044	0.178	0.263	-0.084	0.104	-0.076	**0.620**	**0.620**	-			
COULPET	0.139	-0.224	0.238	0.013	-0.133	-0.010	0.226	**0.475**	-0.163	0.136	-0.099	**0.739**	**0.739**	**0.829**	-		
COULNER	0.106	-0.059	0.189	0.010	-0.125	0.044	0.178	0.263	-0.084	0.104	-0.076	**0.620**	**0.620**	**1.000**	**0.829**	-	
TYPRACI	-0.273	0.124	0.170	-0.041	-0.201	0.312	0.148	0.350	-0.136	-0.236	-0.086	0.330	0.330	**0.635**	**0.505**	**0.635**	-

DLEV: Date of emergence; **DFLO:** Date of flowering; **LONGTIG:** Plant height; **LARTIG:** Stem diameter; **LONGPET:** Petiole length; **LONGLIM:** Blade length; **LARGLIM:** Blade width; **NFEUIL:** Number of leaves; **LONGPAN:** Panicle length; **PROENER:** Vein prominence; **TYPINFL:** Inflorescence type; **COULINF:** Inflorescence colour; **COULTIG:** Stem colour; **COULLIM:** Leaf blade colour; **COULPET:** Petiole colour; **COULNER:** Vein colour; **TYPRACI:** Root type. *Bold values indicate significant correlation coefficients at the 5% level.*

ISSN: 1857-7881 (Print)
e-ISSN 1857-7431 (Online)

Table 5: Performance of discriminant qualitative variables on the three main axes of the PCA

Components	**Axe 1**	**Axe 2**	**Axe 3**
Eigenvalues	5.318	3.583	3.084
Variances explained	31.280	21.075	18.138
Cumulative eigenvalues	5.318	8.901	11.985
Cumulative variances (%)	31.280	52.355	70.494
Variables defining axes and their eigenvalues	LONGTIG (0.649) LARGLIM (0.642) NFEUIL (0.693) COULLIM (0.737) COULTIG (0.790) COULINF (0.790) COULPET (0.795) COULNER (0.737)	LONGPET (0.802) LARTIG (0.722) LONGLIM (0.631)	DLEV (0.917) PROENER (0.915) TYPINFL (-0.426) DFLO (-0.61) TYPRACI (-0.5) LONGPAN (-0.436)

LONGTIG: Plant height; **LARGLIM:** Blade width; **NFEUIL:** Number of leaves; **COULLIM:** Blade colour; **COULTIG:** Stem colour; **COULINF:** Inflorescence colour; **COULPET:** Petiole colour; **COULNER:** Vein colour; **DFLO:** Date of flowering; **LONGPET:** Petiole length; **TYPINFL:** Inflorescence type; **LARTIG:** Stem diameter; **LONGLIM:** Blade length; **DLEV:** Date of emergence; **PROENER:** Vein prominence; **TYPRACI:** Root type; **LONGPAN:** Panicle length.

However, the quality of the representation of each variable on the correlation circles (Figure 4) confirms the result obtained with eigenvalues. These two results suggest that the 11 descriptors mentioned above are discriminating and can be used to select amaranth accessions.

ISSN: 1857-7881 (Print)
e-ISSN 1857-7431 (Online)

Figure 4. Quality of the representation of the variables studied on the correlation circles of the 1&2 and 1&3 planes of the PCA

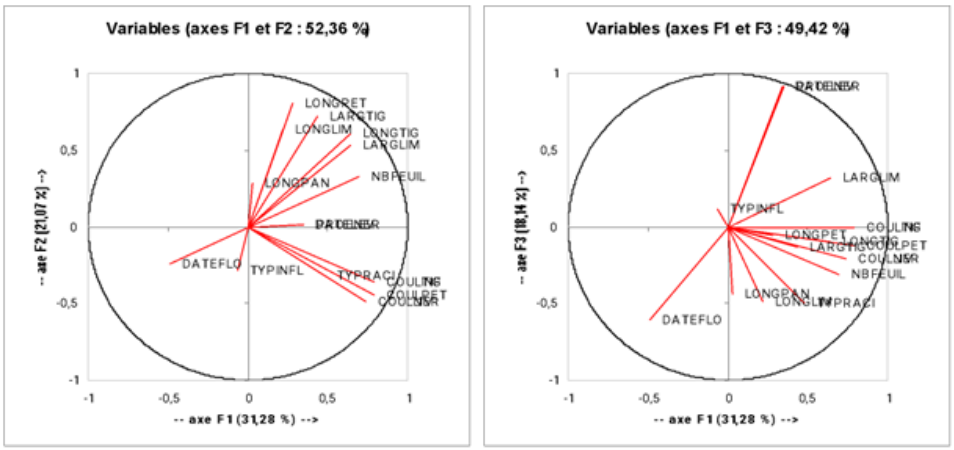

LONGTIG: Plant height ; **LARGLIM**: Width of the blade ; **NFEUIL**: Number of leaves ; **COULLIM**: Colour of the blade ; **COULTIG**: Stem color ; **COULINF**: Colour of the inflorescence ; **COULPET**: Petiole colour ; **COULNER**: Colour of the veins ; **DFLO**: Flowering date ; **LONGPET**: Petiole length ; **TYPINFL:** Inflorescence type ; **LARTIG**: Width of the shank ; **LONGLIM**: Length of the blade ; **DLEV:** Date of emergence ; **PROENER**: Prominence of the veins ; **TYPRACI**: Root type ; **LONGPAN**: Length of the panicle.

Discussion

The domestication of a species is justified by its adaptation to pedoclimatic conditions, its food, economic and medicinal role. The production of *Amaranthus hybridus* L. as an urban and peri-urban market gardening crop in Abidjan and Yamoussoukro could be justified by its socio-economic value for the local population (Fondio et al., 2012). Indeed, amaranth, characterized by intra- and interspecific variability, is domesticated and produced in market gardening as a leafy vegetable.

The selection criteria for a species or morphotype are generally based on agronomic and/or nutritional potential, demand, and market value (Fondio et al., 2012; Missihoun et al., 2012; Adjatin et al., 2017). The strong presence of the green morphotype among the accessions of *A. hybridus* in the present collection is justified by a selection oriented towards this morphotype in particular, because of its preferential characteristics. Indeed, from an agronomic point of view, the green morphotype showed the strongest performance in terms of leaf biomass (29 leaves per plant), stem strength (5.9 cm in diameter), plant height (137 cm) and panicle length (48.7 cm). This suggests that the green colour seems to be a selection criterion used by producers in Abidjan and Yamoussoukro in the production of this leafy vegetable. The green morphotype had also been identified as the most cultivated and consumed in Benin, Niger, Nigeria and Gabon (Soro et al.,

ISSN: 1857-7881 (Print)
e-ISSN 1857-7431 (Online)

2018; Iboune & Assouman, 2023). According to Assogba Komlan et al. (2016), Dinssa et al. (2016), the green morphotype is the most produced and valued by women in all urban, peri-urban and rural regions of tropical Africa.

In addition to amaranth, Kiébré (2016) and Kabré (2019) also observed selection oriented towards the green morphotype on *Cleome gynandra* and *Hibiscus cannabinus*, respectively. In addition, the very high intra- and interspecific variability (Ouédraogo et al., 2021) observed in the collection of *A. hybridus* could be justified by the production system on the one hand and by the mode of reproduction of the plant on the other. These two phenomena lead to the appearance of intermediate forms within the species due to the recombination of morphological traits through gene flow. Indeed, with an outcrossing rate of 25-35%, A. *hybridus* shows a high degree of inter-species hybridization, which would justify the morphological diversity observed (Lanta et al., 2003). Wu et al. (2000) also found wide diversity in stem and leaf colour when assessing China's genetic resource collection. Xiao et al. (2000) also classified 31 amaranth varieties based on 17 biological traits, whose leaf shape and colour were considered to be more discriminating for the classification of amaranth varieties. Thus, the presence of intermediate forms in the collection of *A. hybridus* would be linked to the production of different morphotypes and/or species in the same plot or very close plots, thus leading to spontaneous hybridizations. In addition, certain factors such as pedoclimatic conditions or natural and artificial selection, which can lead to highly variable selective pressures on genotypes, thus leading to morphological variability or the appearance of new phenotypes (Nagarajan & Prasad, 1980; Palomino & Ruby, 1991).

The existence of genetic diversity being the basic condition required for a varietal creation program (Pandey & Singh, 2011), accessions of this study, characterized by significant variability, offer possibilities for improvement of *A. hybridus* in Côte d'Ivoire with a view to meet the food and economic needs of the population. In addition, the different correlations observed between traits can facilitate this genetic improvement insofar as, when traits are positively correlated, the improvement of one will lead to that of the others. Thus, the better agronomic performance of the green morphotype gives it a particular interest in a selection and improvement program for production as a leafy vegetable. The green morphotypes TATROK, AMPT08, ABAN04, YKO07, AKSSI07, YQB06B, YFON01, YFON04, YQR04, YGK05, YQB08, and ABAN17 accessions could be used as potential sires in a breeding program. Indeed, in addition to its agronomic performance, the strongly coloured green morphotype is very rich in β-carotenes and lutein with antioxidant properties capable of preventing certain serious diseases such as cancer and cardiovascular diseases (McLaren & Frigg, 2002; Tiemtoré, 2004).

ISSN: 1857-7881 (Print)
e-ISSN 1857-7431 (Online)

The different correlations provide information on the genetic association between various traits under specific environmental conditions. This can help in the formulation of selection methods in the context of varietal improvement. Thus, the strong positive correlation of plant height with leaf biomass, leaf blade width, stem diameter and petiole length suggests that large plants have robust stems capable of supporting significant leaf biomass. This means that a selection oriented towards one of these traits would generally imply that of the others. As a result, selection oriented towards large plants could contribute to the improvement of leaf yield. Akaneme et al. (2013); Sarker et al. (2014); Abe et al. (2015) also noted that leaf biomass is strongly influenced by vegetative growth parameters such as plant height, number of leaves per plant, and stem diameter. However, the most important negative and significant correlations observed between the emergence date and the flowering date on the one hand, and between the flowering date and each of the variables of leaf blade width and vein prominence on the other, show that long-cycled amaranth plants have a very short emergence time and produce small leaves. This is because these long-cycled plants have not been able to express their photosynthetic potential to the best of their ability, thus allowing them to accumulate enough reserve substances.

Conclusion

This study highlighted the existence of a significant morphological variability within the accessions of *Amaranthus hybridus* from Côte d'Ivoire. This variability was observed on some quantitative variables studied such as organ color, stem diameter, plant height, leaf biomass, blade length and width. Interesting correlations between traits of interest were also noted. Promising accessions of the species have also been identified based on important biometric traits. This includes accessions with tall plants, more leaves, and longer leaf length that can be used as potential sires in an *A. hybridus* breeding program.

Acknowledgments

The authors are very grateful to the International Science Foundation (FIS) Research Grant FIS-CORAF Project/ Leafy Vegetables (K-3891-1). We would like to thank the National Center for Agronomic Research for its technical support in the field.

Conflict of Interest: The authors reported no conflict of interest.

Data Availability: All data are included in the content of the paper.

Funding Statement: The authors did not obtain any funding for this research.

ISSN: 1857-7881 (Print)
e-ISSN 1857-7431 (Online)

References:

1. Abe, S. G, Willem, S., & Patrick, O. A. (2015). Genetic diversity of *Amaranthus spp*. in South Africa. *South African Journal of Plant and Soil*, 32(1), 39-46.
2. Adjatin, A., Balogoun, D., Loko, L., Djengue, W., Bonou-gbo, Z., Honnankpon, Y., Dansi, A., Akoégninou, A., & Akpagana, K. (2017). Phenotypic diversity uses and management of local varieties of *Corchorus olitorius* L. from central Benin. *Journal of Biodiversity and Environmental Sciences*, 11(1), 81-96. ISSN: 2220-6663 (Print) 2222-3045.
3. Akaneme, F. I., & Ani, G. O. (2013). Morphological assessment of genetic variability among accessions of *Amaranthus hybridus*. *World Applied Sciences Journal*, 28(4), 568-577.
4. Assogba Komlan, F., Sikirou, R., Yo, T., Adanguidi, J., & Mensah, A. C. G. (2016). La culture de l'Amarante (Fotêtê en fongbé) au Bénin. *Fiche technique FAO*. Dépôt légal N°8552 du 19/02/16. Bibliothèque Nationale, 1er trimestre. ISBN: 978-99919-2-126-6, 16p.
5. Dinssa, F. F., Hanson, P., Dubois, T., Tenkouano, A., Stoilova, T., Hughes, J. d'A., & Keatinge, J. D. H. (2016). AVRDC - The World Vegetable Center's women-oriented improvement and development strategy for traditional African vegetables in sub-Saharan Africa. *European Journal of Horticultural Science*, 81(2), 91-105. Doi:10.17660/eJHS.2016/81.2.3.
6. Fondio, L., N'zi, J. C., Mahyao, A., Agbo, E., Kouamé, C., Djidji, A. H., & N'gbesso, M. (2011). Bien cultiver l'amarante en Côte d'Ivoire. Direction des programmes de recherche et de l'appui au développement - Direction des innovations et des systèmes d'information CNRA, Côte d'Ivoire, E-mail: info.sqr@cnra.ci. 4p.
7. Fondio, L., N'zi, J. C., Agbo, A. E., Mahyao, A., Djidji, A. H., & N'gbesso, M. F. D. P. (2012). Good agricultural practices for the production of underutilized vegetables in Sub Saharan Africa: case of amaranth (*Amaranthus spp*.) in Côte d'Ivoire. International Society for Horticultural Science (ISHS). *Proceedings of technical consultation workshop held in Arusha, Tanzania*, 7-8 December 2009, Eds R. Nono-Wondim. Scripta Horticulturae, 15, 91-101.
8. Fondio, L., N'zi, J. C., & Kobenan, K. (2015). Comportement agronomique et sanitaire de nouvelles lignées de piment (*Capsicum sp.*) dans le Sud de la Côte d'Ivoire. *Journal of Applied Biosciences*, 92, 8594-8609. http://dx.doi.org/10.4314/jab.v92i1.4.
9. Grubben, G. J. H. (1975). La culture de l'amarante, légume-feuilles tropical avec référence spéciale au Sud-Dahomey. Mededelingen Land bouwhogeschool Wageningen. Wageningen, Netherlands. 233p.

ISSN: 1857-7881 (Print)
e-ISSN 1857-7431 (Online)

10. Grubben, G. J. H., & van Sloten, D. H. (1981). Genetic resources of amaranths: a global plan of action, including a provisional key to some edible species of the family Amaranthaceae by Laurie B. Feine-Dudley. International Board for Plant Genetic Resources, Rome, Italy. 57 pp.
11. Iboune, M., & Assouman, D. A. (2023). Fiche technique pratiques des producteurs pour la culture de l'amarante. Chambre Régionale d'Agriculture (CRA) de Niamey, Niger, 4p.
12. Kabre, V. N. (2019). Diversité génétique de *Hibiscus cannabinus* cultivée dans sept provinces du Burkina Faso. Thèse de doctorat unique, Spécialité : Génétique et Amélioration des Plantes, Université Joseph Ki-Zerbo, Burkina Faso, 127p.
13. Kiebre, Z. (2016). Diversité génétique du Caya blanc (*Cleome gynandra* L.) du Burkina Faso, Thèse de doctorat, Université Ouaga, Burkina Faso, 126p.
14. Lanta, V., Havranek, P., & Ondrej, V. (2003). Morphometry analysis and seed germination of *Amaranthus cruentus, A. retroflexus* and their hybrid (*A. x turicensis*). *Plant Soil and Environment*, 49, 364-369.
15. Mburu, M. W., Gikonyo, N. K., Kenji, G. M., & Mwasaru, A. M. (2012). Nutritional and functional properties of a complementary food based on Kenyan amaranth grain (*Amaranthus cruentus*). *African journal of food agriculture nutrition and development*, 2(2), 1-19.
16. McLaren, D., & Frigg, M. (2002). Voir et vivre, guide pratique sur la vitamine A dans la santé et la maladie. Groupe de travail voir et vivre, seconde Edition. 39 p.
17. Missihoun, A. A., Agbangla, C., Adoukonou-Sagbadja, H., Ahanhanzo, C., & Vodouhè, R. (2012). Gestion traditionnelle et statut des ressources génétiques du sorgho (*Sorghum bicolor* L. Moench) au Nord-Ouest du Bénin. International *Journal of Biological and Chemistry Sciences*, 6(3), 1003-1018.
18. Nagarajan, K., & Prasad, M. N. (1980). Studies in genetic diversity in foxtail millet (*Setaria italica* B.). *Madras Agricultural Journal*, 67, 28-38.
19. National Research Council (1989). Lost Crops of the Incas. Washington, DC, USA: National Academy Press.
20. National Research Council (2006). Lost Crops of Africa. Volume II: Vegetables. The National Academies Press, Washington; ISBN: 0-309-66582-5; 378p. http://www.nap.edu/ catalog/11763.html.
21. N'zi, J. C., Fondio, L., N'Gbesso, M. F. D. P., Djidji, A. H., & Kouamé C. (2015). Bed behavioral assessment of tomato varieties in Côte d'Ivoire. *Journal of Advances in Agriculture*, 4 (3), 513-522.

ISSN: 1857-7881 (Print)
e-ISSN 1857-7431 (Online)

22. Ouedraogo, J., Kiebre, M., Kabore, B., Sawadogo, B., Kiebre, Z., & Bationo, K. P. (2021). Identification and agronomic performance of species of the genus Amaranthus grown in Burkina Faso. *International Journal of Applied Agricultural Sciences*, 7(2), 102-109. https://doi.org/10.11648/j.ijaas.20210702.15
23. Palomino, G., & Rubi, R. (1991). Diferencias cromosomicas entre algunas especies y tipos del genero Amaranthus distribuidos en Mexico: Actas Primer Congreso internacional del Amaranto: 24p.
24. Pandey, R. M., & Singh, R. (2011). Genetic divergence in grain amaranth (*Amaranthus hypochondriacus* L.). *Genetika*, 43(1), 41-49.
25. Písaříková, B., Zralý, Z., Kráčmar, S., Trčková, M., & Herzig, I. (2005). Nutritional value of amaranth (genus Amaranthus L.) grain in diets for broiler chickens. *Czech Journal of Animal Science*, 50(12), 568-573.
26. Sarker, U., Islam, M. T., Rabbani, M. G., & Oba, S. (2014). Genotypic variability for nutrient, antioxidant, yield and yield contributing traits in vegetable amaranth. *Journal of Food Agriculture and Environment*, 12(3 & 4), 168-174. Https: // www.researchgate.net/ publication /267509472.
27. Soro, K., Séguéna, F., Amon, A. D. E., & Konan, B. B. (2018). Caractérisation de la flore dans les espaces de maraîchage : cas d'une parcelle de menthe en zone urbaine à Koumassi (Abidjan), Côte d'Ivoire. *International Journal Biological of Chemical and Sciences*, 12(6), 2547-2563. DOI: https://dx.doi.org/10.4314/ijbcs.v12i6.7.
28. Tiemtore, T.W.E. (2004). Impact de la cuisson hydrothermique sur les micronutriments des légumes feuilles. Thèse de Master ENSIA-SIARC, Montpellier. 62 p.
29. Wu, H., Sun, M., Yue, S., Sun, H., Cai, Y., Huang, R., Brenner, D., & Corke, H. (2000). Field evaluation of an Amaranthus genetic resource collection in China. *Genetic Resources and Crop Evolution*, 47(47), 43-53.
30. Xiao, S., Liu, G., Song, Y., & Yang, G. (2000). Classification of vegetable Amaranthus variety resources. *Journal of Hunan Agricultural University*, 25, 274-2.

ESJ Natural/Life/Medical Sciences Peer-reviewed

Répartition spatiale et identification des ennemis dans le périmètre de culture du fonio (*Digitaria exilis*) à Sédhiou

Amadou Bouye Seydi
Tofféne Diome
Pape Mbacké Sembène
Laboratoire de physiologie animale de la faculté des sciences et techniques de l'Université Cheikh Anta Diop de Dakar FST/UCAD, Dakar, Sénégal

Doi:10.19044/esj.2026.v22n6p141

Submitted: 08 January 2026
Accepted: 25 February 2026
Published: 28 February 2026

Cite As:
Seydi, A.B., Diome, T. & Sembène, P.M. (2026). *Répartition spatiale et identification des ennemis dans le périmètre de culture du fonio (Digitaria exilis) à Sédhiou*. European Scientific Journal, ESJ, 22 (6), 141. https://doi.org/10.19044/esj.2026.v22n6p141

Résumé

Dans le but de cerner les ennemis dans le processus d'évaluation des ravageurs de la culture du fonio (*Digitaria exilis*), une étude a été menée dans le village de Tambananing localisé dans la commune de Sédhiou. L'objectif de cette étude est d'identifier et de faire la répartition spatiale des ennemis de la culture du fonio de manière générale mais aussi de l'aspect entomofaune et des plantes adventices en particulier Pour cela, un dispositif expérimental est mis en place, constitué de 04 parcelles de deux écotypes qui ont été scindées en deux parties égales, l'une semée avec l'écotype *Momo* et l'autre avec l'écotype *Dibong*., dont chacune d'elle est constituée de son témoin négatif sans apport d'engrais organique et de l'autre contenant un apport de fumier organique (témoin positif). La technique d'inventaire et d'identification des nuisibles de la culture du fonio consiste à circuler point par point le long des parcelles autrement dit pied par pied des plants de l'ensemble des parcelles mises en jeu ou encore appelée méthode « tour de champs ». Plusieurs familles d'espèces d'adventices sont inventoriées dans les parcelles de fonio. On note la présence des *poaceae* et des *cyperaceae* qui comptent respectivement 5 et 3 espèces parmi les13 inventoriées dans les champs de fonio. Les espèces *pantropicales* suivant les affinités biogéographiques et celles africaines semblent être plus nombreuses alors que les *thérophytes* représentent le type biologique le plus dominant. L'inventaire des insectes a été fait à travers la

ISSN: 1857-7881 (Print)
e-ISSN 1857-7431 (Online)

capture par le piégeage à l'aide des sachets plastiques et du filet fauchoir. Les résultats ont donné un total de 89 individus capturés à l'aide du filet fauchoir dans notre périmètre d'étude. Ces derniers sont répartis en 5 ordres de groupes d'espèces notamment des *lépidoptères* avec une fréquence beaucoup plus importante de 33 % suivis des *coléoptères* moins importants avec 22 % ensuite des *diptères* 15 %, les *hémiptères* avec 12 % et enfin les *orthoptères* avec 07 %. La protection culturale constitue un maillon essentiel pour prévenir les risques et dangers contre les ennemis des cultures, ce qui revêt une double identité à la fois protéger les végétaux et assurer la sécurité du consommateur.

Mots-clés: Adventices, insectes, nuisibles, fonio, Sédhiou

Spatial Distribution and Identification of Pests in the Fonio (*Digitaria exilis*) Cultivation Area in Sédhiou

Amadou Bouye Seydi
Tofféne Diome
Pape Mbacké Sembène
Animal Physiology Laboratory, Faculty of Science and Technology, Cheikh Anta Diop University of Dakar FST/UCAD, Dakar, Senegal

Abstract

In order to identify pests and enemies in the fonio (*Digitaria exilis*), a crop assessment process was conducted in the village of Tambananing, located in the commune of Sédhiou. The objective of this study was to determine and identify the insect fauna in general, as well as specific pests and enemies. To this end, an experimental setup was established, consisting of four plots of two ecotypes, each divided into two equal parts: one sown with the *Momo* ecotype and the other with the *Dibong* ecotype. Each plot included a control plot without organic fertilizer and another with organic manure. The technique for inventorying and identifying fonio crop pests involved walking point by point along the plots, in other words, inspecting each plant individually across all the plots, a method also known as the "field walk-through" approach. Several families of weed species were identified in the fonio plots. The presence of *Poaceae* and *Cyperaceae* was noted, with 5 and 3 species, respectively, among the 13 identified in the fonio fields. *Pantropical* species, following biogeographical affinities, and African species appear to be more numerous, while *therophytes* represent the most dominant biological type. The insect inventory was conducted through capture using traps with plastic bags and sweep nets. The results yielded a total of 89 individuals captured with sweep nets within our study area. These were distributed across five species groups:

ISSN: 1857-7881 (Print)
e-ISSN 1857-7431 (Online)

Lepidoptera (*butterflies and moths*) were the most frequent (33%), followed by *Coleoptera* (beetles) at 22%, *Diptera* (flies and moths) at 15%, *Hemiptera* (*wingflies and moths*) at 12%, and *Orthoptera* (*grasshoppers and grasshoppers*) at 7%. Crop protection is a crucial element in preventing risks and dangers from crop pests, serving a dual purpose: protecting plants and ensuring consumer safety.

Keywords: Weeds, insects, pests, fonio, Sédhiou

Introduction

Un champ ou une parcelle cultivée est le lieu superficiel où la biodiversité naturelle a largement disparu. En concentrant les espèces cultivées, le cultivateur favorise la pénétration des prédateurs et les épidémies qui sont responsables de la diminution du rendement à l'hectare de la culture. Les conséquences sont des dégâts occasionnés à la production agricole et aux denrées stockées entrainés par les ravageurs, les parasites et les mauvaises herbes, qui représentent souvent plus d'un tiers de la récolte. Les agents responsables de ces pertes non négligeables sont essentiellement les insectes phytophages qui sont de loin les plus nuisibles, les nématodes, les champignons, les virus et les bactéries, sans oublier les adventices. Des stratégies de protection des cultures et des moyens de lutte contre ces ennemis sont alors nécessaires afin de maintenir un niveau élevé de production. Sous l'action combinée des maladies, des attaques des ravageurs et de la concurrence des adventices, on estime que près de 50 % de la production agricole mondiale est perdue avant ou après la récolte (Schiffers, & Moreira, 2018).

Le fonio blanc (*Digitaria exilis*), est une céréale mineure cultivée dans toute l'Afrique de l'Ouest, du Sénégal au lac Tchad. Les plantes, qui atteignent une taille de 30 à 80 cm, produisent de minuscules grains de 1,0 à 1,5 mm de long, d'excellente qualité nutritionnelle et constituant également un aliment précieux et facile à digérer pour la volaille. Le fonio est une source de nourriture pour plusieurs millions de personnes lorsque les autres ressources alimentaires sont rares, apportant ainsi une contribution essentielle à la sécurité alimentaire. En raison de son cycle de croissance court, de 70 à 150 jours, il offre plusieurs possibilités de production. Si les agriculteurs cultivent des cultivars à cycle très court, le fonio leur permet de couvrir la saison critique avant la récolte des principales cultures vivrières. Le fonio pousse sur des sols très pauvres, sur lesquels les autres céréales n'y arrivent pas. Cependant, sa faible capacité de rendement et sa transformation traditionnelle très laborieuse ont freiné son développement (Olugbenga & Weidmann, 2021).

ISSN: 1857-7881 (Print)
e-ISSN 1857-7431 (Online)

Le fonio demande très peu de fertilisants, et occupe donc généralement la dernière place dans les systèmes de rotation avant une jachère de plusieurs années. L'apport d'éléments nutritifs et d'eau n'est généralement pas considéré comme pertinent par les agriculteurs. Pour la préparation du sol, de nombreux agriculteurs brûlent la végétation de la jachère et répandent les cendres. Ce procédé détruit la matière organique de la couche arable, qui est essentielle pour la fertilité et la conservation de l'humidité du sol. La culture du fonio repose principalement sur des variétés rustiques traditionnelles. En raison de la capacité du fonio à s'implanter rapidement, les agriculteurs ne désherbent généralement pas les champs, ce qui provoque une compétition farouche avec les mauvaises herbes, entrainant une réduction de sa capacité à avoir un bon rendement. La sensibilité du fonio aux ravageurs et aux maladies est faible. Néanmoins, certains champignons peuvent affecter la culture en croissance, il faudra noter que les moisissures des grains sont souvent fréquentes. Cependant il faut mettre l'accent sur la mauvaise herbe parasite *striga*, en particulier *Striga rowlandi*, très redoutée, connue pour être abondante en Afrique de l'Ouest, qui peut causer de sérieux dommages à la culture. Les insectes phytophages sont capables de causer des pertes assez importantes associés aux oiseaux qui se nourrissent des grains en cours de maturation (Olugbenga. & Weidmann, 2021).

En Afrique subsaharienne de l'ouest, le fonio constitue à la fois une culture de rente et une culture vivrière. Dans cette zone, cette culture connaît actuellement un regain d'intérêt en zone urbaine du fait de ses vertus diététiques et thérapeutiques (Konkoba. Y, 2004). En zone rurale, le fonio apparaît comme une culture de soudure entrant dans une stratégie de lutte contre l'insécurité alimentaire saisonnière en Afrique de l'Ouest (Vall É et al, 2011). Au Sénégal la filière fonio est cultivée principalement dans la Région Sud du Sénégal, le Centre et l'Est du Sénégal (Issoufou Ouédraogo, 2015).

Le fonio est une céréale dont la production connaît une croissance durant ces dernières années, et pour soutenir cette production, beaucoup de travaux de recherche ont été initiés sur le fonio mais essentiellement orientés vers les technologies post-récolte (Cruz, 2001). Les recherches menées sur les techniques culturales et la fertilisation du fonio sont rares et anciennes (Gigou et al, 2009). Cependant, un accroissement de la production de cette céréale passe par une connaissance des facteurs biotiques qui peuvent influencer l'évolution de la plante durant sa phase végétative (Noba, 2002). Sous l'effet cumulé des ravageurs, des maladies et de la forte présence des adventices, plus de la moitié de la production agricole mondiale est perdue. (Schiffers, 2010). Les estimations de pertes, par région et par culture, publiées en 1965 par H.H. CRAMER ont été revues en 1990 par E.C. OERKE et d'autres auteurs notamment. Ces auteurs mettent en évidence que la différence substantielle qui existe entre la « production potentielle » des variétés utilisées et les «

ISSN: 1857-7881 (Print)
e-ISSN 1857-7431 (Online)

rendements réellement enregistrés », l'attribuant pour la plus large part aux dégâts causés par les parasites aux cultures (Schiffers, 2010). C'est dans ce contexte que s'inscrivent nos travaux qui s'articulent sur l'espace emblavé, la détermination de l'inventaire des nuisibles, c'est-à-dire des adventices et insectes rencontrés dans le périmètre d'étude.

Matériel et Méthodes

Le site d'étude est constitué d'une superficie de ½ ha a été divisé en quatre parcelles identiques de 1250 m^2 chacune. Pour chaque écotype, deux parcelles ont été utilisées l'une servant de témoin (sans apport de fumure) et l'autre de test (avec apport de fumure organique). Les parcelles ont été défrichées, désherbées, nettoyées, labourées au tracteur compact à dents et soumises au paillage ou mulching opéré pendant les deux mois précédents la date de semis avec une quantité de trois tonnes et demi de paille qui devraient suffire pour recouvrir l'ensemble des parcelles de l'étude selon la FAO (FAOSTAT, 2019). De la fumure organique a été ensuite apportée aux parcelles test à la dose de 100 g/m^2, un mois avant la date de semis en vue de permettre son assimilation par le sol.

Matériel végétal

Semence de fonio écotype *Momo*
Semence de fonio écotype *Dibong*

Matériel utilisé au champ est constitué de :

- Daba sert à désherber les mauvaises herbes ;
- Faucille pour couper les mottes de fonio ;
- Décamètre pour délimitation des parcelles ;
- Planchettes pour identifier chaque parcelle ;
- Filet fauchoir pour capturer les insectes ;
- Filets d'attache, servant à attacher les sachets ainsi que le couvercle des bocaux
- Règle décimètre, pour mesurer
- Crayon noir servant à écrire
- Carnet bloc note pour la prise de note
- Sachets plastiques à insérer les insectes capturés
- Bocal en verre pour la mise d'échantillon de fonio pour apprécier les insectes post-récolte

Technique d'identification des adventices du fonio

L'inventaire des adventices a été réalisé pendant la période des inflorescences de ces adventices. La méthode de l'inventaire pied à pied ou itinérant décrite par (Noba, K., 2002) a été mise en œuvre pour l'inventaire

ISSN: 1857-7881 (Print)
e-ISSN 1857-7431 (Online)

des adventices. La technique de relevé floristique utilisée, est celle du tour de champs, qui permet de répertorier les espèces de la surface d'observation de façon exhaustive. Elle consiste à parcourir la parcelle dans différentes directions jusqu'à la découverte d'une nouvelle espèce. Les espèces présentes sont répertoriées avec des codes. Les espèces récoltées sont ensuite identifiées à l'aide de clés entomologiques, puis classées par ordre, famille, genre, voire espèce, selon l'abondance de chaque espèce par comptage, et on calcule la fréquence d'apparition. Les espèces d'adventices ont été identifiées grâce à l'utilisation de guides sur les adventices tropicaux de Berhaut, J. (1967) & H.Merlier & J.Montegut (1982).

La nomenclature employée est celle de (Lebrun J, 1966). Pour les types biologiques, nous avons utilisé la classification de (Raunkiaer C., 1934) adaptée à la zone tropicale où la saison défavorable correspond à la saison sèche. Cette classification distingue 6 formes biologiques qui sont : *les nanophanérophytes (P), les chaméphytes (C), les hémi cryptophytes (H), les géophytes (G), les thérophytes (T) et les plantes parasites (Par).*

Pour les affinités biogéographiques, les informations et les codes utilisés reflètent les travaux de Sarr, E. et Pro, J.C. (1985) qui sont : « *Af* » pour les espèces africaines, « *Am* » pour les espèces afro-américaines, « *Am As* » pour les espèces afro-américaines et asiatiques, « *As* » pour les espèces afro-asiatiques, « *Mas* » pour les espèces afro-malgaches et asiatiques et « *Pt* » pour les espèces *pantropicales*.

Le recensement a consisté à un prélèvement de chaque espèce d'adventice rencontrée dans les parcelles élémentaires. La même opération a été répétée dans les autres parcelles élémentaires en ne tenant plus compte des espèces d'adventices déjà rencontrées. Les échantillons d'adventices récoltés sont ramenés au laboratoire afin de procéder à leur identification. La détermination exacte de toutes les espèces végétales rencontrées dans le champ a été faite en utilisant le guide sur les adventices tropicales (Berhaut, J.,1967).

Méthodologie et technique d'inventaire des ravageurs

L'inventaire des ravageurs a été faite à l'aide d'un filet fauchoir qui est composé de trois éléments : le filet conique proprement dit, l'anneau qui permet de conserver le filet ouvert et la manche, liée à l'anneau, fait en aluminium ou en bois. La parcelle témoin nous a servi d'étude expérimentale, nous avons procédé par une observation par vue panoramique sous la forme Z C'est-à-dire que le surveillant se déplace en forme Z. Ceci s'effectue comme suit : on arpente le champ sur son côté latéral jusqu'à son extrémité d'Ouest en Est, ensuite on traverse le champ par la médiane en déplacement oblique jusqu'au bout du côté opposé au champ, et enfin on suit le côté latéral opposé

ISSN: 1857-7881 (Print)
e-ISSN 1857-7431 (Online)

d'Est en Ouest. L'observation a révélé la présence des fourmis noirs et quelques insectes sans aucune gravité majeure.

Technique d'essai d'identification des insectes post-récolte

Des essais témoin de grain paddy des deux variétés de fonio sont mis dans des bocaux en verre portant sur chaque écotype en vue de déterminer le mode de conservation post-récolte à température ambiante afin d'apprécier les insectes capables d'attaquer le fonio pendant la période post-récolte.

Analyse des données

Les valeurs des résultats de cette étude ont été calculées grâce au programme Excel 10 et les analyses statistiques ont été réalisées par le logiciel Sigma plot.13.0. Les données ont été soumises à une analyse de variance dont l'intervalle de confiance est fixé à 95%.

Résultats

Les résultats de cette étude portant sur l'occupation de manière générale de l'espace cultivé des adventices suivie de leur identification dans les parcelles expérimentales soumises au mulching ont montré une diversité floristique assez riche et diversifiée.

Diversité des espèces adventices

La diversité botanique des adventices au Sénégal est caractérisée par une forte prédominance de plantes herbacées annuelles *(thérophytes*), représentant plus de 77 % de la flore, avec une prédominance des familles *Poaceae, Fabaceae et Malvaceae*. Cette diversité floristique s'adapte aux régions à caractères agroécologiques, avec une représentativité plus élevée en Casamance et au Sénégal oriental, marquée par des espèces pantropicales et africaines. Les données du tableau 01 nous révèlent l'ensemble des familles rencontrées dans l'investigation des adventices répertoriées dans nos parcelles d'étude.

Tableau 1: Tableau de répartition des adventices répertoriés

Familles	*Genres et espèces*
Poaceae	*Brachiaria Lata (Schumach) Hubb*
	Digitaria horizontalis Willd
	Dactyloctenium aegyptium (L.) Willd
	Setaria pallide-fusca (Schumach.) Stapf et Hubb
	Paspalum scrobiculatum L.
Commelinaceae	*Commelina benghalensis L.*
Rubiaceae	*Mitracarpus villosus (Sw.) DC*
Convolvulaceae	*Ipomea eriocarpa R. Br*
Solanaceae	*Physalis angulata L.*
Malvaceae	*Hibiscus asper Hook.f*
	Kyllinga squamulata Thonn.ex Vahl

ISSN: 1857-7881 (Print)
e-ISSN 1857-7431 (Online)

Cyperaceae	*Mariscus cylindristachyus Steud.*
	Cyperus sp.
Amaranthaceae	*Achyranthes aspera L.*
Cucurbitaceae	*Citrullus colocynthis (L.) Schrad.*
Euphorbiaceae	*Acalypha acuta Thunb*
Portulacaceae	*Anacampseros albidiflora Poelln*
Nyctaginaceae	*Boerhavia adscendens Willd*
Scrophulariaceae	*Acanthorrhinum sp. Rothm.*

Répartition géographique des adventices

Types Biologiques

Les espèces ont été identifiées par l'utilisation du guide sur les adventices tropicaux de Berhaut, J. (1967), associées à la nomenclature de Lebrun, J., et la classification de Raunkiaer, C. (1934) a été utilisée pour énumérer les types biologiques suivant les espèces d'adventices inventoriées. Cette classification adaptée à la zone tropicale (Lebrun, 1966,) permet de distinguer, les *Chaméphytes* (C), les *Hémicryptophytes (HCP), les Thérophytes (T), les parasites (Par), Pt (pan tropicale), As (Afro asiatique*), *Af* (*Africaine), Am (Afro américaine), Mas (Afro Malgache Asiatique), Cosm (cosmopolite) G (géophyte).* Le tableau 02 indique la fréquence d'occurrence des différentes espèces d'adventices dans les champs de fonio.

Tableau 2: La fréquence de répartition géographique des espèces et type biologique

Espèces	*Fréquence D'occurrence %*	*Répartition géographique*	*Type Biologique*
Digitaria horizontalis Willd.	*80*	*Pt*	*T*
Spermacoce ruelliae DC	*51*	*Af*	*T*
Cyperus esculentus L.	*25*	*Cosm*	*G*
Fimbristylis hispidula (Vahl) Kunth	*20*	*Af*	*T*
Hibiscus asper Hookf.	*18*	*Af*	*T*
Kyllinga squamulata Vahl	*17*	*Ams As*	*T*
Eragrostis tremula Steud	*16*	*As*	*T*
Dactyloctenium aegyptium	*15*	*Pt*	*T*
Cynodon dactylon (L.) Pors	*14*	*Cosm*	*C*
Andropogon gayanus Kunth	*13*	*Af*	*Hcp*
Striga hermonthica (Delile) Benth	*13*	*Mas*	*Par*
Commelina benghalensis L.	*12*	*As*	*T*
Cassia obtusifolia L.	*11*	*Pt*	*T*
Chloris pilosa Schumach.	*10*	*As*	*T*
Phyllanthus amarus Schumach. Et Thonn.	9	*Pt*	*T*
Cenchrus biflorus Roxb	9	*Cosm*	*T*
Portulaca quadrifida L.	9	*Pt*	*T*
Boerhavia sp	9	*Pt*	*T*
Amaranthus sp.	8	*Pt*	*T*
Hibiscus sabdarifa	03	*Pt*	*T*

Pt (pan tropicale), As (afro asiatique), Af (africaine), Am (afro américaine), Mas (afro malgache asiatique), Cosm (cosmopolite) T (thérophyte), HCP (hémicrytophyte), Par (parasite), G (géophyte), C (chaméphyte), nf (non effectué)

ISSN: 1857-7881 (Print)
e-ISSN 1857-7431 (Online)

Ce tableau 2 renseigne l'état des lieux de la fréquence d'occurrence des différentes espèces d'adventices dans les champs de fonio, dénotant particulièrement l'abondance. Les espèces *Digitaria horizontalis*., *Spermacocea ruelliae* .et *Cyperus esculentus*. suivi de *Fimbristylus hispidula* sont les plus présentes dans le champ d'étude. La plante parasite redoutée *Striga hermonthica* est signalée même si son nombre est inférieur voire faible (13) dans les champs de fonio.

Répartition géographique des espèces
Pourcentage type biologique

Les zones agroécologiques les plus densement peuplées en adventices au Sénégal sont : La Casamance, la région du Fleuve Sénégal, et le Sénégal-Ouest qui sont les endroits les plus diversifiés en espèces adventices. La figure 01 ci-dessous révèle la nature du type biologique rencontrée dans les parcelles montrant le pourcentage d'occupation de l'espace utilisé.

Figure 1: Répartition du type biologique

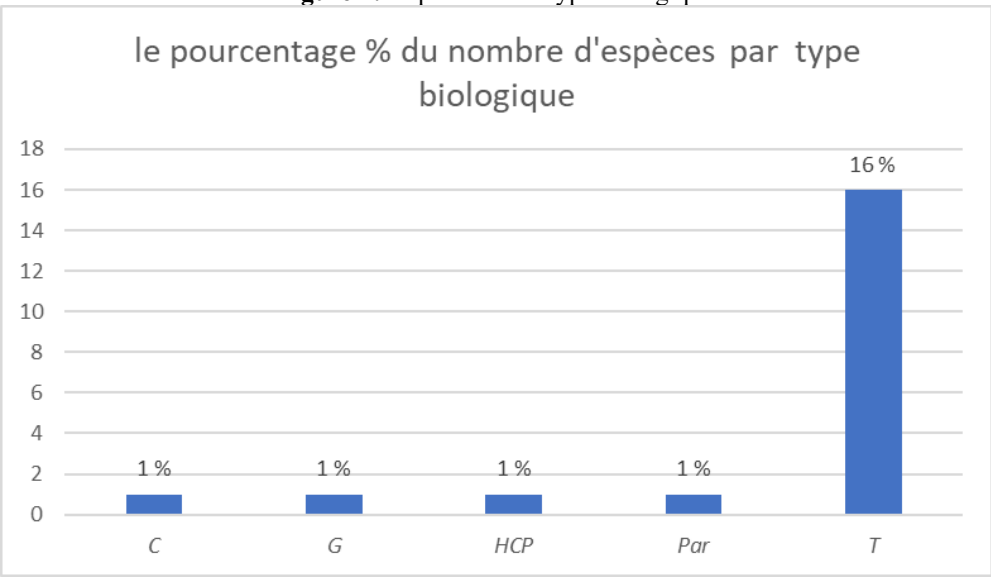

C (chaméphyte) :…G(géophyte) :…HCP(hémicrytophyte), :…..Par(parasite),

Les *thérophytes* sont des plantes qui bouclent leur cycle de vie durant la période favorable et passent la période défavorable en dormance sous forme de graines. La plupart d'entre eux sont capables de réaliser leur cycle de vie en quelques semaines (Haq N.et Dania Ogbe F.,(1995) A travers cette figure 01, nous constatons que le type biologique dominant est constitué des *thérophytes* avec 16%, qui sont en majorité dans la zone de culture ce qui s'illustre très bien par le fait que nous sommes précisément, bel et bien en période d'hivernage où la pluie est observée en abondance, ce qui permet à ce groupe de plantes de se reproduire et de se développer rapidement jalonnant

ISSN: 1857-7881 (Print)
e-ISSN 1857-7431 (Online)

partout les champs et prairies de la place avec une vitesse de propagation inquiétante.

En appui à la figure 02 qui montre la répartition du nombre de fréquence géographique.

Le groupe d'espèce le plus répandu géographiquement dans les parcelles est constitué des *pantropicales* avec la valeur de 7% qui s'affiche largement sur les autres espèces suivies des espèces africaines.

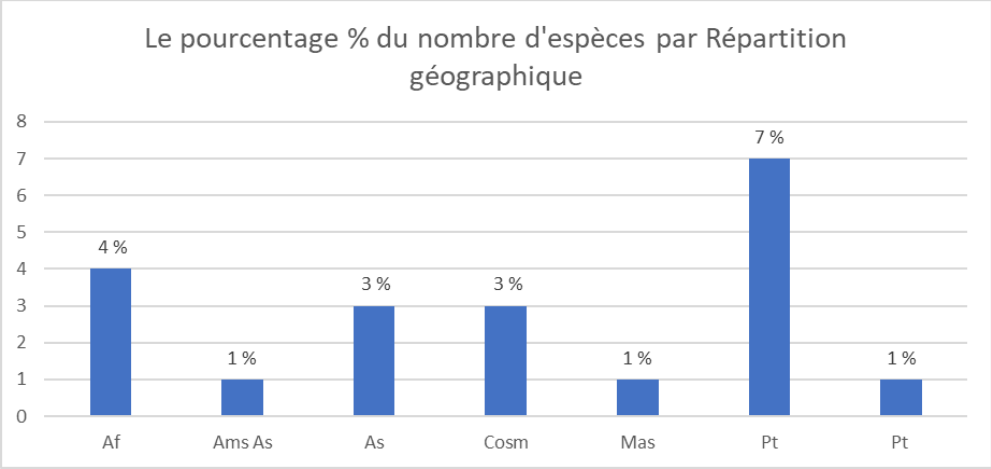

Figure 2: La répartition géographique du nombre d'espèce

La figure 03 ci-après montre le graphique de la fréquence d'occurrence, marquée par la forte présence des *digitaires 80%,* dans les parcelles expérimentales, suivis des *spermacocea 51%.* Cependant même si le striga est redouté dans les parcelles avec 13%, il faut noter que malgré cette présence ceci n'a pas vraiment inquiété la culture en tant que telle.

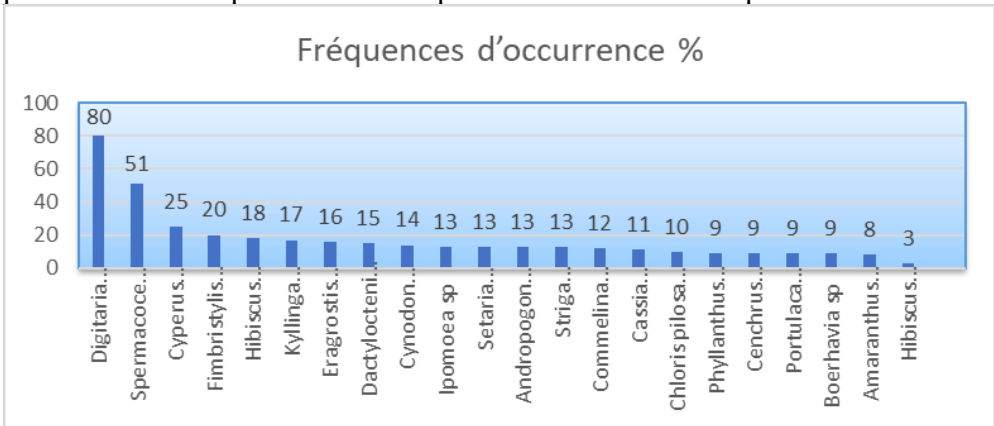

Figure 3: Histogramme de fréquence de l'occurrence

ISSN: 1857-7881 (Print)
e-ISSN 1857-7431 (Online)

Les espèces phytophages

Les espèces phytophages sont des organismes souvent constitués, d'insectes et des invertébrés se nourrissant principalement de substances végétales (feuilles, tige, racines, fruits, écorce, bois, etc.). Elles participent au bon fonctionnement de l'écosystème, parallèlement peuvent provoquer d'importants dégâts aux cultures. Le tableau 03 ci-dessous montre la répartition et la fréquence d'occurrence des espèces inventoriées**.**

Tableau 3: Répartition des ordres et familles des espèces inventoriées dans la parcelle

Ordre d'insectes	*Nombre d'insectes %*	*Nombre de Familles*
Lépidoptère	*33*	*2*
Coléoptère	*22*	*2*
Diptère	*15*	*2*
Hémiptère	*12*	*2*
Orthoptère	*07*	*1*

Au total 89 individus capturées à l'aide du filet fauchoir dans notre périmètre d'étude ce qui a montré 5 ordres de groupes d'espèces notamment des *lépidoptères* avec une fréquence beaucoup plus importante 33 % suivi des *coléoptères* moins importants avec 22 % ensuite des *diptères 15 %, les hémiptères avec 12 % et enfin les orthoptères avec 07 %.*

En se basant sur le guide d'identification et de reconnaissance des familles des espèces nous avons trouvé deux groupes de famille par espèce excepté les orthoptères où on a observé que 01. Le tableau 04 donne une indication de la famille et du genre d'espèces obtenus.

Tableau 4: Tableau des espèces identifiées

Ordre	*Famille*	*Genres et espèces*
Thysanoptères	*Thripidae*	*Thrips tabaci*
	Meloidae	*Mylabris sp.*
Coléoptère		
	Dioipsidae	*Diopsis apicalis*
Diptère	*Syrphydae*	*Syrphus sp*
Lépidoptère	*Arctudae*	*Amsacta spp*
	Noctuidae	*Earias insulana ; Spodoptera littoralis*
Hémiptère	*Aphididae.*	*Aphis gossypii Glover.*
	Aleurodidae	*Bemisia tabaci.*
Orthoptère	*Acridadae*	*Schistocerca gregaria*

Il en ressorte qu'une seule famille chez *l'orthoptère* montrant la présence de *Schistocerca gregaria* (criquet pèlerin), pratiquement toutes les autres familles sont caractérisées par deux genres d'espèces. (Voir tableau 03).

Ravageurs post-récolte

La culture du fonio est principalement menacée par des insectes (piqueurs-suceurs, broyeurs, foreurs), des oiseaux granivores et des rongeurs, avec des dégâts notables au champ et en stockage. Les pertes post-récolte sont

ISSN: 1857-7881 (Print)
e-ISSN 1857-7431 (Online)

causées par des *coléoptères* déprédateurs de stocks. Des maladies fongiques (*helminthosporiose, cercosporiose*)**.** Le tableau 05 ci-après décrit la présence des insectes ravageurs détectés dans les bocaux en verre pendant une période de 7ans. On a noté la présence dans les bocaux en verre suivant le processus d'identification des insectes post-récolte, la présence de *Rizopertha dominica*, de *Trogoderma granarius* et de *Tribolium castaneum* dans l'esquisse des deux écotypes inventoriés. Le classement des différentes espèces rencontrées dans les bocaux suivant l'inventaire a été lancé à la date du 16 Avril 2018.

Tableau 5: Récapitulatif de la présence des ravageurs par espèce et par écotype observé

Variété	*Ryzopertha dominica*	*Trogoderma granarius*	*Tribolium castaneum*	*Total*	*Moyenne*
Dibong	*4*	*2*	*44*	*50*	*16,66 ± 25,53*
Momo	*3*	*3*	*1*	*7*	*2,33 ± 2,51*
Total	*7*	*5*	*45*	*57*	*19 ± 26,45*
Moyenne	*3,5 ± 0,70*	*2,5 ± 0,70*	*22,5 ± 30,40*		

A travers ce tableau 05, on trouve en moyenne une présence assez faible de *Rizopertha dominica* avec une valeur de 3,5 ±0,70, avec P = 0,090 presque semblable à la présence de *Trogoderma granarius* avec 2,5 ± 0,70, avec (P= 0,126). On note une faible présence de ces deux espèces dans le fonio d'une manière générale, ce qui permet de dire une moindre résistance dans le processus post-récolte. Mais contrairement au *Tribolium castaneum* qui montre une forte présence avec 22,5 ± 30,40, (P= 0,486), ce qui nous permet d'affirmer que cette espèce est plus résistante et serait capable de porter plus de nuisance aux cultivateurs mais aussi aux consommateurs de manière particulière. Du coup en comparant les deux écotypes on note bien que le *Momo* présente plus d'aptitude et de propriétés résistantes par rapport au *Dibon*g.

Discussions

A travers cette étude on peut noter que les adventices peuvent avoir une nuisibilité directe sur la culture car ayant un effet de concurrence par rapport aux éléments nutritifs et l'eau et ce, dès le début du développement de la plante cultivée. Ce qui affecte par conséquent l'assimilation chlorophyllienne de la plante cultivée et sa croissance. De plus, certaines adventices ont une rapidité de croissance supérieure à la culture mise en place et peuvent donc être responsable d'un étouffement de la plante. En cours de développement les adventices peuvent héberger différents parasites (virus, bactéries, champignons et insectes ravageurs) et peuvent être source d'infestation (FAO, 2016).

Bien que bénéfiques, les mauvaises herbes peuvent cependant modifier l'environnement de la culture d'une manière négative. Dans des cultures envahies d'adventices, la circulation de l'air et de la lumière est réduite entre

ISSN: 1857-7881 (Print)
e-ISSN 1857-7431 (Online)

les rangs de semis. Alors, dans cet environnement plus sombre et plus humide, les maladies trouvent des conditions idéales pour se propager et infecter les plantes (Lebrun, 1966). Les espèces d'adventices ont été identifiées grâce à l'utilisation de guides sur les adventices tropicaux (Berhaut,1967). La nomenclature employée est celle de (Lebrun J, 1966). Pour les types biologiques, nous avons utilisé la classification de (Raunkiaer , 1934) adaptée à la zone tropicale où la saison défavorable correspond à la saison sèche. Cette classification distingue 6 formes biologiques qui sont : *les nanophanérophytes* (P), *les chaméphytes (C), les hémi cryptophytes (H), les géophytes (G), les thérophytes (T*) et les plantes *parasites (Par).* Pour les affinités biogéographiques, les informations et les codes utilisés reflètent les travaux de (Berhaut, J.,1967) qui sont : « *Af* » pour les espèces africaines, « *Am* » pour les espèces afro-américaines, « *Am As* » pour les espèces afro-américaines et asiatiques, « *As* » pour les espèces afro-asiatiques, « *Mas* » pour les espèces afro-malgaches et asiatiques et « *Pt* » pour les espèces *pantropicales*. Plusieurs familles d'espèces d'adventices sont inventoriées dans les parcelles de fonio. On note la présence des *poaceae* et des *cyperaceae* qui comptent respectivement 5 et 3 espèces parmi les 13 inventoriées dans les champs de fonio. Les espèces *pantropicales* suivant les affinités biogéographiques et celles africaines semble être plus nombreuses alors que les *thérophytes* représentent le type biologique le plus dominant. Les résultats obtenus à travers cette étude sont en parfait adéquation avec ceux réalisés de Issoufou Ouédraogo (2015) et de Cissokho. et al.(2025) qui attestent que l'identification des nuisibles est beaucoup plus riche chez les Poacées, accompagnée de la diversité floristique en phase de croissance.

Les espèces d'insectes capturés appartiennent aux ordres des *Homoptères, Diptères, Hyménoptères, Lépidoptères, Orthoptères et Thysanoptères*. En dehors de cela on peut noter que les insectes observés sont principalement des pucerons et des fourmis noirs qui font bon ménage car les fourmis procurent aux pucerons une défense agressive contre leurs antagonistes prédateurs et parasitoïdes. Cette défense peut être parfois renforcée par l'émission de phéromone d'alarme produite par les pucerons eux-mêmes.et quelques criquets pour la plupart (Chaubet, 2010). Aucune maladie fongique n'a été observée sur le fonio durant le suivi cultural dans les parcelles paysannes. Ces trois espèces sont fréquemment inventoriées dans les parcelles suivies, en particulier aucune méthode de lutte spécifique contre les insectes et les maladies dans les parcelles de fonio n'a été déployée sauf la surveillance par cris accompagnés par des battements de sons de pots de métal abandonnés ou de machettes ça et là et s'il y a un bon nombre d'oiseaux herbivores en présence selon constat, la fronde est l'instrument adéquat pour faire face contre les oiseaux (Gueye, M. 2016). Cependant l'attaque des pucerons est totalement négligeable. Il faut préciser que les résultats trouvés vont dans le

ISSN: 1857-7881 (Print)
e-ISSN 1857-7431 (Online)

même sens que les travaux de (Issoufou Ouédraogo, 2015) qui montrent tantôt la rencontre accidentelle de certains insectes non propres à la culture du fonio. Cependant notons que la détection post-récolte des nuisibles a montré à travers des essais témoin de grain paddy des deux écotypes de fonio mis dans des bocaux en verre en moyenne, une présence assez faible de *Rizopertha dominica* avec une valeur de 3,5 ±0,70, avec P = 0,090 presque semblable à la présence de *Trogoderma granarius* avec 2,5 ± 0,70, avec (P= 0,126) contrairement au *Tribolium castaneum* qui montre une forte présence avec 22,5 ± 30,40, (P= 0,486). On constate une nette dominance de la présence de *Tribolium* castaneum parmi les espèces ravageuses détectées par rapport aux autres comme *Rizopertha dominica* 3,5 ±0,70 et *Trogoderma granarius* 2,5 ±0,70 (P = 0,126) qui ont sensiblement la même valeur moyenne a une unité prés. Cependant on note aucune différence significative parmi les espèces retrouvées dans les bocaux avec (P = 0,09) chez *Rizopertha dominica*. Notons que la répartition par écotype donne chez le *Dibong* une moyenne de 16,66 ± 25,53 ce qui illustre bien que l'écotype *Dibong* est très sensible à la présence des ravageurs ce qui permet de dire que cet écotype ne présente pas suffisamment de propriétés résistantes à l'attaque des ravageurs tandis que chez l'écotype *Momo* avec une moyenne de 2,33 ± 2,51, on note des aptitudes résistantes. En outre il faut noter que l'application de la méthode de mulching a donné beaucoup de satisfaction, parce que cette technique se justifie à travers ces fondements à savoir : protéger le sol de l'érosion éolienne (par le vent) et hydrique (par l'eau). Ceci empêche que les particules du sol ne soient emportées ou lessivées, favorisant l'amélioration de l'infiltration d'eau d'irrigation grâce au maintien d'une bonne structure du sol. On note l'absence de formation de croûte imperméable en surface (parfois appelée croûte de battance) et les pores interstices du sol restent ouverts. De plus cette situation a permis de garder le sol humide en réduisant l'évaporation., obligeant le sol d'être couvert et aussi d'être moins exposé au rayonnement solaire. L'autre aspect bénéfique du mulching, il assure une nourriture et une protection des organismes du sol, constituant une excellente source de carbone pour les organismes du sol et offre des conditions propices à leur croissance à cause du paillis végétal. Le mulching entre autres bloque la croissance des mauvaises herbes, à l'aide d'une couche de paille assez épaisse, le développement des mauvaises herbes (adventices) est stoppé par manque de soleil, d'air, etc. (FAO, 2015). Cette technique a pu réduire de manière drastique une bonne partie de la flore végétale inventoriée dans nos parcelles d'étude, comparée aux études de (Cissokho et al, 2025).

ISSN: 1857-7881 (Print)
e-ISSN 1857-7431 (Online)

Conclusion

Ces travaux donnent une appréciation assez satisfaisante et présentent des avantages plus ou moins intéressants pour la protection culturale et méritent d'être vulgarisés pour contribuer à mieux lutter efficacement contre les problèmes des ennemis des cultures qui montrent des caractères vulnérables pour préserver les cultures des céréales en Afrique de l'Ouest. A cela il faut ajouter la forte diversité des adventices sauvages rencontrés dans le champ de fonio, qui agressent ou freinent le rendement de la productivité agissant sur la qualité du fonio. La présence des insectes permet de ralentir et de compromettre le rendement de la production du fonio. Cependant une meilleure approche, en termes de connaissance et une gestion rigoureuse des insectes nuisibles et des adventices pourraient asseoir les leviers de développement de la filière du fonio en Afrique de l'Ouest. Néanmoins la protection culturale constitue un élément fondamental pour prévenir les risques et dangers contre les ennemis des cultures ce qui permettra de sauvegarder les végétaux et le sol d'une part et d'autre part de garantir la sécurité sanitaire du consommateur.

Conflit d'intérêts : Les auteurs n'ont signalé aucun conflit d'intérêts.

Disponibilité des données : Toutes les données sont incluses dans le contenu de l'article.

Déclaration de financement : Les auteurs n'ont obtenu aucun financement pour cette recherche.

References:

1. Berhaut. J, Crook. J .H, Crowson. R.A, F. Bourlière (1967). Flore du Sénégal, 2ème Ed. Édition. ClaireAfrique., (Flore du Sénégal. 2e Edition plus complète. Avec les forêts humides de la Casamance. Editions Clairafrique,) Dakar. 485p
2. Bernard Chaubet. Journal, INRAE, (Institut National de Recherche pour l'Agriculture, l'Alimentation et l'Environnement). Titre : Pucerons et fourmis. Mutualisme-INRAE. https ://encyclopédie-pucerons.hub.inrae.fr, Date de création : 02 décembre 2010, date de modification : 14 juin 2024.
3. Bruno, Schiffers, PIP. COLEACP, protection des cultures N°7, 96 pages, Programme Initiative Pesticides, Laboratoire de Phytopharmacie de la Faculté universitaire des Sciences agronomiques de Gembloux. P-2. Année 2010.
4. Cissokho.M. K, Samba Laha KA, Ndongo DIOUF, Djibril DIOP, Jules DIOUF, Ghislain KANFANY, Moustapha GUEYE et Mame Samba

ISSN: 1857-7881 (Print)
e-ISSN 1857-7431 (Online)

MBAYE, titre : Caractérisation de la flore adventice du fonio (*Digitaria exilis* (Kippist Stapf.) : une céréale mineure cultivée dans les zones Sud et Sud-Est du Sénégal, Année,2025.

5. COLEACP, Manuel de formation, Production Agricole et Transformation, Fondements de la protection des cultures, 279 pages, P-2, P-7. Cette publication a été rédigée par Bruno Schiffers en collaboration avec Christine Moreira pour les chapitres 1 à 5, 2018.
6. Cruz.J.F. CIRAD. (Centre de coopération Internationale en Recherche Agronomique pour le Développement) Article. Titre : Le Fonio. (Aout 2001) 26.pages (pages 3-4)
7. FAO, (IFOAM)- Fédération Internationale des Mouvements d'Agriculture Biologique. Le paillage (ou mulching) en agriculture biologique, Philippines. Numéro identification 8559, année 2015. Journal de 4 pages, P-1-2
8. FAO. (La gestion des mauvaises herbes en agriculture biologique). Le numéro d'identification 8576. Année de publication 2016, 6 pages 2-6
9. FAO, Faostat 2019. « Production de fonio au Sénégal ». Organisation des Nations Unies pour l'alimentation et l'agriculture. 2019. http://www.fao.org/faostat
10. Gigou. J, D. Stilmant, T.A.Diallo, N.Cissé, M.D. Sanogo, M.Vaksmann et B.Dupuis. , Fonio Millet (*Digitaria Exilis*) Response to N, P and K fertilizers under varying climatic conditions in West Africa. (DOI: 10.1017/S0014479709990421), Aout 2009
11. Guide des adventices (H.Merlier & J.Montegut). 490p, ADVENTICES TROPICALES Flore aux stades plantule et adulte de 123 espèces africaines ou pantropicales. ORSTOM 1982.
12. Gueye M. (2016). « Amélioration des techniques de semis, de fertilisation et de récolte du fonio blanc (*Digitaria exilis* Stapf, Poacea) au Sénégal ». Thèse de doctorat en Biologie, Physiologie et Productions Végétales. Faculté des Sciences et Techniques, Université Cheikh Anta Diop de Dakar (Sénégal), 101 pages + annexes
13. Haq N., Dania Ogbe F., 1995. Fonio (Digitaria exilis and D. iburua). In: Cereals and Pseudocereals (J.T. Williams, éd.), Chapman and Hall, Londres, 225-245
14. Issoufou Ouédraogo, Inventaire et incidence des insectes inféodes à la culture du fonio (Digitaria exilis Stapf) dans la zone ouest du Burkina Faso. December, 2015, Journal of Applied Biosciences94(1):8880, DOI: 10.4314/jab.v94i1.11
15. Konkoba. Y ; Les pratiques alimentaires à Ouagadougou, Burkina Faso : céréales, légumineuses, tubercules et légumes, article publié en 2004

ISSN: 1857-7881 (Print)
e-ISSN 1857-7431 (Online)

16. Lebrun J, 1966. Les formes biologiques dans les végétations tropicales. Bulletin de la Société Botanique de France, 113, 164–175.
17. Noba K. 2002. Sénégal https://hdl.handle.net/20.500.12177/2965. Article publié en Mars 2002. La flore adventice dans le sud du Bassin arachidier (Sénégal) : Structure, dynamique et Impact sur la production du mil et de l'arachide. Thèse de Doctorat d'Etat. UCAD/FST. 137 p
18. Olugbenga oluseyi et Gilles Weidmann, Manuel de formation en agriculture biologique pour l'Afrique (Module 09 Gestion des cultures : Unité 5 Fonio) fiBL, GIZ. 15 pages, 2021 ; Éditeur : Institut de recherche de l'agriculture biologique FiBL, Suisse, www.fibl.org.
19. Raunkiaer C. (1934). The life forms of plants and statistical Plants Geography. Ed. Clarendron, Press, Oxford. 623 p.
20. Sarr, E. & Pro, J.C. (1985). Pénétration et développement des juvéniles d'une souche de Me1oidogiieja~~ariicaet d'une race B de Meloidogyrie iricogiiita dans les racines du fonio (Digitaria exilis Stapf).Rewe de Néiriatologie 8,5945
21. Vall É., Andrieu N., Beavogui F. & Sogodogo D., 2011. Les cultures de soudure comme stratégie de lutte contre l'insécurité alimentaire saisonnière en Afrique de l'Ouest : le cas du fonio (*Digitaria exilis* Stapf). *Cah. Agric*., 20(4), 294-300, doi.org/10.1684/agr.2011.0499

ESJ Natural/Life/Medical Sciences Peer-reviewed

Caractérisation des processus métallogéniques à l'origine des anomalies lithogéochimiques dans la région d'Ubundji, territoire d'Ubundu, RDC

Elukesu Mbula Dimitri
Université de Kisangani, Kisangani, RDC
Makabu Kayembe Gabriel
Université de Lubumbashi, Lubumbashi, RDC
Jamal Abbach
Université Abdelmalek Essaaadi, Maroc
Katembo Kasekete Désiré
Université Officielle de Ruwenzori, Butembo, RDC

Doi:10.19044/esj.2026.v22n6p158

Submitted: 22 January 2026
Accepted: 23 February 2026
Published: 28 February 2026

Cite As:
Elukesu, M.D., Makabu, K.G., Abbach, J. & Katembo, K.D. (2026). *Caractérisation des processus métallogéniques à l'origine des anomalies lithogéochimiques dans la région d'Ubundji, territoire d'Ubundu, RDC.* European Scientific Journal, ESJ, 22 (6), 158. https://doi.org/10.19044/esj.2026.v22n6p158

Résumé

Cette étude évalue l'apport des méthodes statistiques multivariées à la caractérisation des processus à l'origine des anomalies lithogéochimiques observées dans la région d'Ubundji à proximité de la rivière Maiko. Les objectifs ont consisté à la mise en evidence des contextes métallogéniques responsables des anomalies métalliques dans la région. Un total de 23 échantillons de roches prélevés sur le terrain a été analysé par fluorescence X (XRF) afin de déterminer les teneurs en Ta, Sn, Nb, Au, Ag, Cu, et Ni. La matrice de correlation révèlent des corrélations fortes à très fortes entre Sn–Nb–Ta, traduisant un contrôle magmatique felsique différencié, tandis que l'Au (plus ou moins l'Ag) montre une signature distincte, interprétée comme une empreinte hydrothermale. L'Analyse en composantes principales et le clustering K-means mettent en évidence trois groupes géochimiques correspondant respectivement à une signature magmatique, une signature hydrothermale aurifère et un fond géochimique régional. Ces corrélations témoigneraient d'un système hydrothermal polymétallique possiblement

ISSN: 1857-7881 (Print)
e-ISSN 1857-7431 (Online)

associé à des intrusions granitiques différenciées, ainsi qu'une association secondaire avec le Cu et le Ni. Ces résultats permettent d'enrichir la compréhension du contexte métallogénique de la zone étudiée à travers notamment la confirmation de la présence d'anomalie géochimique positive en or et renforcent l'idée que la région d'Ubundji a une configuration géologique particulière comparativement à la géologie régionale qui est marquée par des processus sédimentaires. Son exploration approfondie permettrait d'intégrer non seulement les données géochimiques, mais aussi pétrographiques, des analyses structurales et géophysiques afin de s'assurer de l'extension et la nature des zones minéralisées.

Mots-clés: Statistiques multivariées, processus métallogéniques, anomalies lithogéochimiques, Village Ubundji, République Démocratique du Congo

Characterisation of Metallogenic Processes Responsible for Lithogeochemical Anomalies in the Ubundji region, Ubundu Territory, DRC

Elukesu Mbula Dimitri
Université de Kisangani, Kisangani, RDC
Makabu Kayembe Gabriel
Université de Lubumbashi, Lubumbashi, RDC
Jamal Abbach
Université Abdelmalek Essaaadi, Maroc
Katembo Kasekete Désiré
Université Officielle de Ruwenzori, Butembo, RDC

Abstract

This study assesses the contribution of multivariate statistical methods to the characterization of the processes responsible for lithogeochemical anomalies observed in the Ubundji area, near the Maiko River. The objective was to identify the metallogenic contexts responsible for the metallic anomalies in the area. A total of 23 rock samples collected in the field were analyzed by X-ray fluorescence (XRF) to determine the concentrations of Ta, Sn, Nb, Au, Ag, Cu, and Ni. Statistical analyses reveal strong to very strong correlations among Sn–Nb–Ta, indicating control by differentiated felsic magmatism, whereas gold (± Ag) exhibits a distinct geochemical signature interpreted as reflecting a hydrothermal imprint. Principal component analysis (PCA) combined with K-means clustering highlights three geochemical groups corresponding respectively to a magmatic signature, a gold-bearing

ISSN: 1857-7881 (Print)
e-ISSN 1857-7431 (Online)

hydrothermal signature, and a regional geochemical background. These correlations suggest the presence of a polymetallic hydrothermal system potentially associated with differentiated granitic intrusions, with a secondary association involving Cu and Ni. The results contribute to a better understanding of the metallogenic framework of the study area, notably by confirming the presence of a positive gold geochemical anomaly, and support the interpretation that the Ubundji area displays a particular geological configuration compared to the surrounding region, which is largely dominated by sedimentary processes. Further exploration should therefore integrate not only geochemical data but also petrographic, structural, and geophysical analyses in order to better constrain the extent and nature of the mineralized zones.

Keywords: Lithogeochemical anomalies, metal associations, multivariate statistics, metallogenic processes, Ubundji Village, Democratic Republic of Congo

Introduction

Pour la majorité des campagnes d'exploration de territoires congolais où les connaissances géologiques sont peu développées, la géochimie exerce une influence déterminante sur la nature et l'orientation des travaux de prospection subséquents. M'hammed et al. (1991) montrent que la géochimie permet de mettre en évidence la répartition des éléments chimiques et leur comportement dans les roches lors des processus géologiques. Bellehumer (1992), montre que l'objectif des telles études est d'arriver à reconnaitre les phénomènes géologiques à l'origine des signaux géochimiques complexes et renseigner ainsi sur une existence probable d'un gisement. Dans son ouvrage *Using Geochemical Data: Evaluation, Presentation, Interpretation*, Rollinson (1993), insiste sur le fait que l'analyse multivariée doit être guidée par une hypothèse géologique claire, formulée à partir de données de terrain, de connaissances pétrographiques ou de contextes métallogéniques. Reimann et al. (2008**)** soulignent que l'usage de méthodes statistiques multivariées (comme l'ACP ou l'analyse factorielle) est peu fiable lorsque le nombre d'échantillons est inférieur à 30, sauf si le nombre de variables est également très réduit.

Dans la région d'Ubundje (province de la Tshopo, RDC), où les affleurements sont rares, les couches des sédiments sont épaisses et les connaissances géologiques restent limitées, il est difficile de comprendre les processus à l'origine des anomalies lithogéochimiques et de déterminer leur lien avec des zones potentiellement minéralisées.

Dans ce contexte , la présente étude apprécie dans quelles mesure les méthodes statistiques multivariées permettent-elles d'expliquer et

ISSN: 1857-7881 (Print)
e-ISSN 1857-7431 (Online)

d'interpréter les modèle métallogénique à l'origine des anomalies lithogéochimiques de Sn, Ta, Nb, Ag, Au, Cu et Ni analysées dans les roches à Ubundji, village situé dans la cuvette centrale, une région encore peu documentée sur le plan géologique en raison de la rareté des affleurements.
Les affleurements des roches observées à Ubundji, telles que des pegmatites, des granites, des diorites pourraient expliquer des processus géologiques favorables à une minéralisation polymétallique associée à un système de circulation des fluides chauds dans les roches (hydrothermalisme).
Cette étude a pour objectif de mettre en évidence les processus géologiques (modèle de mise en place) responsables des anomalies métalliques dans la région d'Ubundji (province de la Tshopo, RDC**).** Elle permet d'utiliser les données lithogéochimiques, de les analyser à l'aide des méthodes statistiques multivariées et d'interpréter les résultats afin de mettre en évidence les processus métallogéniques à l'origines des anomalies métalliques.

Matériels et Méthodes

Milieu d'étude

Situation géographique de la zone d'étude

La zone faisant l'objet de la présente étude (Figure1) est située en grande partie dans la province de la Tshopo (Territoire d'Ubundu, village Ubundji) et une partie se retrouve dans la province du Maniema (Figure 1).

ISSN: 1857-7881 (Print)
e-ISSN 1857-7431 (Online)

Carte de localisation de la zone d'étude

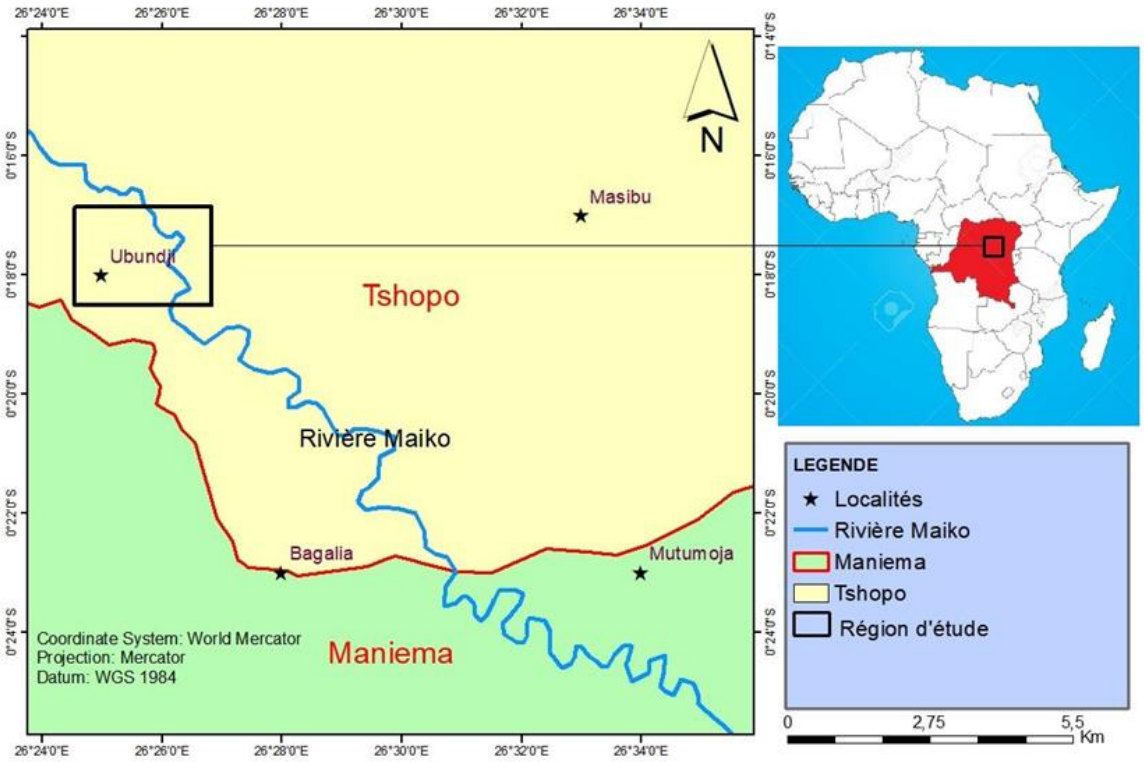

Figure 1: Carte géographique de la zone d'étude

Approche méthodologique

La démarche méthodologique adoptée combine la collecte et l'analyse de données géochimiques, l'utilisation de méthodes statistiques univariées et multivariées en vue de l'interprétation géologique.

Récolte des données

Les données de terrain ont été collectées dans le village d'Ubundji (Territoire d'Ubundu, province de la Tshopo, RDC), près de la rivière Maiko. Pour retrouver facilement les affleurements des roches, nous avons choisi l'itinéraire suivant : les lits des rivières, des vallées encaissées, des zones en hauteur comme des collines, ainsi que des sites d'exploitation artisanale où des creuseurs ont déjà ouvert des puits à la recherche de minéraux utiles. Un total de 23 échantillons de roches (granitoïdes altérés, roches basiques, roches métasédimentaires, roches volcaniques, roches altérées) ont été prélevés. Chaque échantillon, pesant environ 1 kg, a été collecté à l'aide d'un marteau géologique, puis emballé dans un sachet plastique étiqueté. Les coordonnées

ISSN: 1857-7881 (Print)
e-ISSN 1857-7431 (Online)

GPS, les observations sur la roche et son environnement ont été notées pour chaque prélèvement.

Analyses géochimiques des échantillons au laboratoire

Les vingt-trois échantillons de roches prélevés sur le terrain ont été analysés par Fluorescence des Rayons X (notée XRF) au laboratoire du CRGM-Kinshasa (Centre de recherche géologiques et minières de la RDC). La technique XRF repose sur l'excitation des atomes par un rayonnement X primaire, induisant l'émission d'un rayonnement secondaire caractéristique de chaque élément, permettant ainsi une détermination rapide et non destructive des concentrations élémentaires (Beckhoff et al., 2006). Les échantillons ont été préalablement broyés et pressés en pastilles pour garantir l'homogénéité et la précision des mesures. Les éléments métalliques analysés étaient : Cu, Sn, Ni, Ag, Ta, Nb et Au. Les données obtenues ont été compilées dans une matrice (échantillons × éléments) pour traitement.

Analyse des données

Statistique descriptive monovariable

Les travaux de Sinclair (1974) ont montré l'importance des outils de statistique descriptive pour détecter les anomalies dans les données géochimiques. Ainsi, pour chaque élément analysé, nous avons calculé:

- Moyenne, médiane, écart-type, min, max, coefficient de variation (CV),
- Distribution des fréquences (graphiques en histogrammes ou log-probabilité) selon Grunsky (2010)**,** la détection des anomalies suit deux approches :
- Si la distribution est normale , le seuil correspond à la moyenne à laquelle on ajoute deux écart-types (moyenne + 2σ)
- Lorsqu'une distribution est de type lognormale, on procède à une transformation logarithmique puis on le seuil est déterminé à partir de la courbe des fréquences cumulées.
- Une règle pratique (souvent utilisée en géochimie) consiste à comparer la différence entre la moyenne et deux écarts-types (M – 2σ) :
- Si la différence entre la moyenne et deux écart-types reste positive, cela indique que la distribution est normale probable (M – 2σ > 0)
- Si la différence entre la moyenne et deux écart-types est négative, la distribution est asymétrique c'est-à-dire on appliquera le log-transformation.(Si M – 2σ < 0).

Les caractéristiques d'enrichissement ou d'appauvrissement des éléments ont été évaluées par comparaison entre les teneurs moyennes des échantillons et les teneurs de référence crustale (Clarke values), selon la méthode décrite par Rollinson (1993). Un rapport M/Clarke>1 indique un

ISSN: 1857-7881 (Print)
e-ISSN 1857-7431 (Online)

enrichissement, tandis qu'un rapport M/Clarke<1 suggère un appauvrissement.

Statistique multivariable

Corrélation de Pearson

Les coefficients de corrélation de Pearson (r) ont été calculés pour évaluer les relations linéaires entre variables géochimiques**.** Selon Garrett (1983)**,** cette méthode est fiable si les données sont transformées ou standardisées, notamment dans les jeux à faible taille. Les corrélations permettent d'identifier des signatures géochimiques potentielles**,** à interpréter dans un cadre géologique. Dans cette étude un seuil de significativité a été fixé à 95 % afin de tester si les correlations observées different signgificativement de zero. Pour un effectif de 23 échantillons des roches, le degré de liberté égale à 21 et correspond à un coefficient de correlation critique $|r| \geq 0{,}413$. Ce seuil permet donc de déterminer si l'association entre deux éléments géochimiques est fiable du point de vue statistique. Cependant, la significativité ne renseigne pas sur l'intensité de la relation (une corrélation peut être significative mais modérée, ou très forte). Pour caractériser la force des corrélations,la valeur *f* sert d'intervalle de progression des classes. On part d'une valeur de référence $r_0 = 0.091$ (seuil minimal pris pour distinguer les corrélations très faibles) puis on ajoute des multiples de *f*. Dans notre cas la valeur de f a été fixé à 0,227 suivant l'approche proposée par Davis, (2002) ; Rodgers et Nicewander,(1988).

Tableau 1 : Classification des coefficients de corrélation de Pearson selon leur intensité, basée sur la valeur seuil r_0 et f (Davis (2002)

Intervalle	Type de correlation	Valeur de r
r0 à r0 + f	Faible	0,091<r≤0,318
r0 + f à r0+2f	Moyenne	0,318<r≤0,545
r0 + 2f à r0 + 3f	Forte	0,545<r≤0,772
r0 + 3f à r0 + 4f	Très forte	0,772<r≤1

Analyse Factorielle / ACP

Ménard (1991) souligne que l'analyse factorielle permet une réduction de dimension des données tout en mettant en évidence les groupes d'éléments co-variants. Les axes factoriels représentent des regroupements (facteurs) souvent liés à des processus métallogéniques.

Dans la présente étude, une analyse en composantes principales (ACP) a été appliquée à la matrice des données géochimiques préalablement standardisées (transformation en scores centrés-réduits) afin de neutraliser les effets d'échelle entre éléments présentant des concentrations contrastées. L'ACP repose sur la décomposition spectrale de la matrice de corrélation, permettant d'extraire des valeurs propres (valeurs propres) et des vecteurs propres (vecteurs propres). Ces valeurs propres indiquent la proportion de

ISSN: 1857-7881 (Print)
e-ISSN 1857-7431 (Online)

variance totale expliquée par chaque composante principale. Les axes retenus sont ceux présentant des valeurs propres supérieures à 1 (critère de Kaiser), car ils expliquent une part significative de la variance du système.Les charges factorielles (factor loadings) ont été examinées afin d'identifier les éléments et les axes factoriels ainsi obtenus correspondent à des regroupements géochimiques interprétables en termes de processus métallogéniques.

K-means clustering

D'après Carranza (2009), le K-means permet de regrouper les échantillons en clusters géochimiques homogènes. Cette technique est utile pour segmenter l'espace géologique selon des signatures multivariées, en complément de l'analyse factorielle. Le principe consiste à fixer au préalable un nombre de groupes (K), puis à regrouper automatiquement les échantillons présentant des compositions chimiques proches. Chaque cluster est représenté par un centre appelé centroïde, et chaque échantillon est affecté au groupe dont le centroïde est le plus proche, généralement selon la distance euclidienne. Le processus est répété de manière itérative jusqu'à stabilisation des groupes. Ainsi, les échantillons appartenant à un même cluster présentent des caractéristiques géochimiques homogènes, tandis que les clusters sont distincts les uns des autres, permettant d'identifier des domaines géochimiques différenciés.

Matériels et outils de traitement des données

Les matériels utilisés dans cette étude comprennent à la fois des équipements de terrain, de laboratoire et des outils de traitement des données. Les travaux de terrain ont été réalisés à l'aide d'outils géologiques classiques tels que le marteau de géologue, le mètre ruban, les fiches de description et le matériel de prélèvement pour la collecte des échantillons rocheux. Les échantillons ont ensuite été soumis à des analyses en laboratoire afin de déterminer leurs caractéristiques géochimiques. Le traitement et l'analyse des données ont été effectués à l'aide de logiciels spécialisés tels qu'ArcGIS pour la cartographie et l'analyse spatiale, Microsoft Excel pour l'organisation et le traitement préliminaire des données, ainsi que le logiciel R pour les analyses statistiques multivariées et la production des graphiques

Contexte Géologique

Le contexte géologique dans lequel se trouve le terrain d'étude est représenté par le Lindien (Néoprotérozoïque). Cette unité dans la zone est représentée par les unités Lokoma et l'Aruwimi. Le Lindien est composé des sédiments peu ou pas métamorphisés qui reposent sur le substratum cristallin. En l'absence de fossiles, la stratigraphie des formations est entièrement basée sur la lithologie. L'échelle lithostratigraphique comprend trois grandes unités

ISSN: 1857-7881 (Print)
e-ISSN 1857-7431 (Online)

qui sont de haut en bas : L'Aruwimi, le Lokoma et l'Ituri (Verbeek,1972). Celles-ci constituent les unités de base, caractérisées par une lithologie relativement homogène et susceptibles d'être cartographiées. Les limites des formations coïncident généralement avec des contacts lithologiques. Chaque faisceau comprend deux ou plusieurs formations, montrant une certaine parenté lithologique.. Le supergroupe de la Lindi est constitué principalement par les arkoses, grès, quartzites, shales et conglomérats (Verbeek,1970).

Les renseignements relatifs à cette région sont presqu'inexistants et en outre mal localisés. Henry (1923), qui l'a parcourue, y note à plusieurs endroits une discordance entre des grès, conglomérats et des calcaires. Ces roches appartiennent probablement les premières à l'Aruwimi et les secondes à la Lokoma. L'ensemble, qui repose sur le substratum cristallin affleurant localement, pourrait être plissé en une série de synclinaux et d'anticlinaux, dirigés E-W à NW-SE. Dans la fenêtre de Wanie-Rukula, Sluys (1967) a observé des blocs du substratum cristallin encadrés de failles et en contact avec les formations de la Lokoma.

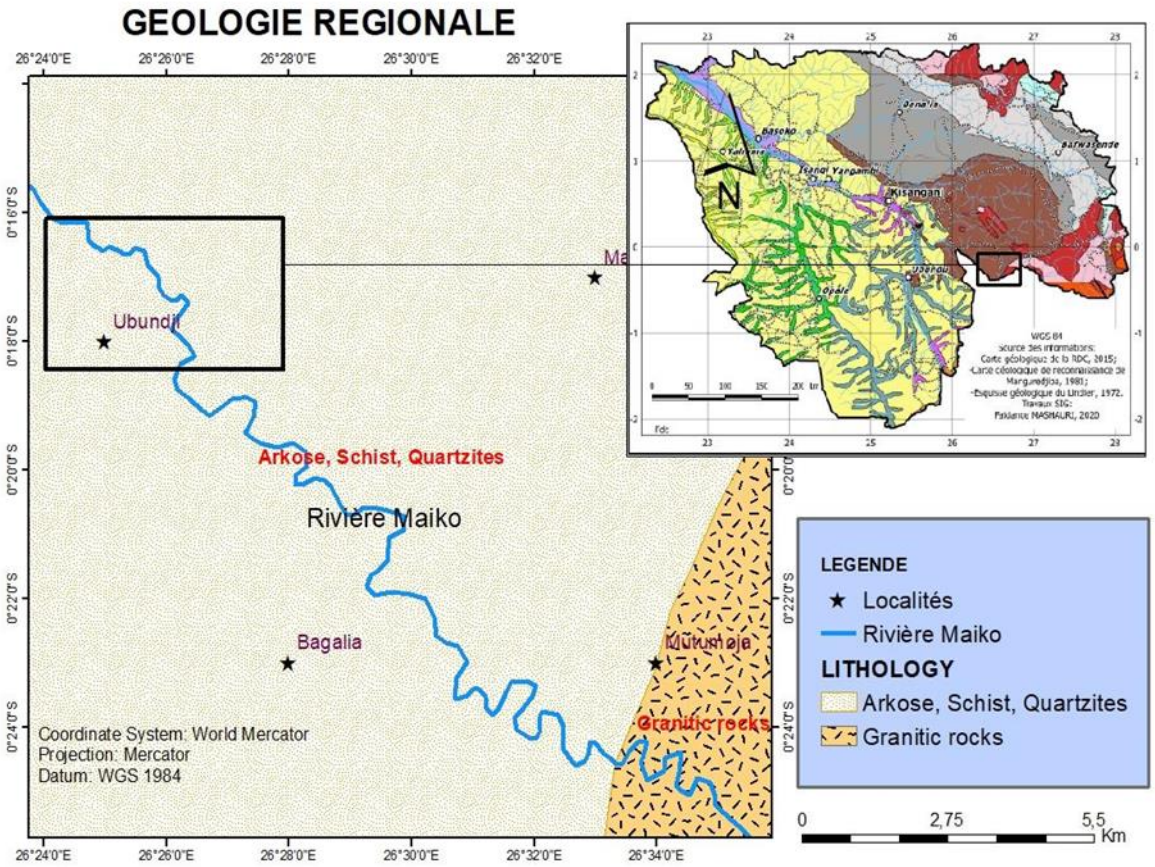

Figure 2 : Carte géologique de la région , extrait de la carte géologique de la RDC, *Fernandez-Alonso et al.,* 2015

ISSN: 1857-7881 (Print)
e-ISSN 1857-7431 (Online)

Resultats

Données géochimiques

Les données issues de l'analyse géochimique des roches sont présentées en annexe.

Résultats obtenus de la statistique descriptive

Paramètre statistique des éléments chimiques et Normalisation des teneurs

Le tableau 2 présente les paramètres statistiques des 7 éléments chimiques analysés dans la zone d'étude et le rapport de normalisation de la teneur moyenne par rapport au Clarke respectif de chaque élément.

Les moyennes de tous les éléments chimiques sont supérieures à leurs valeurs médianes. Ceci indique que la distribution des teneurs est asymétrique à droite.

Un seul élément, notamment l'or, montre un enrichissement dans les échantillons analysés.

Les autres éléments, à savoir : Sn, Ta, Nb, Cu, Ag et Ni présentent un appauvrissement.

Tableau 2: Paramètre statistique des éléments chimiques
(en ppm sauf pour le rapport M/Clarke)

Elem/stat	Min	Max	Moyenne (M)	Médiane	Écart-type	Clarke (Foucault & Raoult, 2010)	M/clarke
Cu	0,001	1,25	0,2793	0,04	0,0775	55	0,005
Sn	0,001	5	0,8915	0,04	0,2934	2	0,445
Ni	0,001	0,03	0,0071	0,003	0,00156	75	0,000094
Ag	0,001	0,33	0,0316	0,002	0,0196	0,1	0,316
Nb	0,001	4	0,6346	0,14	0,2379	20	0,032
Ta	0,001	1,11	0,2634	0,07	0,0844	2	0,132
Au	0,01	2,25	0,73	0,7	0,1193	0,005	146

Distribution des éléments chimiques

Le tableau 3 ci-après donne un aperçu sur les distributions de chaque élément chimique. Il indique que tous les éléments chimiques suivent une distribution lognormale.

Tableau 3 : Distribution des éléments chimiques

Élément	Moyenne(M)	Écart-type(S0)	M-2S0	Distribution
Cu	0,28	0,37	-0,46	lognormale
Sn	0,89	1,41	-1,93	lognormale
Ni	0,007	0,007	-0,007	lognormale
Ag	0,032	0,094	-0,156	lognormale
Nb	0,64	1,14	-1,64	lognormale
Ta	0,26	0,41	-0,56	lognormale
Au	0,73	0,57	-0,41	lognormale

ISSN: 1857-7881 (Print)
e-ISSN 1857-7431 (Online)

Détermination du seuil d'anomalie pour les éléments

Le seuil d'anomalie pour les éléments qui suivent une distribution lognormale est déterminé par la courbe des fréquences cumulées (Graphe a). Ce graphe montre la courbe de fréquence cumulée ou courbe de répartition empirique de l'élément chimique Au.

Le seuil d'anomalie est ici déterminé par la valeur de l'abscisse x correspondant au quartile 75%. Le seuil d'anomalie de l'élément Au est donc la valeur 1,035 g/Tonne.

Le tableau 4 présente les résultats de calcul du seuil d'anomalie pour tous les éléments (Au, Sn, Ta, Nb, Cu, Ag et Ni.)

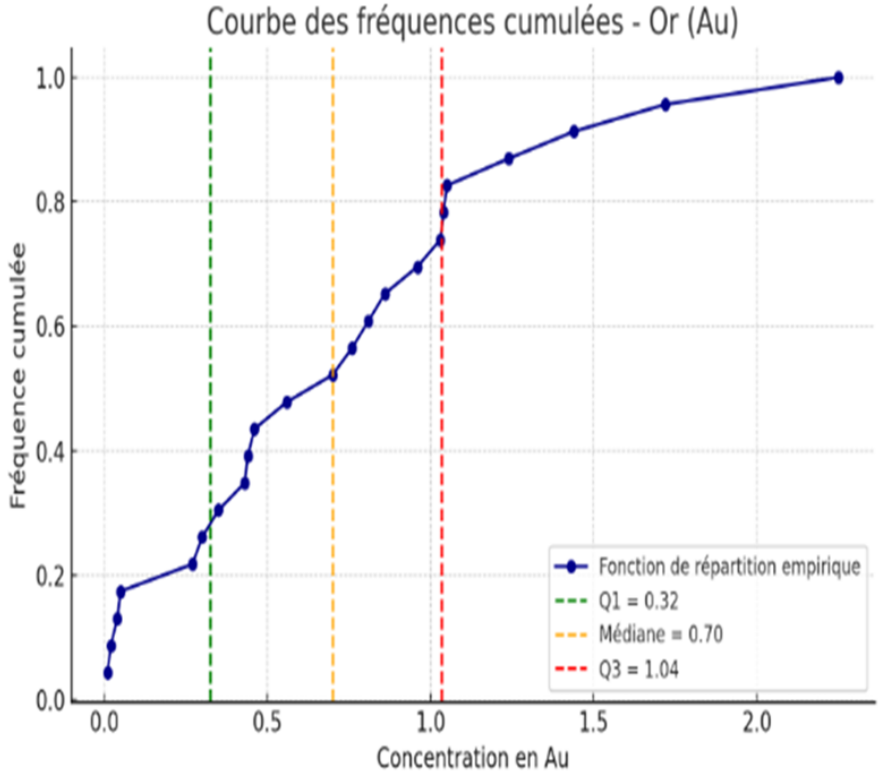

Graphe A : Courbe de répartition empirique de l'or

Tableau 4 : Seuils d'anomalie
(calculés à partir du 3e quartile, Q3) pour chacun des éléments

Élément	Q1 (25%)	Médiane (Q2)	Q3 (75%)	Seuil d'anomalie (≥ Q3)
Cu	0,015	0,040	0,435	0,435
Sn	0,020	0,040	1,010	1,010
Ni	0,002	0,003	0,010	0,010
Ag	0,001	0,002	0,007	0,007
Nb	0,040	0,140	0,360	0,360
Ta	0,025	0,070	0,155	0,155
Au	0,325	0,700	1,035	1,035

ISSN: 1857-7881 (Print)
e-ISSN 1857-7431 (Online)

Résultat de la statistique multivariable

Coefficient de corrélation de Pearson

La matrice de corrélation (Figure 3) , met en évidence une association très forte entre Sn, Nb et Ta (r > 0,88), traduisant un contrôle magmatique felsique différencié. L'or présente des corrélations modérées avec ces éléments, suggérant une origine composite impliquant une remobilisation hydrothermale. Le Cu et Ni montrent des relations plus faibles avec le groupe Sn–Nb–Ta, indiquant une signature géochimique indépendante, probablement liée à des influences lithologiques distinctes. Ces relations confirment la superposition de processus magmatiques et hydrothermaux dans la genèse des anomalies géochimiques étudiées.

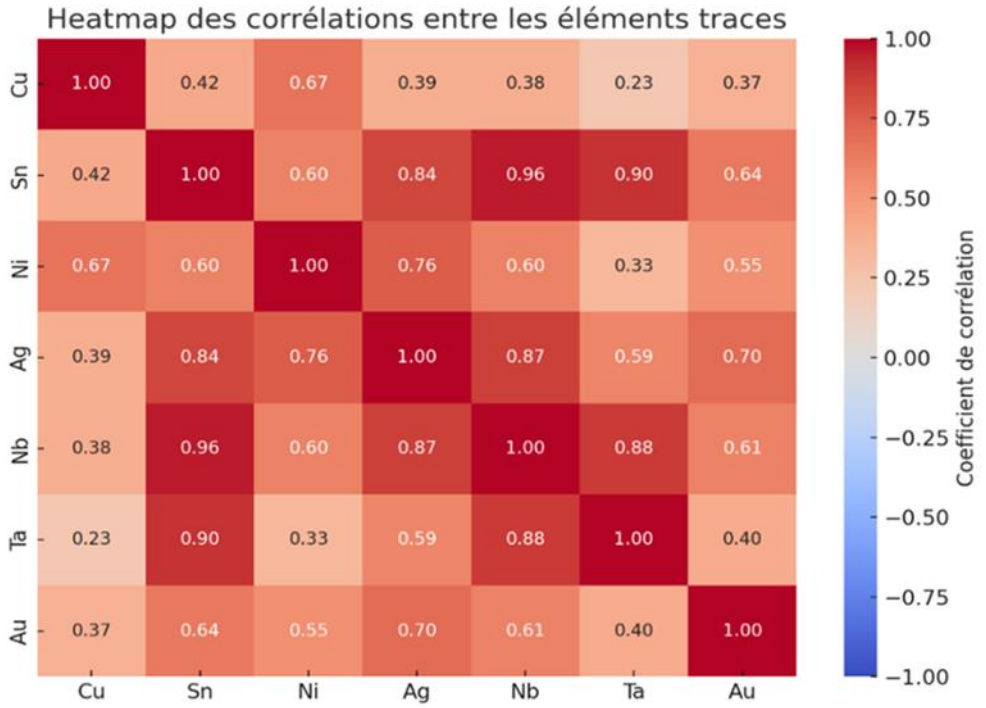

Figure 3 : Carte thermique des coefficients de corrélation de Pearson entre Cu, Sn, Ni, Ag, Nb, Ta, Au), Reimann, C. et al.. (2008)

La corrélation entre les axes factoriels (ACP) et les éléments chimiques

L'Analyse en composantes principales (Figure 4), met en évidence deux axes majeurs contrôlant la variabilité géochimique. L'axe F1, dominé par Sn, Nb et Ta, traduit un processus magmatique felsique différencié, tandis que l'axe F2, dominé par Au ± Ag, reflète une empreinte hydrothermale distincte. La projection des échantillons révèle trois groupes correspondant respectivement à une signature magmatique, une signature hydrothermale et au fond géochimique régional. Ces résultats confirment la superposition de

ISSN: 1857-7881 (Print)
e-ISSN 1857-7431 (Online)

processus magmatiques et hydrothermaux dans la genèse des anomalies géochimiques étudiées.

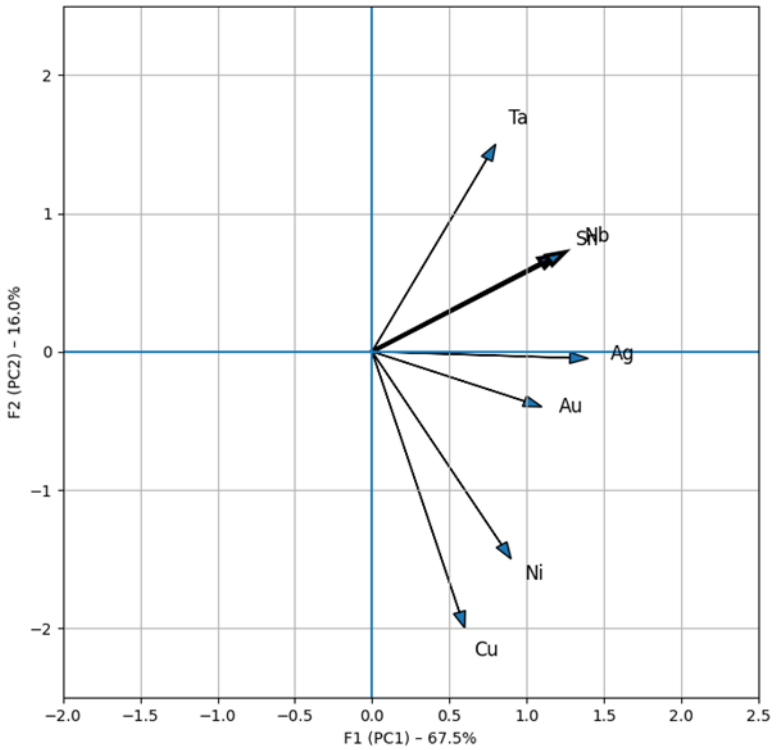

Figure 4 : ACP Biplot F1 et F2

Tableau 5 : Valeur de corrélation entre les axes factoriels

Élément	Corrélation F1	Corrélation F2
Cu	+0.258	**−0.628**
Sn	**+0.439**	+0.234
Ni	+0.356	−0.480
Ag	**+0.421**	−0.022
Nb	**+0.436**	+0.244
Ta	+0.360	**+0.493**
Au	+0.342	−0.130

Regroupements géochimiques issus du K-means

Le regroupement des échantillons par la méthode K-means a permis de mettre en évidence trois clusters géochimiques distincts. Le premier cluster est caractérisé par des teneurs élevées en Sn, Nb et Ta, traduisant un contrôle magmatique felsique différencié (échantillons DBOBU4, MASUD2, DMABA20, DKANG31, DMASUD22, DMAL5, DMABA7, DMABA8, DTCH014, DKANG3 et DTCHO13). Le second cluster est dominé par l'or (± Ag) et reflète une empreinte hydrothermale responsable de la redistribution de l'or (échantillons DISEMB21, DAMBK15, DTCHO12 et DAMBK1) . Le

ISSN: 1857-7881 (Print)
e-ISSN 1857-7431 (Online)

troisième cluster correspond au fond géochimique régional, peu affecté par les processus métallogéniques (DBAS2, DMANG9, DKANG10, DKANG11, DBASH23, DMAIK16, DSW17 et DMABA6) . La cohérence entre les résultats du K-means, de l'ACP et de la matrice de corrélation confirme la superposition de processus magmatiques et hydrothermaux dans la zone étudiée.

Carte conceptuelle (Processus , regroupement géochimique et géologie)

Cette approche intégrée démontre l'apport fondamental des méthodes statistiques multivariées dans la compréhension des processus géologiques à l'origine des anomalies lithogéochimiques, au-delà de toute simple évaluation de potentiel minier.

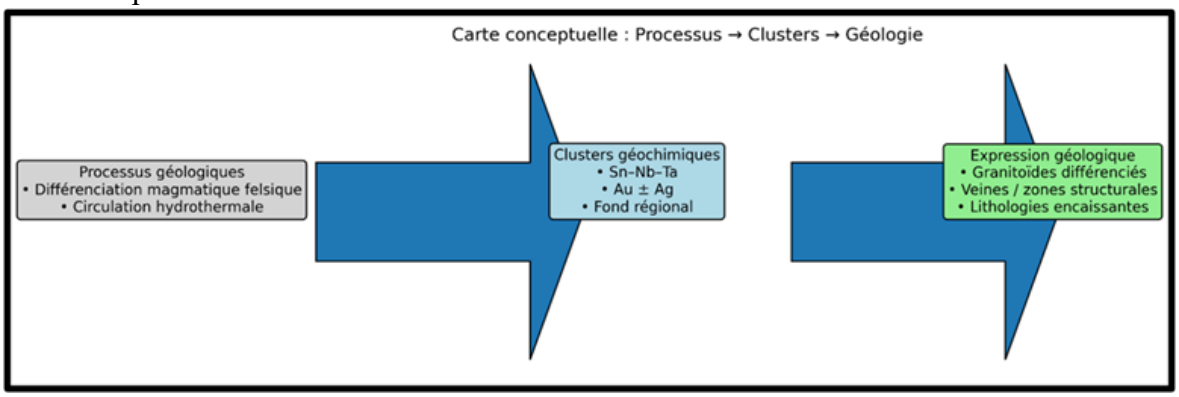

Figure 5 : Carte conceptuelle de processus géologique, regroupement géochimique et géologie

Discussion des résultats

Les résultats obtenus par les méthodes statistiques multivariées appliquées aux données géochimiques mettent en évidence une structuration claire des teneurs en éléments métalliques dans la région d'étude, révélant des signatures minéralogiques potentiellement liées à des systèmes hydrothermaux riches en métaux précieux et critiques.

Distributions et anomalies géochimiques

Les analyses monovariables ont montré que tous les éléments étudiés suivent une distribution lognormale, ce qui est courant dans les milieux géochimiques naturels en contexte minier (Ahrens, 1954 ; Reimann & Filzmoser, 2000 ; Davis, 2002).

L'or (Au), dont la moyenne est largement supérieure à son Clarke (M/Clarke = 146), indique un fort enrichissement dans les roches locales, suggérant une source minéralisée non négligeable. Lavreau, J. (1984) dans son étude intitulée : le géosynclinal de l'Ituri (NE-Zaïre) et son évolution géodynamique, met en évidence des enrichissements très importants en or

ISSN: 1857-7881 (Print)
e-ISSN 1857-7431 (Online)

dans les formations du Kibalien, avec des rapports M/Clarke supérieurs à 100 dans certaines zones aurifères. Des enrichissements aurifères très élevés ont également été rapportés dans plusieurs provinces précambriennes africaines, notamment dans des ceintures de roches vertes, où ils sont associés à des circulations hydrothermales structurées (Milesi et al., 1992 ; Pirajno, 2009)

Corrélations géochimiques

La matrice de corrélation de Pearson montre des associations très fortes entre Sn–Nb, Sn–Ta, Nb–Ta, Sn–Ag et Ag–Nb. Les résultats rejoignent les observations rapportées dans la littérature. Ainsi, plusieurs travaux décrivent l'association Sn–Nb–Ta dans les pegmatites et les granites différenciés (Černý, 1991 ; London, 2008 ; Pollard, 1989). L'intégration de l'argent (Ag) dans ces corrélations a également été signalée dans des systèmes hydrothermaux polymétalliques (Pirajno, 2009 ; Heinrich, 2005), et confirmée dans différents contextes africains, notamment au Kibalien en RDC (Lavreau, 1984) et en Afrique de l'Ouest (Milesi et al., 1992).

Clemens et al. (2018) ont quant à eux démontré que les minéralisations de type Sn–Nb–Ta peuvent être mises en évidence par des signatures géochimiques multivariées dans les granites tardi-tectoniques, ce qui renforce notre hypothèse d'un contexte granitique différencié dans la zone d'étude.

Par ailleurs, les corrélations mises en évidence entre l'or et l'argent ($r = 0,701$), ainsi qu'entre l'or et l'étain ($r = 0,642$), traduisent des associations géochimiques significatives. L'association Au–Ag est largement documentée dans les systèmes hydrothermaux polymétalliques, où ces deux métaux précipitent fréquemment ensemble en raison de leur affinité commune pour les sulfures et les solutions hydrothermales sulfurées. Heinrich (2005) et Pirajno (2009) soulignent que l'or et l'argent se concentrent souvent conjointement dans les fluides magmato-hydrothermaux liés aux intrusions granitiques différenciées. Dans le contexte africain, Lavreau (1984) a également observé cette association au sein des formations du Kibalien en RDC, et Milesi et al. (1992) l'ont rapportée dans plusieurs ceintures de roches vertes aurifères d'Afrique de l'Ouest.

L'association étroite Sn–Nb–Ta observée dans les données multivariées est typique des systèmes felsiques différenciés bien documentés dans les provinces kibariennes, où ces éléments incompatibles se concentrent dans les phases tardives des magmas granitiques et dans les systèmes pegmatitiques associés. L'organisation géochimique observée à Ubundji suggère ainsi un modèle composite, combinant un héritage magmatique felsique différencié et une redistribution hydrothermale ultérieure, dans un contexte géologique dominé par des formations sédimentaires.. (Cahen et al., 1984 ; Pohl, 1994 ; Černý, 1991 ; Tack et al., 2010).

ISSN: 1857-7881 (Print)
e-ISSN 1857-7431 (Online)

Analyse factorielle et clustering géochimique

L'analyse en composantes principales met clairement en évidence deux tendances majeures. Le premier facteur (F1), fortement contrôlé par l'étain, le niobium, le tantale, l'argent et l'or, illustre la signature métallogénique dominante de la zone. Ce regroupement d'éléments est caractéristique des environnements où interviennent des apports magmatiques différenciés, favorisant la mise en place de minéralisations filoniennes polymétalliques.

Le second facteur (F2) traduit une opposition marquée entre le cuivre et les autres éléments. Cette relation suggère que le cuivre ne partage pas le même comportement que les métaux associés au F1, ce qui peut indiquer soit des épisodes de minéralisation distincts, soit des compartiments lithologiques et structuraux différents.

Conclusion

Cette étude lithogéochimique menée dans la région d'Ubundji, au voisinage de la rivière Maiko, a permis de mettre en évidence une structuration géochimique nette des éléments métalliques analysés, révélant des signatures cohérentes avec la superposition de plusieurs processus géologiques et métallogéniques. Les distributions asymétriques des teneurs, les corrélations inter-élémentaires et les résultats des analyses statistiques multivariées témoignent d'un système géochimique non homogène, contrôlé à la fois par un héritage magmatique felsique différencié et par des processus hydrothermaux ultérieurs.

L'association étroite Sn–Nb–Ta, clairement identifiée par la matrice de corrélation, l'analyse en composantes principales et le clustering, constitue un marqueur robuste de différenciation magmatique avancée, typique des environnements granitiques et pegmatitiques enrichis en éléments incompatibles. Cette signature suggère l'intervention de magmas felsiques évolués, dont les phases tardives ont favorisé la concentration de ces éléments dans les roches encaissantes. Par ailleurs, le comportement distinct de l'or, souvent associé à l'argent mais partiellement dissocié du groupe Sn–Nb–Ta, indique une redistribution secondaire contrôlée par des fluides hydrothermaux, probablement canalisés par des structures favorables à la circulation des fluides.

La mise en évidence de trois groupes géochimiques bien individualisés souligne la complexité du système étudié et confirme que les anomalies lithogéochimiques observées ne résultent pas d'un processus unique. Cette organisation spatiale et géochimique reflète un modèle composite dans lequel des apports magmatiques différenciés sont partiellement remobilisés et reconfigurés par des épisodes hydrothermaux postérieurs.

ISSN: 1857-7881 (Print)
e-ISSN 1857-7431 (Online)

Au-delà des résultats locaux, cette étude met en évidence l'apport fondamental des méthodes statistiques multivariées comme outils d'aide à la compréhension des processus géologiques complexes, en particulier dans les régions à faible densité d'affleurements. L'intégration de la géochimie des roches avec les approches statistiques et l'interprétation géologique constitue ainsi une démarche pertinente pour décrypter l'origine et l'évolution des anomalies métalliques. Les travaux futurs gagneraient à intégrer des données pétrographiques détaillées, des analyses structurales et des investigations géophysiques afin de mieux contraindre la géométrie, la chronologie et les mécanismes de mise en place des systèmes minéralisés reconnus dans la région d'Ubundji.

Conflit d'intérêts : Les auteurs n'ont signalé aucun conflit d'intérêts.

Disponibilité des données : Toutes les données sont incluses dans le contenu de l'article.

Déclaration de financement : Les auteurs n'ont obtenu aucun financement pour cette recherche.

References:

1. Ahrens, L. H. (1954). The lognormal distribution of the elements: A fundamental law of geochemistry and its subsidiary. Geochimica et Cosmochimica Acta, 5(2), 49–73. https://doi.org/10.1016/0016-7037(54)90038-2
2. Beckhoff, B., Kanngießer, B., Langhoff, N., Wedell, R., & Wolff, H. (Eds.). (2006). Handbook of practical X-ray fluorescence analysis. Springer.895p
3. Bonham-Carter, G. F. (1994). Geographic information systems for geoscientists: Modelling with GIS. Pergamon Press.398p
4. Cahen, L., Snelling, N. J., Delhal, J., & Vail, J. R. (1984). The geochronology and evolution of Africa. Oxford University Press.
5. Carranza, E. J. M. (2009). Geochemical anomaly and mineral prospectivity mapping in GIS. Elsevier.364p
6. Černý, P. (1991). Rare-element granitic pegmatites. Part I: Anatomy and internal evolution of pegmatite deposits. Geoscience Canada, 18(2), 49–67.
7. Clemens, J. D., Petford, N., & Mawer, C. K. (2018). Rare-metal mineralization in evolved granites: A geochemical approach to targeting Sn–Nb–Ta systems. Ore Geology Reviews, 95, 105–124.
8. Davis, J.C. (2002). Statistics and Data Analysis in Geology, 3rd ed. John Wiley & Sons, New York.612p.

ISSN: 1857-7881 (Print)
e-ISSN 1857-7431 (Online)

9. Garrett, R. G. (1983). The robust multivariate statistical analysis of geochemical data. Journal of Geochemical Exploration, 20(1), 183–198.
10. Fernández-Alonso, M., Kampata, D., Mupande, I.-F., Dewaele, S.,Lagmouc.(2017).Carte géologique de la République Démocratique du Congo à l'échelle 1/2 500 000.Royal Museum for Central Africa (RMCA), Tervuren, Belgique. ISBN: 978-9-4922-4480-2.
11. Foucault, A., & Raoult, J.-F. (2010).Dictionnaire de géologie (8e éd.). Dunod.416p
12. Govindaraju, K. (1994). Compilation of working values and sample description for 383 geostandards. Geostandards Newsletter 18(S1), 1–158.
13. Grunsky, E. C. (2010). The interpretation of geochemical survey data. Geochemistry: Exploration, Environment, Analysis, 10(1), 27–74.
14. Heinrich, C. A. (2005). The physical and chemical evolution of low-salinity magmatic fluids in porphyry environments. Economic Geology, 100(5), 1061–1081.
15. Lavreau, J. (1984). Le Kibalien du Nord-Est du Zaïre : géologie et métallogénie aurifère. Bulletin du Musée Royal de l'Afrique Centrale, Sciences de la Terre.
16. Levinson, A.A. (1974). Introduction to Exploration Geochemistry. Applied Publishing Ltd., Calgary.1965p.
17. Ménard, J.-J. (1991). Statistique multivariée appliquée à la géologie. Éditions Technip, Paris.
18. Milesi, J. P., Ledru, P., Feybesse, J. L., Dommanget, A., & Marcoux, E. (1992). Early Proterozoic ore deposits and tectonics of the Birimian orogenic belt, West Africa. Precambrian Research, 58, 305–344.
19. Pirajno, F. (2009). Hydrothermal Processes and Mineral Systems. Springer, Berlin–Heidelberg.1250p.
20. Pohl, W. (1994). Metallogeny of the Central African Kibaran Belt. Schweizerische Mineralogische and Petrographische Mitteilungen 74, 415–432.
21. Pollard, P.J. (1989). Geochemistry of granites associated with tin and tungsten mineralization. In: Whitney, J.A., Naldrett, A.J. (Eds.), Ore Deposit Models, Vol. 1, Geoscience Canada Reprint Series, pp. 174–207.
22. Reimann, C., Filzmoser, P., Garrett, R. G., & Dutter, R. (2008). Statistical data analysis explained: Applied environmental statistics with R. Wiley-VCH.343p.
23. Rodgers, J.L. & Nicewander, W.A. (1988). Thirteen ways to look at the correlation coefficient. The American Statistician 42(1), 59–66.

ISSN: 1857-7881 (Print)
e-ISSN 1857-7431 (Online)

24. Rollinson, H.R. (1993). Using Geochemical Data: Evaluation, Presentation, Interpretation. Longman Scientific & Technical, London.261p.
25. Sinclair, A.J. (1974). Selection of threshold values in geochemical data using probability graphs. Journal of Geochemical Exploration 3(2), 129–149.
26. Sluys, M. (1967). La fenêtre tectonique de Wanie-Rukula et ses implications géologiques. Bulletin de la Société belge de Géologie, de Paléontologie et d'Hydrologie 75(2), 221–242.
27. Tack, L., Wingate, M.T.D., Liégeois, J.-P., Fernandez-Alonso, M. & Deblond, A. (2010). The Kibaran belt of Central Africa: A Proterozoic accretionary belt. Precambrian Research 180, 63–91.
28. Verbeek, T. (1970). Géologie et lithologie du Lindien (Précambrien supérieur du nord du Zaïre). Annales du Musée Royal de l'Afrique Centrale, Sciences géologiques, n°66, 311 p.
29. Verbeek, T. (1972). Carte géologique de la République du Zaïre au 1:2 000 000 et notice explicative. Musée Royal de l'Afrique Centrale, Tervuren.

ISSN: 1857-7881 (Print)
e-ISSN 1857-7431 (Online)

Appendix

Tableau: Données géochimiques (ppm)

N°Echant	Cu	Sn	Ni	Ag	Nb	Ta	Au
1	0,02	0,04	0,01	0,008	0,02	0,01	0,76
2	0,002	0,001	0,008	0,002	0,04	0,02	0,01
3	0,04	1	0,002	0,01	0,06	0,03	1,05
4	0,43	5	0,02	0,33	4	1,11	2,25
5	1,25	1,02	0,01	0,01	0,46	0,2	0,86
6	0,21	0,002	0,001	0,002	0,024	0,09	0,35
7	0,75	0,77	0,01	0,007	0,24	0,11	0,96
8	0,78	0,7	0,02	0,006	0,24	0,11	1,03
9	0,04	0,01	0,008	0,002	0,001	0,001	0,04
10	0,001	0,001	0,001	0,001	0,01	0,008	0,02
11	0,26	0,04	0,008	0,001	0,26	0,1	0,05
12	0,14	0,03	0,002	0,001	0,07	0,03	0,81
13	0,04	0,08	0,008	0,003	0,14	0,03	1,24
14	0,74	0,7	0,01	0,006	0,23	0,07	0,46
15	0,18	0,04	0,001	0,001	0,06	0,04	1,04
16	0,01	0,001	0,001	0,001	0,21	0,08	0,3
17	0,01	0,02	0,003	0,001	0,14	0,06	0,27
18	0,44	2,26	0,003	0,001	2,46	1	0,56
19	0,01	0,04	0,001	0,001	0,04	0,02	1,44
20	0,03	2,24	0,002	0,001	1,14	1,03	0,43
21	0,01	0,02	0,003	0,001	0,04	0,01	0,44
22	0,03	2,24	0,002	0,001	1,15	0,96	0,7
23	1	4,25	0,03	0,33	3,56	0,94	1,72

ESJ Natural/Life/Medical Sciences Peer-reviewed

Évaluation du niveau de connaissances et d'exposition aux risques sanitaires de la cysticercose porcine dans la commune d'Oti Sud 1 au Togo en 2023

Binamlé Bagna
Station de Kolokopé, Centre de Recherche Agronomique de la Savane Humide, Institut Togolais de Recherche Agronomique (ITRA/CRASH), Togo
Matéyendou Lamboni
Département de Santé Animale et Production Halieutique, Institut Supérieur des Métiers de l'Agriculture de l'Université de Kara (ISMA/UK), Togo
Secrétariat Général du Ministère des Ressources Halieutiques, Animales et de la Règlementation de la Transhumance (SG MRHART), Togo
Ali Kpatcha Kadanga
Département de Santé Animale et Production Halieutique, Institut Supérieur des Métiers de l'Agriculture de l'Université de Kara (ISMA/UK), Togo

Doi:10.19044/esj.2026.v22n6p178

Submitted: 26 August 2025
Accepted: 18 February 2026
Published: 28 February 2026

Cite As:
Bagna, B., Lamboni, M. & Kadanga, A.K. (2026). *Évaluation du niveau de connaissances et d'exposition aux risques sanitaires de la cysticercose porcine dans la commune d'Oti Sud 1 au Togo en 2023.* European Scientific Journal, ESJ, 22 (6), 178.
https://doi.org/10.19044/esj.2026.v22n6p178

Résumé

La cysticercose est une zoonose parasitaire classée parmi les maladies tropicales négligées, liée à la consommation de viande de porc crue ou insuffisamment cuite. Une étude transversale à visée descriptive à travers une enquête pour évaluer le niveau de connaissance de la cysticercose porcine au sein de la population de la commune d'Oti Sud 1, au Togo, en 2023 a été menée. Un total de 249 acteurs de la filière porcine (éleveurs-commerçants, charcutiers et consommateurs), sélectionnés à partir de listes officielles et par échantillonnage aléatoire a été enquté. Les résultats révèlent que 78,71% des enquêtés sont des hommes. Parmi eux, 70,28% sont des éleveurs-commerçants, 4,41% des charcutiers et 89,15% des consommateurs de viande porcine. Un taux élevé de précarité en matière d'assainissement a été observé, avec 54,62% des répondants ne disposant pas de latrines. L'élevage est

ISSN: 1857-7881 (Print)
e-ISSN 1857-7431 (Online)

majoritairement traditionnel (97,14%), sans enclos (85,71%), sans déparasitage (97,71%) et basé sur une alimentation non contrôlée. La divagation des porcs en saison sèche concerne 97,14% des cas. Bien que 92,77% des participants déclarent connaître la cysticercose porcine, 99,57% en ignorent la cause. De même, si 100% des répondants connaissent l'épilepsie humaine, 97,99% n'en connaissent pas le lien avec la cysticercose. Ce contexte traduit une forte vulnérabilité à la transmission de la maladie. Il apparaît nécessaire de renforcer les actions de sensibilisation, d'améliorer les pratiques d'élevage et de consolider le contrôle vétérinaire dans la commune d'Oti Sud 1 pour une lutte efficace contre cette zoonose.

Mots-clés: Cysticercose porcine, élevage, connaissances, viande de porc, Togo

Assessment of the Level of Knowledge and Exposure to Health Risks of Porcine Cysticercosis in the Commune of Oti Sud 1 in Togo in 2023

Binamlé Bagna
Station de Kolokopé, Centre de Recherche Agronomique de la Savane Humide, Institut Togolais de Recherche Agronomique (ITRA/CRASH), Togo
Matéyendou Lamboni
Département de Santé Animale et Production Halieutique, Institut Supérieur des Métiers de l'Agriculture de l'Université de Kara (ISMA/UK), Togo
Secrétariat Général du Ministère des Ressources Halieutiques, Animales et de la Règlementation de la Transhumance (SG MRHART), Togo
Ali Kpatcha Kadanga
Département de Santé Animale et Production Halieutique, Institut Supérieur des Métiers de l'Agriculture de l'Université de Kara (ISMA/UK), Togo

Abstract

Cysticercosis is a parasitic zoonosis classified as a neglected tropical disease, linked to the consumption of raw or undercooked pork. A descriptive cross-sectional study using a survey to assess the level of knowledge about porcine cysticercosis among the population of the Oti Sud 1 commune in Togo in 2023 was conducted. A total of 249 stakeholders in the pork sector (farmers, traders, butchers, and consumers), selected from official lists and through random sampling, were surveyed. Among the respondents, 78.71% were men. Of the participants, 70.28% were pig farmer-traders, 4.41% were butchers, and 89.15% were pork consumers. Poor sanitation was evident, with 54.62%

ISSN: 1857-7881 (Print)
e-ISSN 1857-7431 (Online)

lacking access to latrines. Traditional pig farming was predominant (97.14%), with most respondents lacking pig enclosures (85.71%), deworming practices (97.71%), and relying on unregulated feed sources. Seasonal roaming of pigs during the dry season was reported by 97.14%. While 92.77% of participants claimed to know about porcine cysticercosis, 99.57% were unaware of its actual cause. Similarly, although 100% recognized epilepsy in humans, 97.99% did not understand its link to cysticercosis. These findings highlight a context highly conducive to the transmission of the disease. Strengthening community awareness, improving husbandry practices, and enforcing veterinary meat inspections are essential to combat this zoonotic threat effectively in Oti Sud 1.

Keywords: Porcine cysticercosis, husbandry, knowledge, pork meat, Togo

Introduction

La cysticercose à *Taenia solium,* une des maladies parasitaires du porcs transmissible à l'homme à partir de l'ingestion des viandes souillées non inspectées est très répandue chez les porcs et les humains (Mopoundza et al., 2019). En effet, la cysticercose porcine, associée au téniasis humain, forme un complexe parasitaire endémique dont plusieurs foyers ont été identifiés dans plusieurs pays tropicaux (Sciutto et al., 2000).Les porcs acquièrent la cysticercose en ingérant les œufs de *T. solium* contenus dans les fèces du porteur de *Tænia* tandis que chez l'homme, la maladie est due essentiellement à l'ingestion d'eau ou d'aliments contaminés par les œufs de *T. solium*, et parfois lors de l'ingestion accidentelle d'œufs de *Tænia* par auto-infestation (Bouteille, 2014 ; N'Dri, 2023). La cysticercose porcine est très répandue en raison du manque de logements adéquats pour les porcs, aux porcs errants dans les zones rurales et aux mauvaises conditions d'élevage et d'hygiène fécale (Costard et al., 2009). Cette zoonose constitue la principale cause d'épilepsie en Afrique et occasionne des lourdes pertes économiques de l'élevage des porcs (Porphyre et al., 2015). Cette maladie fait l'objet des saisies dans les abattoirs de porcs à Ouagadougou au Burkina Faso (Dahourou et al., 2018). Considérée comme une des zoonoses majeures endémiques négligées à travers le monde, elle représente un fardeau considérable pour la santé publique, affectant plus de 50 millions de personnes dans le monde (OMS, 2011) et entraîne plus de 50 000 décès chaque année (Murrell et al., 2005).

Hormis les régions où l´élevage et surtout la consommation du porc constituent un tabou, la cysticercose porcine affecte probablement tous les pays d´Afrique (Quet et al., 2010). En Afrique occidentale, les prévalences sont de 11,7% au Ghana 8,41% au Benin ,0,6% au Burkina-Faso et de 17% au Togo (Zoli et al., 2003).

ISSN: 1857-7881 (Print)
e-ISSN 1857-7431 (Online)

Au Togo les préparations dérivées de la viande de porc, sont très recherchées et appréciées par les communautés qui les consomment dans les charcuteries ou à l'occasion des fêtes et différentes cérémonies. La probabilité que ce type de viande soit contaminée par différents parasites dont le *T. solium* dans les autres régions du pays, encore très rurales, n'est pas négligeable (Dorny et al., 2004 ; Mariska et al., 2008). Dans une étude sur les raisons d'échec du traitement antiépileptique aux Centres Hospitaliers Universiaires (CHU) au Togo, il a été reçu en consultation neurologique externe (3 410 patients dont 1 920 au CHU Campus, 1 010 au CHU SO et 480 au CHU Kara) entre le 1er janvier et le 31 mas 2014). Il est ressorti un total de 310 patients épileptiques soit une fréquence de 9,1% (Anayo et al., 2023).

Ainsi, il est question de savoir si les acteurs de la filière porcine de la commune de l'oi sud 1 connaissent-ils les risques sanitaires liés à la cysticercose porcine? C'est pour apporter une contribution à la lutte contre cette zoonose et proposer des mesures de lutte que cette étude a été initiée pour évaluer le niveau de connaissance des risques sanitaires de la cysticercose porcine dans la commune de l'Oti Sud1.

Méthodologie

Zone d'étude

La commune de l'Oti Sud 1 est située dans la préfecture de l'Oti-Sud, dans la région des Savanes, au nord du Togo. Elle couvre une superficie de 1 459 km² (oti-sud1.mairie.tg, 2024). Le chef-lieu de la commune est Gando, une ville située à environ 537 km de Lomé et à 45 km de Mango, au sud-est (oti-sud1.mairie.tg, 2024). Selon les données du Recensement Général de la Population et de l'Habitat (RGPH-5) de novembre 2022, la commune de l'Oti Sud 1 compte une population totale de 106 052 habitants, dont 51 610 hommes et 54 442 femmes (INSEED, 2022). La population est majoritairement rurale, avec 89 706 habitants vivant en milieu rural, contre 16 346 habitants en milieu urbain (City Population, 2024). La commune dispose d'un centre hospitalier préfectoral, de cinq unités de soins périphériques et d'un poste de contrôle vétérinaire assurant la surveillance des maladies animales à travers le Réseau d'Épidémiosurveillance des Maladies Animales au Togo (REMATO) (Ministère de l'Agriculture, 2021).

La population de la commune est essentiellement agricole. La majorité pratique l'élevage des gros et petits ruminants, ainsi que de la volaille de manière traditionnelle. Les porcs sont également élevés dans cette commune (Direction Régionale de l'Agriculture, 2019). La commune est composée d'une majorité d'animistes, ainsi que de musulmans et de chrétiens. Elle regroupe plusieurs ethnies, notamment les Gangam, les Anoufoh (Tchokossi), les Moba, les Kabyè et les Éwé (oti-sud1.mairie.tg, 2024).

ISSN: 1857-7881 (Print)
e-ISSN 1857-7431 (Online)

Figure 1 : Carte administrative des cantons de la commune de l'Oti Sud 1

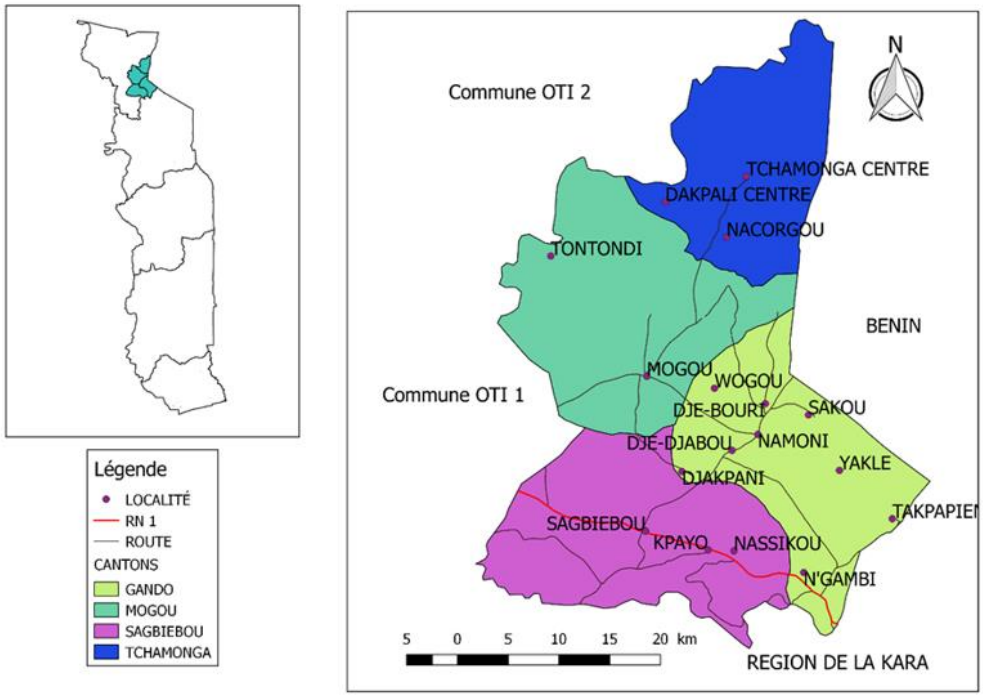

(source: BAGNA)

Type et période de l'étude

Il s'est agi d'une étude de type transversale à visée descriptive à travers une enquête auprès des acteurs de la filière porcine dans la commune de l'Oti Sud 1. Elle s'est réalisée en octobre 2023.

Population d'étude et échantillonnage

La population d'étude était constituée des acteurs de la filière porcine de la commune de l'Oti Sud 1. Elle est composée des éleveurs-commerçants de porcs, les charcutiers, les consommateurs de la viande de porc. Dans cette étude, est considéré comme éleveur de porcs ceux qui disposent d'un effectif minimal de 5 sujets dans leur exploitation. Les charcutiers de porcs et les éleveurs ont été sélectionnés sur la base de la liste des charcutiers et éleveurs de la commune détenue par la Section Contrôle Vétérinaire. Ils ont été choisi par recrutement progressif en suivant la liste disponible. Quant aux consommateurs, ils ont été choisis de façon aléatoire aux points de vente de viande. Ces acteurs ont été retenus pour leurs proximité avec les porcs. De plus, ils constituent les premières catégories socio-professionnelles à être exposées et à favoriser la propagation de la cysticercose porcine à travers leurs pratiques et attiudes.

ISSN: 1857-7881 (Print)
e-ISSN 1857-7431 (Online)

Technique et outils de collecte

Le questionnaire a été administré en face à face en français et en langue locale. Un questionnaire a été conçu et paramétré dans l'application Kobocollect. Ce questionnaire a été administré aux acteurs enquêtés après avoir obtenu leur consentement oral et volontaire. Cependant, des observations directes aux points de visites ont été effectuées pour réduire les biais d'informations.

Variables d'étude

Les questions ont porté sur les caractéristiques socio démographiques des acteurs (sexe, âge, niveau d'étude, activité de l'acteur...), les connaisssances sur la cysticercoses porcine et les épilepsies (existance, causes), les pratiques liées au comporement humains et à l'élevage de porc en lien avec la cysticercose porcine (système d'élevage, soins vétérinaires, alimentation des porcs, hygiène des mains, consommation des viandes de porcs, inspection de la viande de porc...).

Traitement des données et analyses statistiques

Les données collectées par l'application Kobocollect ont été téléchargées pour constituer un fichier Excel. La base de données ainsi obtenue a été traitée. Le traitement à consister à corriger les erreurs, à supprimer les doublons et à recoder de nouvelles variables. Le recodage a été fait en créeant des nouvelles variables (tranche d'âge, les catégories professionnelles). La base apurée a été téléchargée dans le logiciel EpiInfo7 pour les analyses statistiques descripives. Les résultats sont présentés en effectifs et proportions pour les variables qualitatives sous forme de tableau.

Considérations éthiques

L'étude réalisée a été autorisée par la Direction Régionale du Ministère en charge de l'Elevage de la région des Savanes. Les acteurs enquêtés ont donné leur consentement oral et volontaire avant l'administration du questionnaire. Avant toute chose, le bien fondé de l'étude et l'accord de la direction régional pour cette étude ont été expliqués aux acteurs qui étaient libres de participer à l'enquête ou de refuser. La gestion des données collectées a assuré l'anonymat et la confidentialité informations.

Résultats

Caractéristiques socio-démographiques de la population enquêtée

Un total de 249 acteurs a été enquêté dans la commune de l'Oti Sud 1. Les hommes étaient majoritaires (78,71%) pour une minorité de femmes (22%) et en ce qui concerne l'âge, 65,46% avait moins de 40 ans et 34,54% d'âgés de plus de 40 ans (tableau 1).

ISSN: 1857-7881 (Print)
e-ISSN 1857-7431 (Online)

Tableau 1 : Caractéristiques socio-démographiques des personnes enquêtées

Variables	Modalité	Effectif	Pourcentage (%)
Classe sociale	Particulier	2	0,80
	Fonctionnaire	247	99,20
Niveau d'étude	Non scolarisé	160	64,26
	Primaire	40	16,06
	Secondaire	47	18,88
	Supérieur	2	0,80
Sexe	Homme	196	78,71
	Femme	53	21,29
Tranche d'âge	Moins de 40 ans	163	65,46
	Plus de 40 ans	86	34,54
Elevage de porcs	Oui	175	70,28
	Non	74	29,72
Charcutier	Oui	11	4,41
Canton de provenance	Gando	131	52,61
	Mogou	84	33,73
	Sagbiebou	21	8,43
	Tchamonga	13	5,22

Niveau de connaissance de la cysticercose

Il ressort de cette étude que la majorité des enquêtés connaissent l'existence la cysticercose porcine (92,77%) et la cysticercose humaine à travers l'épilepsie (100%). Par contre pour la maitrise des causes réelles, un taux de 0,80% connait les causes de la cysticercose porcine et 2,01% maitrise les causes exactes de la cysticercose humaine (tableau 2).

Tableau 1: Niveau de connaissance de la cysticercose

Variable	Modalité	Effectif	Proportion (%)
Connaissance du ténia	Non	2	0,80
	Oui	247	99,20
Connaissance de la cysticercose porcine (n= 249)	Oui	231	92,77
	Non	18	7,23
Connaissance de la cause exacte de la cysticercose porcine (n=231)	Oui	1	0,43
	Non	230	99,57
Connaissance des tænias (n=249)	Oui	247	99,20
	Non	2	0,80
Connaissance de l'existence de l'épilepsie (n=249)	Oui	249	100
Connaissance de la cause exactes de l'épilepsie (n =249)	Oui	5	2,01
	Non	244	97,99

Pratiques sanitaires à risque avec la cysicercose porcine

Pratiques à risque liées au système d'élevage des porcs

L'étude a montré que l'élevage pratiqué dans la commune de l'Oti sud1 est essentiellement traditionnel (99,43%). Sur cet effectif un taux de 85,71% des éleveurs n'ont pas des enclos. En saison sèche, 97,14% d'éleveurs laissent les porcs en divagation. Par rapport à la prophylaxie des porcs, 2,28%

ISSN: 1857-7881 (Print)
e-ISSN 1857-7431 (Online)

éleveurs bénéficient de l'assistance d'un vétérinaire pour les traitements et déparasitages. L'alimentation des porcs est assurée par plusieurs sources de matières premières. Une proportion de 100%, 99,42% et 70,28% utilise respectivement le reste de repas de cuisine, la drêche de bière locale et les herbes fourragers dans l'alimentation des porcs (tableau 3).

Tableau 3 : Pratiques à risque liées au système d'élevage des porcs

Variable (n=175)	Modalité	Effectifs	Pourcentage (%)
Système d'élevage	Traditionnel	174	99,43
	Semi intensif	1	0,57
Liberté en saison sèche	Oui	170	97,14
	Non	5	2,86
Disponibilité d'enclos	Non	150	85,71
	Oui	25	14,29
Nettoyage hebdomadaire des enclos (n=25)	Oui	25	100
Déparasitage	Non	171	97,71
	Oui	4	2,28
Source d'alimentation	Reste de repas	175	100
	Drèche de bière locale	174	99,42
	Herbes	123	70,28
	Son de riz	5	2,86

Pratiques à risque liées au comportement humain

Sur 249 personnes enquêtées, 45,38% disposaient des latrines dans leur concession. Pour l'hygiène des mains, seulement 6,43% ont affirmé se laver les mains après les toilettes. Une proportion de 96,39% de personnes enquêtées consomme la viande du porc et ont tous affirmé que la viande de porc est inspectée par un vétérinaire, un assistant d'hygiène ou les deux types d'inspecteur respectivement dans 55,42% ; 43,78% et 0,8% de cas (Tableau 4).

Tableau 4 : Pratiques à risque liées aux comportements humains

Variable	Modalité	Effectif	Proportion (%)
Source d'eau	Forage	243	97,59
	Puits	9	3,61
	Togolaise des eaux	7	2,81
	Fleuve	1	0,40
Disponibilité de latrines	Non	136	54,62
	Oui	113	45,38
Lavage des mains après toilettes	Non	233	93,57
	Oui	16	6,43
Utilisation de savons lors de lavage des mains (n=16)	Oui	14	87,50
	Non	2	12,50
Consommation de viande	Oui	240	96,39
	Non	9	3,61

ISSN: 1857-7881 (Print)
e-ISSN 1857-7431 (Online)

Inspection de la viande de porc	Oui	246	98,80
	Non	3	1,20
Possible de consommer la viande ladre (n=231)	Non	229	99,13
	Oui	2	0,87
Inspection de la viande de porc	Vétérinaire	138	55,42
	Assistant d'hygiène	109	43,78
	Vétérinaire et assistant d'hygiène	2	0,80

Discussion

Caractéristiques socio démographiques des enquêtés

La majorité des personnes enquêtées étaient des hommes. Cette supériorité des hommes pourrait s'expliqué par le fait qu'une partie de notre échantillon a été interrogée au point de vente de viande de porc au marché. En effet les femmes ont plus tendance à acheter la viande de porc fraiche pour la cuisine à la maison contrairement aux hommes qui préfèrent consommer la viande déjà préparée sur les sites de vente. Ils étaient donc plus retrouvés au point de vente où la consommation de viande déja préparée se vend accompagné de boisson locale. De plus l'activité d'élevage des porcs est l'apanage des hommes qui confient la surveillance des sujets aux femmes dans cette communauté ; et ces femmes parcontre s'adonnent plus à l'élevage des volailles. Ce résultat est conforme à ceux de Dahourou et al., (2018) dans leur étude dans la région de la Boucle de Mouhoun (Burkina Faso) et ont attribué cette supériorité masculine aux activités des femmes lors de l'enquête. La plupart des enquêtés ne sont pas scolarisées et sont dans une tranche d'âge de plus de 40 ans. Ceci est dû au fait que les apprenants ne sont pas retrouvés dans les marchés et dans les ménages lors des enquêtes ; l'homme, le chef de la maison est le répondant dans plupart des ménages. Bien que les enfants soient inscrits à l'école, les parents par contre n'avaient pas eu cette chance d'y aller dans cette zone pratiquement rurale. Ces résultats sont conformes à ceux de Kungu et al., (2017) en Uganda et Dahourou et al., (2018) où respectivement 68% et 89,4% des personnes enquêtées étaient des hommes.

Niveau de connaissance de la cysticercose

La majorité des personnes enquêtées ont connaissance de l'exixtence de la cysticercose porcine et de la cysticercose humaine à travers l'épilepsie mais ne maitrisent pas les causes exactes de cette maladie. Ce résultat témoigne de l'existence effective de cette zoonose dans la communauté. La non maitrise des causes est liée aux croyances erronées sur l'épilepsie varant d'un pays à l'autre et au déficit de sensibilisation et d'information de la population en général sur l'épilepsie (Maiga et al., 2012; Agbétou et al.,2021). Or des études ont que chez l'homme, le téniasis se contracte par la consommation de viande de porc crue ou insuffisamment cuite contenant des

ISSN: 1857-7881 (Print)
e-ISSN 1857-7431 (Online)

larves de ténia et chez l'animal, la cysticercose survient par ingestion d'œufs de ténia avec de l'eau et des aliments (Melki et al., 2018). L'existence des carcasses de porc ladres traduit également une forte propagation d'œufs infestants, éliminés par des humains porteurs de vers adultes. Selon Andriantsimahavandy et *al*., (2003), au Madagascar, deux facteurs épidémiologiques majeurs sont constamment présents pour expliquer l'importance de la cysticercose : la promiscuité homme-porc notamment dans les régions d'élevage des hautes terres et le péril fécal. Ce résultat concorde avec ceux de Assana et al., (2001) où deux tiers des chefs d'exploitation connaissaient la cysticercose porcine, et que très peu de gens se rendaient compte de sa relation avec la taeniose et la cysticercose humaine. Des insuffisances dans la connaissance de cycle de transmission, de l'épidémiologie de la cysticercose porcine et humaine sont des facteurs qui favorisent la propagation de cette maladie à travers des comportement qui facilitent sa transmission et le maintien des infestations à *Taenia solium (*Shey-Njila et al., 2003).

Pratiques à risque liées au système d'élevage des porcs

Le système d'élevage essentiellement traditionnel sans suivi vétérinaire est lié au fait que l'élevage des porcs étant une activité secondaire dans la communauté, les éleveurs n'utilisent donc pas suffisamment de ressources pour la construction des porcheries, le suivi sanitaire et une bonne gestion de l'alimentation. Le système d'élevage en divagation, les types des gorets élevés et le système d'alimentation contribuent à l'infestation des porcs à la cysticercose et à la propagation de la maladie tant chez l'animal que chez l'être humain qui est le consommateur de première place (Kayeye et al., 2025). De plus, selon Tahina, (2015), l'absence de son de riz dans l'alimentation des porcs était un facteur de risque. Dans les élevages où les éleveurs ne donnaient que des fourrages verts ainsi que des déchets de cuisine, les porcs seraient exposés aux carences tant en vitamines que minéraux or ces derniers sont nécessaires pour le système de défense d'un animal. Cette situation dans la commune est aussi lié au fait qu'aucours de la période de 1997 à 2009, le Togo a connu des épizooties de Peste Porcine Africaine qui ont dévasté une grande partie du cheptel porcin, augmentant la vulnérabilité socio-économique de nombreux ménages ruraux (Somenutsè, 2022). De plus il ressort et un faible appui technique et financier des institutions spécialisées au niveau national, pour un meilleur encadrement de l'activité porcine.

Pratiques à risque liées aux comportements humains

Une forte proportion des élevages sont sans enclos et plus de la moitié des ménages ne disposent pas de latrine ce qui constituent des facteurs favorisant l'endmicité de la cysticercose dans la commune de l'Oti Sud 1. Ces

ISSN: 1857-7881 (Print)
e-ISSN 1857-7431 (Online)

résultats sont conformes à ceux de Waiswa et *al*., (2009) qui ont rapporté dans leur étude que dans les districts de Kamuli et Kaliro en Uganda, le mode d'élevage des porcs en liberté, peut constituer un risque majeur pour la santé des animaux car les foyers qui ne disposent pas de latrines peuvent faciliter l'accès des porcs aux matériel infestant. Kungu et al., (2015), au Nigéria ont incriminé la divagation des animaux, le manque de latrines, les défécations à l'air libre à des endroits facilement accessibles aux porcs comme les principaux facteurs de risque de l'infestation des porcs. Pour Tassou et al., (2022), la pauvreté rurale marquée par la rareté de latrines est un facteur favorisant la contamination des porcs par ingestion de matières fécales souillées émises sur les décharges d'ordures ou dans les végétations en agglomération.

Nos résultats rapportent une faible proportion de la population qui se lave systématiquement les mains après les toilettes et la plupart consomment la viande de porcs. Il ressort ainsi un risque lié à l'hygiène des mains et une importance à accorder à l'inspection post mortem des viandes de porcs. Phiri et al. (2006) ont rapporté qu'en dehors de la divagation, la cysticercose est associée au manque d'inspection de la viande, la méconnaissance de la maladie ainsi que le manque de mesures sanitaires et hygiéniques appropriées.

Conclusion

Cette étude, qui a consisté en une évaluation du niveau de connaissances de la population de la commune de l'Oti Sud 1 sur la cysticercose, a permis de mettre en évidence plusieurs facteurs socio-culturels, sanitaires et structurels favorisant la persistance de la cysticercose porcine et humaine dans la commune de l'Oti Sud 1. Il ressort de cette étude, la prédominance masculine parmi les enquêtés, l'analphabétisme, la méconnaissance des causes exactes de la cysticercose porcine et humaine. Le système d'élevage, largement traditionnel, non encadré et pratiqué en divagation, combiné au manque d'infrastructures sanitaires telles que les latrines, constitue un environnement favorable à la transmission de *Taenia solium*. L'absence d'hygiène individuelle, notamment le lavage des mains après défécation, et la consommation de viande de porc constituent les attitudes à risque. Les acteurs de la filière porcine de la commune de l'Oti Sud 1 ne maitrisent pas les risques sanitaires liés à la cysticercose porcine. Ces résultats soulignent l'urgence de mettre en place des stratégies multisectorielles incluant l'éducation sanitaire, l'amélioration des pratiques d'élevage, le renforcement de l'inspection vétérinaire, ainsi que la promotion de l'hygiène et de l'assainissement communautaires. L'approche « Une Seule Santé » (*One Health*) s'avère particulièrement pertinente pour répondre efficacement à cette problématique complexe.

ISSN: 1857-7881 (Print)
e-ISSN 1857-7431 (Online)

Remerciements

Nous remercions le personnel des services vétérinaires de la Direction Régionale de l'Agriculture, de l'Elevage et du Développement Rural de la région des savanes et les acteurs de la section contrôle vétérinaire préfectorale de l'Oti Sud.

Conflit d'intérêts : Les auteurs n'ont signalé aucun conflit d'intérêts.

Disponibilité des données : Toutes les données sont incluses dans le contenu de l'article.

Déclaration de financement : Les auteurs n'ont obtenu aucun financement pour cette recherche.

References:

1. Agbetou, M. A., Nganhou, C. H., Sowanou, A., Dovoedo, N., donné Gnonlonfoun, D., Adoukonou, T., Adjien, C., & Houinato, D. (2021). Epilepsie en milieu scolaire: Connaissance des enseignants sur l'épilepsie au sud du Bénin. African & Middle East Epilepsy Journal, 10(1)
2. Anayo, K. N., Guinhouya, K. M., Apetse, K., Agba, L., Assogba, K., Belo, M., & Balogou, A. K. A. (2023). Raisons d'échec du traitement antiépileptique aux CHU au Togo. Journal De La Recherche Scientifique De l'Université De Lomé, 24(3-4), 31–39. Https://doi.org/10.4314/jrsul.v24i3-4
3. Andriantsimahavandy, A., Rasamoelina, H., & Randrianasolo, R. (2003). La cysticercose humaine et porcine à Madagascar : aspects épidémiologiques et contrôle. *Revue Médicale de Madagascar*, 13(2), 87–93.
4. Assana, E., Zoli, A. P., & Geerts, S. (2001). Prevalence of porcine cysticercosis in the North province of Cameroon. *Veterinary Parasitology*, 99(3), 233–239.
5. Bouteille, B. (2014). La neurocysticercose : aspects cliniques et thérapeutiques. *Médecine Tropicale et Santé Internationale*, 4(1), 23–27.
6. City Population. (2024). *Oti Sud 1 - Population*. https://www.citypopulation.de/en/togo/mun/admin/oti_sud/5061__oti_sud_1/
7. Costard, S., Mur, L., Lubroth, J., Sanchez-Vizcaino, J. M., & Pfeiffer, D. U. (2009). Epidemiology of African swine fever virus. *Virus Research*, 150(1–2), 1–13. https://doi.org/10.1016/j.virusres.2010.09.003

ISSN: 1857-7881 (Print)
e-ISSN 1857-7431 (Online)

8. Dahourou, D. L., Ouedraogo, R., & Tapsoba, A. S. R. (2018). Perception paysanne et connaissance de la cysticercose porcine dans la Boucle du Mouhoun (Burkina Faso). *Revue Africaine de Santé et de Productions Animales*, 16(2), 103–112.
9. Direction Régionale de l'Agriculture, Région des Savanes. (2019). *Rapport sur l'état de l'agriculture et de l'élevage dans la région des Savanes*.
10. Dorny, P., Praet, N., Deckers, N., & Gabriel, S. (2009). Emerging food-borne parasites. *Veterinary Parasitology*, 163(3), 196–206. https://doi.org/10.1016/j.vetpar.2009.05.026
11. Institut National de la Statistique et des Études Économiques et Démographiques (INSEED). (2022). *Recensement général de la population et de l'habitat (RGPH-5)*.
12. Kayeye, P. B., Mushobekwa, J. T., Mudekereza, C. B., & Bujiriri, J. B. (2025). Contribution du système d'élevage du porc en divagation sur la transmission de la cysticercose porcine dans le Groupement de Miti, Sud-Kivu en République Démocratique du Congo. *Annales de l'UNIGOM*, *15*(3).
13. Kungu, J. M., Mwanza, A. M., & Dione, M. M. (2015). Assessment of farmer knowledge and risk factors of porcine cysticercosis in Nigeria. *Tropical Animal Health and Production*, 47(4), 751–761.
14. Kungu, J. M., Mwanza, A. M., & Muwonge, A. (2017). Prevalence and risk factors of porcine cysticercosis in Uganda: A systematic review. *BMC Veterinary Research*, 13(1), 1–9.
15. Maiga, Y., Albakaye, M., Kuate, C., Christian, N., & Koumaré, B. (2012). Epilepsie en Afrique subsaharienne: Connaissances, Attitudes et Pratiques face à l'épilepsie. *African & Middle East Epilepsy Journal*, 1(4).
16. Mariska, M. A., Ramiandrasoa, F., & Rasamoelina, H. (2008). Prevalence of porcine cysticercosis and risk factors in Madagascar. *Tropical Animal Health and Production*, 40(5), 347–352.
17. Melki, J., Koffi, E., Boka, M., Touré, A., Soumahoro, M. K., & Jambou, R. (2018). Taenia solium cysticercosis in West Africa: status update. Parasite, 25, 49.
18. Ministère de l'Agriculture, de la Production Animale et de la Pêche. (2021). *Rapport annuel du Réseau d'épidémiosurveillance des maladies animales au Togo (REMATO)*.
19. Mopoundza, P. N., Madingou, E. L., Nguema, P. P. A., & Mavoungou, S. (2019). Étude de la prévalence de la cysticercose porcine dans les abattoirs de Libreville. *Revue Africaine de Santé et de Productions Animales*, 17(2), 89–95.

ISSN: 1857-7881 (Print)
e-ISSN 1857-7431 (Online)

20. Murrell, K. D., & Crompton, D. W. T. (2005). Food-borne parasitic zoonoses: The problem of taeniasis and cysticercosis. In *WHO/FAO/OIE Guidelines for the Surveillance, Prevention and Control of Taeniasis/Cysticercosis*. World Health Organization.
21. N'Dri, K. M. (2023). La cysticercose porcine : une revue des connaissances et de l'impact en Afrique subsaharienne. *Revue Ivoirienne des Sciences et Technologies*, 42(1), 55–65.
22. Organisation mondiale de la Santé (OMS). (2011). *Taeniasis/cysticercosis: Fact sheet N°376*. https://www.who.int/news-room/fact-sheets/detail/taeniasis-cysticercosis
23. oti-sud1.mairie.tg. (2024). *Notre commune*. https://oti-sud1.mairie.tg/notre-commune/
24. Phiri, I. K., Dorny, P., Gabriel, S., & Sikasunge, C. S. (2006). Assessment of routine inspection methods for detecting porcine cysticercosis in Zambian village pigs. *Journal of Helminthology*, 80(1), 69–72.
25. Porphyre, T., Raboisson, D., & Etter, E. (2015). Control of pig-related zoonoses in sub-Saharan Africa: A review. *Zoonoses and Public Health*, 62(5), 254–269. https://doi.org/10.1111/zph.12139
26. Quet, F., Guerchet, M., Pion, S.D.S., Ngoungou, E.B., Nicoletti, A., & Preux, P.M.(2010). Meta-analysis of the association between cysticercosis and epilepsy in Africa. *Epilepsia,* 51(5), 830-837
27. Sciutto, E., Fragoso, G., Fleury, A., Laclette, J. P., Sotelo, J., Aluja, A., & Larralde, C. (2000). *Taenia solium* disease in humans and pigs: An ancient parasitosis disease rooted in developing countries and emerging as a major health problem of global dimensions. *Microbes and Infection*, 2(15), 1875–1890.
28. Shey-Njila, N., Zoli, A. P., & Assana, E. (2003). *Taenia solium* cysticercosis in pigs raised in the rural area of Cameroon: Sero-prevalence and risk factors. *Acta Tropica*, 87(2), 15–23.
29. Somenutse, K.G., Bankolé, A.A. et Djiwa, O. 2022. Guide de bonnes pratiques d'élevage, de transport, de commercialisation et d'abattage des porcs. Lomé, FAO. https://doi.org/10.4060/cc0221fr
30. Tahina, R. (2015). *Facteurs de risque de la cysticercose porcine dans la région Analamanga, Madagascar* [Thèse de doctorat vétérinaire, Université d'Antananarivo].
31. Tassou, S. A., Houngbegnon, R. C., Adoligbe, C., & Youssao, A. K. I. (2022). Facteurs environnementaux favorisant la transmission de la cysticercose porcine au Bénin. *Bulletin de la Recherche Agronomique du Bénin*, 101, 23–30.

ISSN: 1857-7881 (Print)
e-ISSN 1857-7431 (Online)

32. Waiswa, C., Fèvre, E. M., & Kabasa, J. D. (2009). Porcine cysticercosis and risk factors in rural Kamuli and Kaliro districts, Uganda. *Journal of Helminthology*, 83(4), 347–354.
33. Zoli, A. P., Shey-Njila, N., Assana, E., Nguekam, J. P., Dorny, P., Brandt, J., & Geerts, S. (2003). Regional status, epidemiology and impact of *Taenia solium* cysticercosis in western and central Africa. *Acta Tropica*, 87(1), 35–42.

ESJ Natural/Life/Medical Sciences Peer-reviewed

Intégration des contextes locaux dans le programme scientifique de sciences de la vie et de la terre (SVT) au cycle qualifiant : Cas des contextes du Haut Ziz, sud-est marocain

Mohamed Manaouch, PhD
Mohamed Aghad, PhD
Laboratoire Environnement, Sociétés et Territoires (LEST),
FSHS, Université Ibn Tofail, Maroc
Mohamed Sadiki, MCH
Laboratoire Géosciences et Ressources Naturelles, FS,
Université Ibn Tofail, Maroc
Jamal Al Karkouri, PES
Laboratoire Environnement, Sociétés et Territoires (LEST),
FSHS, Université Ibn Tofail, Maroc

Doi:10.19044/esj.2026.v22n6p193

Submitted: 19 January 2026
Accepted: 28 February 2026
Published: 28 February 2026

Cite As:
Manaouch, M., Aghad, M., Sadiki, M. & Al Karkouri, J. (2026). *Intégration des contextes locaux dans le programme scientifique de sciences de la vie et de la terre (SVT) au cycle qualifiant : Cas des contextes du Haut Ziz, sud-est marocain.* European Scientific Journal, ESJ, 22 (6), 193. https://doi.org/10.19044/esj.2026.v22n6p193

Résumé

Il est désormais essentiel d'intégrer les contextes locaux dans le programme des sciences de la vie et de la terre (SVT) du tronc commun scientifique (TCS) dans le cycle qualifiant, afin de répondre aux enjeux contemporains relatifs à la propagation des savoirs scientifiques, ainsi qu'au développement de la pensée critique et de la conscience environnementale chez les élèves. L'inclusion de contextes locaux dans le curriculum des SVT vise à aider les apprenants à surmonter ces enjeux. Dans cette optique, notre recherche se concentre sur l'intégration des contextes géoenvironnementaux locaux dans le cursus des SVT. L'objectif est d'analyser et de comparer cette intégration ainsi que son impact sur le niveau d'apprentissage des élèves du TCS. À cette fin, deux analyses ont été menées. La première examine le programme scientifique des SVT du TCS afin d'évaluer les contextes actuellement utilisés. La seconde se concentre sur l'identification des contextes

ISSN: 1857-7881 (Print)
e-ISSN 1857-7431 (Online)

locaux pertinents pour proposer leur intégration dans le curriculum des SVT. Les résultats révèlent la possibilité de proposer 30 contextes locaux. Selon les indicateurs retenus, cette intégration semble favoriser l'amélioration du processus d'apprentissage des concepts en SVT.

Mots-clés: Contexte locaux, Cycle qualifiant, Curriculum, Sciences de la vie et de la Terre (SVT)

Integrating Local Contexts Into the Scientific Program of Life and Earth Sciences (SVT) in the Qualifying Cycle: Case of the Upper Ziz, Southeastern Morocco

Mohamed Manaouch, PhD
Mohamed Aghad, PhD
Laboratoire Environnement, Sociétés et Territoires (LEST),
FSHS, Université Ibn Tofail, Maroc
Mohamed Sadiki, MCH
Laboratoire Géosciences et Ressources Naturelles, FS,
Université Ibn Tofail, Maroc
Jamal Al Karkouri, PES
Laboratoire Environnement, Sociétés et Territoires (LEST),
FSHS, Université Ibn Tofail, Maroc

Abstract

It is now essential to integrate local contexts into the curriculum for Life and Earth Sciences (SVT) within the common scientific curriculum (TCS) during the qualifying cycle, in order to address contemporary challenges related to the dissemination of scientific knowledge, as well as to the development of critical thinking and environmental awareness among students. The inclusion of local contexts in the LES curriculum aims to assist learners in overcoming these issues. In this regard, our research focuses on the integration of local geo-environmental contexts into the LES curriculum. The objective is to analyze and compare this integration and its impact on the learning outcomes of CSC students. To this end, two analyses have been conducted. The first examines the scientific curriculum of LES in the CSC to evaluate the contexts currently used. The second focuses on identifying relevant local contexts to propose their integration into the LES curriculum. The results indicate the potential to introduce 30 local contexts. According to the selected indicators, this integration appears to enhance the learning process of concepts in LES.

ISSN: 1857-7881 (Print)
e-ISSN 1857-7431 (Online)

Keywords: Local contexts, Qualifying cycle, Curriculum, Life and Earth Sciences

Introduction

L'enseignement des sciences de la vie et de la terre (SVT) au cycle secondaire demande plusieurs éléments clés tels que des connaissances solides en concepts fondamentaux, une pédagogie adaptée aux différents styles d'apprentissage, et des expérimentations pratiques pour illustrer la théorie (Legendre, 1994). Il se voit convoqué pour contribuer au développement de l'esprit critique des élèves tout en intégrant des outils technologiques modernes (Fuchs-Gallezot & Bächtold, 2023). Par conséquent, la formation continue des enseignants est cruciale pour rester à jour avec les évolutions scientifiques et pédagogiques.

Au Maroc, les résultats des rapports récents sur les performances en sciences provenant d'évaluations internationales, comme 'Trends in International Mathematics and Science Study ' (TIMSS) et 'Programme for International Student Assessment ' (PISA), soulignent un niveau préoccupant chez les élèves, qui est inférieur à celui d'autres pays (Loubaki et al., 2015). En effet, 69 % des élèves ne maîtrisent pas les compétences essentielles en sciences (MEN PISA 2018). Ces constats représentent un signal d'alerte pour inciter à des actions visant à améliorer cette situation.

Pour optimiser l'enseignement des sciences au Maroc, une approche combinant des méthodes pédagogiques innovantes et des outils appropriés est nécessaire. Cela favorise non seulement une meilleure compréhension des apprenants, mais également l'éveil de leur intérêt et leur curiosité pour les sciences. L'optimisation peut être envisagée sous deux angles principaux : les méthodes pédagogiques et les outils éducatifs, chacun étant fondamental pour l'efficacité de l'enseignement et de l'apprentissage. Pour les méthodes pédagogiques, les modes d'apprentissage et l'intégration des technologies sont parmi les plus répandus.

L'intégration des technologies de l'information et de la communication (TIC) sont considérées comme des outils éducatifs essentiels (Maouni et *al.,* 2014 ; Nafidi et *al.,* 2018). Diverses initiatives ont été prises pour les intégrer dans le système éducatif marocain. Par ailleurs, des chercheurs comme Iwzane et *al.* (2025) soulignent la nécessité d'introduire une approche d'investigation dans l'enseignement des sciences de la vie et de la terre au niveau collégial et qualifiant. De même, Abid et *al.* (2025) insistent sur l'importance d'intégrer l'éducation au développement durable dans le curriculum des sciences de la vie et de la terre. Enfin, Ameziane (2018) appelle les responsables à intégrer des aspects environnementaux dans les curriculums marocains de ces disciplines au cycle secondaire.

ISSN: 1857-7881 (Print)
e-ISSN 1857-7431 (Online)

L'intégration des contextes locaux dans l'enseignement des sciences, en particulier les SVT revêt une importance essentielle pour plusieurs raisons. À l'heure où la mondialisation et les avancées technologiques transforment rapidement notre monde, il devient impératif d'ancrer l'enseignement dans les réalités que vivent les apprenants. Le sud est marocain, par exemple, offre une richesse de spécificités géographiques, culturelles et économiques qui, lorsqu'elles sont intégrées au cursus scolaire, permettent de créer un enseignement plus pertinent et adapté. En plus, l'intégration des spécificités locales permet de rendre l'enseignement plus attractif. En liant les concepts scientifiques aux réalités locales comme la gestion des ressources en eau dans une région aride ou la biodiversité des écosystèmes locaux, les élèves perçoivent immédiatement la pertinence des sciences dans leur quotidien. Cette approche favorise leur engagement et stimule leur curiosité scientifique.

Pour les apprenants eux-mêmes, les bénéfices sont évidents. En intégrant les contextes locaux dans leur éducation, ils acquièrent une connaissance approfondie de leur environnement et développent un sentiment d'appartenance. Cette connexion avec leur terre natale leur permet de mieux comprendre et protéger leur patrimoine environnemental et culturel.

Pour atteindre cette intégration, nous avons réalisé une analyse des contextes actuels présents dans le programme scientifique du tronc commun scientifique (TCS), suivie d'une étude des contextes locaux pouvant être intégrés pour faciliter l'apprentissage des concepts scientifiques. Cette approche va constituer une démarche essentielle pour répondre aux besoins des apprenants de la région du sud est marocain. En créant un pont entre les savoirs scientifiques et les réalités locales. Enfin, nous avons mené une enquête sur l'effet de cette intégration sur l'apprentissage des SVT via un questionnaire convenable destiné aux enseignants des SVT à l'échelle locale.

Materiels et Methodes

Présentation du contexte du Haut Ziz, Sud-Est marocain

Le pays du Haut Ziz (HZ) en amont du barrage Hassan Eddakhil est une surface géographique délimitée sur 4435 km² avec un périmètre de l'ordre de 613 km renfermant toute la vallée de Ziz et ses affluents. Cette zone est comprise entre les latitudes : 32° 64' 19'' et 32° 05' 48'' Nord et les longitudes 05° 46'20'' et 04° 11' 72'' Ouest (fig. 1). À plus de 1200 m d'altitude, cette vallée est en grande partie située dans le Haut Atlas oriental. Elle est administrativement gérée par les deux provinces d'Errachidia et de Midelt de la région de Darâa-Tafilalet qui compte trois autres provinces : la province de Tinghir, la province d'Ouarzazate et la province de Zagora (HCP, 2022).

ISSN: 1857-7881 (Print)
e-ISSN 1857-7431 (Online)

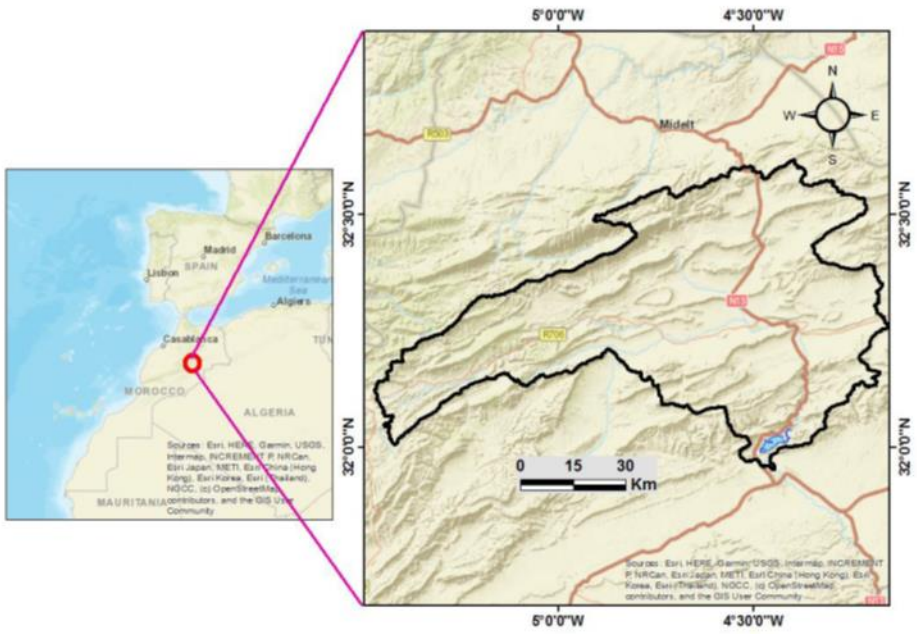

Figure 1 : Carte de localisation du bassin versant du Haut Ziz (Haut Atlas oriental, Maroc)

Le HZ se caractérise par un climat de type aride à semi-aride dont les principaux traits sont : un écart thermique important entre les températures élevées de l'été (26,2 °C comme moyenne au mois de juillet) et celles basses de l'hiver (8,6 °C comme moyenne au mois de décembre) ; une pluviométrie qui se caractérise par une importante irrégularité dans le temps (fig. 2), ainsi que son caractère torrentiel et très violent ; des vents venant de l'Atlantique et descendant des Hauts plateaux enregistrant des vitesses moyennes d'environ 84 km/h (Manaouch et al., 2023).

ISSN: 1857-7881 (Print)
e-ISSN 1857-7431 (Online)

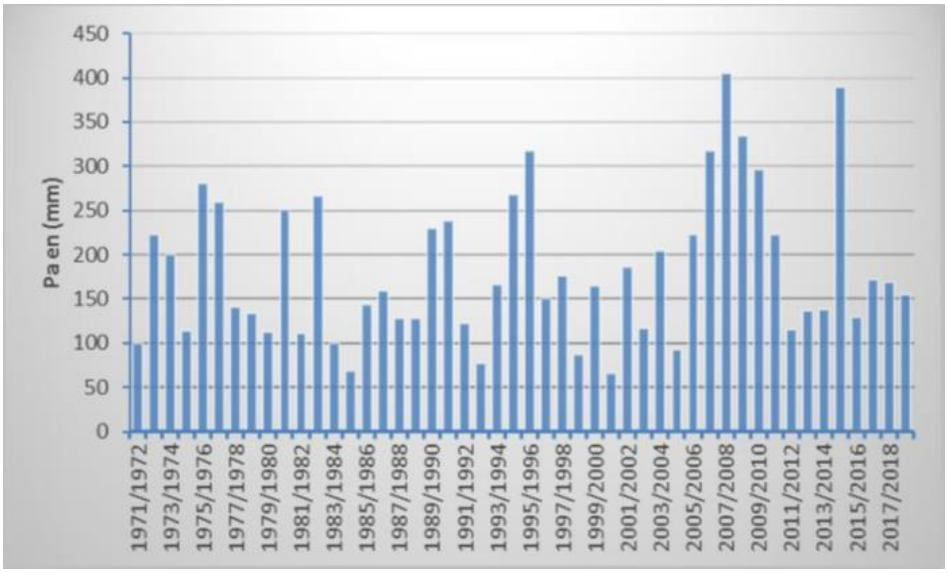

Figure 2 : Précipitations annuelles recueillies dans la station de M'zizel entre 1971 et 2018 au niveau du bassin du Haut Ziz

Le montage du réseau hydrographique principal est assuré par l'oued Ziz (cours d'eau principal) sur une longueur d'environ 172 km avec un nombre de 13 principaux affluents (fig. 3) qui l'alimentent en plus de plusieurs autres petits ravins et de sources (Manaouch et al., 2024).

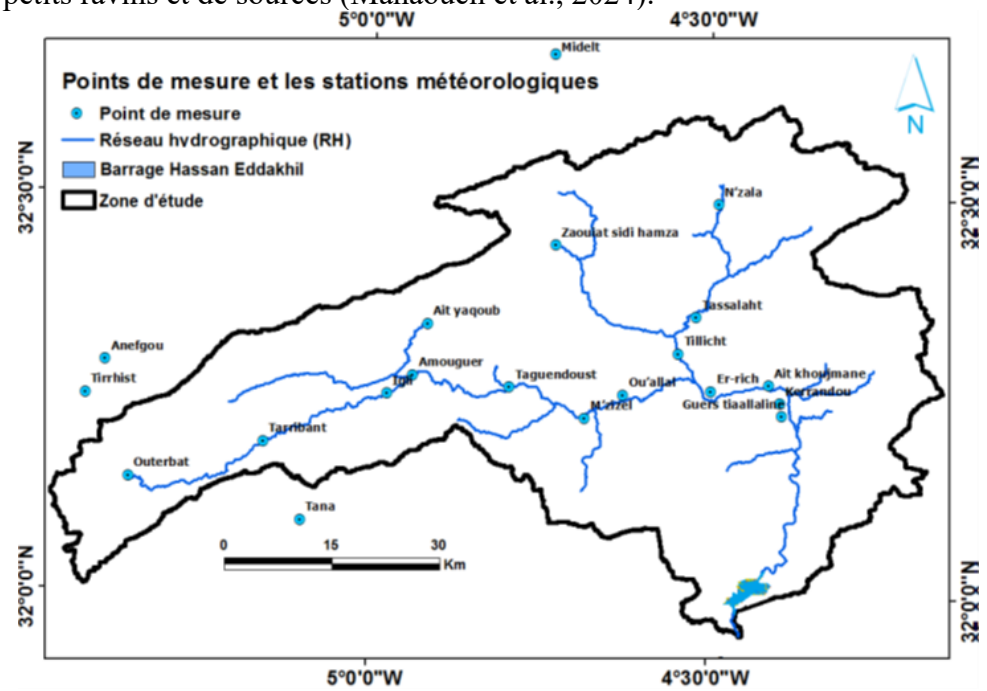

Figure 3 : Carte de la répartition des stations météorologiques et les points de mesure de précipitations dans le bassin du Haut Ziz

ISSN: 1857-7881 (Print)
e-ISSN 1857-7431 (Online)

Le réseau routier est très limité, une seule route nationale (N°13) reliant les deux provinces d'Errachidia et Midelt et une seule autre régionale (R706) reliant Imilchil et Er-Rich assurent le désenclavement du HZ (fig. 1). Ces deux routes traversent le HZ dans sa grande partie, tandis que les pistes carrossables existantes reliant toutes les autres grandes agglomérations (Sadiki et *al.,* 2024). Parmi elles, quelques pistes sont actuellement en train d'être goudronnées, il s'agit de la piste menant de Zaouiat Sidi Hamza vers Anfergal, la route reliant Er-Rich à Tamagourt à travers Tillicht et Ouallal et celle reliant la route nationale N°13 et les douars de Tawahit, Ait Attou et Imghi de la commune de Guers Tiaallaline.

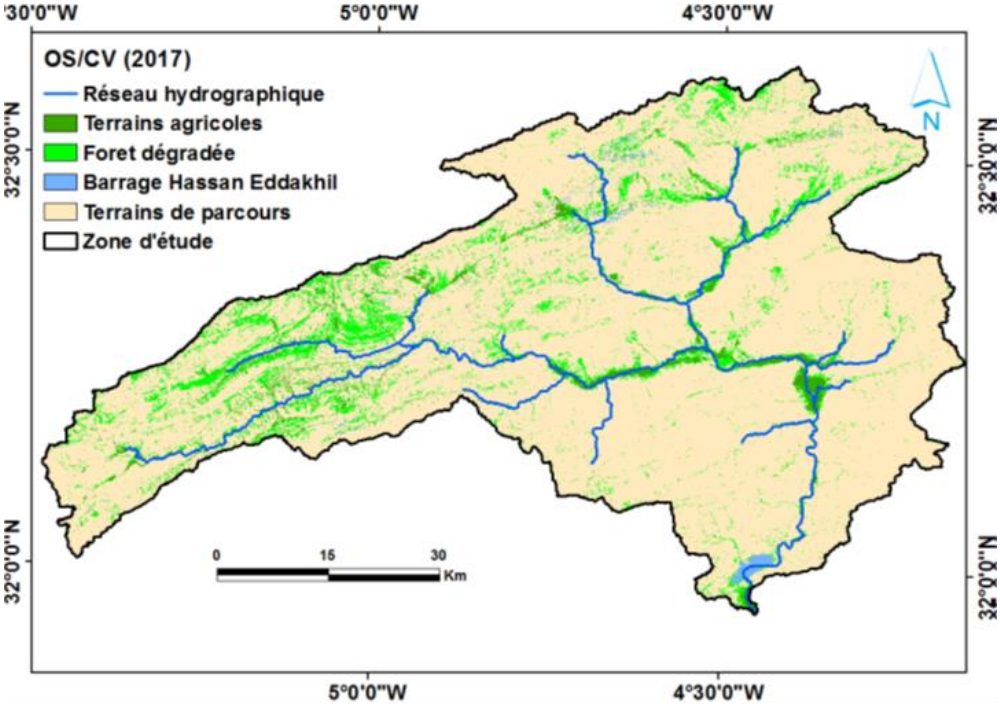

Figure 4 : Carte de localisation des terrains agricoles dans le HBZ

L'agriculture suit un système de type oasien, notamment en aval d'oued Ziz (fig. 5), en se développant exclusivement sur ses bords (fig. 4) et aux alentours de quelques principaux affluents (Tazarine, Zaouiat Sidi Hamza, Outerbate, Ait Yakoub, …) (Manaouch et *al.,* 2021).

ISSN: 1857-7881 (Print)
e-ISSN 1857-7431 (Online)

Figure 5 : Paysage de système oasien d'Ait Atmane (photographie prise le 05 octobre 2022)

Les systèmes de cultures pratiqués sont encore traditionnels et assurent une agriculture vivrière complémentaire aux autres activités comme l'élevage (fig. 6), le tourisme, l'artisanat et les mines. Ces activités occupent la population active selon des taux différents (Naimi et *al.,* 2024).

Figure 6 : Troupeau de moutons dans un Agdal (source : Abba)

ISSN: 1857-7881 (Print)
e-ISSN 1857-7431 (Online)

Pour l'élevage, il constitue la principale source de revenu pour les petits douars de montagne (Afraskou, Taneghrift, Tazrouft, Michlifene, …) et se base exclusivement sur les terrains de parcours (fig. 7) comme source de fourrage gratuite et collective.

Figure 7 : Exemple de groupements de Thym à Tazrouft (photographié le 5 octobre 2022)

L'agriculture offre un supplément de fourrage à travers la pratique à grande échelle de la céréaliculture et des cultures fourragères. Malgré la production limitée et les faibles rendements réalisés, cette supplémentation assure la survie des bétails en périodes de neige et de faible production sur parcours, notamment en amont du HZ.

ISSN: 1857-7881 (Print)
e-ISSN 1857-7431 (Online)

Figure 8: Un ensemble de femmes du milieu rural ayant fourni du bois de chauffage pour les foyers à Ait Ali Ouikkou, en amont du Haut Ziz

La problématique de l'érosion dans la vallée de Ziz est très remarquable. À l'instar des autres régions du Maroc, plusieurs facteurs contribuent à rendre la situation préoccupante, car la survie de la population dépend fortement de l'état du milieu environnant, qui offre des potentialités d'améliorer leurs principales activités, à savoir l'agriculture sur les bords des principaux affluents d'oued Ziz et l'élevage. Néanmoins, le développement de leur niveau de vie est intimement lié à eux-mêmes, car ils sont responsables de la dégradation massive (fig. 8) et continue ainsi que de l'usage non rationnel des ressources naturelles disponibles (Naimi et *al.,* 2024).

ISSN: 1857-7881 (Print)
e-ISSN 1857-7431 (Online)

Figure 9 : Inondation d'un affluent de l'oued Ziz en amont du Haut Ziz au niveau du douar de Tabouarbite (photographie prise le 10 octobre 2022)

Cette dégradation entraîne une intensification des crues, dont l'ampleur s'aggrave avec le temps : fréquence élevée, zones affectées en croissance, et dégâts de plus en plus coûteux (fig. 9). Malgré les efforts et initiatives prises par la population et d'autres intervenants, la situation semble souvent dépassée, laissant de nombreux efforts à déployer.

L'étude approfondie du HZ est révélatrice de la richesse exceptionnelle de ses paysages géographiques, qui se distinguent par leur diversité et leur complexité (Manaouch et *al.,* 2025). Ce territoire présente une variété de contextes écologiques et géomorphologiques, allant des montagnes majestueuses aux vallées verdoyantes. Ces caractéristiques variées offrent une multitude d'opportunités d'exploration et d'analyse pour les élèves. Celles-ci peuvent être intégrées de manière significative dans les programmes

ISSN: 1857-7881 (Print)
e-ISSN 1857-7431 (Online)

scientifiques de la discipline des SVT du TCS, permettant ainsi aux étudiants de mieux comprendre les interactions entre l'environnement et les organismes vivants, ainsi que les enjeux de la conservation des habitats et de la biodiversité.

Méthodologie du questionnaire

Pour clarifier le processus d'échantillonnage, il est essentiel d'établir des critères de sélection ciblant spécifiquement les enseignants de SVT des lycées du HZ. Ces critères incluent des caractéristiques telles que l'âge, le sexe, le lieu de travail et le grade, tout en veillant à leur alignement avec les objectifs de l'étude. L'échantillonnage a été effectué de manière aléatoire, en utilisant des quotas basés sur les différentes régions du HZ. Cette approche permet de minimiser les biais de sélection, garantissant ainsi que chaque membre de la population a une chance égale d'être inclus.

Pour évaluer les attitudes des enseignants vis-à-vis de l'intégration des contextes locaux dans le programme de SVT du TCS, nous avons réalisé une enquête à l'aide d'un questionnaire, administré conformément à la méthodologie reconnue décrite ci-dessous. (fig. 10). Le questionnaire a été élaboré et mis en ligne via Google Forms, la population d'étude a été sollicitée pour remplir les questionnaires par courriers électroniques et par les réseaux sociaux, principalement Facebook, via les groupes des enseignants des SVT. Cette méthode a été choisie du fait qu'elle permet de toucher une large population dispersée sur le HZ. Pour le traitement des données, nous avons utilisé Excel. Cette approche a été sélectionnée en raison de sa capacité à réaliser des analyses statistiques et de sa grande flexibilité dans la manipulation et la visualisation des données.

Les auteurs reconnaissent certaines limites dans cette méthodologie, notamment la participation de tous les enseignants, la fiabilité et la véracité des réponses, ainsi que l'absence de participation des inspecteurs de SVT. Cependant, ils estiment que les enquêtes et les questionnaires sont des outils efficaces pour ce type de recherche et qu'ils permettent de recueillir des données pertinentes et significatives. Ils seraient enthousiastes à l'idée de réaliser des questionnaires à l'échelle nationale et d'inviter un plus grand nombre de participants, y compris les inspecteurs, afin de discuter de cette méthodologie plus en détail et d'explorer toute suggestion pouvant renforcer notre approche.

ISSN: 1857-7881 (Print)
e-ISSN 1857-7431 (Online)

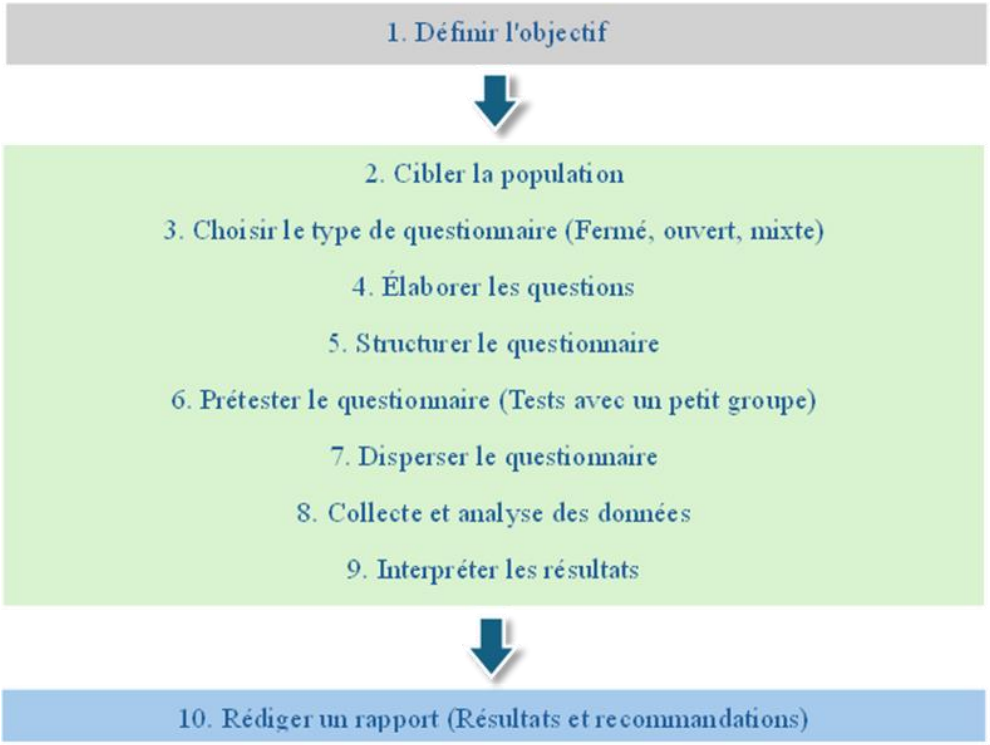

Figure 10 : Schéma méthodologique suivi pour la création du questionnaire

Présentation du programme scientifique des SVT du TCS

Le programme des SVT du TCS (tab. 1) présente une approche intégrée permettant aux élèves d'explorer et de comprendre les diverses dimensions de leur environnement. Ce cursus, riche et varié, commence par une unité sur l'écologie, où sont abordées les techniques utilisées et une introduction aux écosystèmes. Il met en lumière les facteurs édaphiques, tels que les propriétés du sol, leur impact sur la répartition et l'évolution des êtres vivants, ainsi que l'influence de l'Homme. Les facteurs climatiques, également cruciaux en agriculture, influencent la distribution des espèces. De plus, les relations trophiques, ainsi que les pyramides de biomasse et d'énergie, illustrent la dynamique des écosystèmes. Enfin, il est essentiel de considérer les risques liés à l'exploitation non durable des ressources et la nécessité de préserver les équilibres naturels.

La deuxième unité aborde la reproduction sexuée des plantes à fleurs, notamment chez les angiospermes, implique l'observation de fleurs, l'organisation de leur appareil reproducteur, et le rôle des grains de pollen dans la pollinisation et la formation des fruits. Ce processus comprend la germination des grains de pollen et la double fécondation, menant à la formation des graines. Les gymnospermes et la reproduction chez les plantes sans fleurs, comme les algues, fougères et mousses, sont également abordés.

ISSN: 1857-7881 (Print)
e-ISSN 1857-7431 (Online)

De plus, le cycle de développement des plantes, la reproduction asexuée via la multiplication végétative (greffage, bouturage, marcottage), et les enjeux de la modification génétique des plantes (PGM) sont explorés, tout comme la classification des plantes.

Tableau 1 : Le cursus scientifique en sciences de la vie et de la terre au sein du tronc commun scientifique

Unité	Contenu à enseigner	Enveloppe horaire
U1	*Sortie écologique* -Quelques techniques du terrain -Réalisation de la sortie -Première approche du concept écosystème	12h
	Les facteurs édaphiques et leurs relations avec les êtres vivants -Propriétés du sol. -Rôle du sol dans la répartition des êtres vivants. -Rôle des êtres vivants dans l'évolution du sol. -Impact de l'Homme sur le sol	09h
	Les facteurs climatiques et leurs relations avec les êtres vivants -Les facteurs climatiques. -Rôle des facteurs climatiques dans la répartition des êtres vivants. -L'importance de connaître et de maîtriser les facteurs climatiques dans le domaine agricole.	09h
	Flux de la matière et flux de l'énergie dans l'écosystème -Les relations trophiques -Les réseaux trophiques -Les pyramides de biomasse et les pyramides d'énergie -Définition du concept écosystème. -Aspects dynamiques de l'écosystème.	09h
	Les équilibres naturels -Dangers de l'exploitation irrationnelle des ressources naturelles -Nécessité de préserver les équilibres naturels et rôle de l'Homme dans la protection de la nature	06h
U2	*La reproduction sexuée des plantes à fleurs:* -La reproduction chez les angiospermes -Observation et dissection de différentes fleurs. -Organisation de l'appareil reproducteur.	12 h
	-Rôles des grains de pollen dans la formation du fruit: Pollinisation; ses différents types et son importance agricole. -Germination des grains de pollen. -La double fécondation; formation de la graine et sa germination.	06h
	-La reproduction chez les gymnospermes	03h
	La reproduction sexuée des plantes sans fleurs : -Chez les algues -Chez une fougère et chez une mousse	
	Cycles de développement des Plantes	06h

ISSN: 1857-7881 (Print)
e-ISSN 1857-7431 (Online)

	La reproduction asexuée -La multiplication végétative -Les applications de la multiplication végétative dans le domaine agricole: greffage; bouturage et marcottage. *La modification génétique des plantes (PGM)* -Techniques de la modification génétique des plantes. -Problématique de la modification génétique des plantes. *Classification des plantes*	 06h 06h 03h 03h

Analyse des contextes utilisés dans le programme scientifique des SVT du TCS

L'analyse des contextes utilisés dans le programme scientifique des SVT du TCS révèle une grande variabilité entre les manuels scolaires. Cette situation illustre une intégration aléatoire des contextes, souvent déconnectée des réalités locales, ce qui pourrait aider les apprenants à mieux saisir les concepts des SVT. En effet, de nombreux exemples de contextes étrangers sont présentés (tab. 2), sans que les élèves aient une idée claire des lieux ou des environnements concernés. Par exemple, une chaîne alimentaire polaire est souvent mentionnée, alors que les apprenants n'ont aucune compréhension de qui consomme qui dans ce contexte, ce qui limite leur capacité à établir des liens significatifs avec le sujet étudié. L'exemple de la reproduction chez les algues marines illustre également cette situation où les apprenants font preuve d'ignorance à l'égard de ces espèces non locales. L'exemple de la dynamique de l'écosystème, qui concerne le nombre de lynx et de lièvres, illustre bien cette situation où les apprenants ignorent le lynx qui est une espèce non locale.

Tableau 2 : Quelques contextes utilisés actuellement dans le programme des SVT du TCS

Contenu à enseigner	Contextes actuels utilisés	Figures / schéma
Le choix de la station d'inventaire	Zone qui ressemble aux alentours du lac Aguelmam Azigza	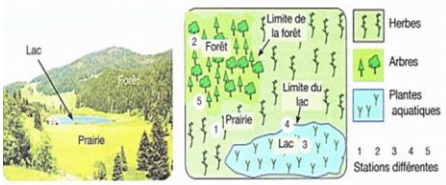
Rôle du sol dans la répartition des espèces végétales.	La forêt du chêne de liège à Maamoura. Entre la forêt de Témara et le plateau des Zaers.	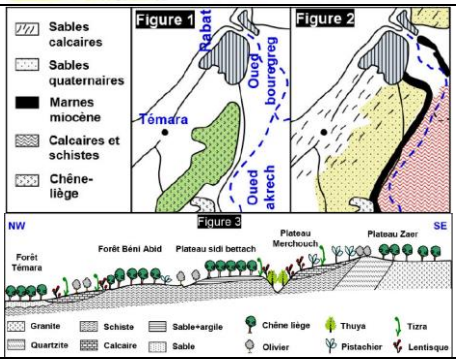

ISSN: 1857-7881 (Print)
e-ISSN 1857-7431 (Online)

L'étude d'un milieu aquatique	Daya de Sidi Boughaba	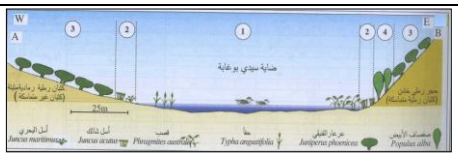
Première approche du concept écosystème	Océan – forêt -	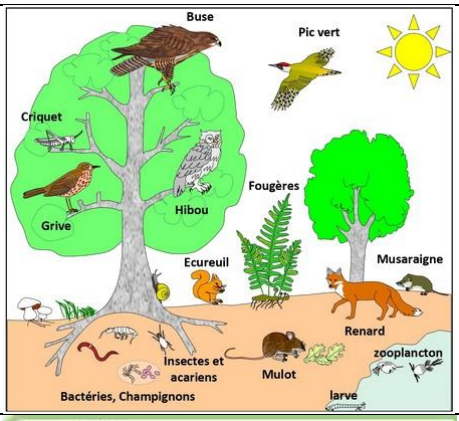
L'importance de connaître et de maîtriser les facteurs climatiques dans le domaine agricole	Les fermes de clémentine de Berkane Les fermes de tomates d'Agadir	
Impact négatif de l'Homme sur le sol	Source inconnue	
Aspects dynamiques de l'écosystème	Lynx et les lapins	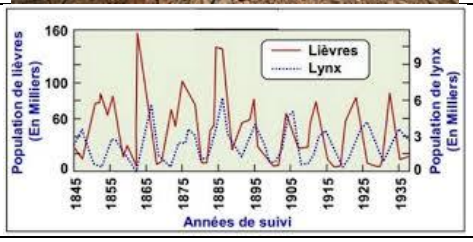

ISSN: 1857-7881 (Print)
e-ISSN 1857-7431 (Online)

Rôle des facteurs climatiques dans la répartition des êtres vivants.	Les deux versants de Bouiblane	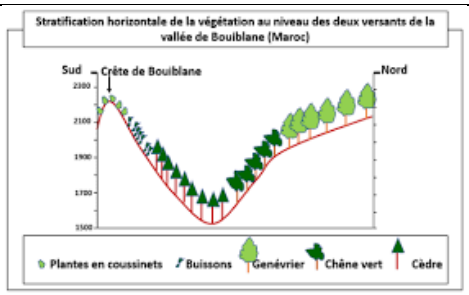
Les équilibres naturels	Exemple de lièvres et lynx	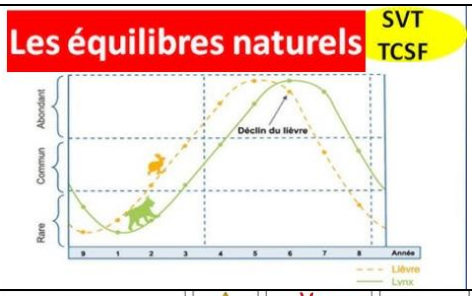
La reproduction sexuée des plantes à fleurs	Espèces non reconnues localement	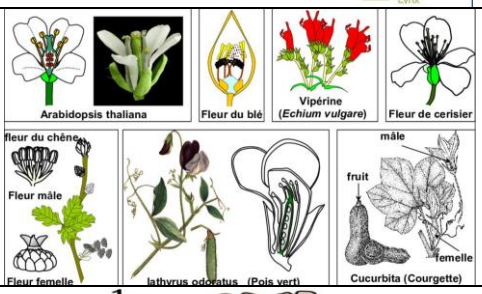
La reproduction sexuée des plantes sans fleurs	Fucus vésiculeux : espèce non reconnue localement	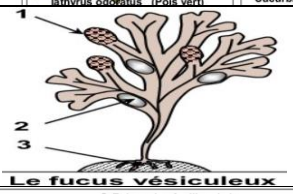
Les applications de la multiplication végétative dans le domaine agricole : bouturage Marcottage greffage	Exemples d'expériences étrangères	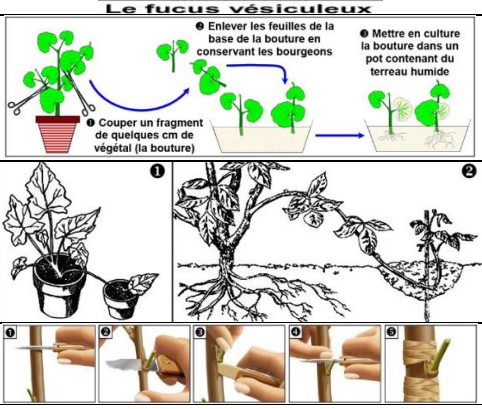

ISSN: 1857-7881 (Print)
e-ISSN 1857-7431 (Online)

Resultats

Les contextes locaux proposés :

Le HZ se distingue par une diversité remarquable de contextes géographiques et de paysages (tab. 3), qui en font un territoire particulièrement riche et fascinant. De ses montagnes comme El Ayyachi et Aberdouz aux vallées verdoyantes, en passant par ses oasis luxuriantes et ses plaines subdesertiques, cette région offre une multitude d'écosystèmes variés. Cette richesse naturelle constitue un terrain d'étude idéal pour les élèves, permettant d'aborder des thématiques essentielles du programme des SVT du TCS. Les élèves peuvent explorer les interactions entre les êtres vivants et leur environnement, étudier la biodiversité présente dans les différents habitats, et comprendre les dynamiques des équilibres naturels. En intégrant ces propriétés uniques du HZ dans le cursus scolaire.

Certaines figures proposées dans le cursus de SVT du TCS peuvent effectivement manquer d'analyse, étant donné la diversité des paysages présents dans le HZ. Il est donc vrai que ces résultats restent principalement descriptifs et pourraient tirer profit d'une analyse plus approfondie. Pour renforcer notre analyse critique, il convient de noter l'absence de travaux antérieurs similaires.

Tableau 3 : Les contextes locaux proposés

Contenu à enseigner	Contextes locaux proposés	Figures
Le choix de la station d'inventaire	Lac Tislite	
Rôle du sol dans la répartition des espèces végétales.	Berges de la vallée de Ziz	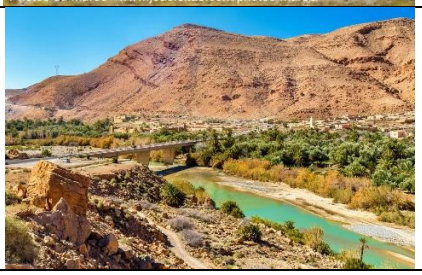

ISSN: 1857-7881 (Print)
e-ISSN 1857-7431 (Online)

Première approche du concept écosystème	Les oasis de Ziz	
L'importance de connaître et de maîtriser les facteurs climatiques dans le domaine agricole	Fermes du palmier dattiers Mejhoul à Boudnib	
	Fermes du pommier au niveau de Bouzmou à Imilchil	
Impact négatif de l'Homme sur le sol	Erosion hydrique – Déforestation	
Impact positif de l'Homme sur le sol	Lutte antiérosive au niveau du HZ (digues en pierres)	

ISSN: 1857-7881 (Print)
e-ISSN 1857-7431 (Online)

	Reboisement (alentours du lac Tsilit)	
Aspects dynamiques de l'écosystème	L'évolution des mouflons à manchettes au niveau du parc national du Haut Atlas oriental (PNHAO)	
Rôle des facteurs climatiques dans la répartition des êtres vivants	Chêne vert/ cèdre / sapin/ palmier dattier -	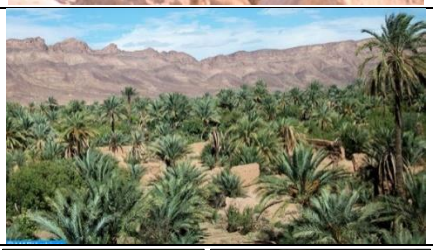
La reproduction sexuée des plantes à fleurs	Espèces locales : Pommier – Palmier dattier – Olivier -	

Les résultats du questionnaire

Après le recueil des réponses des enseignants des SVT représentant des groupes d'âge différents, ayant des expériences professionnelles et répartis sur l'ensemble du HZ (tab. 4). Le traitement pour l'analyse des données a été réalisé à l'aide du logiciel Excel : ce dernier a été utilisé essentiellement pour le traitement descriptif des répartitions des modalités des différents items du questionnaire.

ISSN: 1857-7881 (Print)
e-ISSN 1857-7431 (Online)

Tableau 4 : Les caractéristiques des professeurs ayant répondu au questionnaire

Nom	Âge	Sexe	Grade	Zone	Utilisation des contextes locaux
Prof 1	35	Homme	première	centre	Oui
Prof 2	29	Homme	première	sud	Non
Prof 3	30	Homme	deuxième	centre	Oui
Prof 4	35	Femme	première	nord	Oui
Prof 5	29	Homme	deuxième	nord	Non
Prof 6	45	Homme	principale	nord	Oui
Prof 7	50	Homme	principale	centre	Oui
Prof 8	48	Femme	principale	centre	Oui
Prof 9	33	Homme	première	centre	Oui
Prof 10	28	Femme	deuxième	sud	Non
Prof 11	26	Homme	deuxième	sud	Oui
Prof 12	24	Femme	deuxième	nord	Oui
Prof 13	52	Homme	principale	centre	Oui
Prof 14	39	Femme	première	ouest	Oui
Prof 15	40	Homme	première	ouest	Oui
Prof 16	37	Femme	première	ouest	Non
Prof 17	53	Homme	principale	ouest	Oui
Prof 18	26	Femme	deuxième	centre	Oui
Prof 19	29	Homme	deuxième	centre	Non
Prof 20	31	Homme	deuxième	centre	Oui
Prof 21	27	Homme	deuxième	sud	Oui
Prof 22	30	Femme	deuxième	ouest	Non
Prof 23	57	Homme	principale	sud	Oui
Prof 24	28	Homme	deuxième	nord	Oui
Prof 25	39	Homme	première	nord	Non
Prof 26	35	Femme	première	sud	Oui
Prof 27	45	Homme	première	sud	Oui
Prof 28	34	Femme	deuxième	nord	Non
Prof 29	60	Homme	principale	ouest	Non
Prof 30	61	Homme	principale	centre	Oui

Sept enseignants sur huit de grade principal estiment que l'intégration des contextes locaux aide les apprenants à mieux comprendre les concepts des SVT. De plus, sept sur dix des enseignants de première grade partagent également cet avis, tandis que seulement sept sur douze des professeurs de deuxième grade le confirment (fig. 11).

ISSN: 1857-7881 (Print)
e-ISSN 1857-7431 (Online)

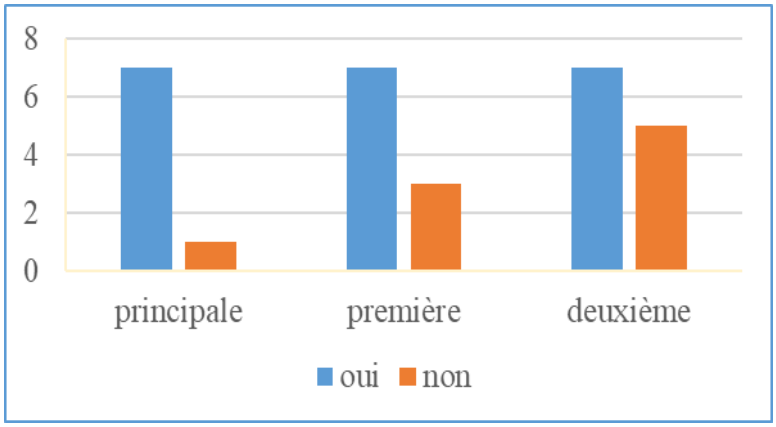

Figure 11 : Répartition des réponses des professeurs selon leur grades

En ce qui concerne la répartition des réponses selon le genre, quinze enseignants sur vingt de sexe masculin estiment que l'intégration des contextes locaux aide les apprenants à mieux saisir les concepts des SVT (fig. 12). Par ailleurs, six enseignants sur dix de sexe féminin sont également d'accord avec cette opinion.

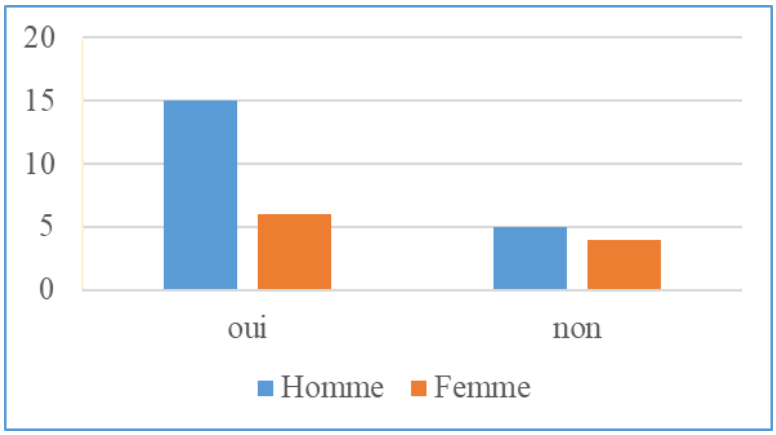

Figure 12 : Répartition des réponses des professeurs selon leur sexe

Discussion

Merlo-Leurette et Forissier (2009) affirment que l'enseignement des sciences traverse un processus d'adaptation que nous caractérisons par le terme de contextualisation. Forissier (2019) a par la suite souligné l'importance de la didactique de la contextualisation et de ses effets sur l'apprentissage des sciences.

D'un autre côté, Moore (2008) a étudié, à travers des comparaisons, la relation entre la contextualisation et l'universalisme dans le champ de l'enseignement des langues. De plus, Hussard-Wang (2025) a examiné l'impact de la contextualisation dans l'enseignement et l'apprentissage du

ISSN: 1857-7881 (Print)
e-ISSN 1857-7431 (Online)

français en France auprès des apprenants allophones. Daghé et *al.* (2025) se sont penchés sur la manière de contextualiser l'enseignement de l'oral dans les classes d'accueil, tandis que Doussot & Fink (2024) ont mis en avant l'importance de la contextualisation en histoire à travers une étude didactique sur les relations entre l'épistémologie scolaire et l'épistémologie de référence. En ce qui concerne les SVT, l'examen des travaux antérieurs révèle un manque de recherche dans ce domaine.

Le contexte du HZ présente une diversité remarquable de paysages et de caractéristiques géo-environnementales. Cette richesse peut être utilisée comme un cadre d'apprentissage intégré dans l'enseignement des SVT pour les élèves du TCS. En reliant les concepts scientifiques à leur environnement, les enseignants peuvent favoriser une compréhension approfondie chez les élèves. Par exemple, l'exploration des écosystèmes locaux permet aux élèves d'appréhender des notions telles que la biodiversité, les cycles de vie et l'impact des activités humaines sur leur milieu. Par conséquent, l'intégration de ces contextes locaux dans le cursus de SVT du TCS revêt une importance cruciale pour rendre l'enseignement plus pertinent et engageant pour les élèves du HZ.

Les résultats de notre enquête, menée auprès des enseignants de SVT dans cette région, mettent en évidence des variations significatives dans la perception de cette intégration en fonction des caractéristiques des ensegnants telles que l'ancienneté, l'age, le sexe et le lieu de travail.

Pour l'expérience, ceux ayant plus d'expérience partagent une vision favorable envers l'intégration des exemples locaux dans l'enseignement des SVT (fig. 13). Ils reconnaissent conjoncturellement que les élèves se sentent davantage concernés et intéressés par des sujets qui se rapportent à leur quotidien et à leur environnement immédiat. Cette constatation est en consonance avec des recherches antérieures portant sur l'intégration des contextes locaux en français (Hussard-Wang, 2025) qui soulignent que des exemples pertinents facilitent la compréhension du français chez les apprennants allophones en France, car ils établissent un lien entre la théorie et la réalité observée par les élèves.

De même, les enseignants ayant une ancienneté intermédiaire partagent des avis semblables, soulignant que l'intégration des contextes locaux contribue non seulement à capter l'attention des élèves mais aussi à faciliter l'assimilation des concepts scientifiques. Ils mettent en avant l'idée que les exemples issus de la réalité quotidienne des élèves rendent l'apprentissage plus significatif, ce qui est essentiel pour leur développement cognitif. En utilisant des réalités que les élèves expérimentent chaque jour, ces enseignants parviennent à enrichir le processus éducatif, transformant des notions abstraites en applications concrètes.

ISSN: 1857-7881 (Print)
e-ISSN 1857-7431 (Online)

À l'inverse, les enseignants récemment intégrés dans le système éducatif montrent une réticence palpable à adopter cette approche d'intégration des contextes locaux. Leur scepticisme peut être attribué à leur manque d'expérience dans l'enseignement et à leur récente découverte des méthodologies pédagogiques. Il est possible qu'ils aient besoin de temps pour observer les avantages concrets de cette intégration dans leur pratique pédagogique. Cela soulève la nécessité de les accompagner par des formations et des ressources pédagogiques qui leur permettent de se familiariser davantage avec les avantages de l'intégration des contextes locaux et de ses impacts sur l'apprentissage des élèves.

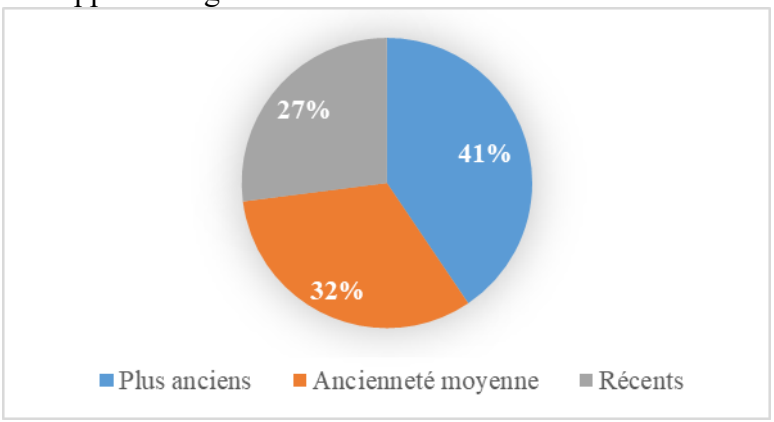

Figure 13 : Pourcentages d'enseignants favorables à l'intégration des contextes locaux selon leur ancienneté

Les résultats montrent également que les enseignants masculins sont globalement plus favorables à l'intégration des contextes locaux dans le cursus de SVT que leurs homologues féminins (fig. 14). Les hommes soulignent l'engagement accru des élèves grâce à cette approche, tandis que les femmes expriment des réserves concernant son application pratique. Cette divergence de perspectives souligne la nécessité de prendre en compte les expériences et points de vue des deux genres pour développer une approche pédagogique inclusive et efficace.

ISSN: 1857-7881 (Print)
e-ISSN 1857-7431 (Online)

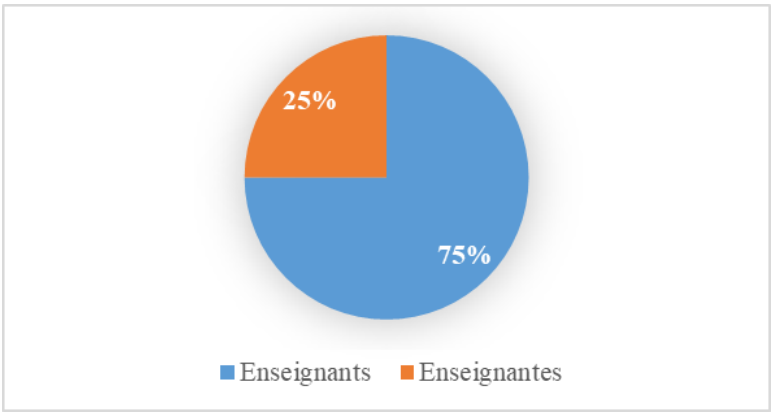

Figure 14 : Pourcentages d'enseignants favorables à l'intégration des contextes locaux selon leur sexe

En conclusion, l'intégration des contextes locaux dans le cursus de SVT est perçue positivement par les enseignants expérimentés et ceux ayant une ancienneté moyenne, qui constatent ses bénéfices sur l'engagement et la compréhension des élèves. En revanche, il est crucial de soutenir les nouveaux enseignants pour les encourager à adopter cette approche innovante et d'identifier les raisons qui expliquent pourquoi les enseignantes sont moins favorables à l'intégration des contextes locaux. Des formations et des ressources adaptées pourraient leur fournir la confiance nécessaire pour utiliser efficacement les contextes locaux dans leur enseignement, favorisant ainsi un apprentissage significatif pour tous les élèves.

Conclusion

L'analyse des contextes présents dans le programme des SVT du TCS marocain indique que la majorité des exemples ne reflètent pas la réalité locale des élèves du HZ. Par conséquent, il est essentiel d'intégrer ces contextes locaux. Les résultats du questionnaire révèlent que de nombreux enseignants perçoivent un impact positif de cette intégration sur l'enseignement des SVT. Cette adaptation permet de rendre l'apprentissage plus pertinent et engageant pour les élèves, en se basant sur des exemples concrets issus de leur environnement. En ajustant le contenu pédagogique à la réalité locale, les enseignants favorisent non seulement la compréhension des concepts scientifiques, mais améliorent également la motivation et l'implication des élèves dans leurs études.

Cependant, pour tirer pleinement parti de cette approche, il est essentiel d'élargir et de diversifier le nombre de participants au questionnaire en y intégrant les inspecteurs et d'autres intervenants. Il est également important de proposer cette idée à l'échelle nationale pour évaluer son utilité. De plus, il serait judicieux d'élargir cette recherche à d'autres disciplines afin

ISSN: 1857-7881 (Print)
e-ISSN 1857-7431 (Online)

d'évaluer l'impact global de l'intégration des contextes locaux sur la performance de l'apprentissage des élèves sur le long terme. Ces pistes de réflexion ouvriront des avenues prometteuses pour une amélioration continue de l'enseignement des SVT au Maroc.

Conflit d'intérêts : Les auteurs n'ont signalé aucun conflit d'intérêts.

Disponibilité des données : Toutes les données sont incluses dans le contenu de l'article.

Déclaration de financement : Les auteurs n'ont obtenu aucun financement pour cette recherche.

References:

1. Abid, C., Essedaoui, A., & Selmaoui, S. (2024). Intégration de l'éducation au développement durable dans le curriculum des sciences de la vie et de la terre: Étude comparative entre les filières Sciences Expérimentales, Sciences Mathématiques et Lettres et Sciences Humaines au cycle secondaire au Maroc. ESI Preprints (European Scientific Journal, ESJ), 20(35), 106-106.
2. Ameziane, N. (2018). Place de l'environnement dans les curricula marocains des Sciences de la Vie et de la Terre au cycle secondaire. The Journal of Quality in Education, 8(11), 19-19.
3. Daghé, S. A., Silva-Hardmeyer, C., Cordeiro, G. S., & Roux-Mermoud, A. (2025). Contextualisation de l'enseignement de l'oral en classe d'accueil: structure et gestes didactiques. *Tréma*, (64).
4. Doussot, S., & Fink, N. (2024). La contextualisation en histoire: une étude didactique sur les rapports entre épistémologie scolaire et épistémologie de référence. *Revue française de pédagogie*, *223*(2), 9-26.
5. Forissier, T. (2019). *Contextualisation et effets de contextes dans l'apprentissage des Sciences* (Doctoral dissertation, Université des Antilles).
6. Fuchs-Gallezot, M., & Bächtold, M. (2023). L'esprit critique dans l'enseignement des sciences: quelles approches? Quelles prises en charge par la recherche? Quelles prises en charge scolaires?. RDST. Recherches en didactique des sciences et des technologies, (28), 9-30.
7. Hussard-Wang, J. (2025). Contextualiser l'enseignement et l'apprentissage du français en France parmi les publics allophones. *Contextes et didactiques. Revue semestrielle en sciences de l'éducation*, (26).

ISSN: 1857-7881 (Print)
e-ISSN 1857-7431 (Online)

8. Iwzane, M., Ouardi, J., Benhadi, B., Chennaoui, M., El Idrissi, B. E. F., & Afquir, M. (2025). Apprentissage par la démarche d'investigation dans le cycle collégial et qualifiant au Maroc: Exemples de progressions en SVT. In SHS Web of Conferences (Vol. 214, p. 01029). EDP Sciences.
9. Legendre, M. F. (1994). Problématique de l'apprentissage et de l'enseignement des sciences au secondaire: Un état de la question. Revue des sciences de l'éducation, 20(4), 657-677.
10. Loubaki, G. N., Potvin, P., Hijazi, L. R., & Vàzquèz-Abad, J. (2015). Diagnostic des conceptions en sciences susceptibles d'expliquer les différences de performances à une évaluation internationale entre le Québec et le Maroc. Comparative and International Education, 44(1).
11. Manaouch, M., Mohamed, S., & Imad, F. (2021). Integrating WaTEM/SEDEM model and GIS-based FAHP Method for Identifying Ecological Rainwater Harvesting Sites in Ziz upper watershed, SE Morocco.
12. Manaouch, M., Naimi, L., Haynou, M., Aghad, M., Sadiki, M., Pham, Q. B., & Jakimi, A. (2025). Enhancing Geotourism in Southeastern Morocco through Machine Learning-Based Geomorphosite Identification. Geoheritage, 17(1), 1-19.
13. Manaouch, M., Sadiki, M., Aghad, M., Bao Pham, Q., Batchi, M., & Al Karkouri, J. (2024). Assessment of landslide susceptibility using machine learning classifiers in Ziz upper watershed, SE Morocco. Physical Geography, 45(2), 203-230.
14. Manaouch, M., Sadiki, M., Pham, Q. B., Zouagui, A., Batchi, M., & Al Karkouri, J. (2023). Predicting potential reforestation areas by Quercus ilex (L.) species using machine learning algorithms: case of upper Ziz, southeastern Morocco. Environmental Monitoring and Assessment, 195(9), 1094.
15. Maouni, A., Mimet, A., Khaddor, M., Madrane, M., & Moumene, M. (2014). L'intégration des TIC dans l'enseignement des SVT au Maroc: réalité et attentes. Radisma, 10, 27.
16. MEN PISA (2018) acessible via https://www.csefrs.ma/wp-content/uploads/2023/04/Rapport-PISA-V-Fr.pdf
17. Merlo-Leurette, S., & Forissier, T. (2009). La contextualisation dans l'enseignement des sciences et techniques en Guadeloupe. *Grand N, Revue de mathématiques, de sciences et technologie pour les maîtres de l'enseignement primaire*, *83*.
18. Ministère de l'éducation national du préscolaire et des sports, Rapport National Maroc-PISA 2018 publié février 2023, Centre National de l'Evaluation et des Examens. Royaume du Maroc. Accessible via le lien: https://www.men.gov.ma/

ISSN: 1857-7881 (Print)
e-ISSN 1857-7431 (Online)

19. Moore, D. (2008). Contextualisation et universalisme. Quelle didactique des langues pour le 21ème siècle?. *Perspectives pour une didactique des langues contextualisée.*, 183-203.
20. Nafidi, Y., Alami, A., Zaki, M., El Batri, B., Hassani, M. E., & Afkar, H. (2018). L'intégration des TIC dans l'enseignement des sciences de la vie et de la terre au Maroc: état des lieux et défis à relever. European Scientific Journal, 14(1), 97-121.
21. Naimi, L., Benaddi, L., Jakimi, A., & Manaouch, M. (2024). Assessing habitat suitability for aoudad (Ammotragus lervia) reintroduction in southeastern morocco to promote ecotourism. Scientific African, 26, e02444.
22. Naimi, L., Ouaddi, C., Benaddi, L., Bouziane, E. M., Jakimi, A., & Manaouch, M. (2024). Machine Learning Approach to Identify Promising Mountain Hiking Destinations Using GIS and Remote Sensing. International Journal of Advanced Computer Science & Applications, 15(10).
23. Sadiki, M., Manaouch, M., Aghad, M., Batchi, M., & Al Karkouri, J. (2023). Identifying landslides prone-areas using GIS-based fuzzy analytical hierarchy process model in ziz upper watershed (Morocco). Ecological Engineering & Environmental Technology, 24.